Final Report for the Task 6 Modeling of the San Joaquin River

A Deliverable
for
CALFED Project ERP-02D-P63
Monitoring and Investigations for the San Joaquin River and Tributaries Related to Dissolved Oxygen
Task 6 Model Calibration and Forecasting

Prepared by

Joel Herr, Carl W. Chen, and Katie van Werkhoven
Systech Water Resources, Inc.
Walnut Creek, CA 94596

May 16, 2008

TABLE OF CONTENTS

List of Figures

List of Tables

ABSTRACT

Dissolved oxygen concentrations in the Stockton Deep Water Ship Channel (DWSC) have often dropped below 5 mg/l needed to protect aquatic life in general and upstream migrating salmon in particular. A predictive model was needed to serve as a tool for calculating the necessary load reduction of oxygen consuming materials to meet the dissolved oxygen standard. This project developed the San Joaquin River Model that comprised two models: 1) A GIS based watershed model (WARMF) for the upstream non-tidal section of the San Joaquin River and 2) the Link-Node Model for the downstream tidal section of the San Joaquin River that including the DWSC. A graphical user Interface was developed to link the two models together, so that the output of the upstream watershed model would automatically become the input to the downstream estuary model. Given the input data of meteorological and operating conditions, the model predicted dynamic river flow and water quality at various river segments throughout the simulation time period. Field programs collected flow and water quality data at various stations in water years 2000 to 2005. The meteorology and operating conditions (waste discharges, river inflow, diversions, irrigations, etc.) of 2000 to 2005 were compiled and used to drive the model. The flow and water quality predicted by the model matched the observed data collected by the field programs. Hydrologic and water quality calibrations were performed to reduce model errors. This report described the calibration results by comparing the simulation results to the observed data in graphs as well as in statistics. The matches were found to be very good. Some discrepancies occurred that require further investigation. The final model was found to be suitable for calculating DO TMDLs of oxygen consuming materials to eliminate chronic low DO in the DWSC. It was also found suitable for developing real time water quality management plans to eliminate the episodic low DO in the DWSC.

t

1 MODEL CALIBRATION

INTRODUCTION

Background

The Stockton Deep Water Ship Channel ("DWSC") has often experienced low dissolved oxygen concentration, impairing the passage of salmon upstream to spawn in San Joaquin River and its tributaries. The California Central Valley Water Quality Control Board and the California Water Resources Control Board placed the San Joaquin River on the 303d list for violating the dissolved oxygen standard to protect the beneficial use of fishery and aquatic life. Being placed on the 303d list triggered federal law requiring the development of TMDL (total maximum daily load) of dissolved oxygen consuming materials that enter the water body. The loading of these materials had to be curtailed to meet the minimum dissolved oxygen criterion of 6 mg/l from September through November and 5 mg/l the rest of the year.

In the 1990s, the Central Valley Water Quality Control Board concentrated its regulatory effort on the point source control of the Stockton Regional Wastewater Treatment Plant, which received high loads of cannery wastes in the summer. It is a secondary treatment plant with its final effluent polished by an algae pond. Under summer operating conditions, the effluent from the algae pond contained low concentrations of BOD and ammonia. In the critical fall month of September, however, the algae pond turned over, became ineffective, and released ammonia to the effluent with a concentration as high as 25 mg/l. The Water Quality Control Board demanded the construction of a nitrification unit to convert ammonia to nitrate before its discharge to the San Joaquin River.

Considerable scientific studies have been conducted to investigate the causes of low DO in the DWSC, including data collections, data analyses, and modeling. The City of Stockton conducted monthly field sampling of DO, BOD, temperature, and chlorophyll-a in the San Joaquin River at nine stations. The data were used to calibrate the EPA Link-Node estuary model (Shanz and Chen 1993). The model was used to evaluate how the export pumping at Tracy would divert water from the upstream San Joaquin River through the Old River, which reduced the river inflow, increased the hydraulic residence time, and decreased DO in the DWSC (Chen and Tsai 1996). The model was also used to evaluate alternatives to increase DO in the DWSC and show that low DO conditions would persist even if the point source discharge from Stockton Regional Wastewater Treatment Plant were completely eliminated (Chen and Tsai 1997a and b). Low river inflow and high DO demanding substances from the upstream would continued to cause a low DO in the DWSC.

Jones and Stokes (1998) compared the seasonal variations of chlorophyll-a at Vernalis and DO concentration in the DWSC. High chlorophyll-a concentration was associated with a super saturation of DO at Vernalis. It was also associated with low DO in the DWSC. The algae grown in the upstream appeared to have been transported downstream to DWSC, where the algae died and respired to consume dissolved oxygen. Controlling algae at Vernalis might be a potential solution for achieving the dissolved oxygen objective at the DWSC.

In 1999, the San Joaquin River DO TMDL study was initiated to seek a watershed approach to solve the low DO problem for the DWSC. CALFED funded a study to collect field data by California Department of Water Resources. Analysis of data showed that ammonia was a significant DO sink, which could be derived in part from the ammonia discharge of Stockton Regional Wastewater Treatment Plant and in part from the decomposition of dying algae from the upstream (Lehman, Sevier, Giulianotti, and Johnson. 2004). The Link Node estuary model was improved and calibrated with the new data collected (Chen and Tsai 2002). The model was used to calculate the relative contribution of DO sinks to the DWSC (Chen and Tsai 2000). The river load from upstream was substantial. Foe, Gowdy, and McCarthy (2002) showed that the river load was primary contributed by algae seeded by agriculture drains, which was then doubled by growth during the transport downstream to Vernalis.

In 2003, CALFED funded the directed action project for monitoring and investigations of the San Joaquin River and tributaries related to dissolved oxygen. A comprehensive field program was established to measure flow and water quality in the Upper San Joaquin River and its tributaries. Meanwhile, USGS and University of California Davis have collaborated to measure sources and transport of nutrients and algae during summer and fall of 2000 and 2001 (Kratzer at al. 2004). Jones & Stokes (2005) created a data atlas by compiling all these data into a CD to support data analysis and modeling. Task 6 of the upstream study was for the development, calibration, and application of the San Joaquin River Model.

Modeling Objective

The objective was to develop a predictive model of San Joaquin River. The model accepted meteorology (daily maximum and minimum temperatures, precipitation, wind speed etc.) and operating conditions (daily point source waste discharges, reservoir releases, water diversion, application of irrigation water and fertilizer to the agriculture lands, etc.) as input. The model predicted the daily nonpoint source load of pollutants and the flow and water quality of San Joaquin River as output.

The model was used to serve multiple purposes:

1. To provide an integrated interpretation of the field data collected in the past as well as during the directed action project. The model was used to predict flow and water quality, based on known scientific principles of heat budget, mass balance, hydrology, hydrodynamics, chemical transformations, algal growth, and nutrient uptake. The predictions were compared to the observed data for confirmation.

2. To develop the DO TMDL plan that can eliminate the chronic low DO problem in the DWSC. The model was used to calculate the reductions of point and nonpoint loads of oxygen consuming materials needed to meet the DO objectives of the DWSC.

3. To develop real time water quality management plan for episodic low DO events in the DWSC. The model was used to forecast water quality problem (low DO) two to three weeks ahead of time, when it was anticipated that the water of San Joaquin River will be diverted through Old River to Tracy for export pumping. Under such circumstance, the model was used to explore various remedial measures to raise the DO of the DWSC, including various means to release more water back to the San Joaquin River, hold back wetlands releases, and/or turn on the U tube aerator to inject dissolved oxygen into the DWSC.

4. To support the stakeholder processes of DO TMDL. The model served as a decision support system for stakeholders to learn about the watershed behaviors, to identify the sources and magnitudes of oxygen demanding materials, to formulate alternatives to reduce the point and nonpoint loads, and to evaluate the expected improvements of water quality. The decision support system guided stakeholders to discuss the issues and learn about management plans that were scientifically correct and politically and economically acceptable.

5. To develop a TMDL and water quality management framework for other pollutants. The model simulated many chemical species. When a need arises in the future, the model can be used to address the water quality issues of TDS (EC), pesticides, specific ions (e.g. sodium), DOC, among others.

San Joaquin River Modeling System

The San Joaquin River has two very different sections. The Lower San Joaquin River, which includes the DWSC, is tidal. The violation of DO standard occurred in this section. Yet, most of the nonpoint loads of oxygen consuming materials were derived from the agricultural lands in the Upper San Joaquin River Watershed, which is non-tidal. For that reason, the San Joaquin River model required a tidal estuary model and a non-tidal river model.

An estuary model had already been developed for the Lower San Joaquin River, extending from The Old River junction near Mossdale to the Stockton DWSC at Venice Island (Schanz and Chen 1993, and Chen and Tsai 2002). Another model for the non-tidal portion of the San Joaquin River needed to be linked to it.

Initially, the plan was to use a special version of the DWR DSM2 model called DSM2-SJR that does not have a tidal boundary. DWR had done some initial work to extend DSM2-SJR to the non-tidal section of the San Joaquin River (Pate 2001). The non-tidal section of San Joaquin River flows west from its headwaters in the Sierra National Forest and then north along the central valley floor to the tidal section of the San Joaquin River to form the Sacramento-San Joaquin Delta.

This river section has three eastside tributaries (Stanislaus River, Tuolomne River, and Merced River) that drain the Sierra-Nevada western slope westward to San Joaquin River. On the west side, there are six tributaries (Hospital/Ingram Creek, Del Puerto Creek, Orestimba Creek, Los Banos Creek, Mud Slough, and Salt Slough) that drain the Diablo Coastal Range eastern slope eastward to the San Joaquin River. The total drainage area of this river section is approximately 32,000 square miles, including the largest and most productive agriculture lands of California.

The initial work of DWR concentrated on the main stem of the San Joaquin River. Bathymetric data was obtained from the US Army Corps of Engineers and was used to generate the cross sections for each river mile (node) of the San Joaquin River. The invert elevations of the river cross sections were taken off topographic maps. Using these data as input, DSM2-SJR was used to perform hydrodynamic simulation to calculate the travel time. The simulated travel time was compared to the travel time measured by tracer studies. The invert elevations and channel geometries were adjusted to match the observed and simulated travel time (Wilde 2005).

The extension of DSM2-SJR to the eastside tributaries was proven more difficult because the bathymetry data needed to develop the channel geometry could not be obtained from the Corps of Engineers. More seriously, the DSM2-SJR was a river model that does not simulate the hydrology and nonpoint source loads of pollutants from the agricultural lands. It relied on the SJRIO model (Kratzer et al. 1987) to provide semi empirical estimates of groundwater accretions from agriculture lands. There were changes in agriculture practices since 1985. The empirical estimate, based on the historical data prior to 1985, was not necessarily still applicable. With the SJRIO estimated groundwater accretions, the DSM2-SJR could not simulate the river flow to match the measured flow of recent years. An arbitrary "add water" term was introduced to account for the missing water and salt (Brown and Huber 2004 and Wilde 2005). DSM2-SJR was not a mature model for ready application. It requires substantial effort of further development and testing.

The upstream study used an adaptive research approach that allows for the adjustment of methodology during the course of investigation. With the difficulties of DSM2-SJR, the principal investigators of the upstream study decided to change the upstream model to WARMF model. A request for the change was made and approved by CALFED in 2005.

WARMF is a GIS based watershed model for TMDL analysis. It is a public domain model, available from US EPA website (Google EPA WARMF). The model is a mature model that is compatible with other watershed models contained in the EPA BASINS. It could readily be applied to the San Joaquin River Basin without modification. The model is well documented (Chen et. al. 2001) and peer reviewed (Keller, 2000, 2001, Driscoll, Jr. et al. 2004). The User's Manual is available (Herr et al. 2001).

WARMF could simulate the watershed processes to calculate hydrology and nonpoint source loads of pollutants from various land uses (urban, forested, and agricultural areas). The input data included the locations of agricultural diversions, daily diversions, and amount of irrigation water applied to the agriculture lands. The model simulated percolation of irrigation water through soil, evapotranspiration of water through crops, change of groundwater table,

agricultural return flow, and groundwater accretion to the river reaches. The model also simulated the nonpoint loads of pollutants due to fertilizer and pesticide applications, leaching of cations and anions from the soil, and erosion of soils from land.

Thus, the modeling system of San Joaquin River contained the Link-Node estuary model for the tidal lower section and the WARMF watershed model for the upper non-tidal section. The interface point of the two models was established at the Old River junction near Mossdale.

San Joaquin River Model Interface

The San Joaquin River Modeling Interface ("Interface") was designed to integrate the Link-Node estuary model and WARMF watershed model under user-friendly software. Figure 1.1 shows the GIS map displayed by the Interface.

The tributary areas upstream of the eastside reservoirs (New Melones Reservoir, Don Pedro Reservoir, and Lake McClure) were excluded from the WARMF watershed model. The WARMF watershed model was set up for the watershed from the confluence with Bear Creek near Stevinson to the Old River confluence (near Mossdale).

The Link-Node estuary model extended from the DWSC Light 18 through the lower San Joaquin River upstream to the junction with the Old River (near Mossdale). The Link-Node estuary model only simulated the tidally influenced waterways. The runoff and nonpoint loads from lands draining directly to the tidal waterways were ignored.

The San Joaquin River Model Interface automatically transfered the output of river flow and associated pollutants from the watershed model to the input of the estuary model. The user could therefore run both the watershed model and the estuary model through the Interface with one command.

The Interface transformed the model from an old fashioned DOS based model to a modern Windows based model. The DOS based model works with the concept of punch cards, data files, data lines, formats, and batch processing, which are difficult to set up, modify, or run. The Windows based model works directly on the computer screen and uses menu, dialog box, picture, GIS map, graphic, and point and click system. The users could simply point and click on menu to set up a simulation run directly in a dialog box. The model system was created with a data module to store all kinds of input data including inflow, inflow water quality, diversion record, meteorology, air quality, measured flow and water quality, and pictures. The users could point and click on the GIS map to view the data associated with the location, displayed in dialog boxes with their variables names spelled out in plain English. The users could make changes directly on the dialog box without having had to worry about their formats.

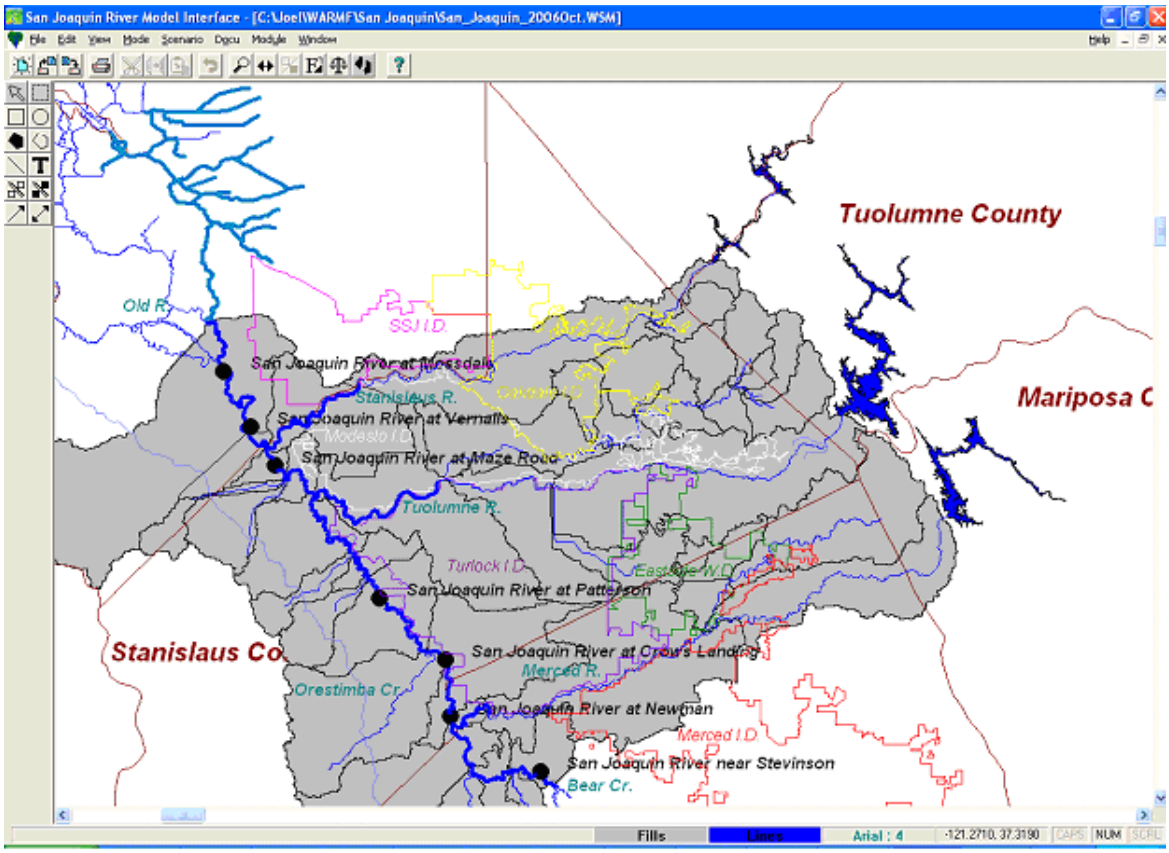

Figure 1.1 The San Joaquin River Model Interface.

The user friendly features of the Interface encouraged the principal investigators of the upstream study, who were not necessarily modelers, to run the model and examine the data within it. Stakeholders were trained to use the model and provided feedback during the project. To promote the collaborations among investigators and interested stakeholders, the San Joaquin River Modeling System, completed with the model and database, was placed on an FTP site for download.

The Interface was developed to link the WARMF watershed model to the Link-Node estuary model. Effort was expended to make sure that both models could be executed through the Interface. Updating and recalibration of the Link-Node model was done to improve its predictive performance. The use of the linked models to prepare and implement the real time water quality management plan was documented in the forecasting procedure report (Herr and Chen 2006) and forecasting results report (Herr and Chen 2007).

UPSTREAM WATERSHED MODEL

Model Setup

WARMF was set up to simulate the San Joaquin River and its watershed that extends from the confluence with Bear Creek to the junction with the Old River near Mossdale. The San Joaquin River included in the watershed model is shown in yellow in Figure 1.2 The dark gray areas on the GIS map show lands simulated by the model that receive natural precipitation and irrigation water. The remaining area on the map, including the west side tributaries and the east side tributaries upstream to the major reservoirs, was not simulated but may be at a later time, when the need arises and funding is made available.

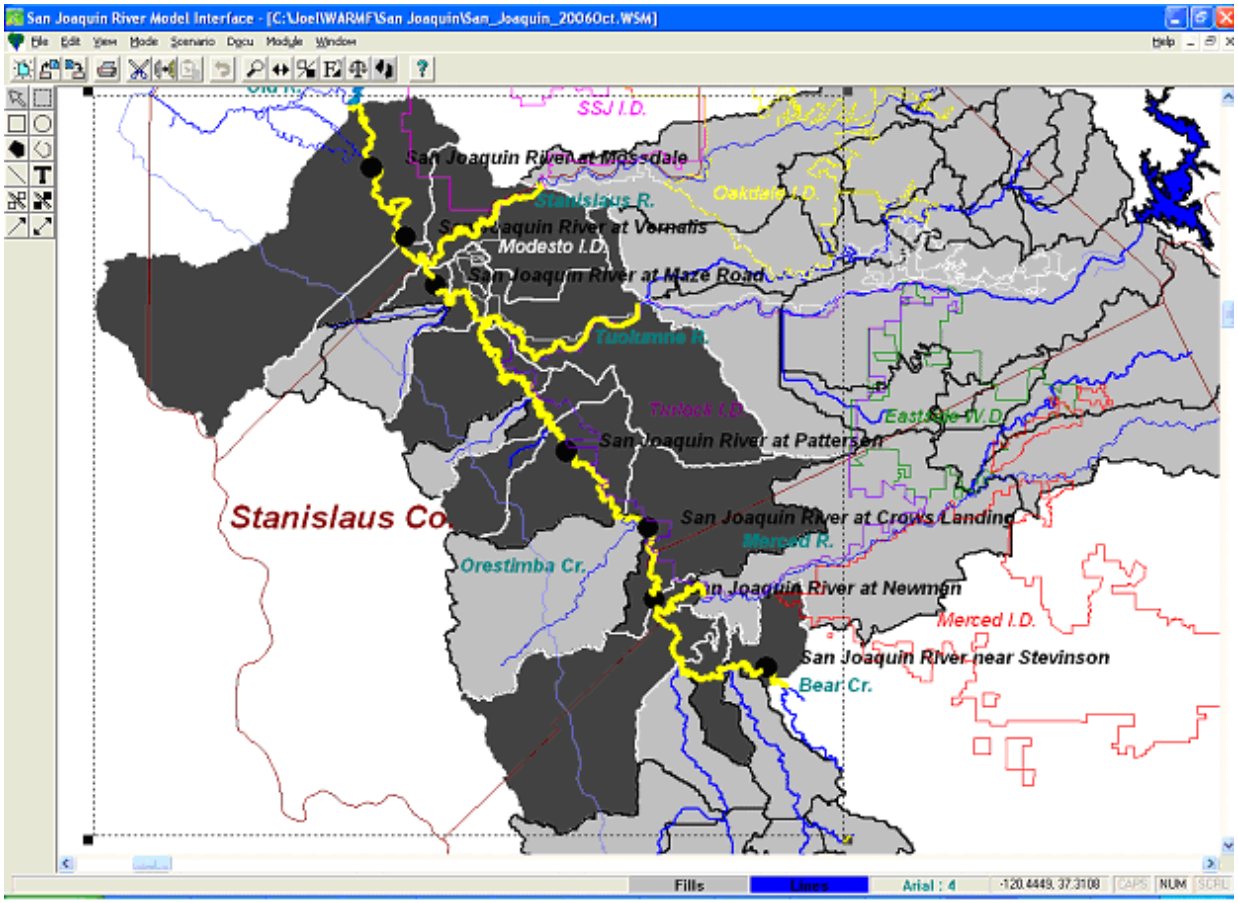

Figure 1.2 The Domain of WARMF San Joaquin River Model.

The San Joaquin River within the watershed was divided into 93 river segments. The irrigated lands were divided into 17 land catchments. The model simulated natural storm water runoff,

irrigation return flow, groundwater table of land catchments, groundwater lateral flow from land catchments to their respective receiving river segments

With this model set up, the boundary conditions were the San Joaquin River and its tributaries that intersect with the model domain. For those boundary conditions, there were gage stations that provided measured inflows as inputs to the model. For example, there were three gages for the three major east side tributaries (Stanislaus, Tuolumne, and Merced Rivers). For the agricultural lands, the model inputs included daily diversions, location of diversion, and areas upon which the irrigation water was applied. Based on the locations of diversions, the model used the water quality of the source water when applying that water as irrigation.

Hydrologic Simulation

WARMF simulates hydrology based on water balance and physics of flow. It begins with precipitation on the land surface. Precipitation and irrigation water can percolate into the soil. Within the soil, water first goes to increase the moisture in each soil layer up to field capacity. Above field capacity, water percolates down to the water table, where it flows laterally out of the land catchment according to Darcy's Law. Water on the soil or within the soil is subject to evapotranspiration, which is calculated based on temperature, humidity, and season. The amount of water entering and leaving each soil layer is tracked. If more water enters the soil than leaves it, the water table rises. If the water table reaches the surface, the soil is saturated and overland flow occurs. The overland flow is calculated by Manning's equation.

Rivers accept the subsurface and overland flow from catchments linked to them. They also receive point source discharges and flow from upstream river segments. Diversion flows are removed from river segments. The remaining water in the river is routed downstream using the kinematic wave algorithm. The channel geometry, Manning's roughness coefficient, and bed slope are used to calculate depth, velocity, and flow. The velocity is a measure of the travel time down the river, which in turn affects the water quality simulation. A thorough description of the processes simulated by WARMF is in the WARMF Technical Documentation (Chen, Herr, and Weintraub 2001).

Water Quality Simulation

The fundamental principle which guides WARMF simulation of water quality is heat and mass balance. Heat enters the soil in water from precipitation and irrigation. Heat is exchanged between catchments and the atmosphere based on the thermal conductivity of the soil. Heat in water leaving the catchments enters river segments, which combine the heat from multiple sources. As in catchments, there is thermal exchange with the atmosphere based on the difference in temperature between the water and the air. Temperature is then calculated by heat balance throughout the model.

Chemical constituents enter the model domain from atmospheric deposition and from point source discharges. They can also enter the land surface in irrigation water and fertilizer application. Chemical species move with water by percolation between soil layers, groundwater lateral flow to rivers, and surface runoff overland. Each soil layer is considered to be a mixed

reactor, as is the land surface within each land use. Within the soil, cations are adsorbed to soil particles through the competitive exchange process. Anions are adsorbed to the soil using an adsorption isotherm. A dynamic equilibrium is maintained between dissolved and adsorbed phases of each ion. Reactions transform the dissolved chemical constituents within the soil. The dissolved oxygen concentration is tracked, and as D.O. goes to zero, anoxic reactions take place. When overland flow takes place, sediment is eroded from the catchment surface according to the modified universal soil loss equation. The sediment carries adsorbed ions (e.g. phosphate) with it to the river.

Rivers accept the water quality which comes with each source of flow. Each river segment is considered a completely mixed reactor. Ions form an equilibrium between dissolved and adsorbed to suspended sediment. Sediment can settle to the river bed and is scoured from the river bed when velocity is high enough. Chemical reactions are based on first order kinetics with their rate adjusted with a temperature correction. Algae are represented by three types: greens, blue-greens, and diatoms. Each has their own optimum growth rate, nutrient half-saturation concentrations, light saturation, optimum temperature, and temperature range for growth. At each time step, algal growth is a function of nutrient limitation, light limitation, and temperature limitation. Light penetration is a function of the algae, detritus, and total suspended sediment concentrations. Light intensity is integrated over the depth of the river segment.

Simulated Parameters

In order to model the dissolved oxygen in the DWSC, the models simulated an array of hydrologic, chemical, and physical variables. Table 1.1 are the parameters simulated the WARMF and Link-Node models.

Table 1.1 Parameters Simulated by WARMF and Link-Node Models

Parameter	WARMF	Link-Node
Flow	X	X
Depth	X	X
Velocity	X	X
Temperature	X	X
pH	X	
Ammonia (as N)	X	X
Calcium	X	
Magnesium	X	
Potassium	X	
Sodium	X	
Sulfate	X	
Nitrate (as N)	X	X
Chloride	X	
Phosphate (as P)	X	X
Alkalinity	X	
Inorganic Carbon	X	X
EC or TDS	X	X

Parameter	WARMF	Link-Node
Fecal Coliform	X	X
BOD	X	X
Dissolved Oxygen	X	X
Blue-green Algae	X	
Diatoms	X	
Green Algae	X	
Periphyton	X	
Pheophytin		X
Detritus (Volatile Solid)	X	X
Clay	X	X
Silt	X	X
Sand	X	X
Total Suspended Sediment	X	X
Total Phosphorus	X	
Total Kjeldahl Nitrogen	X	
Total Nitrogen	X	
Total Organic Carbon	X	
Total Phytoplankton	X	X
Total Dissolved Solids (TDS)	X	X

WARMF modeled electrical conductivity (EC) in two forms. One form is an independent constituent. In this case, ECs of inflows, precipitation and irrigation water were specified in the input. The model simply tracked the EC concentration as a conservative substance. The other form was a non-conservative EC, in which WARMF modeled individual cations and anions of water. The individual ions underwent adsorption, desorption, cation exchange with soil, and reactions. The resulting concentrations of individual ions were summed for TDS. The TDS was then converted to EC by multiplying 1.667, which is a factor found to be applicable to the water in San Joaquin River.

Three species of algae were included in WARMF. The biomass concentrations of algae species were converted to chlorophyll and summed for total chlorophyll. Sediment was represented by sand, silt, and clay fractions in WARMF. Sand was considered bed load, while silt and clay were part of suspended load. Total Suspended Sediment was the sum of silt and clay. Total Sediment included sand as well.

Model Inputs

WARMF is a dynamic watershed model. It requires six categories of input data: 1) geometric dimensions of land catchments and river segments and their elevations, 2) soil characteristics of the watersheds 3) model coefficients, 4) land uses of land catchments, 5) meteorological condition, and 6) operating condition.

The first 4 categories of data are time invariant variables, which do not change values during the model simulation. Their input values are prepared only once during model set up. The model coefficients include reaction rates and their temperature correction factors. WARMF does allow for land use changes, which can occur once every few years. In that case, WARMF uses a "warm start" procedure to run the simulation in sequence. In this procedure, WARMF uses a set of land use data to perform simulation for a period of few years. WARMF will save the results at the end of the simulation and use them as the initial condition to start the simulation for the next few years with the new land use data.

The last two categories of data are time varying. These are sometimes referred to as the driving variables. The meteorology affects the annual and seasonal variations of hydrology (i.e. dry years and wet years) and water quality (i.e. hot summers and cold winters). The operating condition includes such man-made activities as fertilizer application, reservoir releases, diversions, irrigation and waste discharges, which can be modified by management alternatives to improve water quality.

The daily values of driving variables are compiled and imported into the Data module of WARMF. During the simulation, the Data module automatically feeds these daily values to the model.

The following sections described the site specific input data for the San Joaquin River Model.

Geometric Data

The Digital Elevation Model (DEM) data available from the EPA BASIN were imported to WARMF. WARMF used the DEM data to delineate the Upper San Joaquin River Basin into land catchments and river segments. WARMF also calculated the geometric dimensions and slope of land catchments and the length and slope of river segments. River segments were further divided manually to match the delineation used by the DSM2-SJR model and the preliminary extension to the east side tributaries performed by Huckelbridge (2006). The stage-width relationships from DSM2-SJR and its east side extensions were transcribed into WARMF.

Land Use Data

Each land catchment had various land uses on its surface. The San Joaquin River watershed model was set up to have the land uses of deciduous forest, coniferous forest, mixed forest, orchard, cropland/pasture, confined feeding, rangeland, forested wetland, non-forested wetland, barren, residential, commercial/industrial, and water.

The 1980 land use shape files of the USGS were imported into WARMF. WARMF calculated the percent land use area by overlaying the shape files of land use layers with the boundaries of land catchments.

Model Coefficients

Model coefficients include such parameters as BOD decay rate, ammonia nitrification rate, algal growth rate, algal mortality rate, algal respiration rate, half saturation constants for light, nitrate, and phosphate, percent compositions of nitrogen and phosphorus for algal biomass, etc. Temperature correction factors are also included in the model coefficients to adjust the rates for

temperature, which changes dynamically with time during the simulation. WARMF already contains default values of those parameters, which were used as the initial values for the model. Their values are adjusted during the model calibration. Refer to Appendix A for details about the model coefficients adjusted during calibration.

Meteorology Data

In WARMF, each land catchment was assigned to a meteorology station. The Modesto, Manteca, and Los Banos stations were used as inputs to WARMF. Each land catchment was assigned to the nearest available station.

The meteorological data of the meteorology stations for the period of 2000 to 2007 were compiled from the California Irrigation Management Information System (CIMIS). The stations report hourly temperature, dew point temperature, wind speed, and precipitation.

There was no cloud cover data. Cloud cover was estimated from precipitation (P), average temperature (T_{ave}), and dew point temperature (T_{dew}) as follows:

When there is precipitation:

2 cm/day < P	CC = 1
1 cm/day < P ≤ 2 cm/day	CC = 0.9
0 cm.day < P ≤ 1 cm/day	CC = 0.8

When there is no precipitation:

$(T_{ave} - T_{dew}) < 4$ ˚C	CC = 0.6
4 ˚C ≤ $(T_{ave} - T_{dew}) < 6$ ˚C	CC = 0.3
6 ˚C ≤ $(T_{ave} - T_{dew})$	CC = 0

If WARMF were run with a time step longer than 1 hour, the meteorology data would be aggregated over each time step.

Air Quality and Rain Chemistry Data

Air quality was used to calculate the atmospheric dry deposition of ammonia, nitrate, and other constituents to the land and canopy surfaces. Weekly air quality data was obtained from the US EPA's Clean Air Status and Trends Network (CASTNET).

Rain chemistry data was used to calculate wet deposition falling onto the land catchment. Data for rain chemistry was compiled from the Yosemite National Park station of National Atmospheric Deposition Program (NADP). Data from this station was entered on a weekly basis for input to the WARMF model.

Boundary River Inflows

Boundary river inflows were external inputs to the model. These inputs were treated like "point sources", with data for inflow quantity and associated water quality.

Table 2.2 presents the data sources for river inflows to the watershed boundary. Major river inflows include three east side tributaries (Stanislaus River, Tuolumne River, Merced River), the

San Joaquin River at Stevinson (Bear Creek), and seven west side tributaries (Salt Slough, Mud Slough, Los Banos Creek, Orestimba Creek, Del Puerto Creek, Ingram Creek, and Hospital Creek).

The time series of daily flow, temperature, and water quality constituent concentrations of the boundary river inflows were compiled from available data sources for input to WARMF model. The data period of interest was water years 2000 to 2007. For this period, daily flow data was available for all river inflows except Hospital Creek and Ingram Creek. For these two creeks, the inflows were synthesized as described in notes 6 and 8 of Table 1.2.

Water quality data was not available on a daily basis. Data availability for water quality varied considerably among stations and water quality constituents. Available data was used to create daily concentrations for an average year for each constituent at each location. For each month, average concentrations were calculated based on all the data available for that month from 1984 through 2007. If no data was ever collected in a particular month, its value was interpolated from other monthly averages. Those average values were then assigned to the 15th of each month and then the values were interpolated between those days to generate the concentration for each day of the year.

For certain time periods and stations, electrical conductivity was measured but not individual ions. The measured EC in μs/cm was divided by 1.67 to become total dissolved solids (TDS). The individual ion concentrations are scaled up in equal proportion so that their sum matched the TDS calculated from EC. If alkalinity was measured, the cations were multiplied by one factor and anions by the other factor to simultaneously match the measured values of EC and alkalinity.

Table 1.2
Data Sources for Boundary River Inflows

Upstream Boundary	Source of Flow Data	Source of Water Quality Data
Stanislaus River at Tulloch Dam	Stanislaus River at Ripon	Stanislaus River at Caswell S.P. Stanislaus River at Goodwin Dam Stanislaus River at Ripon[1]
Tuolumne River at Don Pedro Dam	Tuolumne River at Modesto	Tuolumne River at Shiloh Road Tuolumne R. below LaGrange Dam[2]
Merced River at New Exchequer Dam	Merced River near Stevinson	Merced River near Stevinson
San Joaquin River at Bear Creek	San Joaquin River near Stevinson	San Joaquin River near Stevinson
Salt Slough at Confluence with SJR	Salt Slough at Highway 165	Salt Slough at Highway 165
Mud Slough at Confluence with Los Banos Creek	Mud Slough near Gustine	Mud Slough near Gustine
Los Banos Creek at Confluence with Mud Slough	Los Banos Creek at HWY 140[3] Mud Slough near Gustine	Los Banos Creek at HWY 140[4]
Orestimba Creek at Confluence with SJR	Orestimba Creek at River Rd	Orestimba Creek at River Road
Del Puerto Creek at Confluence with SJR	Del Puerto Creek at Vineyard Road	Del Puerto Creek at Vineyard Road[5]
Ingram Creek at Confluence with SJR	Ingram Creek[6] Del Puerto Creek at Vineyard Road	Ingram Creek[7] Del Puerto Creek at Vineyard Road
Hospital Creek at Confluence with SJR	Hospital Creek[8] Del Puerto Creek at Vineyard Road	Hospital Creek[9] Del Puerto Creek at Vineyard Road

1 A complete set of data was not available from a single location. Caswell State Park was used for nutrients, organic carbon, and algae. Goodwin Dam was used for major cations and anions. Ripon was used for suspended sediment and electrical conductivity.

2 A complete set of data was not available from a single location. Shiloh Road was used for nutrients, organic carbon, algae, and sediment. LaGrange Dam was used for the major cations and anions.

3 Flow data was only available for 2005. Previous years were estimated by starting with Mud Slough flow and adjusting with monthly average flow multipliers

4 Major cations and anions were estimated from EC and ion ratios for west side tributaries for which there is data; suspended sediment concentrations were copied from Mud Slough data.

5 Major cations and anions were estimated from EC and ion ratios for west side tributaries for which there is data.

6 Flow data was only available for 6/15/2005-12/31/2005. Flow was estimated by multiplying Hospital Creek flow by a common factor for 5/17/2005-6/14/2005. Flow from 5/17/2005

through 12/31/2005 was copied to previous years. For wet season when there was no data (1/1-5/16), flow data for Del Puerto Creek was copied and scaled based on the ratio of watershed area between Del Puerto Creek and Ingram Creek.

7 Major cations and anions were estimated from EC and ion ratios for west side tributaries for which there is data; suspended sediment concentrations were copied from Del Puerto Creek data.

8 Flow data was only available for 5/17/2005-12/31/2005. Flow from 5/17/2005 through 12/31/2005 was copied to previous years. For wet season when there was no data (1/1-5/16), flow data for Del Puerto Creek was copied and scaled based on the ratio of watershed area between Del Puerto Creek and Hospital Creek.

9 Major cations and anions were estimated from EC and ion ratios for west side tributaries for which there is data; suspended sediment concentrations were copied from Del Puerto Creek data.

Point Source Discharge Data

The Modesto Water Quality Control Facility is the only point source discharge in the upstream watershed. Its daily flow and associated water quality concentrations were compiled from the EPA Pollution Control System (PCS) database for input to WARMF. The Stockton Water Pollution Control Facility discharges to the estuary portion of the river upstream of the DWSC. Its discharge data as compiled in the San Joaquin River Data Atlas was used to update the Link-Node point source file.

Agricultural Drains and Spills Data

The is data available for 14 agricultural canals and drains that discharge water to the Upper San Joaquin River. The water quality of these discharges depending on the water source: in some cases the discharges are of excess delivery water while other discharges are of drainage from agricultural lands. There are 4 discharges from the Modesto Irrigation District (MID), 6 from the Turlock Irrigation District (TID), and 4 drains on the west side of the San Joaquin River. They are distributed along the San Joaquin River from the Merced River to the Stanislaus River and along the lower reaches of the east side tributaries. The TID Harding Drain includes the discharge from the City of Turlock Wastewater Treatment Plant.

Available flow data were used to create the input data of agriculture drains and spills. To the extent possible, daily flow data were compiled and used. Monthly average flows were interpolated for periods without measured data. Some drains have EC data, which were converted to TDS and then used to estimate the concentrations of cations and anions. The ratios of the various ions were taken from the applicable irrigation water source: the Tuolumne River for MID and TID and the Delta-Mendota Canal for the west side drains. Some drains have one or more measurements of nutrients. These measured concentrations were used as the daily concentrations for input to WARMF. When there is no measured value for a drain, the average concentration of nearby drains was used.

Fertilizer Application Data

Fertilizer was applied to Orchard and Cropland/Pasture land uses in WARMF. The application rates were:

Orchard: 14.5 kg/ha/month nitrogen, ½ as ammonia and ½ as nitrate, from April 15 through October 15
4 kg/ha/month phosphorus, from April 15 through October 15
Cropland/Pasture: 2.1 kg/ha/month nitrogen, ½ as ammonia and ½ as nitrate, all year
1.4 kg/ha/month phosphorus, all year

Irrigation Water

Irrigation from 11 districts was simulated in the WARMF San Joaquin River model. Where the district boundaries overlapped the land catchment boundaries, irrigation water was applied to the land in the model. The irrigation waters were diverted from various sources shown in Table 1.3.

Table 1.3
Sources of Irrigation Water

Irrigation District	Water Source
South San Joaquin Irrigation District	Stanislaus River
Modesto Irrigation District	Tuolumne River
Turlock Irrigation District	Tuolumne River
Central California Irrigation District	Delta-Mendota Canal
Del Puerto Water District	Delta-Mendota Canal
Oak Flat Water District	Delta-Mendota Canal
Patterson Water District	San Joaquin River
West Stanislaus Irrigation District	San Joaquin River
El Solyo Water District	San Joaquin River
Banta-Carbona Irrigation District	San Joaquin River
Plain View Water District	Delta-Mendota Canal

The locations of diversions from the San Joaquin River are shown with white dots in Figure 1.3. Available diversion data is summarized in Table 1.4. The irrigation districts which diverted from various locations on the San Joaquin River had their diversion points within the model domain, and thus were simulated dynamically by WARMF. During the model simulation, WARMF diverted the quantity of irrigation waters from their respective diversion points and uses the simulated water quality for the irrigation water.

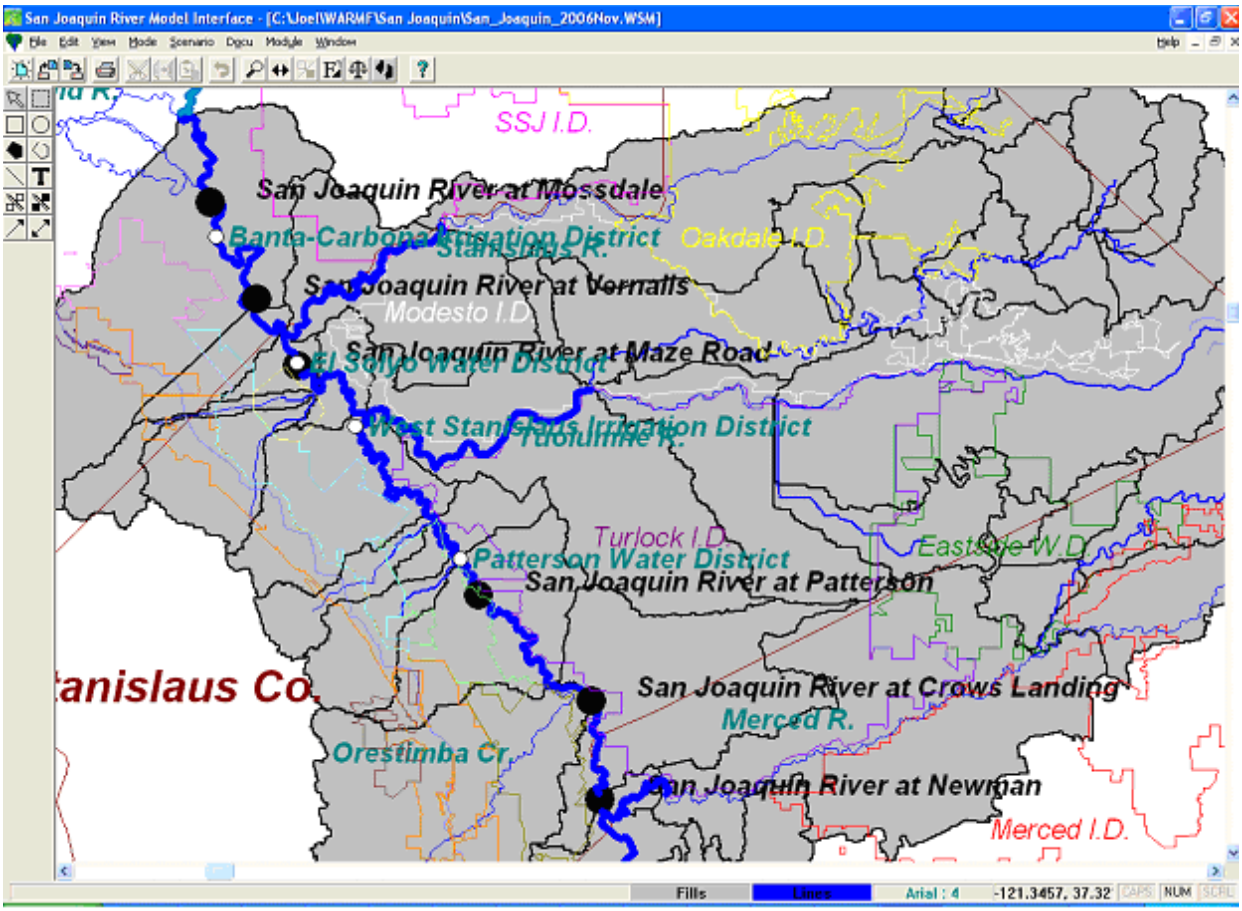

Figure 1.3 Locations of District Diversions from the San Joaquin River

Table 1.4
Diversions of Irrigation Water from San Joaquin River

Diversion	Data Available	Average Flow, cfs
Patterson Water District	2000-2005: monthly measured flow 2006: daily measured flow 2007: copied from 2004	54
West Stanisluas Irrigation District	2000-2004: monthly averages of 2005 2005-2007: daily measured flow	108
El Solyo Water District	2000-2004 estimated from SJRIO 2005-06: monthly delivery + 15% loss 2007: copied from 2004	20
Banta-Carbona Irrigation District	2000-2006: daily flow data 2007: copied from 2004	70

The sources of irrigation water allow us to estimate the quality of water applied to the crop. The water quality of the Delta-Mendota Canal was taken from measurements of nutrient and individual ion concentrations. EC data collected from the canal was used to scale the concentrations of all the individual ions up or down.

The water quality of the irrigation water for Modesto and Turlock Irrigation Districts was estimated from water quality data of the Tuolumne River. The water quality of the irrigation water for South San Joaquin Irrigation District was assumed to be the same as for the Modesto and Turlock districts.

The irrigation rate was assumed to be proportional to the diversion of each irrigation district. The diversions typically follow a seasonal pattern: near zero before February, increasing until midsummer, and then decreasing until November. The cumulative amount irrigation was 4 feet per year.

At a stakeholder outreach meeting in Modesto on October 18, 2006, representatives of the Modesto and Turlock Irrigation districts brought to our attention the existence of riparian diversions. Farms with their farm lands adjacent to rivers but outside of the irrigation district can draw water from the river for irrigation. These diversions are not measured, so they must be estimated. The flow was estimated by calculating the irrigated acreage not served by irrigation districts for each land catchment and then applying a typical irrigation rate. The white dots in Figure 1.4 show the locations where estimated riparian diversions were removed from the San Joaquin River and its tributaries.

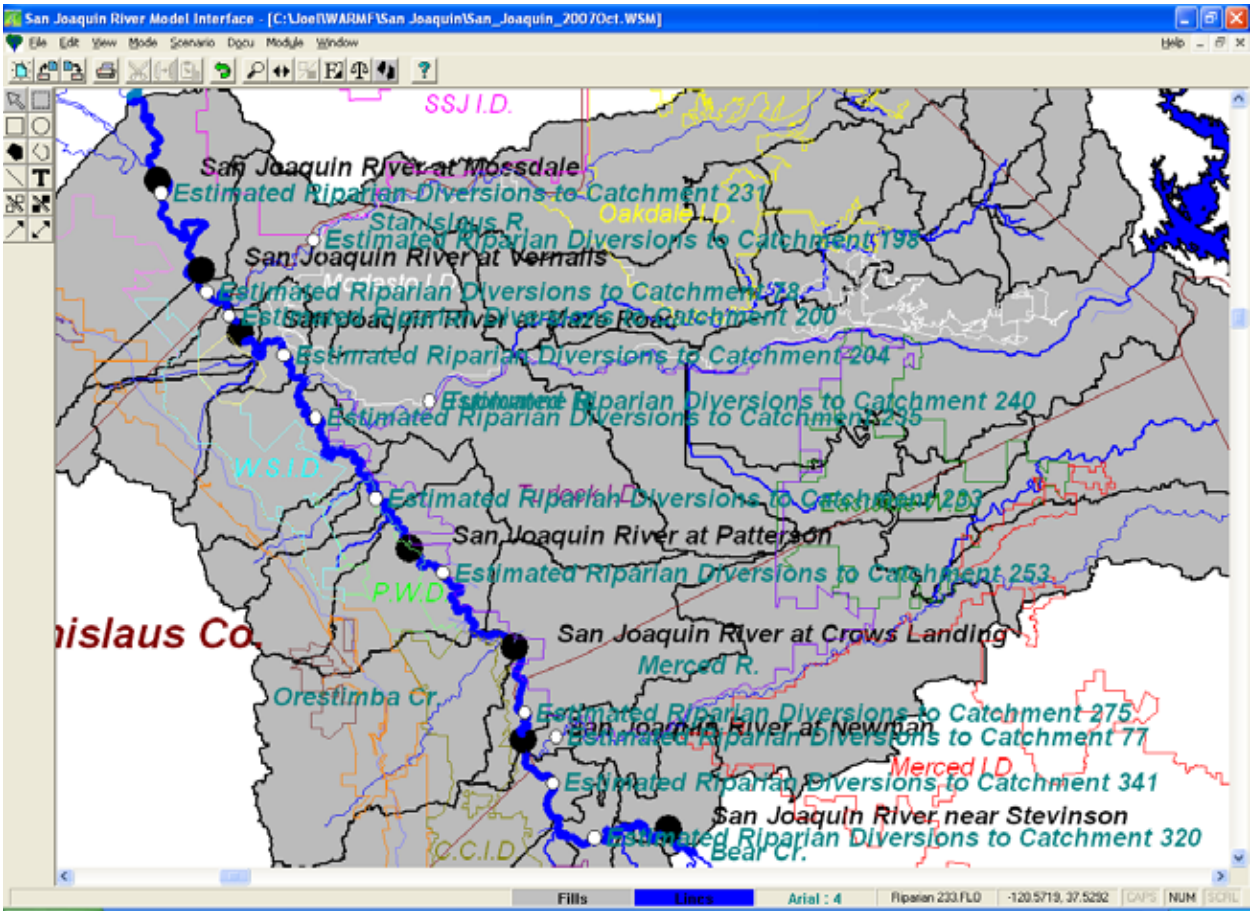

Figure 1.4 Locations of Estimated Riparian Diversions from the San Joaquin River

DOWNSTREAM ESTUARY MODEL

Model Set Up

The Link-Node estuary model was set up prior to the San Joaquin River DO TMDL upstream studies for the Lower San Joaquin River extending from Light 18 of the DWSC to the junction with the Old River (near Mossdale). The model domain included French Camp Slough, Mormon Slough, Smith Canal, the Turning Basin, Burns Cutoff, the lower Calaveras River, Fourteen Mile Slough, and Turner Cut as shown in Figure 1.5.

The Link-Node model divided the estuary water body into a series of nodes, shown in red. Nodes are linked by channels. Nodes are numbered in the Link-Node model. Node 1 was the upstream boundary that receives river inflow from the Upper San Joaquin River. Nodes 70, 94, and 96 were the downstream boundaries that accepted tides as input. Nodes 30, 40, 44, 59, 60, 61, 91, 92, 95, and 96 were the DWSC.

The model performed a hydrodynamic simulation to calculate the tidal flows in the channels and the tidal elevations at nodes with a time step of 1 minute. The hydrodynamic solutions are integrated to hourly results. The water quality simulation is then performed to calculate temperature and concentrations of various water quality constituents in nodes.

As described earlier, the Link-Node model was originally developed for USEPA. Improvements have been made since its delivery to the USEPA. The model was modified to accept real time tides to follow the natural spring tide and neap tide cycles. The model could therefore perform real time hydrodynamic and water quality simulation for the entire period of simulation over several years, unlike the USEPA version that can only perform simulation over few tidal cycles to reach a dynamic steady state. An anti numerical dispersion algorithm was added to reduce the numerical dispersion typically found in the Link-Node model, which uses an Euler grid system. The model was modified to simulate multiple water quality parameters simultaneously, unlike the original version that could only simulate a conservative substance and a non-conservative substance. The model implemented a tidal exchange algorithm to simulate the concentrations of water quality parameters entering the tidal boundary during the flood tides, unlike the original version that used a constant concentration value.

The Link-Node model as applied to the Lower San Joaquin River Estuary has been documented in Shanz and Chen (1993) and Chen and Tsai (2002). The user's manual has been prepared by Chen and Tsai (2002).

The Link-Node model is a DOS based simulation model. In this project, the Graphical User Interface was developed to allow user to run the Link-Node model through Windows. Due to budget limitation, model inputs for Link-Node can not be modified through the Interface, but simulation results are displayed by point-and-click on the map.

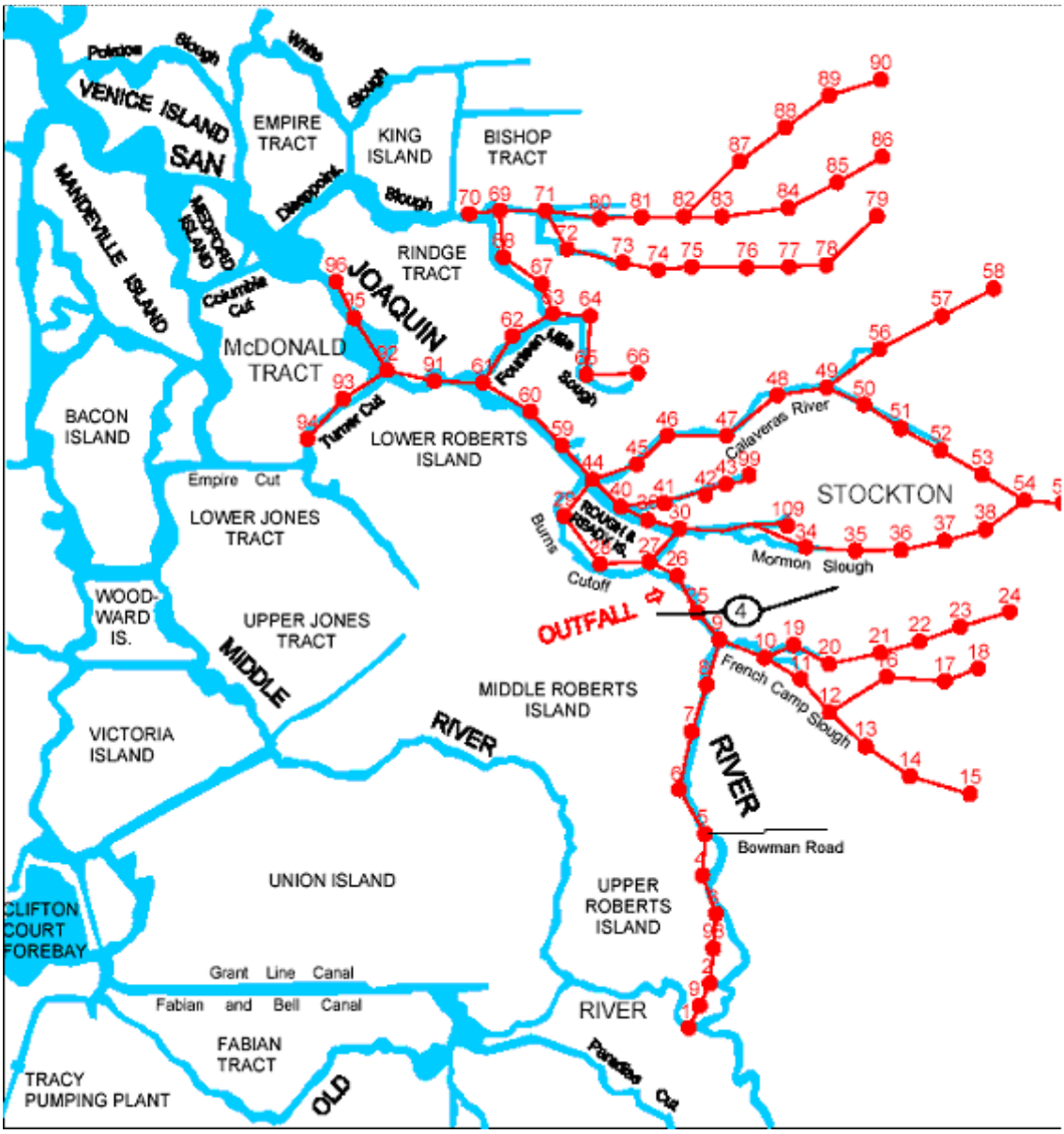

Figure 1.5 Link-Node Model Domain

The Link-Node model is a receiving water quality model. It was set up to receive the point source load of the Stockton Regional Waste Water Treatment Plant at Node 26, where there is an arrow for "OUTFALL", as shown in Figure 1.5. It did not simulate the watershed processes of runoff from the land adjacent to the estuary.

Simulated Parameters

The Link-Node model simulated a host of variables necessary to predict dissolved oxygen, oxygen consuming materials, algal growth and respiration. Hydrologic parameters included

flow, water depth, and flow velocity. Water quality parameters included temperature, ammonia, nitrate, phosphate, BOD, dissolved oxygen, algae, and phaeophytin (dead algae).

The compatibility of variables between WARMF and Link-Node models is compared in Table 1.1. Generally speaking, they were quite compatible. The compatibility allowed the graphical Interface to translate the output of WARMF model to the input of Link-Node model.

Model Inputs

The model inputs for the Link-Node model were previously prepared for the conditions of 1991-1992 and 1999-2000. In order to run both WARMF model and Link-Node model together, it is necessary to update the input data of the Link-Node model to the same periods of simulation or 2000 to 2007. The Link-Node simulations in the new time period showed a good match to observed data for some parameters and some locations, but needed recalibration to improve the simulation in other areas. Brown (2002) noted that some adjustments of the model coefficients may be needed to account for higher mortality of algae from the Old River confluence to the channel point. One change was made to Link-Node coefficients, increasing the phytoplankton settling rate to 1 m/d to match the settling rate used by WARMF in the relatively quiescent reaches of the upstream San Joaquin River between the Stanislaus River and the Old River.

The Link-Node model coefficients originally had single values for reaction rates which applied over the entire Link-Node model domain. The model has been upgraded to allow for different reaction rates in different nodes. With this change, the model is better able to simulate the different processes which occur in the DWSC versus the San Joaquin River upstream of Channel Point.

The following sections describe various input data that have been updated in this project.

Update of Meteorological Data

The Link-Node model used hourly meteorology data recorded at Stockton. The data included temperature, dewpoint temperature, cloud cover, air pressure, and wind speed. The data was updated for years 2000 to 2007.

Update of River Inflow Data

The Link-Node model required the river inflow data from the Upper San Joaquin River. This river inflow was the flow at Vernalis less the diversion through the Old River to Tracy export pumping station. During the early model development in the 1990s, the diversion to the Old River was estimated by two DWR empirical equations, depending on whether the temporary barrier at the head of Old River was up or not. It was found that the empirical equations were not accurate.

We recommended to the City of Stockton to sponsor the installation of a gaging station at Garwood Bridge by the USGS. The USGS has since posted the measured the tidal velocity and tidal flow for the station on their website on a regular basis with a time delay of about 30 days. The use of measured flow as input to the model substantially improved the model predictions.

The gaged flow for 1991-1992 and 2000 had already been compiled for input to the Link-Node model. For this project, the gaged flow at the Garwood Bridge was updated to 2000 to 2007.

Due to the lack of an accurate method to calculate the diversion to the Old River, the WARMF output of flow at the Old River confluence can not be used directly. The Interface has been programmed to ignore the WARMF output of flow and to use the gaged flow instead. The water quality output of WARMF was translated to the water quality of the gaged river inflow according to Table 1.1.

Update of Point Source Data

The Stockton Regional Wastewater Treatment Plant is the only point source discharge to the lower San Joaquin River estuary. The point source data of flow, temperature, ammonia, nitrate, phosphate, BOD, DO, TDS, algae, and sediment in the effluent was updated for years 2000-2007.

Update of Tidal Data

There were three tidal boundary locations at Light 16 (Node 96), Tiki Lagoon on Turner Cut (Node 94), and Paradise Point on Disappointment Slough (Node 70). The tidal elevation data for those nodes was updated for the years 2000 to 2007.

The Link-Node model requires the water quality of background water outside of the tidal boundaries. The background water quality is updated for the years 2000 to 2007, using the water quality data monitored at the City of Stockton's monitoring station R8. The reason is that the water sample collected during the flood tides at station R8 may simply represent the background water.

The background water quality was used by the Link-Node model to calculate the water quality for the parcels of water entering the tidal boundary nodes during the flood tide. During the ebb tide, the model used the simulated water quality of the tidal boundary nodes to export the mass of pollutants outside of the tidal boundaries. The parcels of water that exited the tidal boundaries were tracked. The model uses a tidal exchange algorithm to calculate the exchange of the water parcels with the background water as a function of time. The water quality of the water parcels was returned back to the estuary system during the flood tide.

MODEL CALIBRATION

Calibration Procedure

Given meteorological and operational data, the San Joaquin River Model made predictions for stream flow and water quality at various river segments. At locations where monitoring data was collected, the model predictions should match the measured stream flow and water quality. Initially, some model coefficients, such as physical properties of the watershed, are known. Other coefficients are left at default or typical literature values. The initial predictions made did not necessarily match the observed values very well. Model calibration was performed by

adjusting model coefficients within reasonable ranges to improve the match between model predictions and observed data.

The model predictions and observed data were compared graphically. In the graph, the time series of model predictions were plotted in a curve on top of measured data. If the observed values fell on top of the curve, the match could be determined as good or poor by visual inspection.

The model predictions and observed data were also compared statistically. The differences between the predicted and observed values are errors. The magnitudes of the errors were calculated in the statistical terms of relative error, absolute error, root mean square error, and correlation coefficient.

Both graphical and statistical comparisons were made with WARMF. WARMF has a scenario manager, where each scenario is a set of model input coefficients and corresponding simulation results. Scenario 1 may be used to represent a set of numerical values of model coefficients used in the simulation. Scenario 2 may be used to represent a second set of modified model coefficients used in the simulation. After the simulation, WARMF can plot the observed data as well as the model predictions for both scenarios on the same graph. By visual inspection, it is relatively easy to see whether the changes to model coefficients improve the match.

Likewise, WARMF calculates the values of various error terms for the model predictions. The comparison of the numerical values of errors for two scenarios can lead the user to adjust the model coefficients in the right way to reduce the errors.

Model calibration followed a logical sequence. Hydrological calibration was performed first, because an accurate flow simulation is a pre-requisite for accurate water quality simulation. The calibrations for temperature and conservative substances were performed before the calibration of nutrients (phosphate, ammonia, and nitrate), algae and dissolved oxygen concentrations.

Only a few model coefficients were adjusted for each calibration. For hydrological calibration, the boundary river inflows were checked for their accuracy as discussed in Chapter 2 of this report. Evapotranspiration coefficients, field capacity, saturated moisture, and hydraulic conductivity are then adjusted so that the simulated agricultural return flow and groundwater accretion can account for flow changes between the monitoring stations. For water quality calibration, the growth rate and half saturation constants of algae have been measured in the field program. The measured values were used to replace the default values contained in WARMF.

After submission of the Calibration Report (Herr and Chen 2006a), riparian diversions were added to WARMF in response to feedback from the Modesto and Turlock Irrigation Districts. A review of the model performed by Flow Science (List and Paulsen 2008) recommended several improvements to the calibration. The calibration was modified in response to this feedback.

Hydrologic Calibration

Simulated Years

Since the field data were collected in 2000 to 2007, the calibration period discussed in this report extends from 10/1/1999 to 9/30/2007. The first six years, 2000-2005, were used for model calibration. 2006 and 2007 were used for model verification to determine the predictive power of the model for time periods not previously simulated. Table 1.5 presents the average annual flows for the water years 2000 to 2007 at Vernalis. The table also shows the percentile of the annual flows based on the flow records of 1984 to 2007.

Table 1.5
Average Annual Flows at Vernalis for Water Years 2000 to 2007

Water Year	Average Flow at Vernalis, cfs	Percentile (based on 1984-2007)
2000	3,920	62
2001	2,390	48
2002	1,930	38
2003	1,920	33
2004	1,890	29
2005	5,230	71
2006	10.153	96
2007	2.198	39

Year 2000 was a wet year at 62nd percentile. Year 2005 was also a wet year at 71st percentile, while 2006 was the second wettest in the 24 year record analyzed. 2003, 2004, and 2007 were dry years at 29th percentile and 33rd percentile respectively. Year 2001 was a normal year at the 48th percentile. It appears that the San Joaquin River has not experienced any critically dry years since the drought of 1988-1992.

Ideally, field data should be collected in a variety of wet and dry years. However, the field investigators had no control over the natural meteorological and hydrological variability. Model calibration must be performed for the period that the field data were collected.

Even though there is a lack of extreme dry and wet years, the years of simulation cover a variety of flow conditions ranging from 29th percentile to 96th percentile. The middle ground hydrologic conditions can serve as the base case to evaluate management alternatives for TMDL analysis. The meteorological conditions of extreme dry years or wet years can be used to drive the calibrated model to predict the water quality conditions of extreme years.

Time Series Output

In the graphs that follow, simulation results are shown in blue lines and observed data in black circles. Ideally, the blue lines pass through all the black circles, but that does not always occur because of a combination of model error, data error, and data measurement uncertainty.

Hydrologic Calibration Results

There are three levels of hydrologic calibration: global, seasonal, and event. Global means that the simulated annual volume of water passing a gage is the same as the volume measured. Seasonal means that the simulated seasonal variation of hydrology follows the same pattern of measured hydrograph. The measured hydrograph typically has a high flow during the rainfall season and a recession to base flow during the dry season. Event means that the simulated peak flows match the observed peaks during precipitation events.

There were seven gaging stations along the San Joaquin River where simulated flow can be compared against observed data. Figure 1.6 through Figure 1.12 show the comparison of simulated and observed hydrographs for Stevinson (Lander Ave.), Fremont Ford, Newman, Crows Landing, Patterson, Maze Road, and Vernalis.

In these plots, the simulated results are shown in blue lines and the observed data is in black circles. The good match between the model predictions and flow measurements collected in the field program is evident. The plots demonstrate that WARMF can simulate the agricultural return flow and groundwater accretion to the river from irrigated lands reasonably well. No artificial “add water” term was used to make up the difference between simulation results and observed data. The simulations do show brief peak flows from storm events lasting less than one day much greater than the daily average measured data.

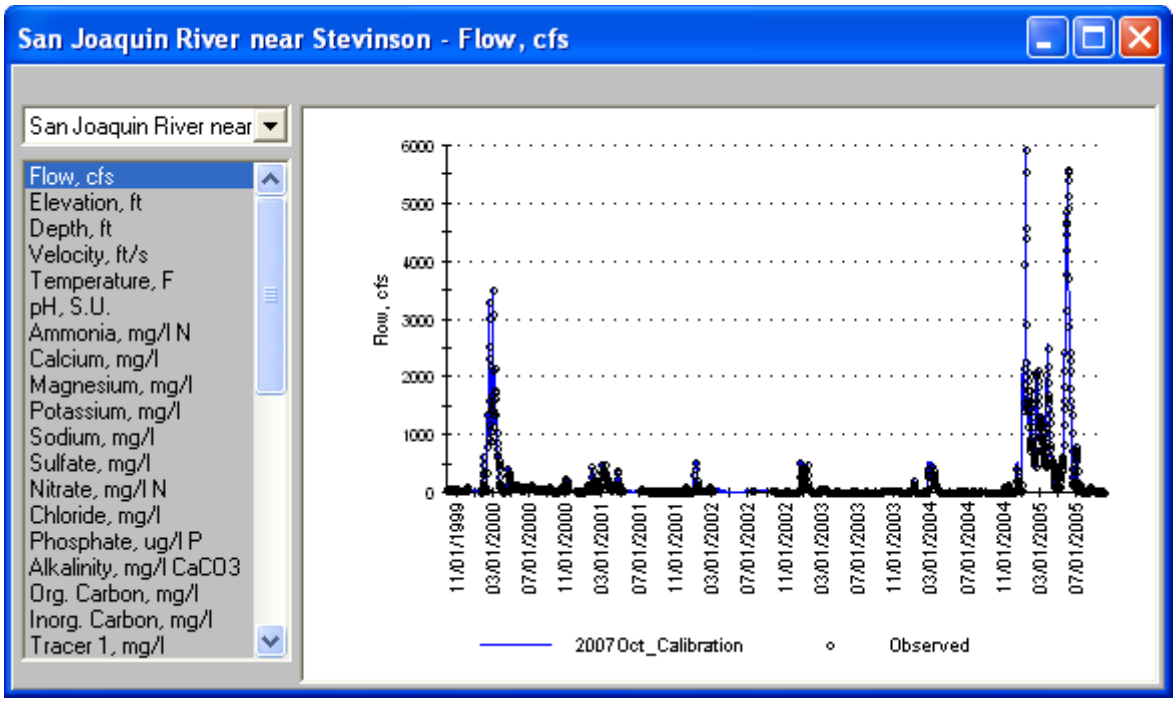

Figure 1.6 Simulated vs Observed Flow at Stevinson (Lander Ave.)

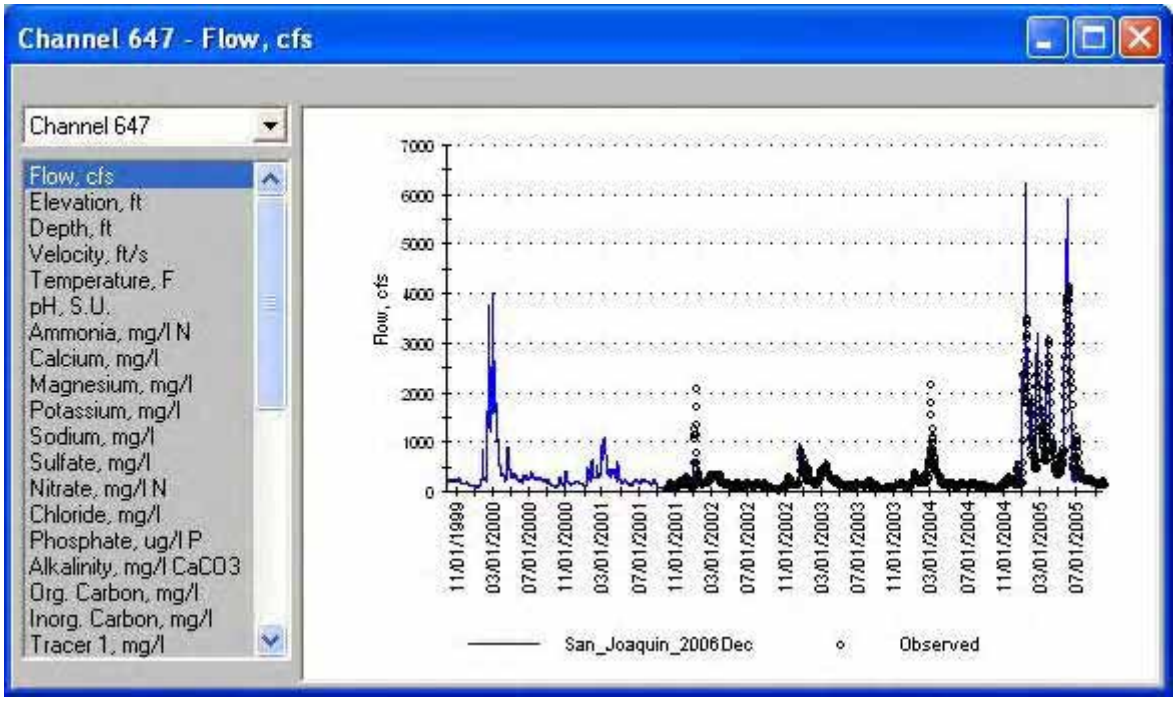

Figure 1.7 Simulated vs Observed Flow at Fremont Ford

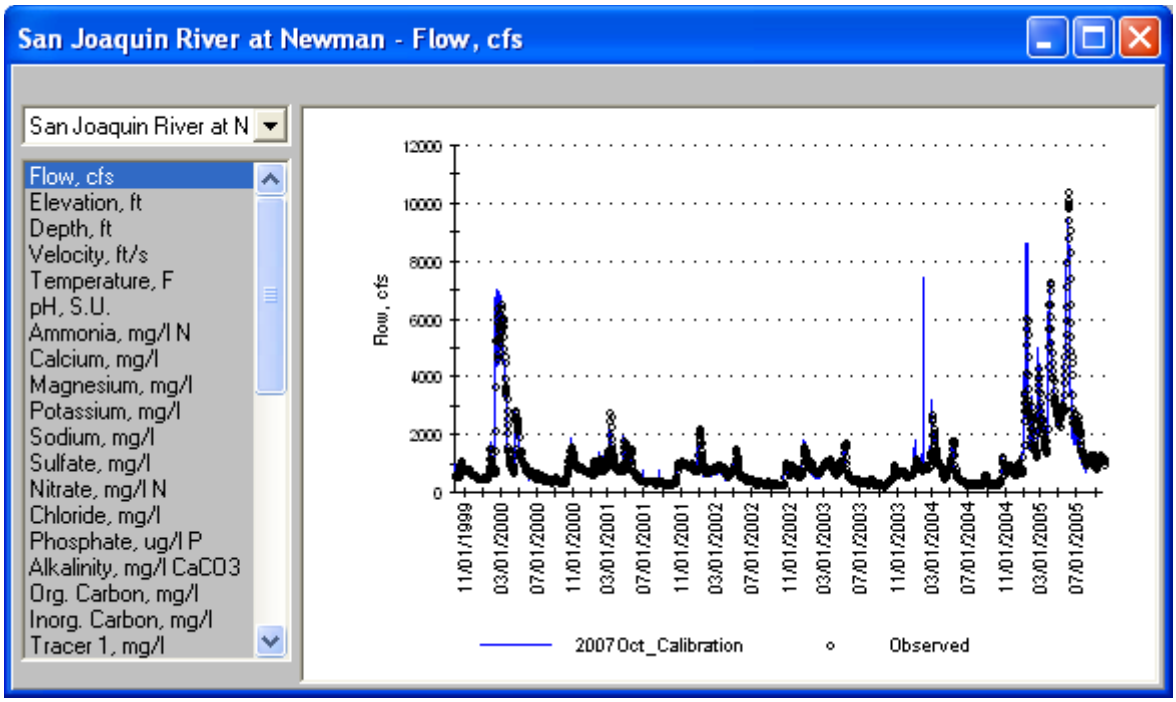

Figure 1.8 Simulated vs Observed Flow at Newman

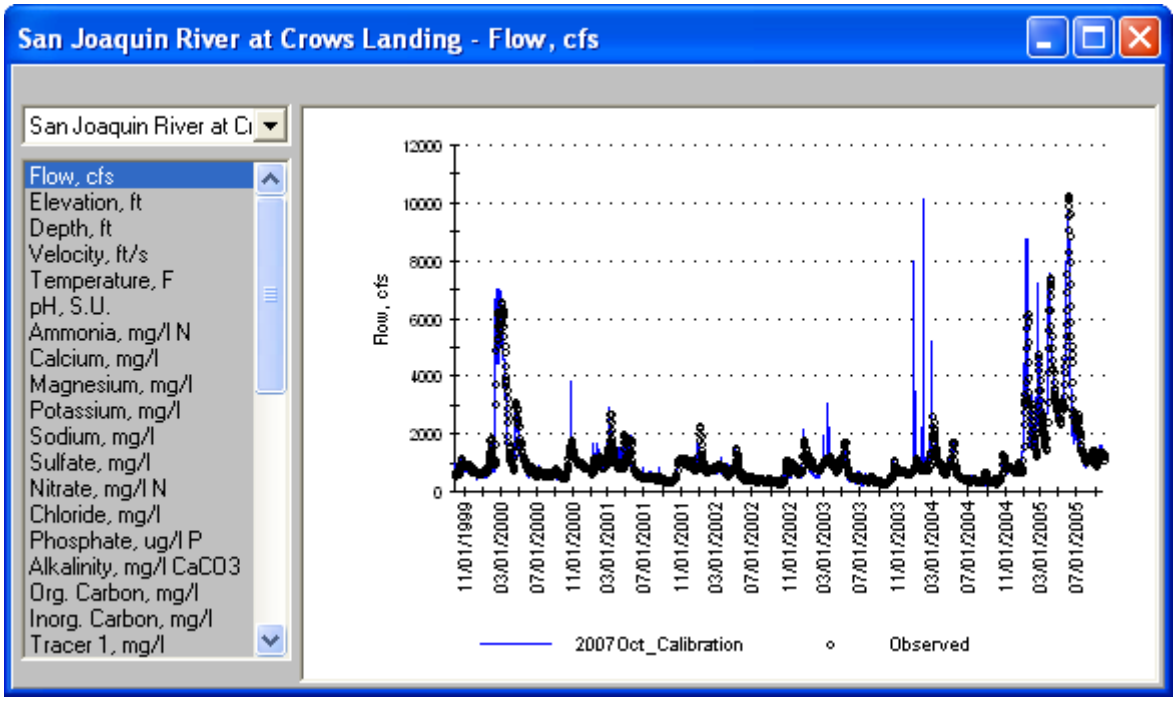

Figure 1.9 Simulated vs Observed Flow at Crows Landing

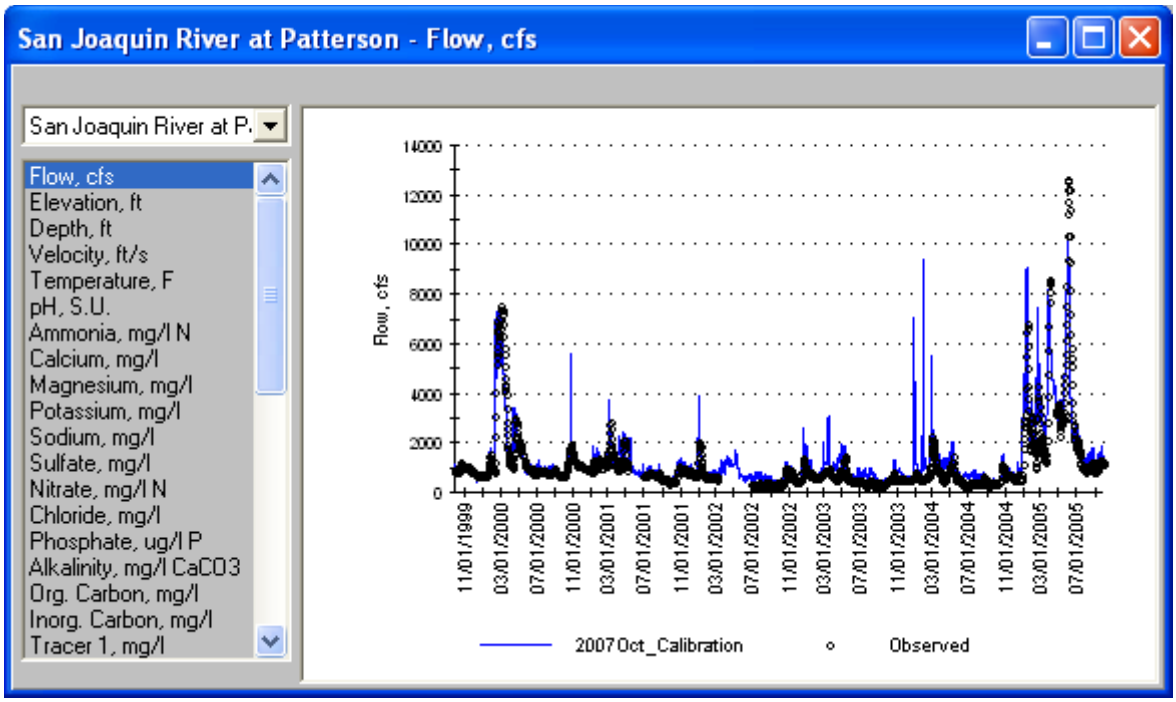

Figure 1.10 Simulated vs Observed Flow at Patterson

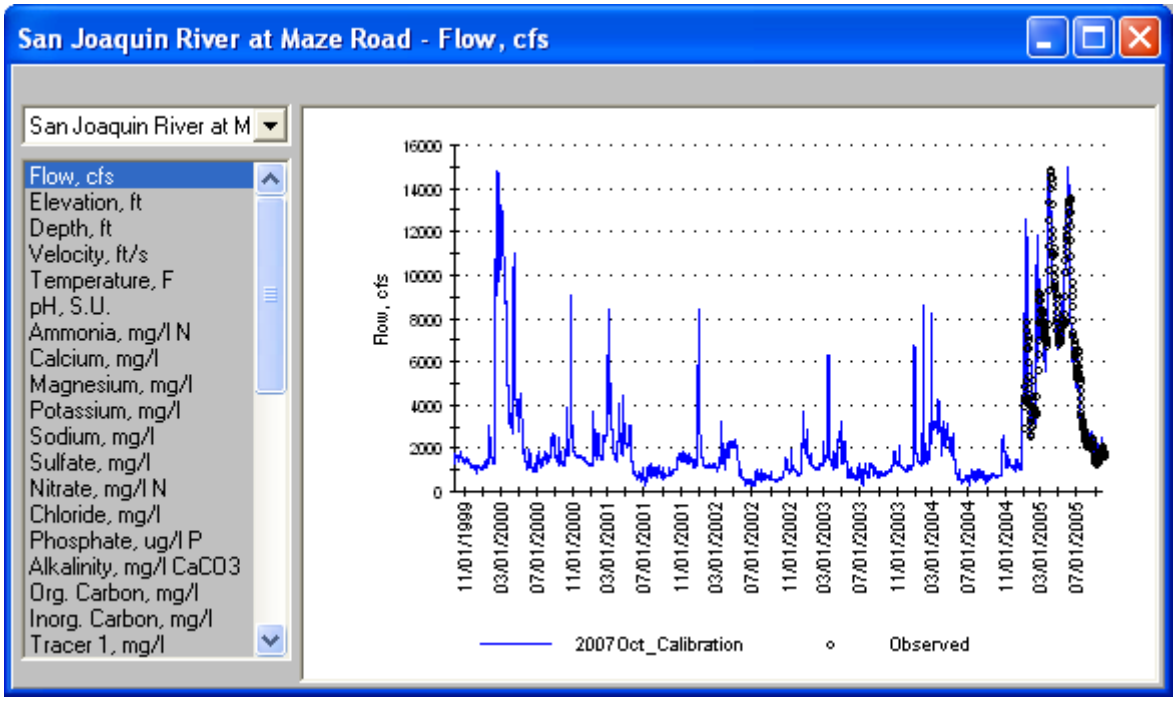

Figure 1.11 Simulated vs Observed Flow at Maze Road

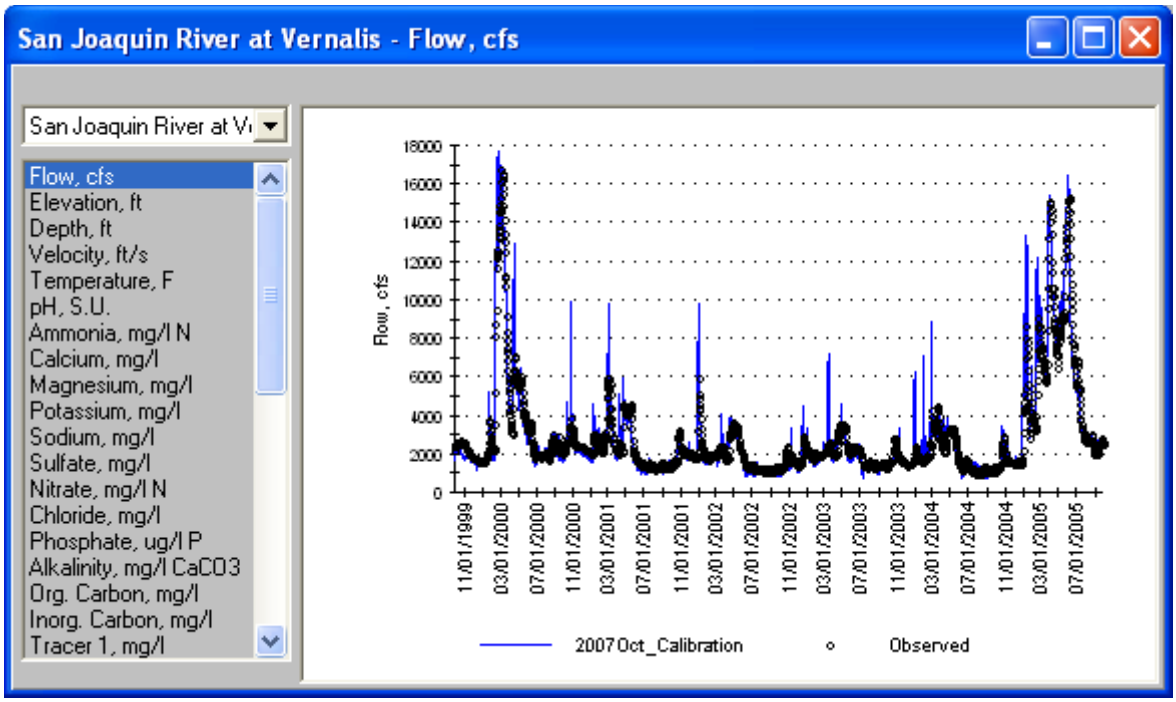

Figure 1.12 Simulated vs Observed Flow at Vernalis

Table 1.6 provides the summary statistics of model errors, assuming the measured flows are accurate. Relative error is the average of the deviations between simulated and observed. Absolute error is the average of the absolute differences between model predictions and observations. The goal of calibration is to have the relative error below 5% and the absolute error below 10%. These values are believed to be within the accuracy of instruments used to measure the flow.

Table 1.6
Statistics of Model Errors for Flow Simulation

Gaging Station	Relative Error	Absolute Error
Stevinson	+1%	18%
Fremont Ford (data begins 10/2001)	+2%	18%
Newman	-6%	11%
Crows Landing	0%	11%
Patterson	+15%	27%
Maze Road (data begins 1/2005)	-2%	11%
Vernalis	-1%	13%

The relative errors were very good for all the gages except Patterson. After the model was initially calibrated and the discrepancy at Patterson was presented, investigators went to the field to determine if the error could have been in the flow measurement. It was determined that indeed the stage-flow relationship at the Patterson gage was not correct.

An important point to make here is that the WARMF model pointed out the discrepancies between model predictions and observed data. A similar situation has occurred when the

SJRIODAY model was used to estimate the agricultural return flows, which led to the need of "add water" to account for missing water in the DSM2-SJR model. These discrepancies prompt the investigators to find out the reason for the discrepancies. The reason for the "add water" was found to be the inaccuracy of SJRIODAY model. The discrepancy of simulated and observed flows at the Patterson gage remains to be investigated and corrected later in this project.

Travel Time

In addition to correct predictions of time varying stream flows at given locations as discussed in the section above, the model must also simulate the travel time of water between stations along the San Joaquin River. The time required for water to flow downstream is important for determining the extent of chemical decay, algal growth and nutrient uptake that can take places in the river. The travel time predictions can be compared to the travel times measured by tracer studies.

The travel time is defined by dividing the river length by the averaged flow velocity. Velocity is the flow rate divided by the cross-sectional area of the river. The key in modeling velocity correctly is having good river cross-section data and good simulation of water depth (and therefore the cross-section area) as a function of flow. Previous works on the extension of DSM2 to the Upper San Joaquin River provided good cross sectional area data for WARMF to use (Pate 2001, Wilde 2005, and Huckelbridge 2006). WARMF uses the kinematic wave method for flow routing, which uses mass balance of water and Manning's equation to calculate the depth correctly.

The travel time was simulated by adding a spike of virtual tracer to the model and then tracking the peak concentration of that spike as it moves downriver. The tracer was added to the river at Lander Avenue on the first day of each month. The simulation was performed on an hourly time step. The simulation results were analyzed to determine travel time.

Figure 1.13 shows the travel time down the San Joaquin River as a function of flow at Vernalis. Note that for a given flow at Vernalis, the travel time was highly dependent upon the flow in individual tributaries.

The very long travel times were for periods when there was very little flow in the San Joaquin River at Lander Avenue. Under summer low flow conditions, it took approximately three to four days for the water to travel down the San Joaquin River from Lander Avenue to Vernalis, and one additional day to reach the Old River.

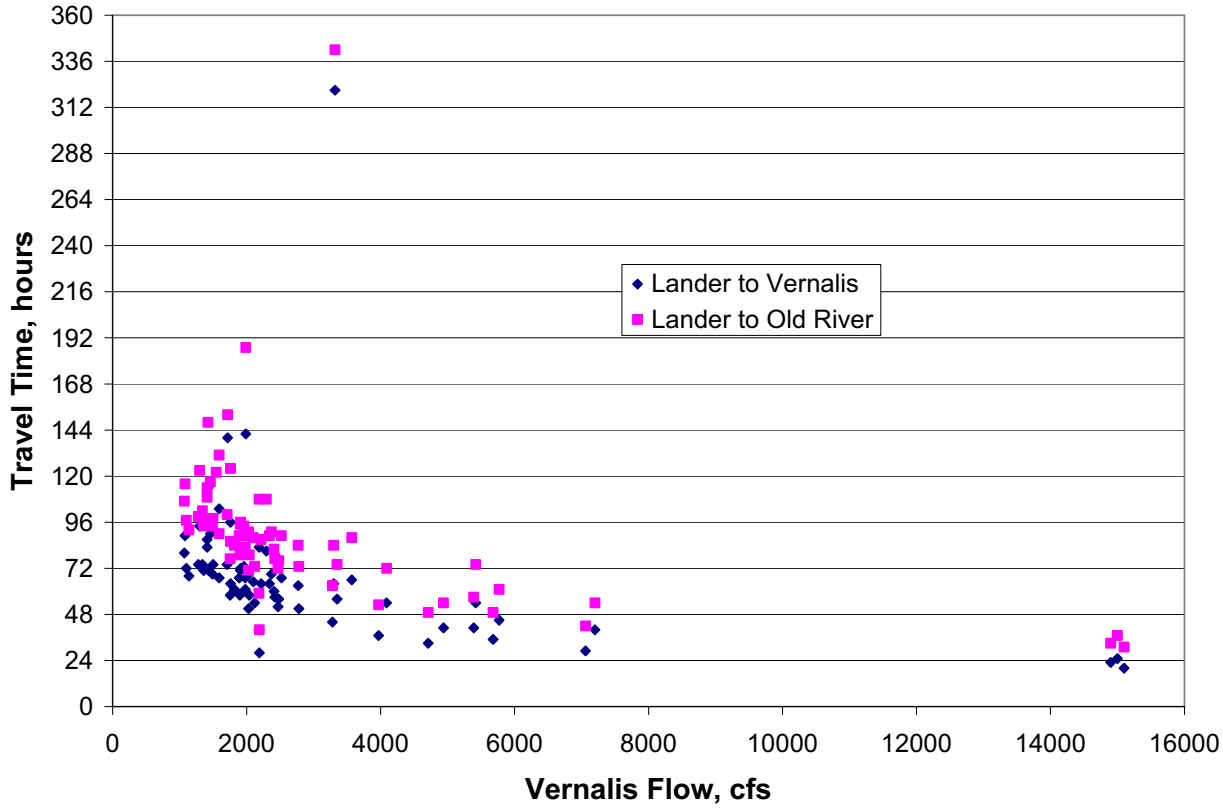

Figure 1.13 Simulated Travel Time from Lander Avenue to Vernalis and Old River

A field tracer study was conducted under two different flow regimes in 1994. The first test put dye in the Merced River near Stevinson on February 9th when the flow at Vernalis was approximately 2,800 cfs (high flow). It took 38 hours for the dye plume to reach Vernalis. In the second test, dye was added to the San Joaquin River at its confluence with Salt Slough on June 20th, when the flow at Vernalis was about 1,000 cfs (low flow). The dye took 74 hours to reach Vernalis (Wilde 2005).

The model predicted a wide range of residence time as a function of river flow at Vernalis. The times the tracer studies were conducted are not within the model simulation period. To compare simulation results against the tracer studies, similar flow regimes must be found during the simulation period matching the historical flow in the San Joaquin River and its major tributaries when the tracer studies were conducted. Table 1.7 shows the historical flow for the two tracer studies in 1994 and the times during the simulation period whose flow regimes most closely matched those in the tracer studies. August 1, 2005 was used to compare against the high flow tracer study and August 1, 2004 was compared with the low flow tracer study.

Table 1.7
Flows Used for Comparison of Simulated vs Observed Travel Time

	High Flow Comparison		Low Flow Comparison	
Location	Flow, 2/9/1994 cfs	Flow, 8/1/2005 cfs	Flow, 6/20/1994 cfs	Flow, 8/1/2004 cfs
SJR at Lander Ave	Not measured	15	Not measured	10
Merced River near Stevinson	800	544	137	80
Tuolumne River at Modesto	1,130	1.400	126	261
Stanislaus River at Ripon	430	317	590	412
SJR at Vernalis	2,780	2,770	1,150	1,070

The time periods used for comparison have significant differences in tributary flow, so results of the comparison are not definitive. The simulated travel time for the 8/1/2005 actual flow condition was 37 hours, which is very close to the 38 hours measured on 2/9/1994. The simulated travel time for the 8/1/2004 actual flow condition was 61 hours, 18% less than the 74 hours measured on 6/20/1994.

Water Quality Calibration

After the hydrologic calibration, water quality calibration was performed. As stated earlier, the water quality calibration followed a certain order, reflecting the dependence of a constituent over the others. Temperature was calibrated first, followed by total suspended sediment, conservative substances, nutrients, then algae and dissolved oxygen.

Six water quality stations were used for WARMF calibration along the San Joaquin River: Lander Avenue (Stevinson), Crows Landing, Patterson, Maze Road, Vernalis, and Mossdale. Crows Landing and Patterson are between the confluences of the Merced and Tuolumne Rivers. Maze Road is between the Tuolumne and Stanislaus Rivers. Vernalis and Mossdale are downstream of all the major east side tributaries. Additional stations at Garwood Bridge, Rough & Ready Island, and Buckley Cove were calibrated in the Link-Node model domain.

The following sections describe the calibration results for various water quality parameters. For each water quality parameter, the simulated results (blue lines) and observed data (black circles) are compared from the most upstream station to the most downstream station.

Water Temperature

Figure 1.14 through Figure 1.19 show the time series of simulated and observed water temperature at various stations along the San Joaquin River. The algorithms used by WARMF in the original calibration of 2006 were modified based on the Flow Science review. WARMF always conducted heat balance and convective exchange of heat with the atmosphere, but complete accounting of short wave radiation, long wave radiation, and evaporative cooling were

added to the temperature calculations in rivers. This upgrade of the algorithm increased the predicted temperature and reduced the error between simulated results and measured data. The model is shown to follow the observed seasonal variations of water temperature from 2000 to 2005.

The temperature simulation for Garwood Bridge, Buckley Cove (Station R6) was based on the output of the Link-Node model. The good match demonstrates that the model was verified with the data of years 2000 to 2005. The predictive capability of the Link-Node model is evident.

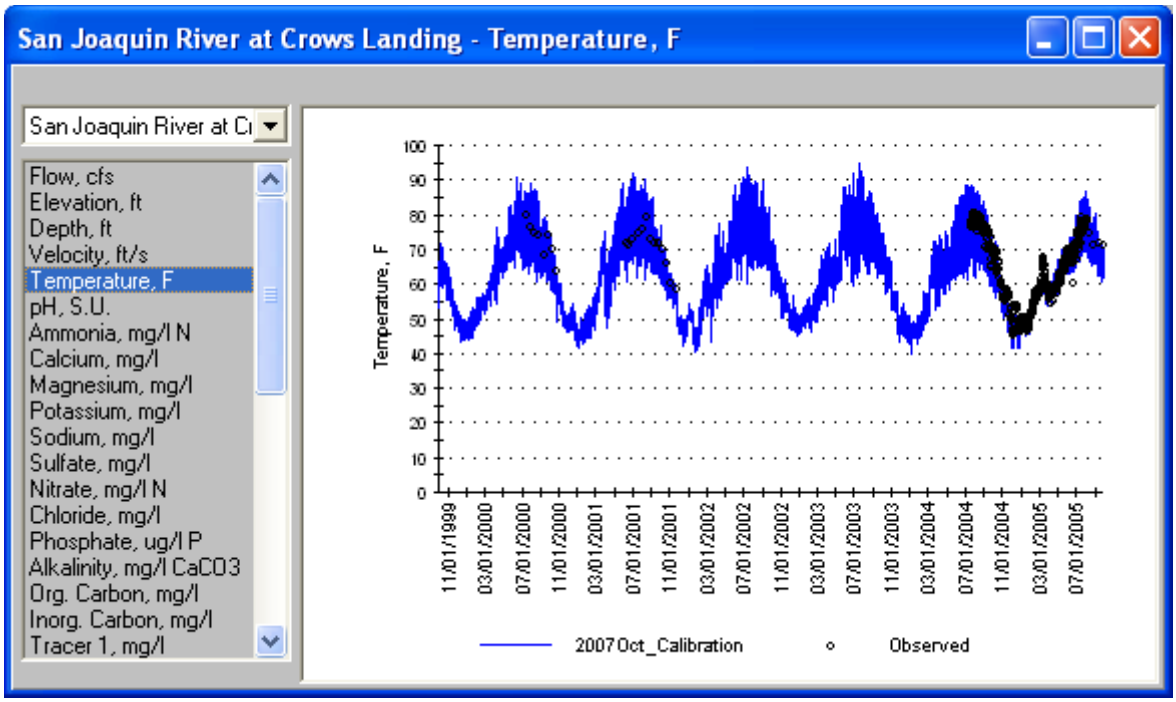

Figure 1.14 Simulated vs Observed Temperature at Crows Landing

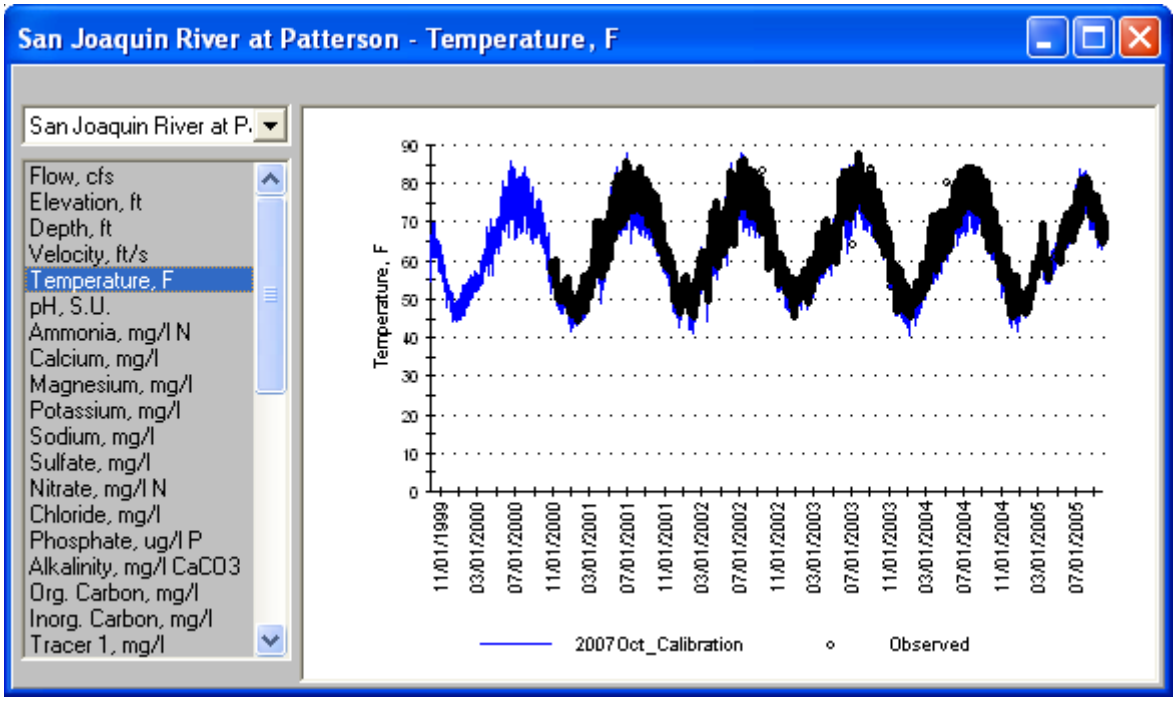

Figure 1.15 Simulated vs Observed Temperature at Patterson

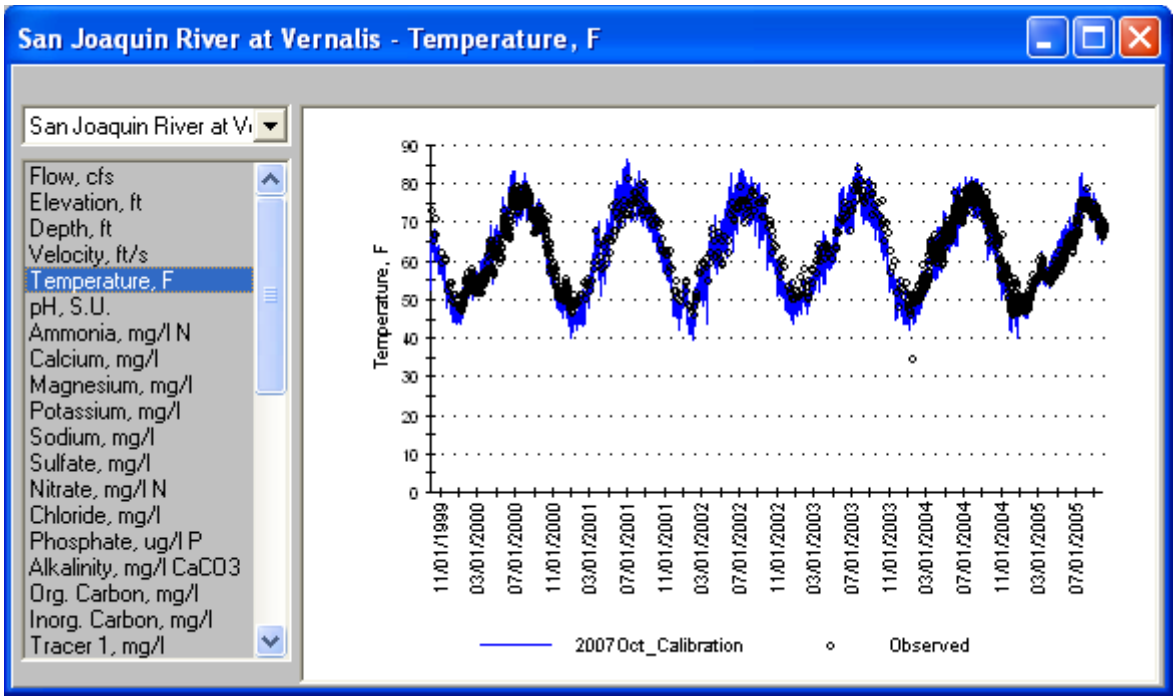

Figure 1.16 Simulated vs Observed Temperature at Vernalis

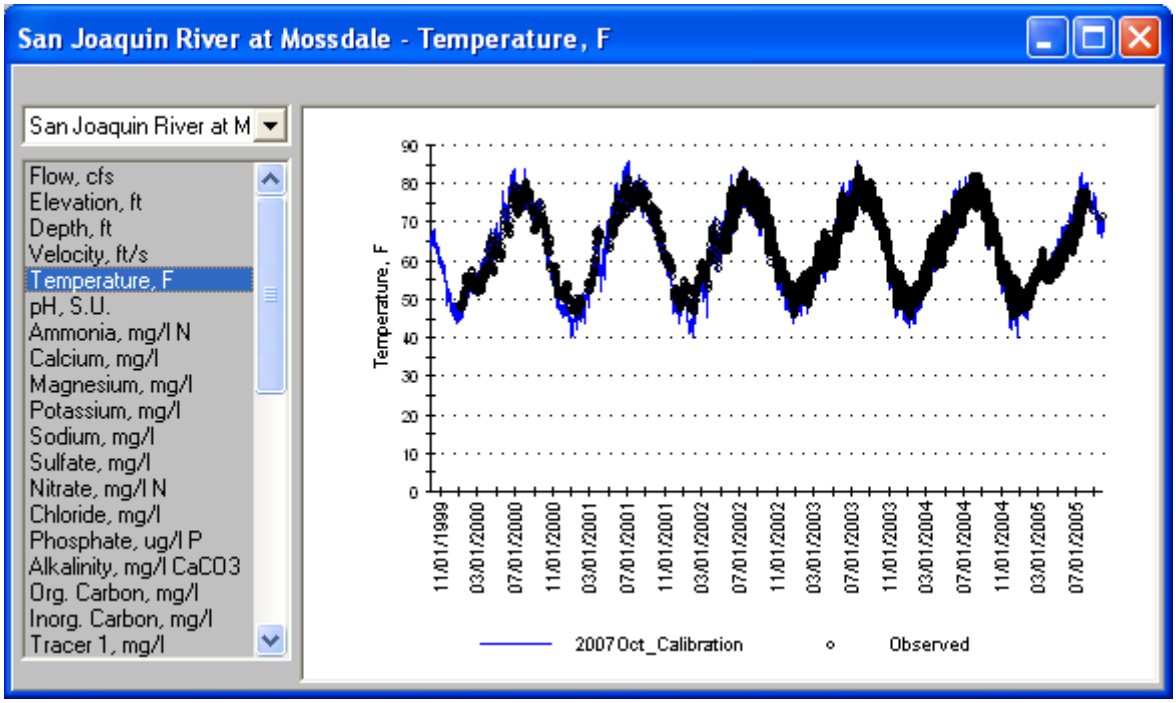

Figure 1.17 Simulated vs Observed Temperature at Mossdale

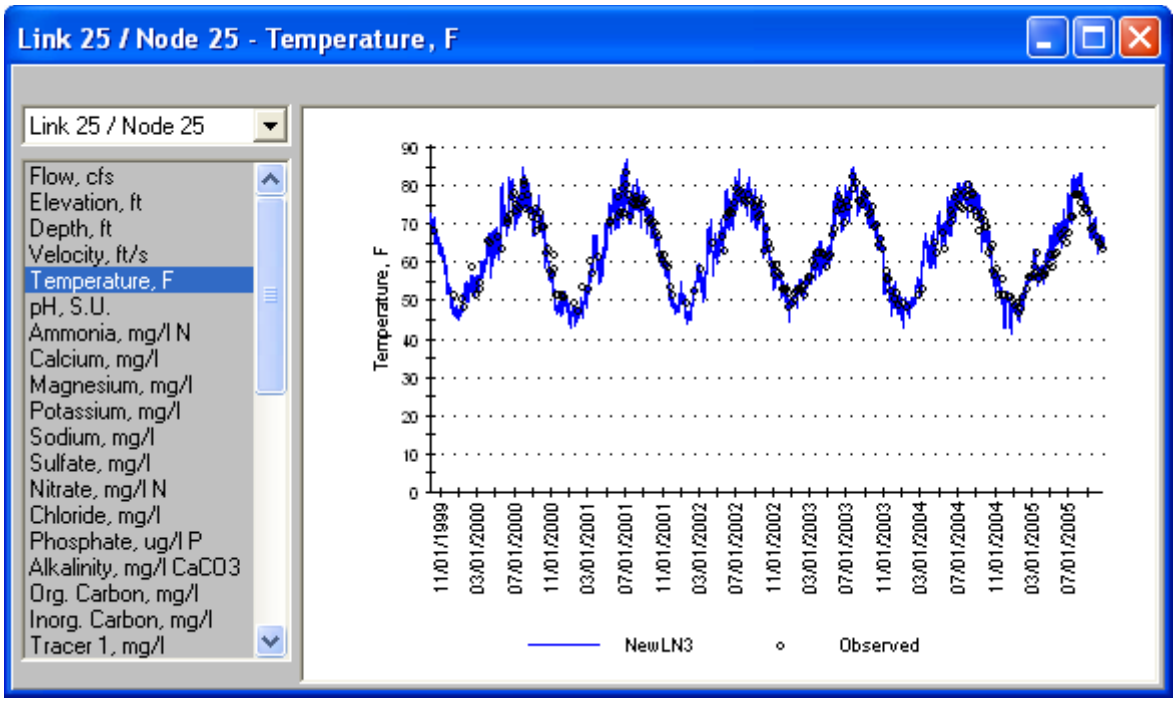

Figure 1.18 Simulated vs Observed Temperature at Garwood Bridge

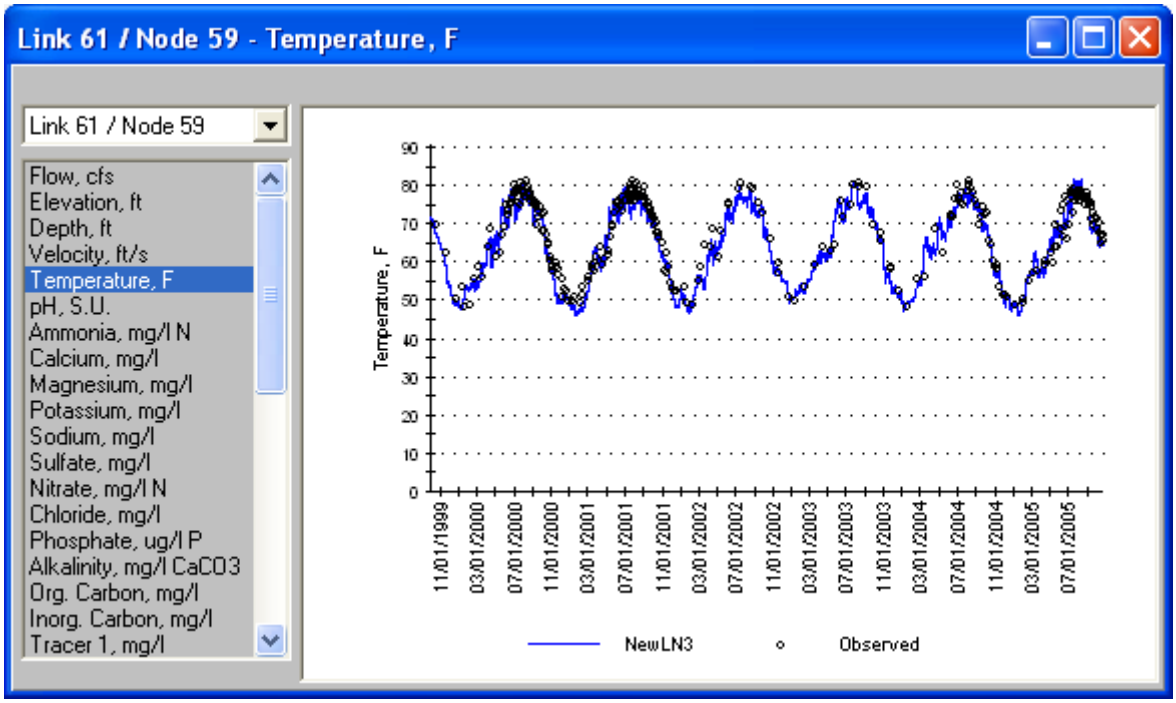

Figure 1.19 Simulated vs Observed Temperature at Buckley Cove (Station R6)

Table 1.8 provides a summary of model errors for various stations, assuming that the observed data are accurate. The goal of calibration was to reduce the relative error below 1 degree C (1.8 degrees F). The model achieved that goal, although it still tends to slightly underpredict the temperature.

Table 1.8
Model Errors of Water Temperature for San Joaquin River

Monitoring Station	Relative Error	Absolute Error
Stevinson	-0.2 ^{o}F	0.8 ^{o}F
Crows Landing	-1.4 ^{o}F	1.6 ^{o}F
Patterson	-1.6 ^{o}F	1.9 ^{o}F
Maze Road	+0.7 ^{o}F	2.1 ^{o}F
Vernalis	-0.5 ^{o}F	2.0 ^{o}F
Mossdale	-0.8 ^{o}F	2.0 ^{o}F
Garwood Bridge	-0.4 ^{o}F	1.8 ^{o}F
Buckley Cove (Station R6)	-1.3 ^{o}F	2.3 ^{o}F

Total Suspended Sediment

Figure 1.20 through Figure 1.24 show the simulated and observed time series of total suspended sediment at various stations along the San Joaquin River. The observed seasonal variations of total suspended sediment were generally simulated by the model. However, the model simulated high peak concentrations resulting from storm runoff which were not observed in biweekly monitoring data. Daily monitoring data was collected for 2004-2005 at Vernalis (Figure 1.22), which shows peak values from storm runoff.

Thus, the model predictions of high total suspended sediment were confirmed by the daily measurements at Vernalis, but not confirmed by the biweekly measurement at other stations. Literature has shown that most total suspended sediment of a river is carried only by a few large storms, which is consistent with the prediction of WARMF. These let us to conclude that the model predictions were accurate despite large discrepancies between the predicted and observed values for certain days during the storms. The simulation results from Buckley Cove in the Link-Node model domain show a similar pattern as the stations farther upstream, but without the high peak concentrations.

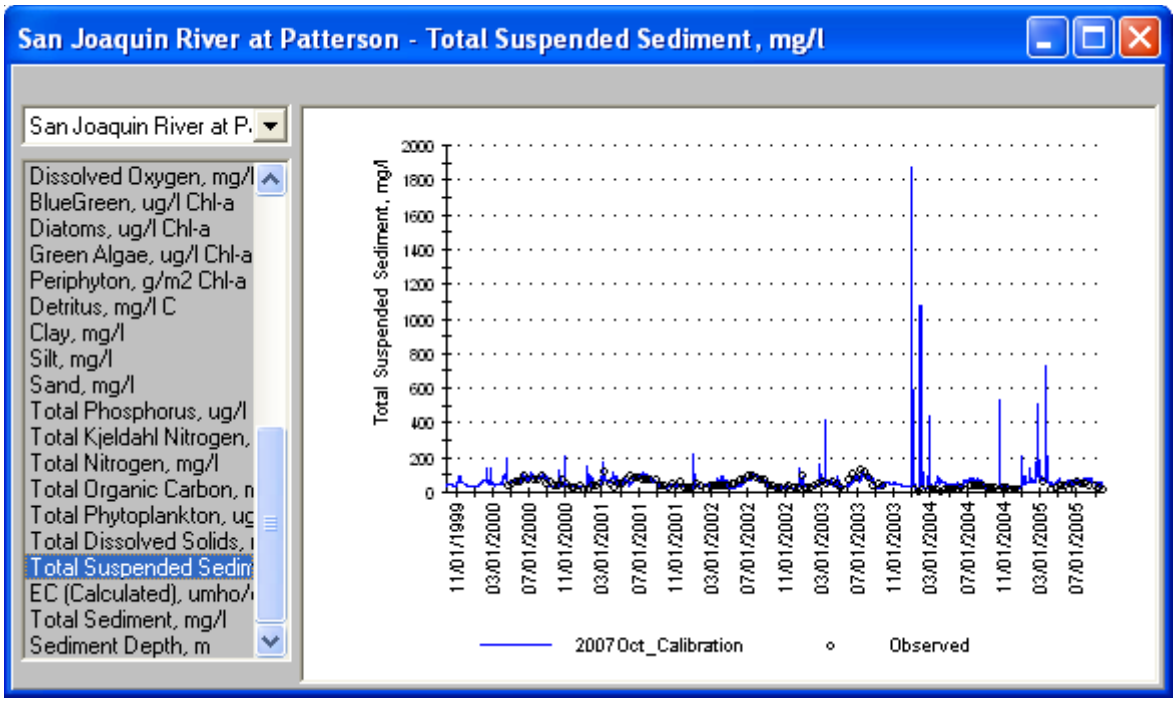

Figure 1.20 Simulated vs Observed Total Suspended Sediment at Patterson

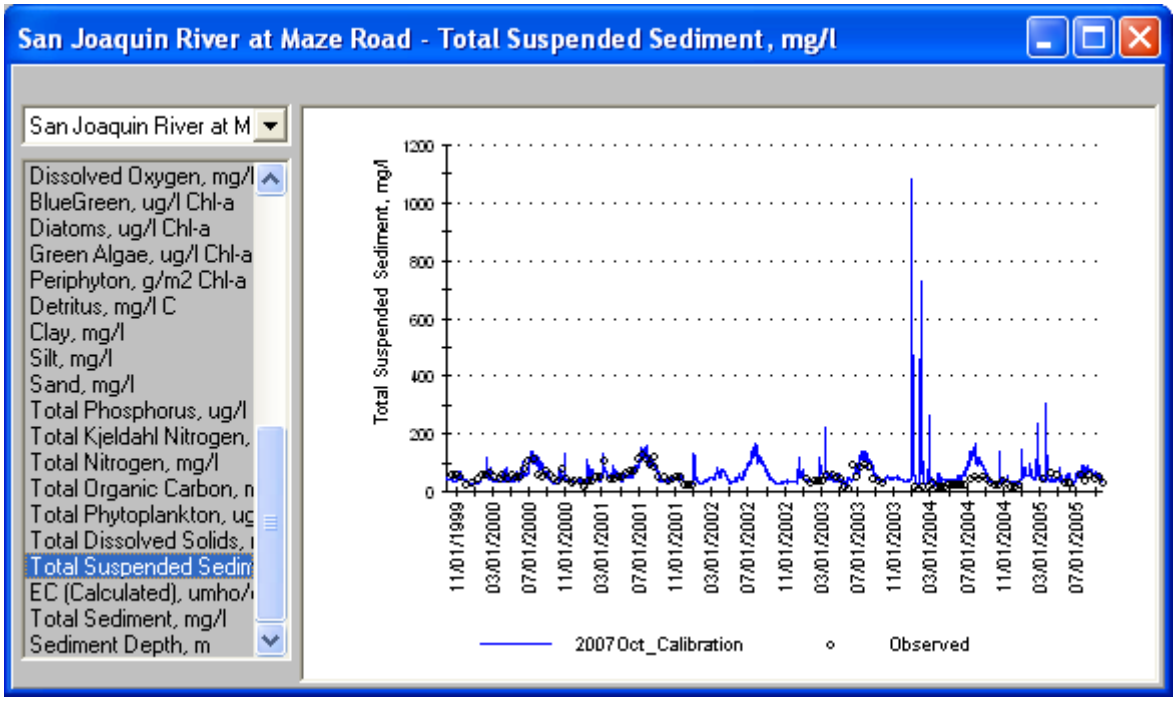

Figure 1.21 Simulated vs Observed Total Suspended Sediment at Maze Road

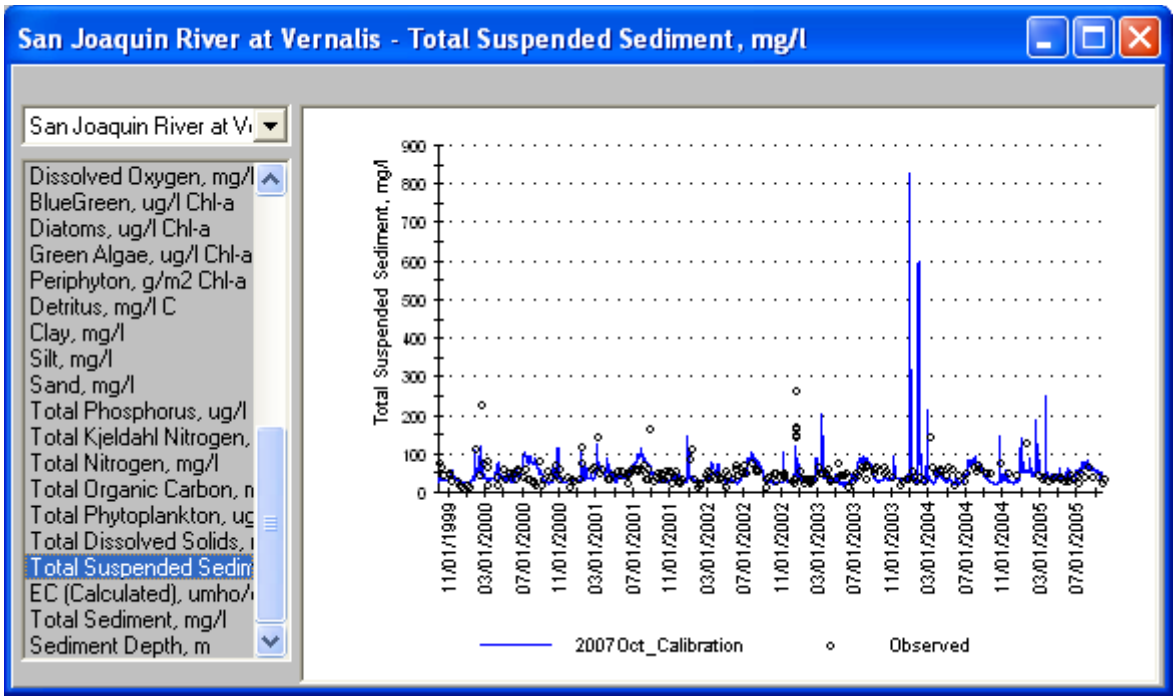

Figure 1.22 Simulated vs Observed Total Suspended Sediment at Vernalis

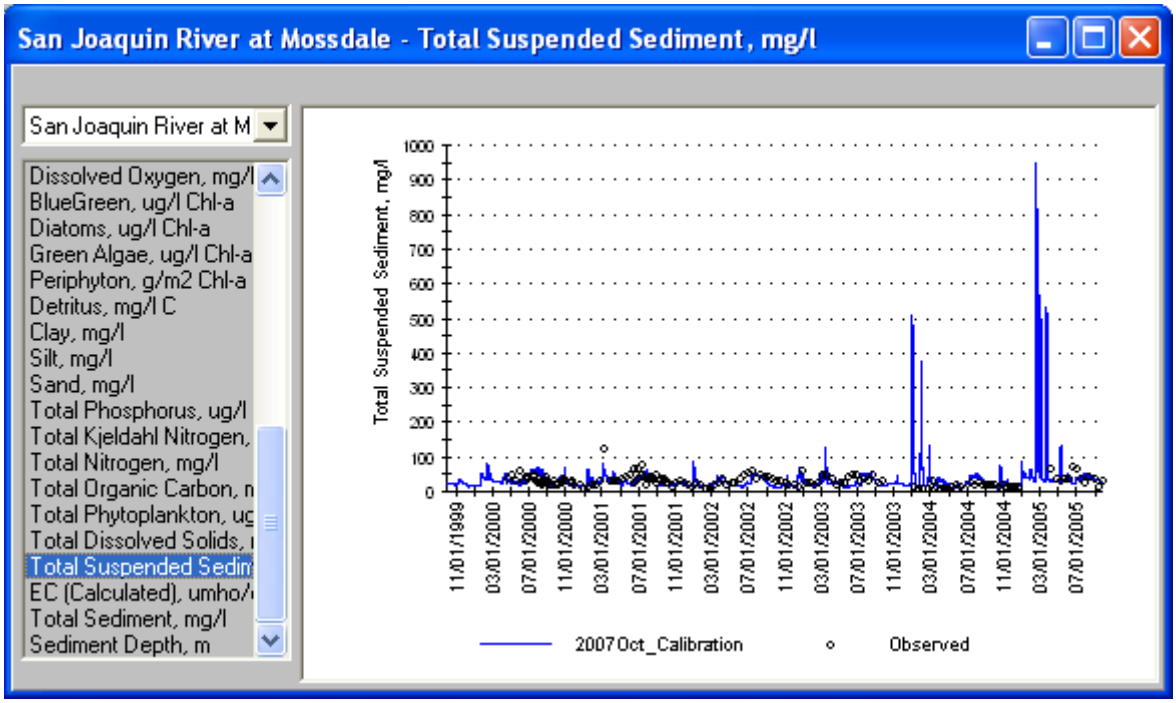

Figure 1.23 Simulated vs Observed Total Suspended Sediment at Mossdale

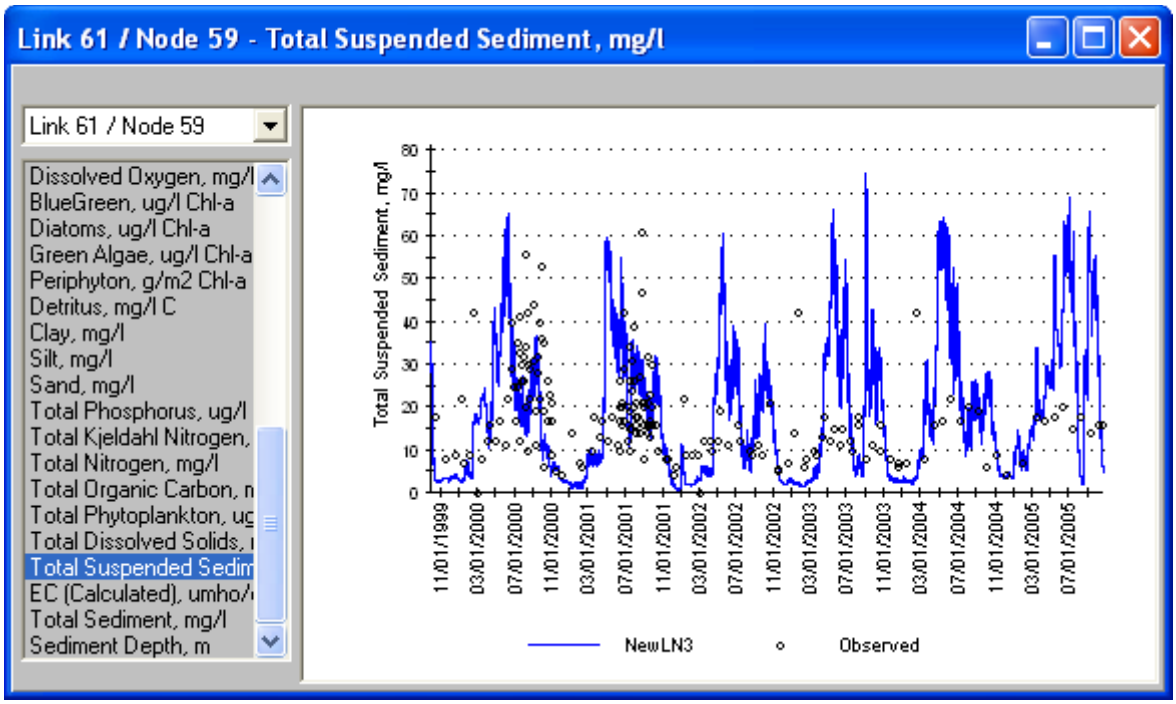

Figure 1.24 Simulated vs Observed Total Suspended Sediment at Buckley Cove

Sediment load to the San Joaquin River came from boundary river inflows and overland flows from land catchments. Once in the river, sediment could settle out or be scoured from the river bed. The model simulated total suspended sediment by its three components of clay, silt, and sand. Because clay settles very slowly, it was assumed that suspended sediment in boundary river inflows was clay. Clay, silt and sand fractions were simulated in the storm runoff from land catchments. The monitoring data from the San Joaquin River had more total suspended sediment than can be explained by boundary river inflows alone. The monitoring data suggested the likelihood of scouring in the river bed that was predicted by the WARMF model using the default settling rate, scouring shear stress and velocity embedded in the model database. The settling velocity for clay was set at 0.0003 m/d for most of the river segments due to turbulence. Between Vernalis and Mossdale, the river is much deeper and slower, so a clay settling rate of 1 m/d was set in that reach.

Table 1.9 shows the errors of model predictions for various monitoring stations on the San Joaquin River. The goal for calibration was to keep relative error below 10% and absolute error below 50%. The model generally meets this goal. At Crows Landing, where there are relatively few measured data points, the model is overpredicting the measured values.

Table 1.9
Model Errors for Total Suspended Sediment in the San Joaquin River

Monitoring Station	Relative Error	Absolute Error
Stevinson	+8%	12%
Crows Landing	+28%	54%
Patterson	-1%	32%
Maze Road	+3%	32%
Vernalis	-10%	40%
Mossdale	-12%	39%
Buckley Cove (Station R6)	+25%	72%

Calcium

Figure 1.25 through Figure 1.29 compare the simulated and observed time series of calcium concentration at various stations along the San Joaquin River. The simulated calcium concentration was higher than observed at Crows Landing, probably due to error estimating the ion ratios in agricultural return flows or error in initial conditions within the soil. The model predictions for other stations were in the correct ranges and all show a good match to the magnitude and seasonal pattern of the observed data.

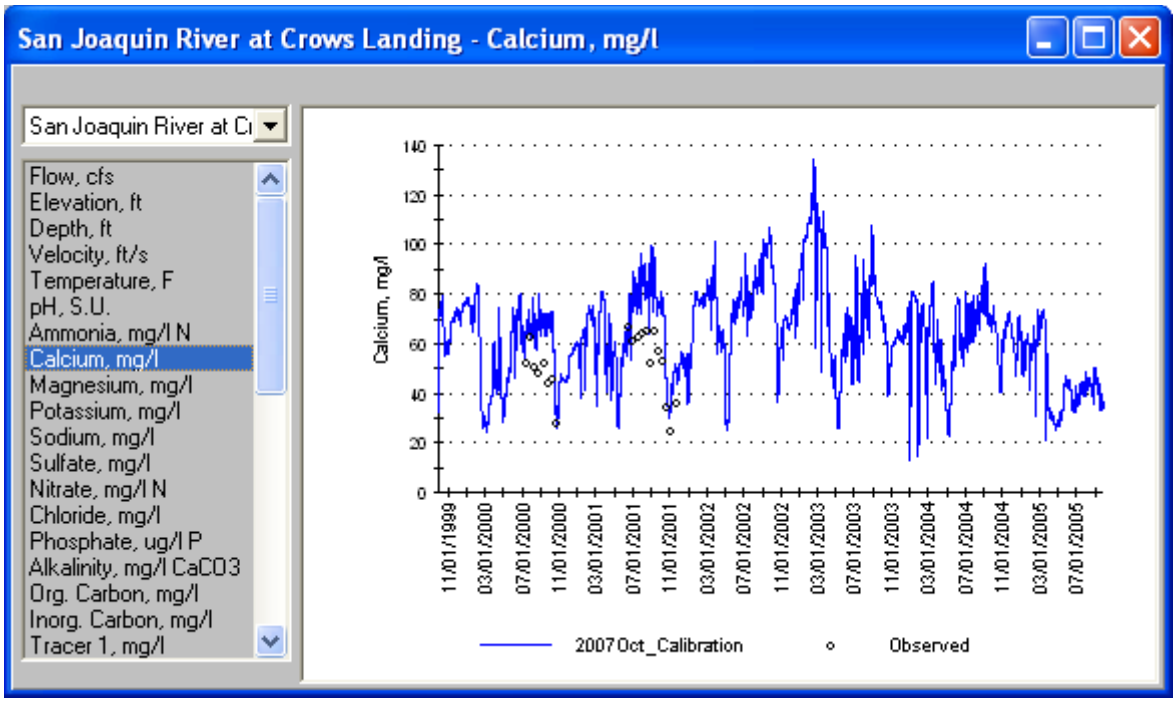

Figure 1.25 Simulated vs Observed Calcium at Crows Landing

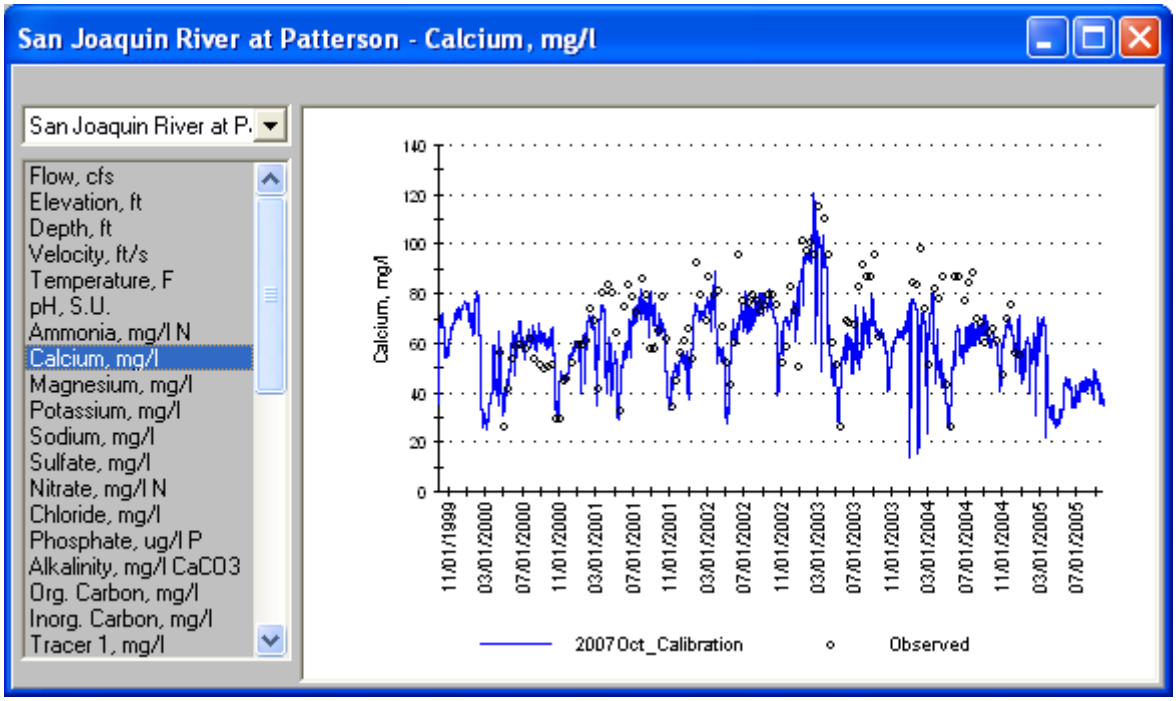

Figure 1.26 Simulated vs Observed Calcium at Patterson

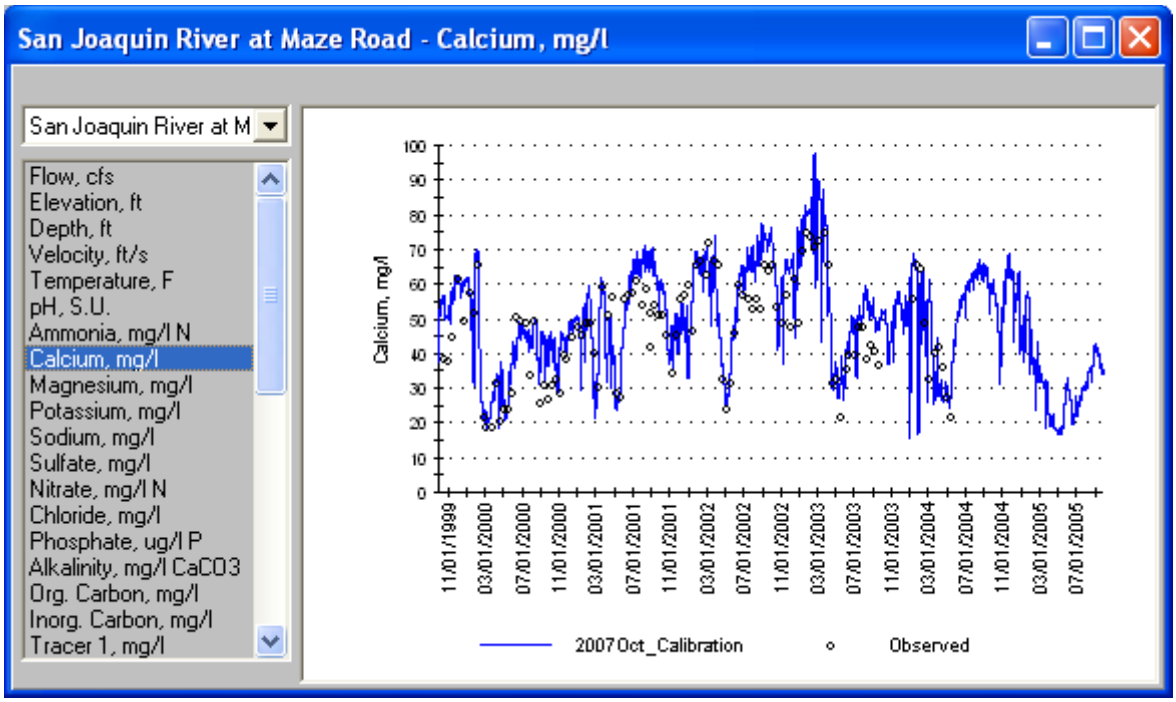

Figure 1.27 Simulated vs Observed Calcium at Maze Road

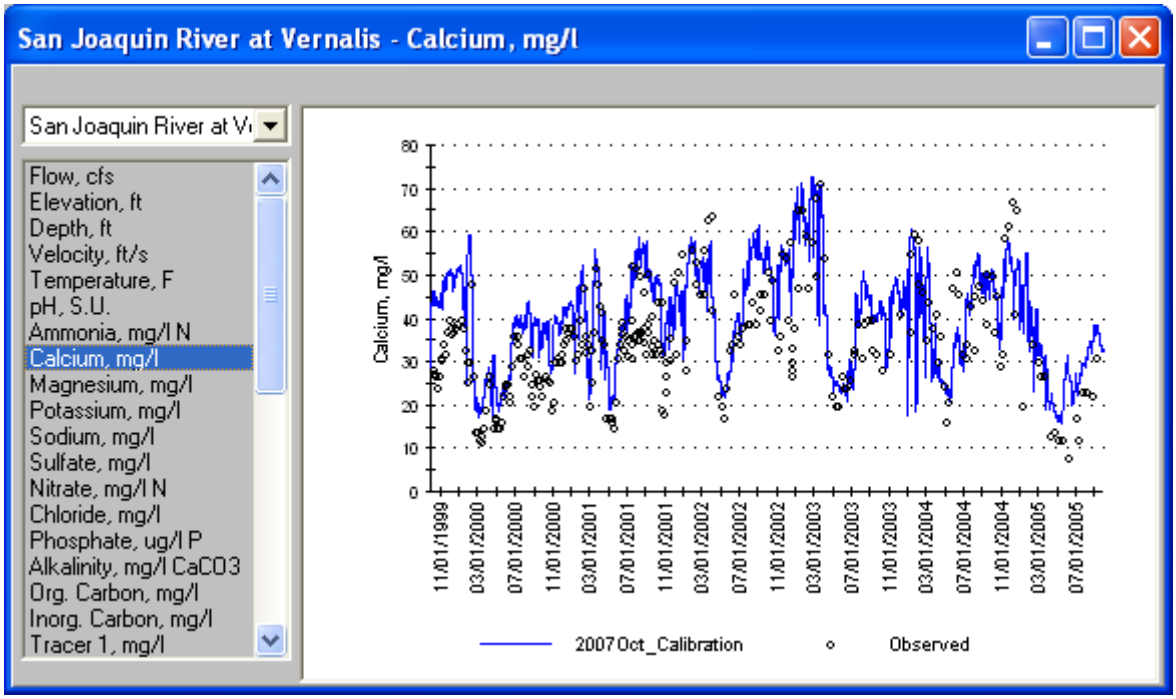

Figure 1.28 Simulated vs Observed Calcium at Vernalis

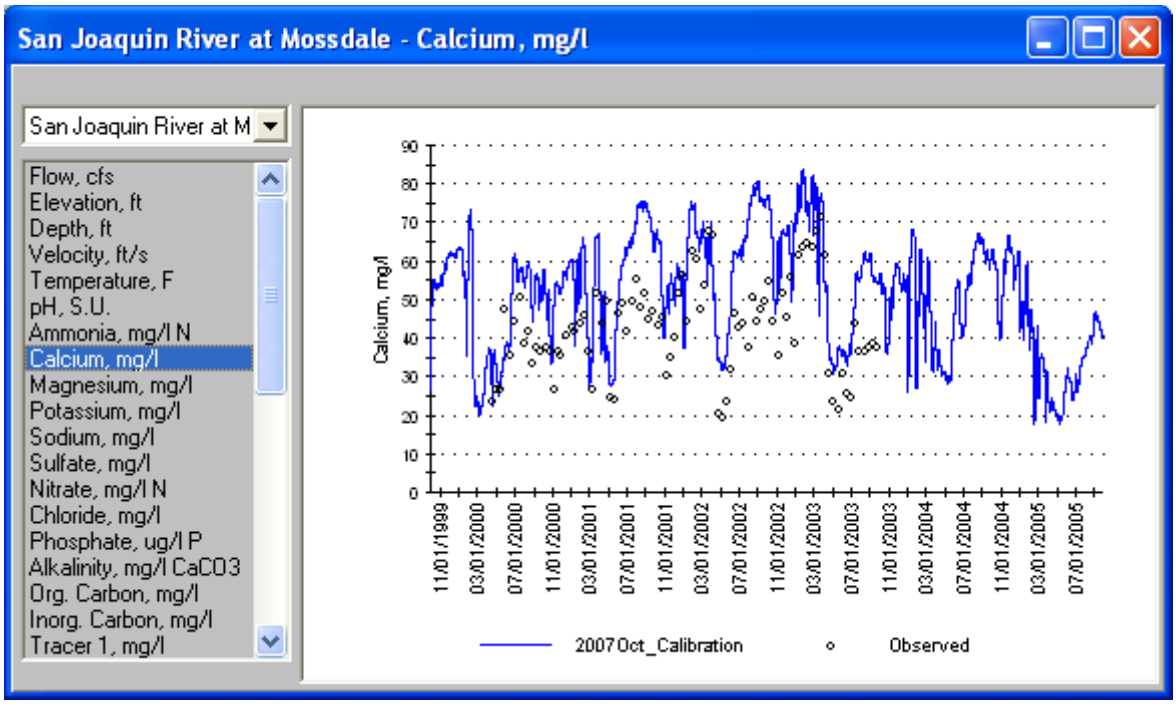

Figure 1.29 Simulated vs Observed Calcium at Mossdale

Table 1.10 shows the errors of model errors for calcium ion concentration in San Joaquin River. The goal of calibration was to achieve a relative error below 10% and absolute error below 20%. The goal for relative error was reached in 4 stations out of 6 stations. The error above the criteria at Vernalis and Mossdale might be caused by the model simulating too much calcium in the shallow groundwater near those monitoring stations.

Table 1.10
Model Errors for Calcium Concentration in San Joaquin River

Monitoring Station	Relative Error	Absolute Error
Stevinson	+0%	3%
Crows Landing	+31%	31%
Patterson	-9%	15%
Maze Road	+8%	15%
Vernalis	+18%	24%
Mossdale	+30%	32%

Magnesium

Figure 1.30 through Figure 1.34 compare the time series of simulated and observed magnesium ion concentrations at various stations along the San Joaquin River. WARMF simulated the magnitude and seasonal pattern of magnesium well. The magnesium concentration must be estimated for agricultural return flows as a ratio relative to other ions and as a function of measured or estimated EC. Some error is introduced as a result of these assumptions.

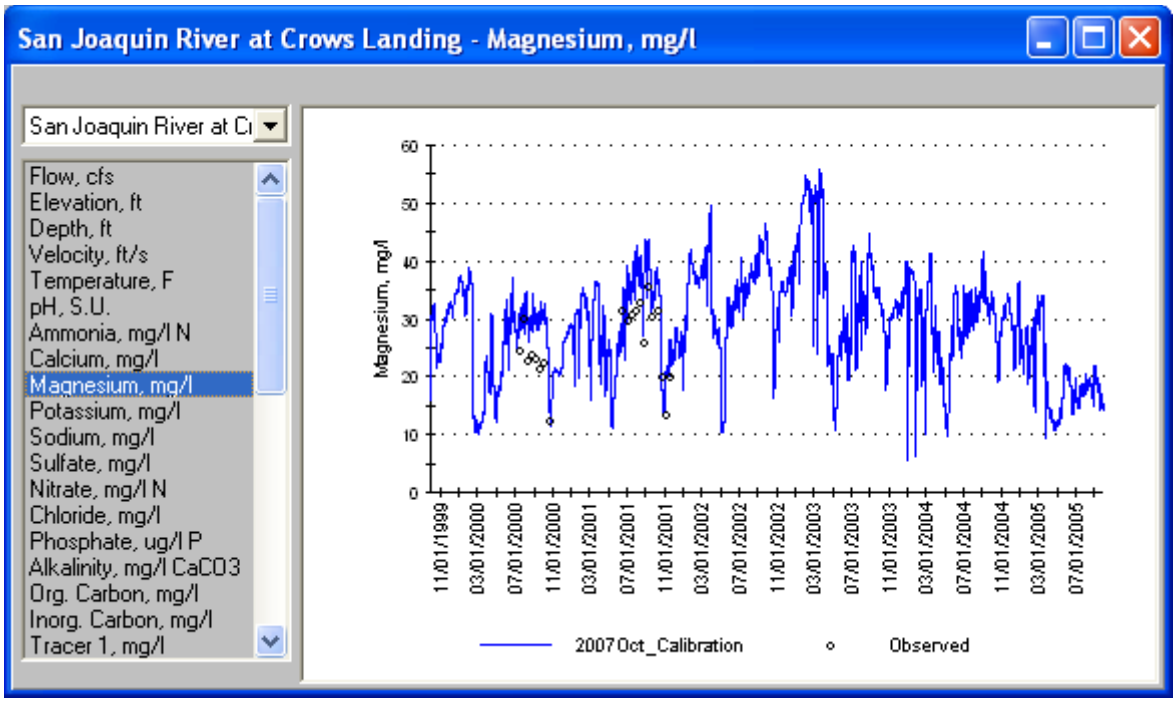

Figure 1.30 Simulated vs Observed Magnesium at Crows Landing

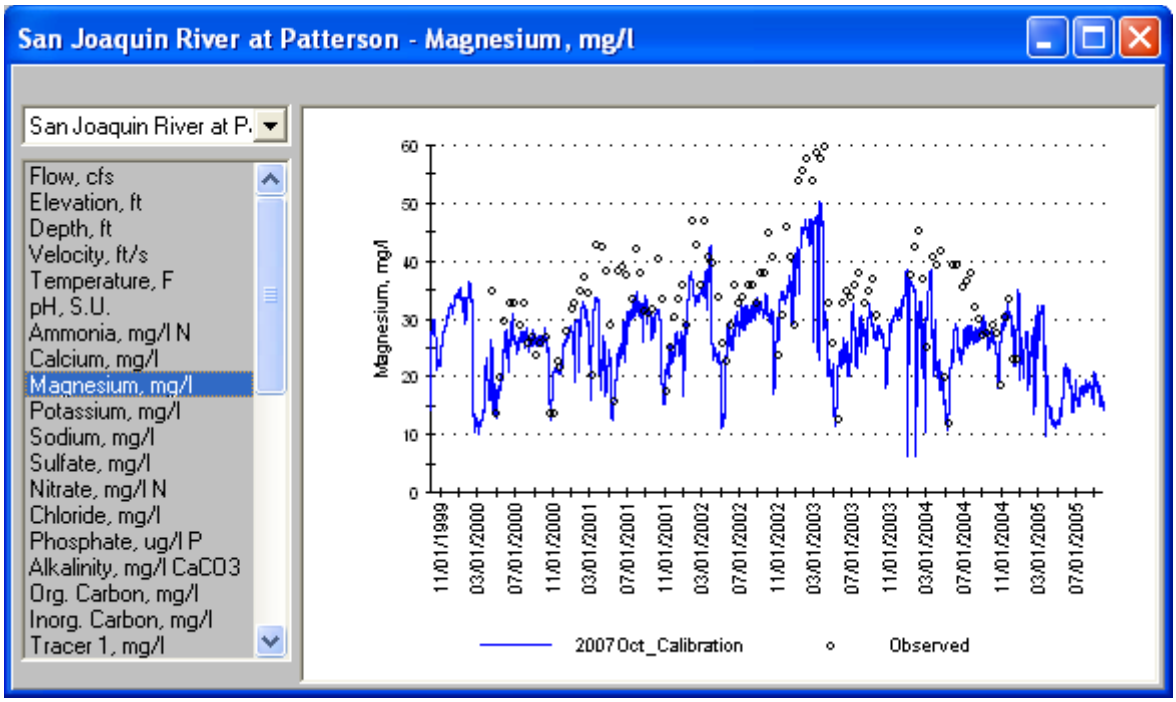

Figure 1.31 Simulated vs Observed Magnesium at Patterson

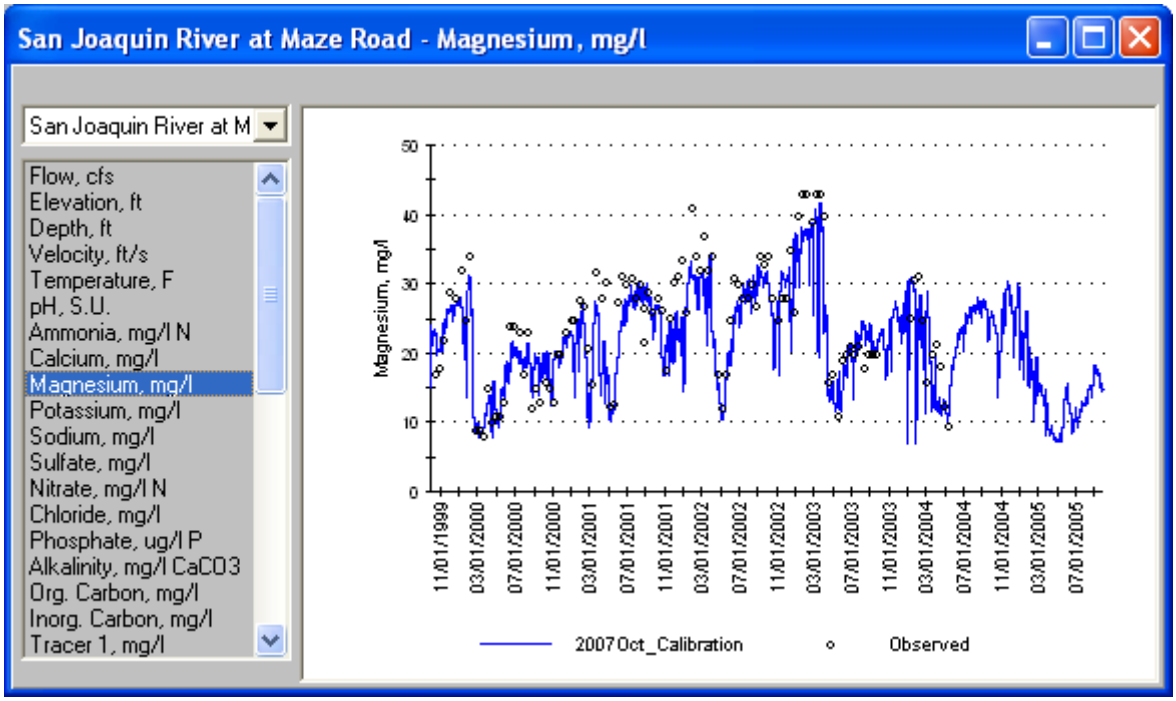

Figure 1.32 Simulated vs Observed Magnesium at Maze Road

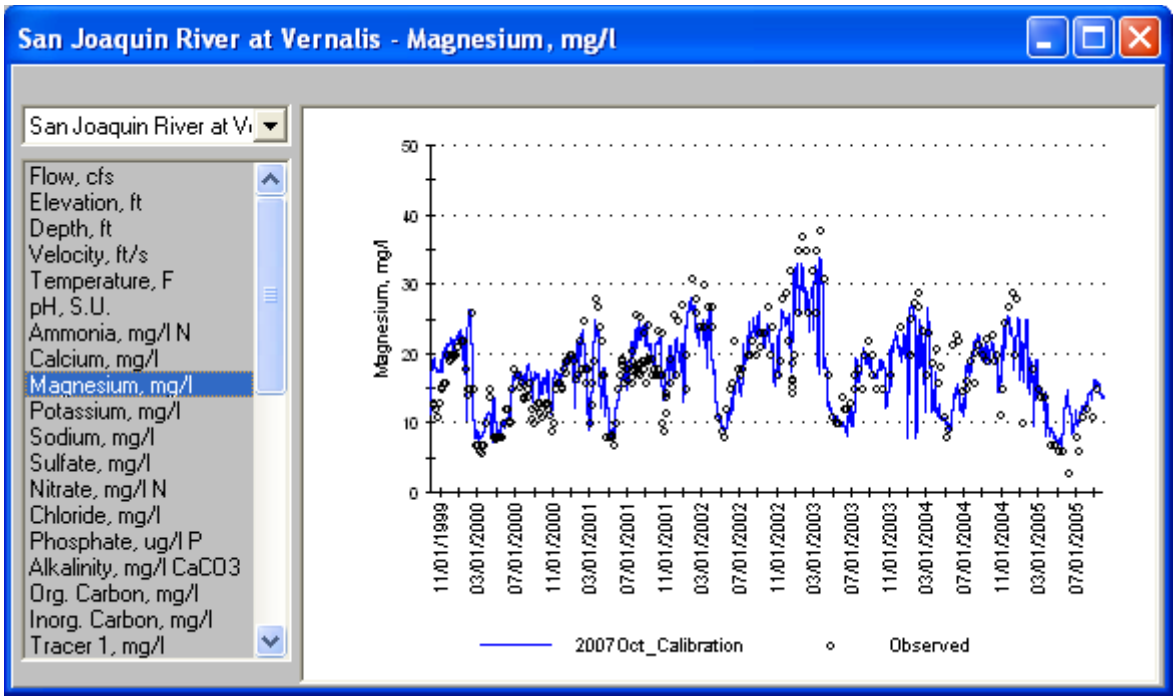

Figure 1.33 Simulated vs Observed Magnesium at Vernalis

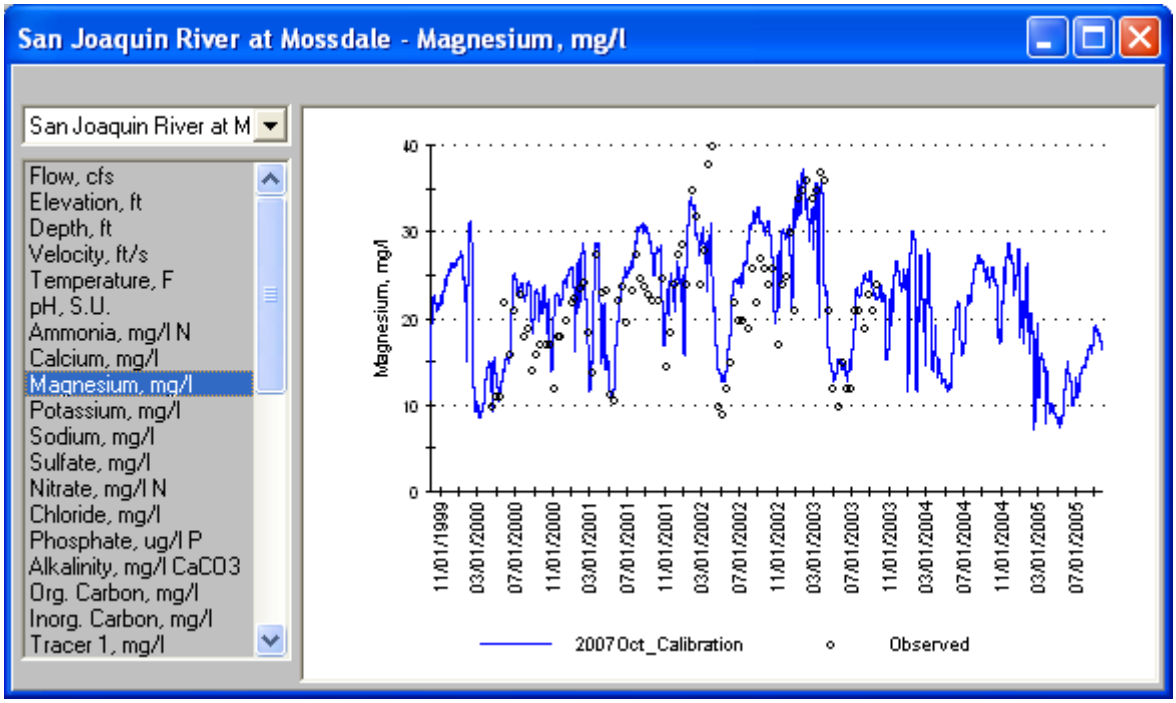

Figure 1.34 Simulated vs Observed Magnesium at Mossdale

Table 1.11 shows the model errors for dissolved magnesium concentrations in San Joaquin River. The goal of calibration was to achieve a relative error below 10% and absolute error below 20%. The goal for relative error was reached in 4 out of 6 stations.

Table 1.11
Model Errors for Magnesium Concentration in San Joaquin River

Monitoring Station	Relative Error	Absolute Error
Stevinson	+1%	3%
Crows Landing	+20%	21%
Patterson	-18%	20%
Maze Road	-7%	14%
Vernalis	+2%	17%
Mossdale	+8%	17%

Potassium

Figure 1.35 through Figure 1.39 compare the predicted and observed time series of potassium ion concentration at various stations along the San Joaquin River. The predicted concentrations were generally higher than observed values. Much of the observed data is only accurate to +/- 1 mg/l (up to 50% measurement error), which makes it difficult to discern the seasonal pattern of potassium concentration.

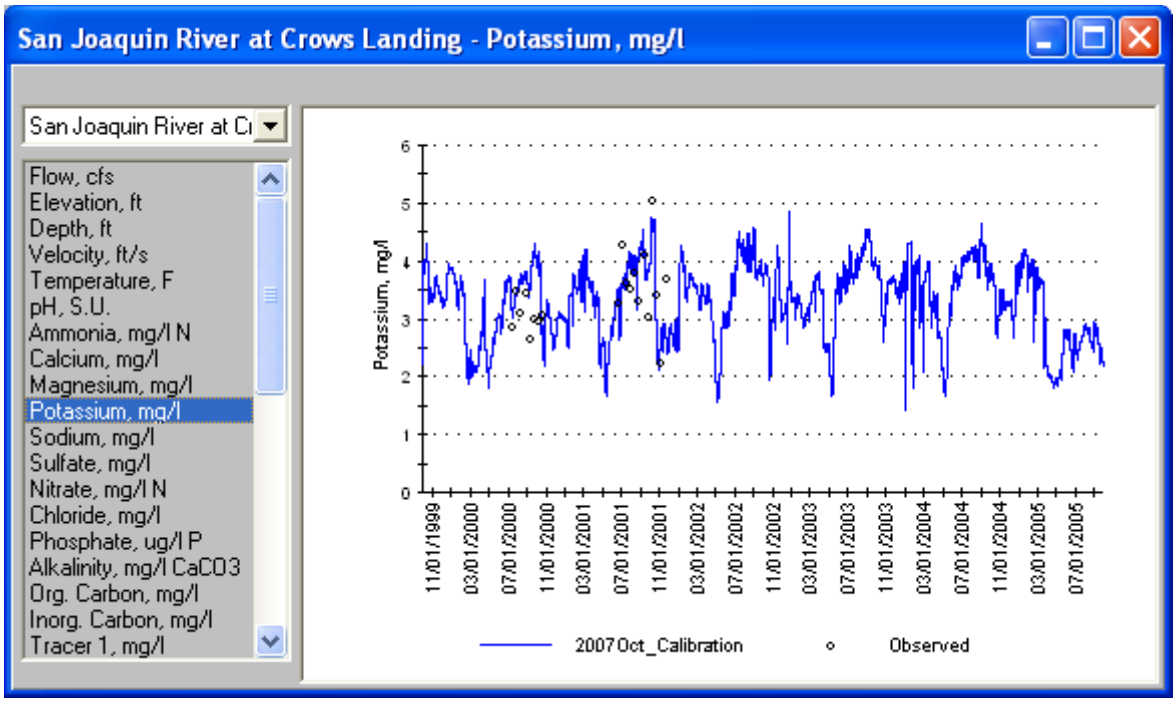

Figure 1.35 Simulated vs Observed Potassium at Crows Landing

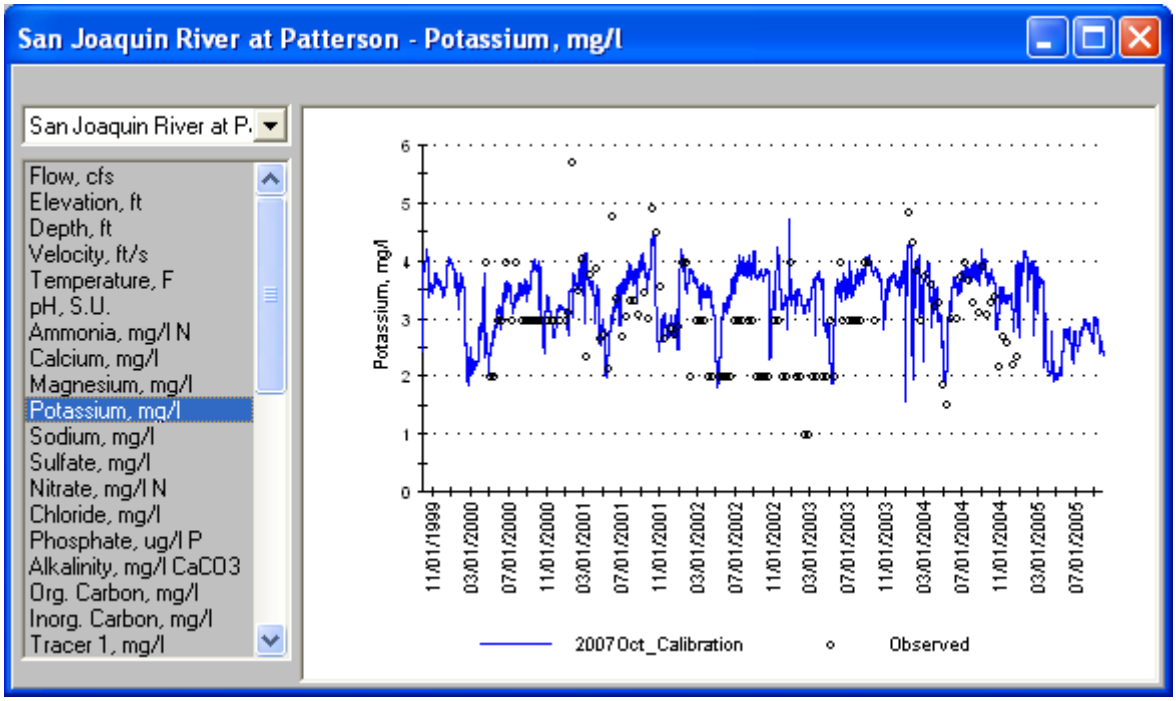

Figure 1.36 Simulated vs Observed Potassium at Patterson

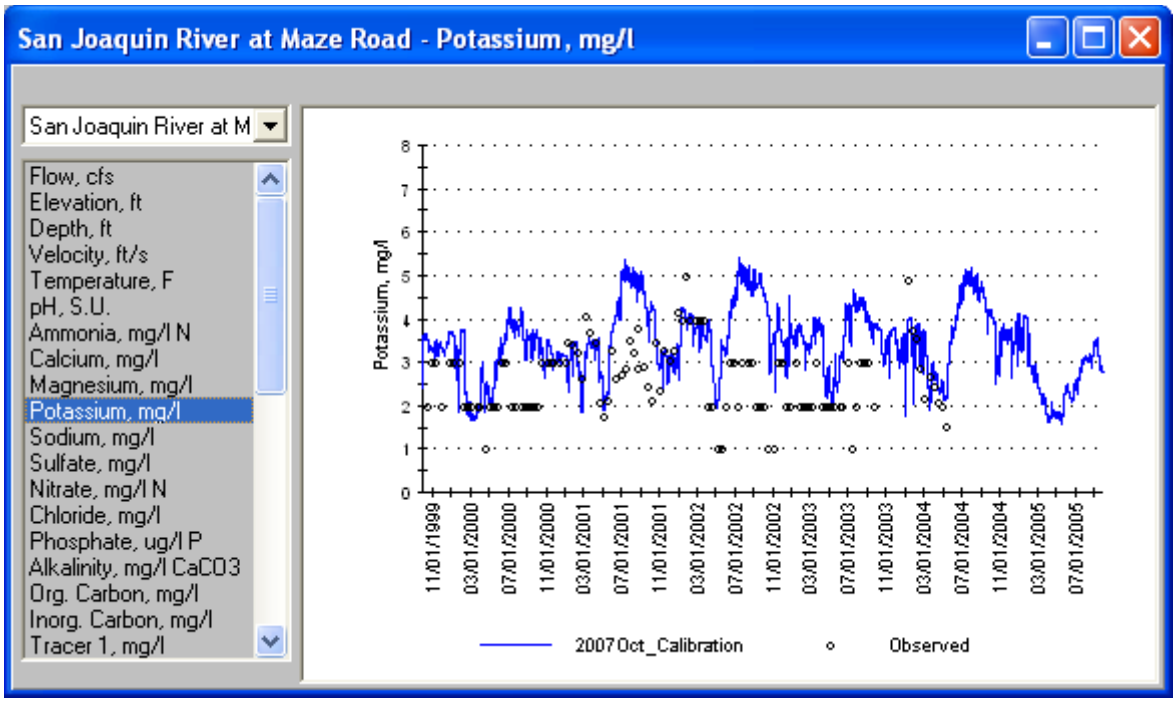

Figure 1.37 Simulated vs Observed Potassium at Maze Road

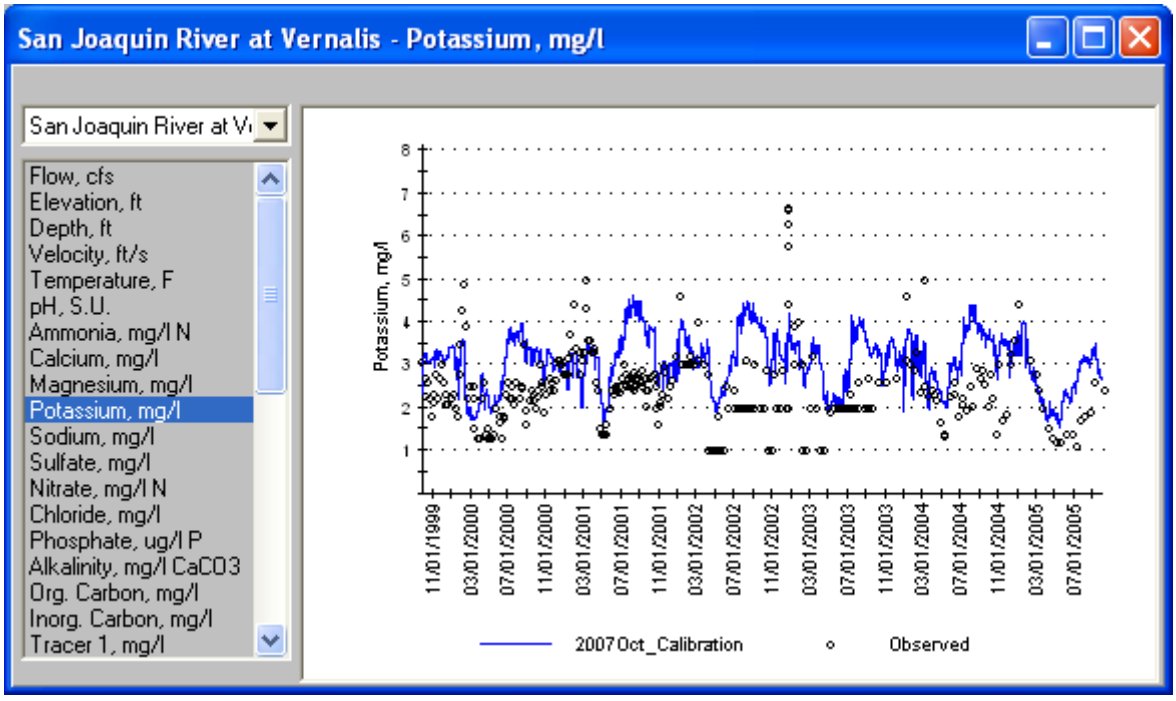

Figure 1.38 Simulated vs Observed Potassium at Vernalis

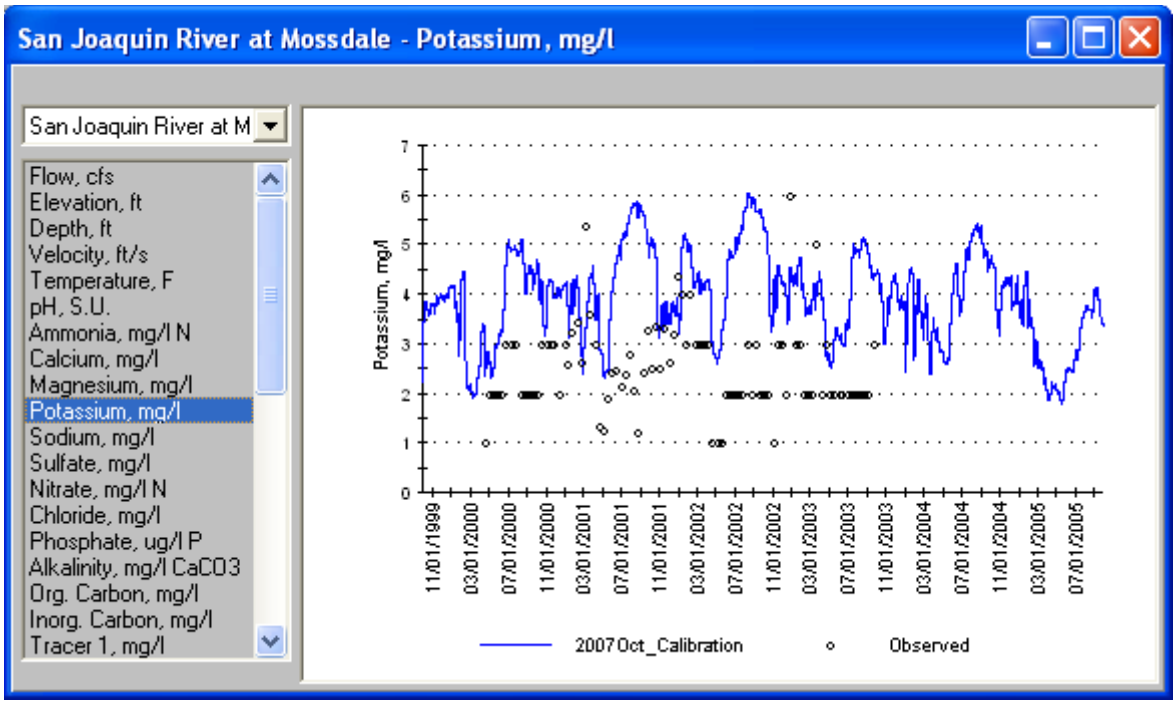

Figure 1.39 Simulated vs Observed Potassium at Mossdale

Table 1.12 shows the model errors for dissolved potassium concentrations in San Joaquin River. The model has increasing errors going downstream. The model was likely predicting more potassium in shallow groundwater than is actually occurring. This was not considered a primary concern because potassium has no affect the prediction of DO in the DWSC and little effect on the overall salt/EC load.

Table 1.12
Model Errors for Potassium Concentration in San Joaquin River

Monitoring Station	Relative Error	Absolute Error
Stevinson	-0%	2%
Crows Landing	+6%	15%
Patterson	+15%	22%
Maze Road	+34%	39%
Vernalis	+26%	36%
Mossdale	+66%	72%

Sodium

Figure 1.40 through Figure 1.44 compare the predicted and observed time series of dissolved sodium concentration at various stations along the San Joaquin River. The model predictions followed the observed seasonal pattern of sodium concentration very well.

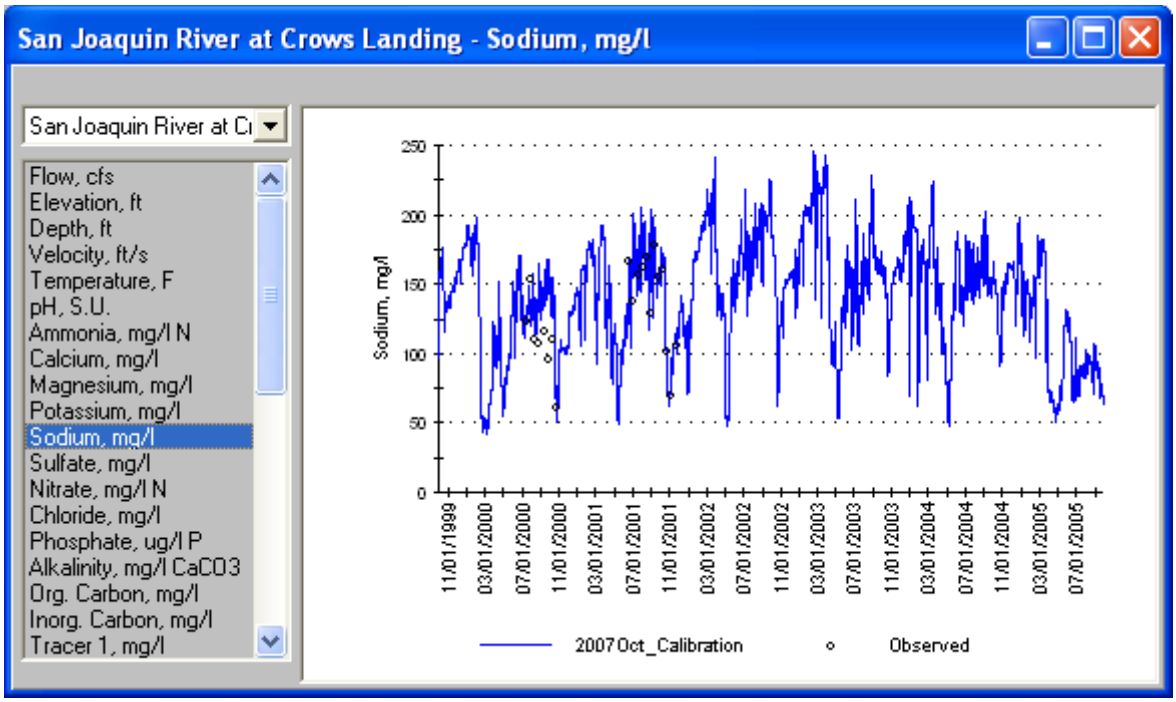

Figure 1.40 Simulated vs Observed Sodium at Crows Landing

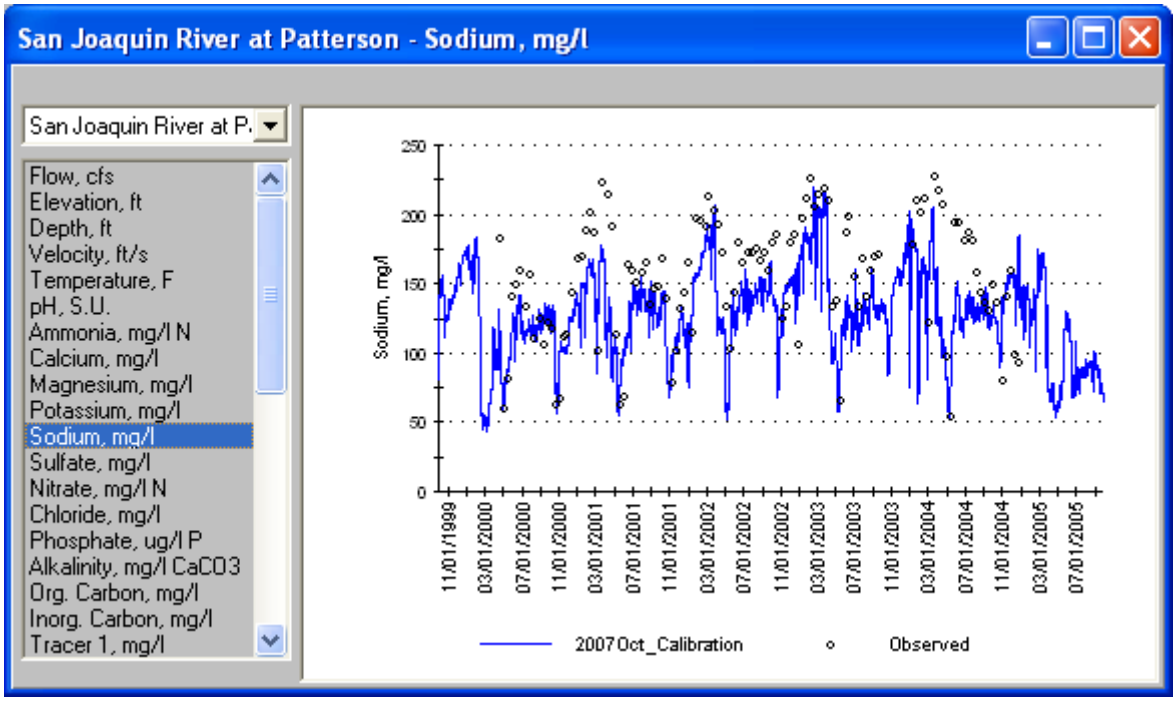

Figure 1.41 Simulated vs Observed Sodium at Patterson

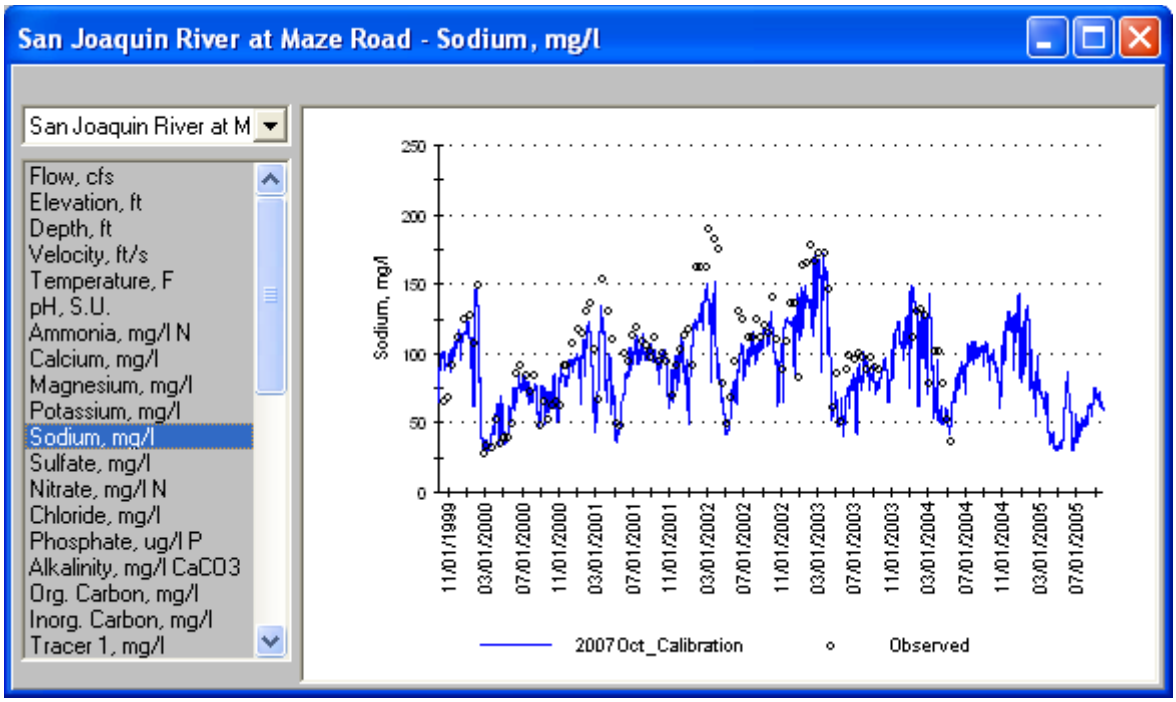

Figure 1.42 Simulated vs Observed Sodium at Maze Road

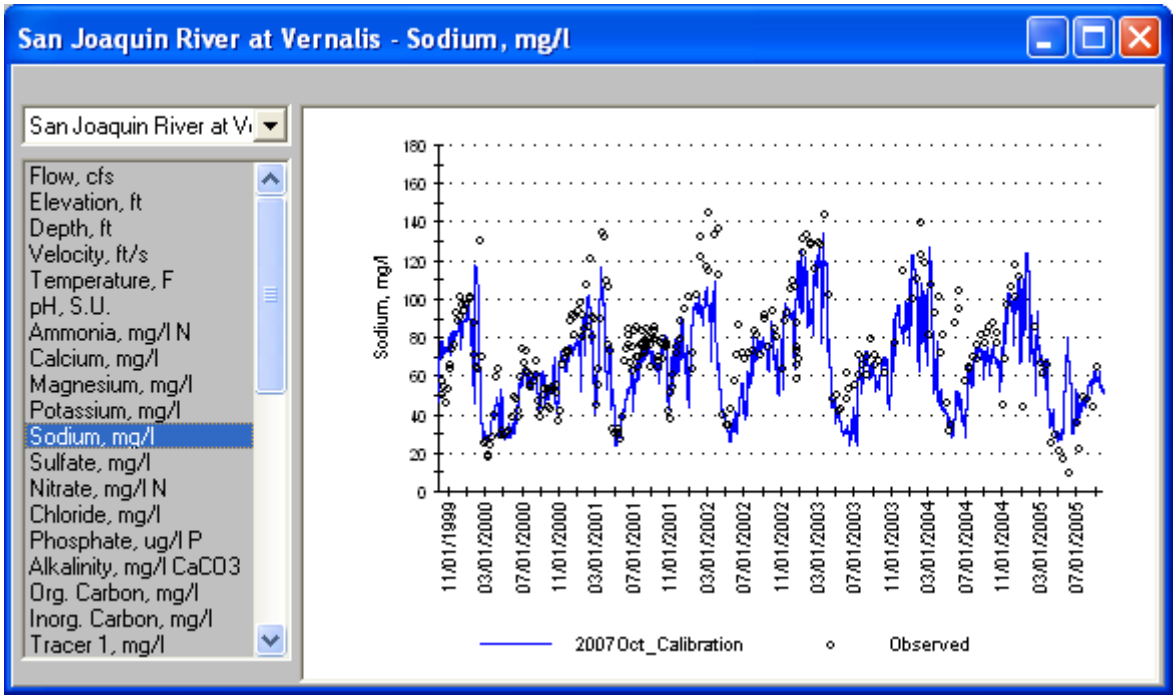

Figure 1.43 Simulated vs Observed Sodium at Vernalis

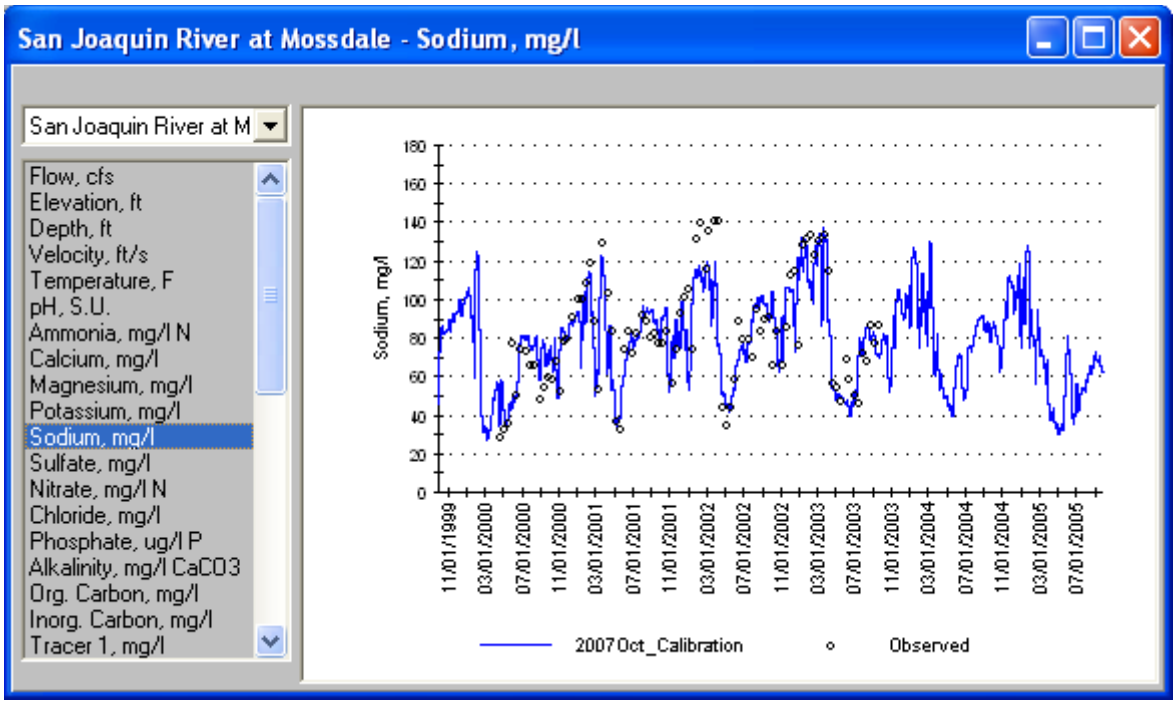

Figure 1.44 Simulated vs Observed Sodium at Mossdale

Table 1.13 shows the model errors for sodium concentration, assuming the observed data are accurate. The model was within 10% relative error at 3 of 6 stations with a bias toward predicting too little sodium, but the model was within 20% absolute error at all stations.

Table 1.13
Model Errors for Sodium Concentration in San Joaquin River

Monitoring Station	Relative Error	Absolute Error
Stevinson	-1%	3%
Crows Landing	+9%	17%
Patterson	-15%	19%
Maze Road	-11%	16%
Vernalis	-11%	19%
Mossdale	-2%	13%

Sulfate

Figure 1.45 through Figure 1.49 compare the predicted and observed the time series of sulfate concentration at various stations along the San Joaquin River. The model predictions had a good match with the magnitude and seasonal pattern of observed sulfate concentration.

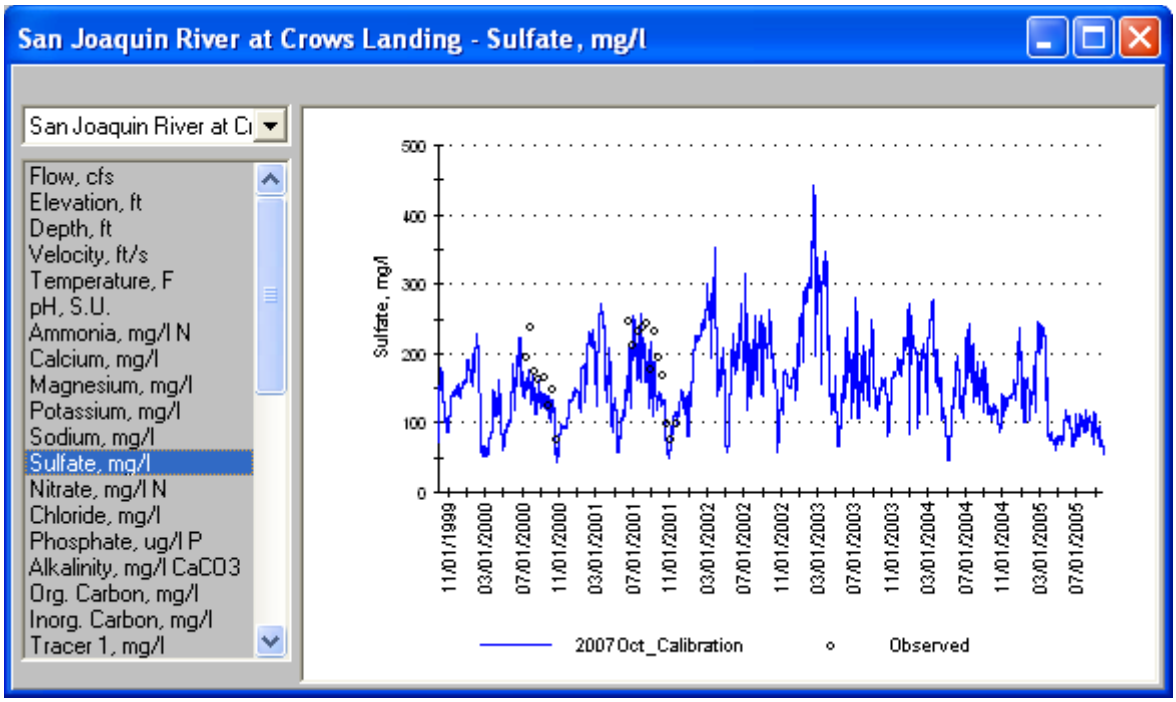

Figure 1.45 Simulated vs Observed Sulfate at Crows Landing

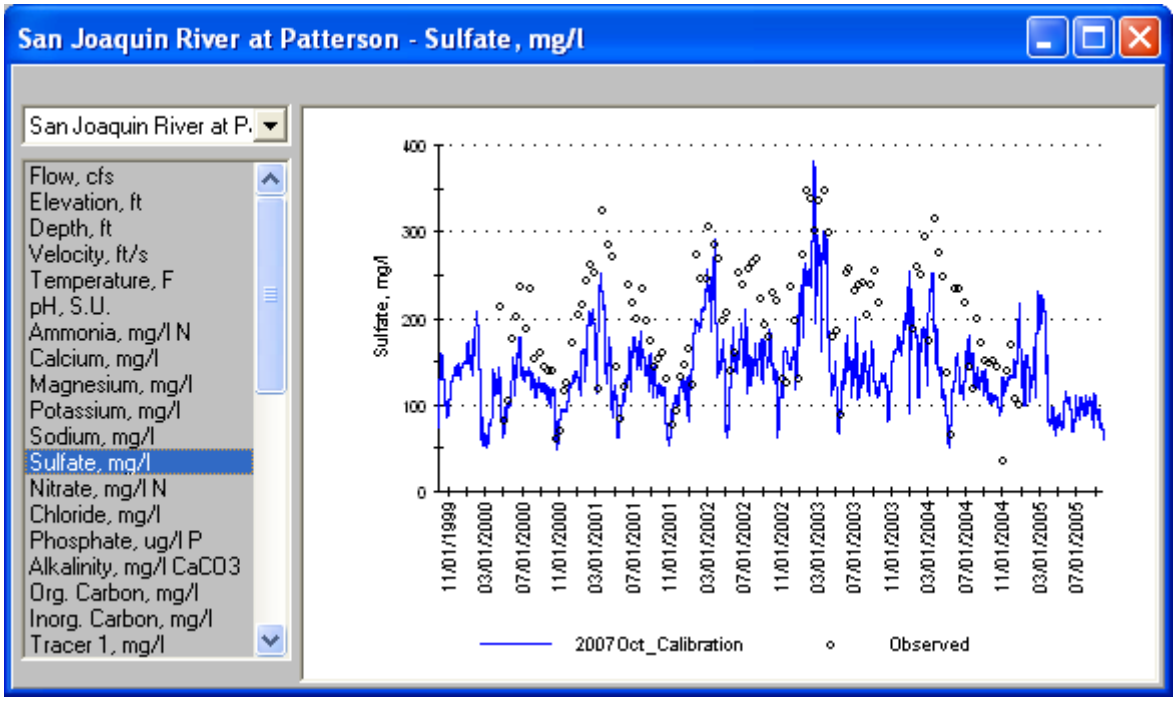

Figure 1.46 Simulated vs Observed Sulfate at Patterson

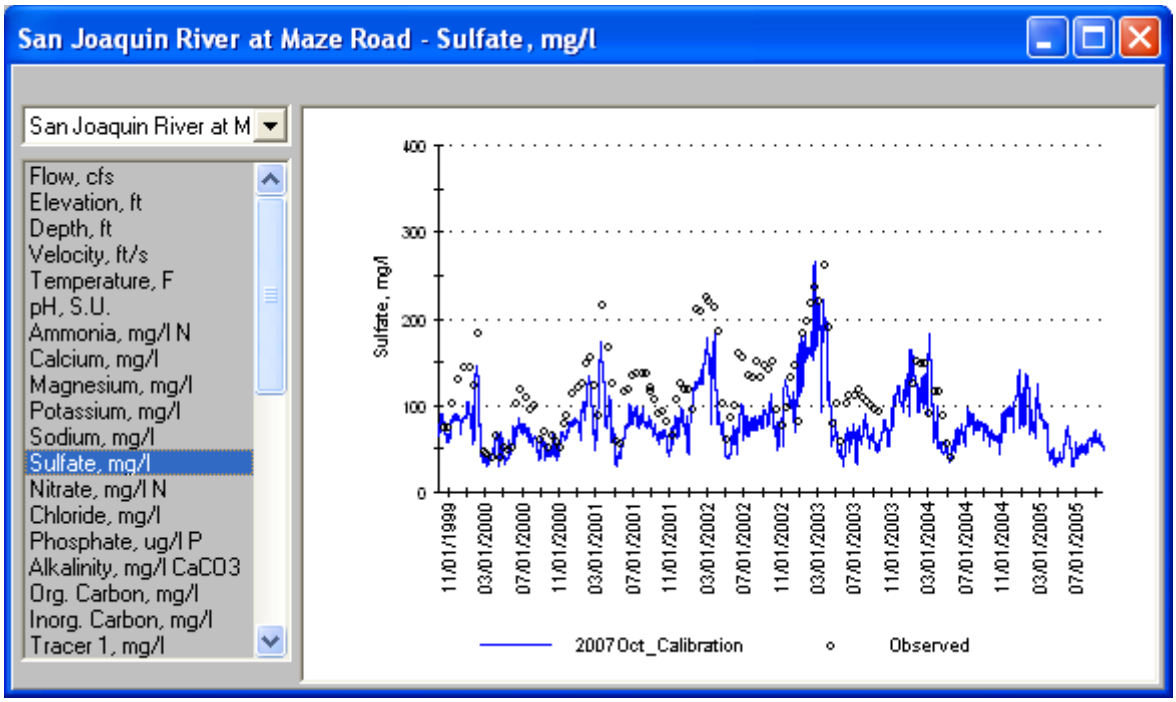

Figure 1.47 Simulated vs Observed Sulfate at Maze Road

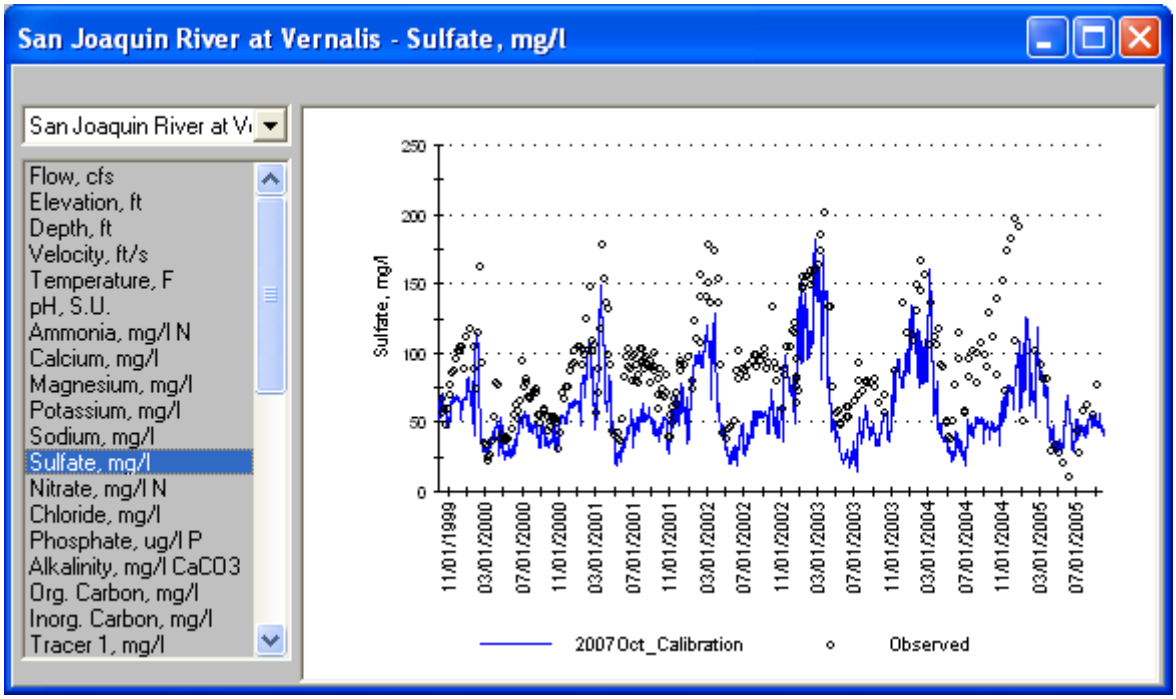

Figure 1.48 Simulated vs Observed Sulfate at Vernalis

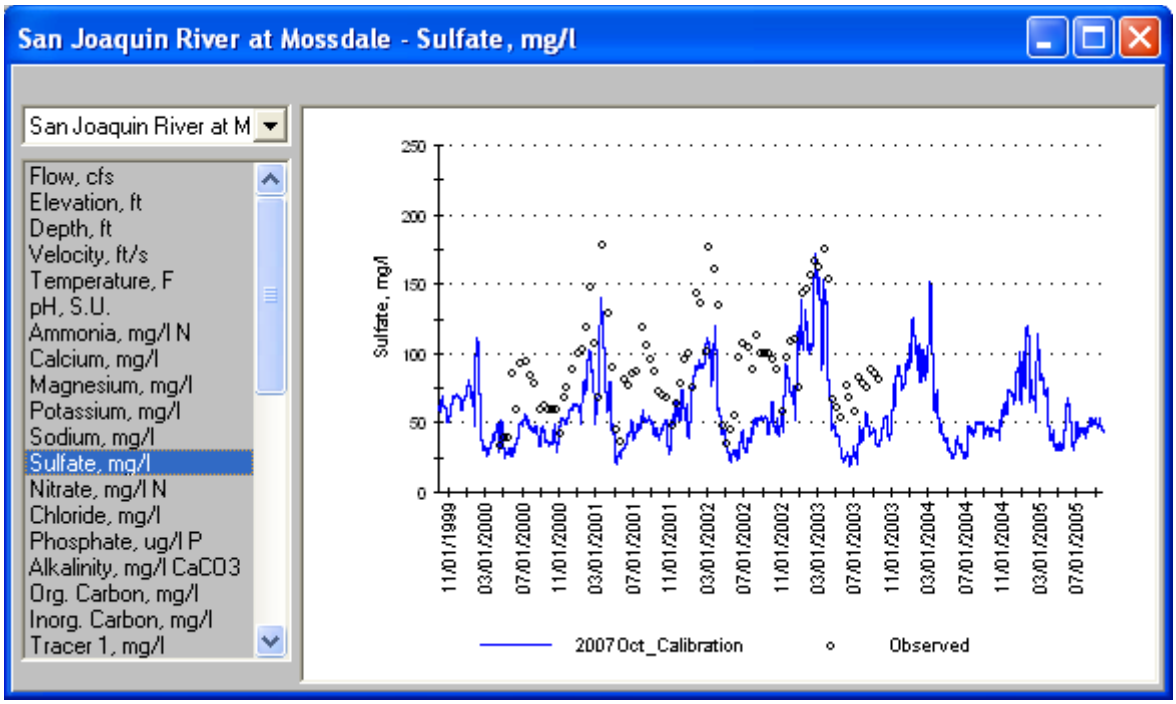

Figure 1.49 Simulated vs Observed Sulfate at Mossdale

Table 1.14 shows the model errors for sulfate concentration at various monitoring stations on the San Joaquin River. The model under predicted the observed sulfate concentrations, with the error increasing going downstream. This was likely caused by the model not simulating enough sulfate in shallow groundwater, which in turn may be caused by an overestimate of the amount of sulfate reduction taking place in the soil or an underestimate of the amount of sulfate in irrigation water.

Table 1.14
Model Errors for Sulfate Concentration in the San Joaquin River

Monitoring Station	Relative Error	Absolute Error
Stevinson	+1%	4%
Crows Landing	-20%	23%
Patterson	-26%	30%
Maze Road	-28%	31%
Vernalis	-34%	36%
Mossdale	-37%	37%

Chloride

Figure 1.50 through Figure 1.54 compare the predicted and observed time series of chloride concentration at various stations along the San Joaquin River. The model followed the observed seasonal pattern of chloride concentration for all stations. But, the model systematically under predicted the chloride concentrations for stations downstream of Patterson. The reason for the under prediction of chloride could be caused by the input errors for the water quality of irrigation

water. The chloride data for the irrigation water were sparse. For the source of irrigation water from the east side tributaries, we typically used low chloride concentrations for the irrigation water, which might introduce errors.

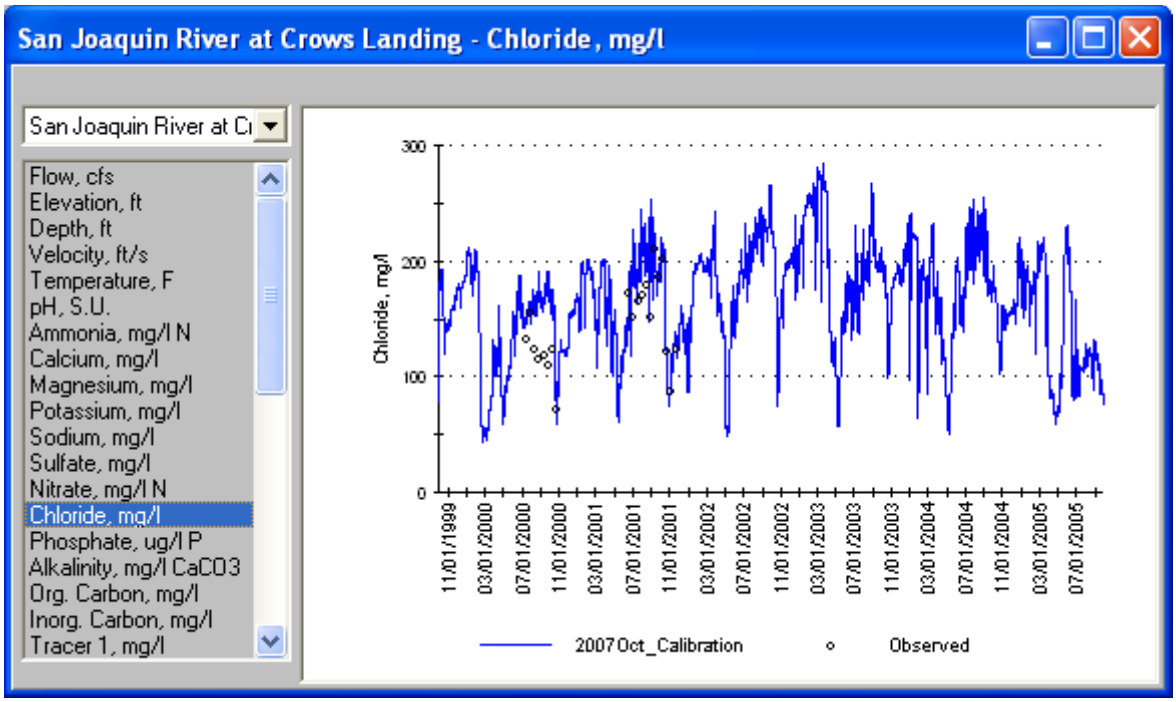

Figure 1.50 Simulated vs Observed Chloride at Crows Landing

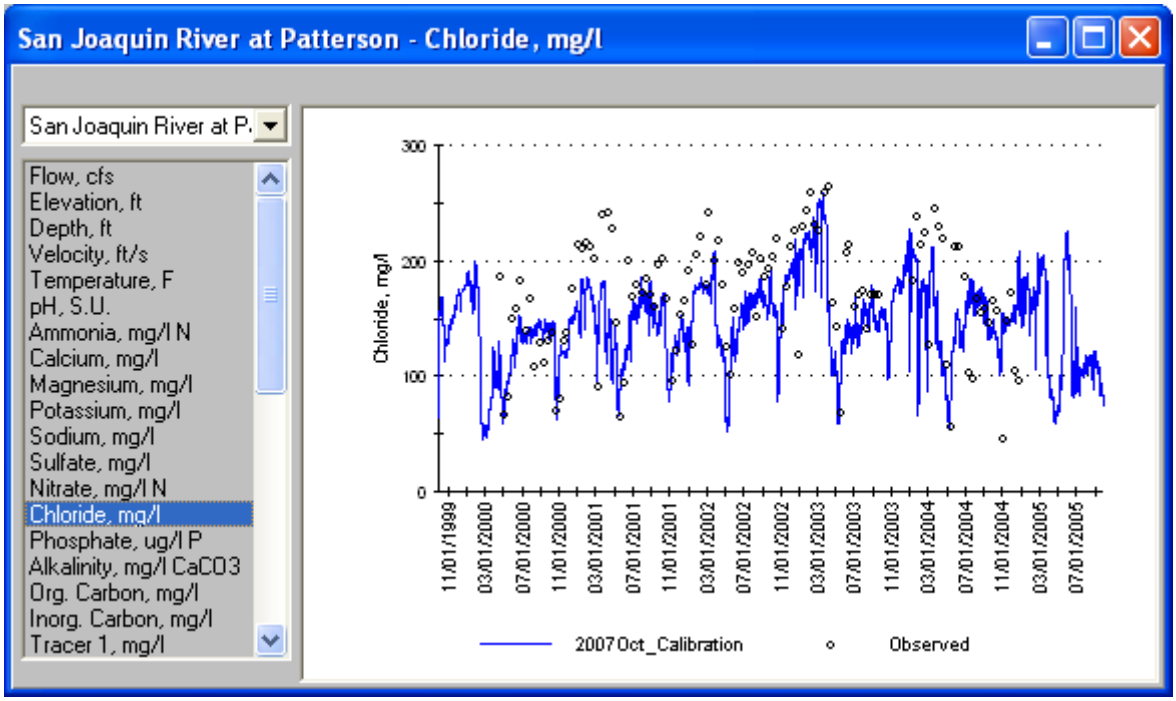

Figure 1.51 Simulated vs Observed Chloride at Patterson

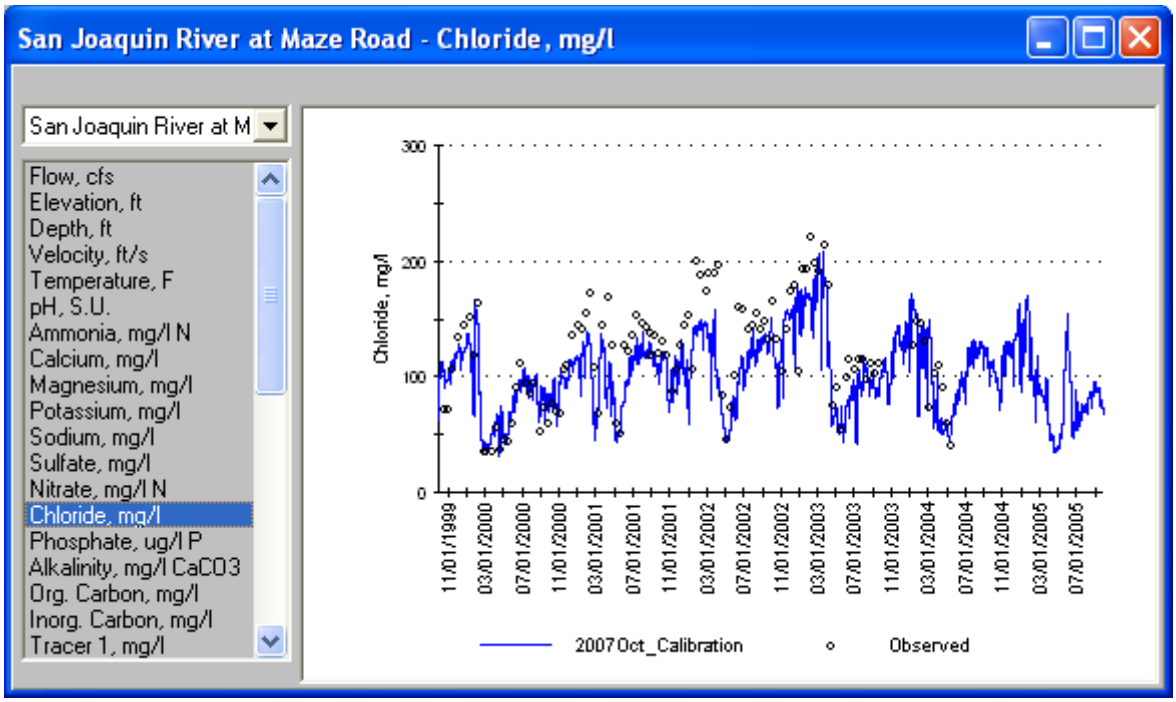

Figure 1.52 Simulated vs Observed Chloride at Maze Road

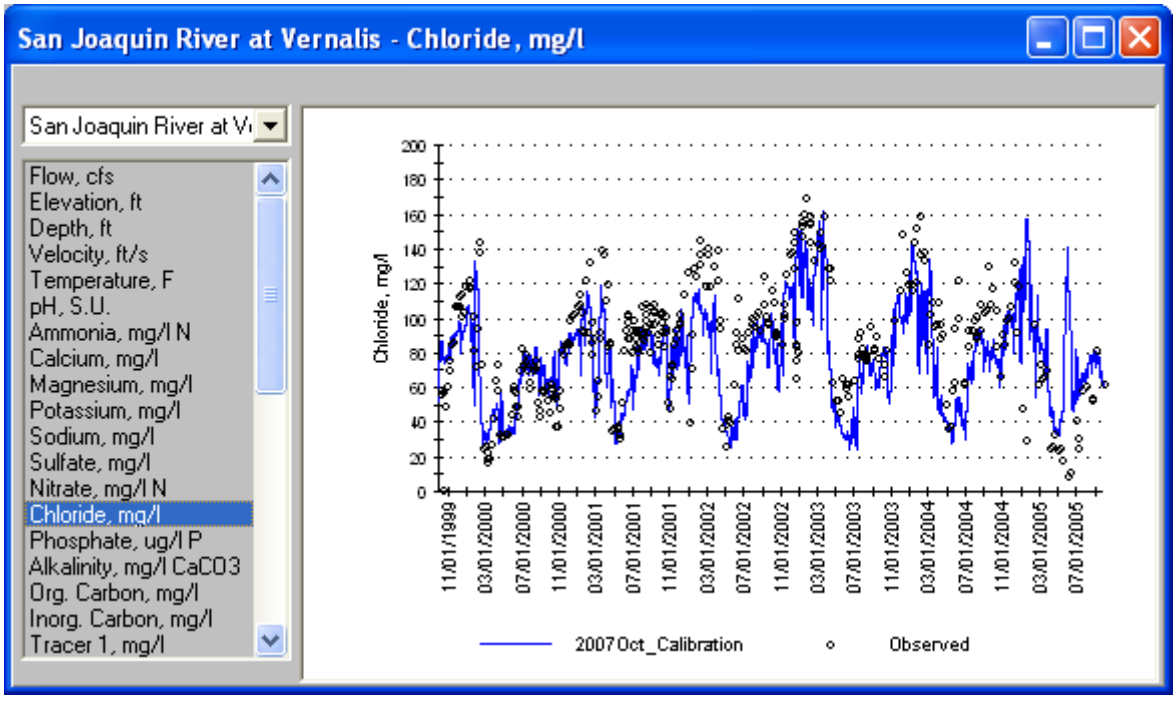

Figure 1.53 Simulated vs Observed Chloride at Vernalis

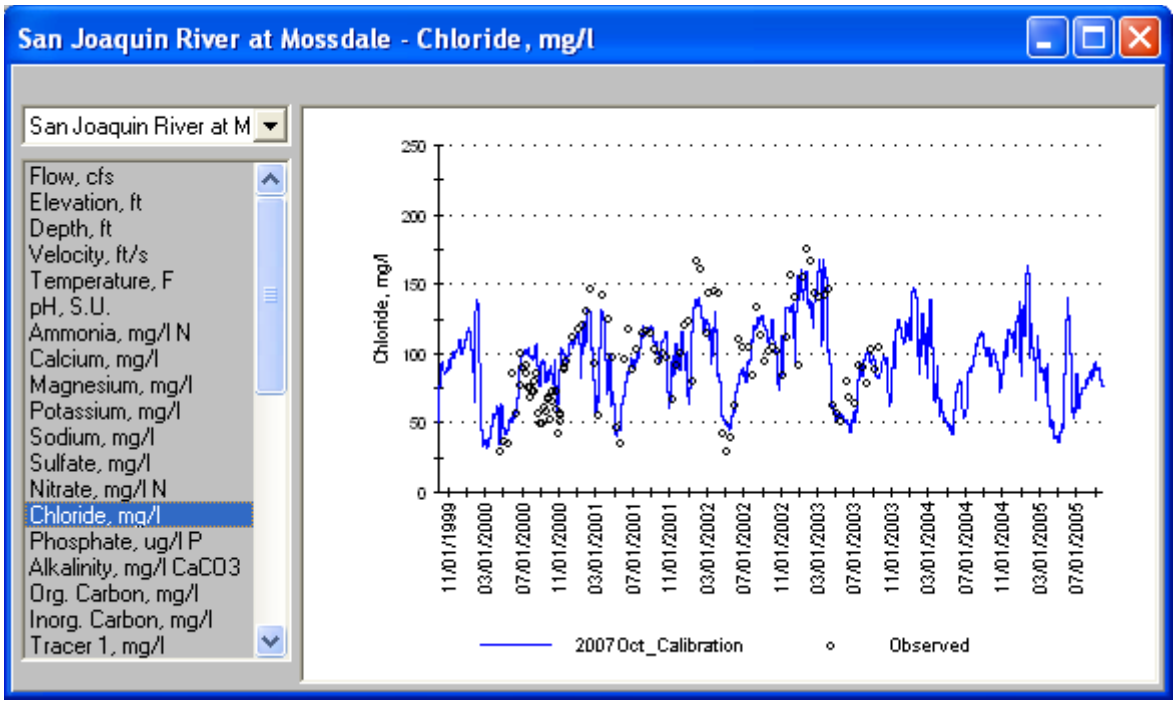

Figure 1.54 Simulated vs Observed Chloride at Mossdale

Table 1.15 shows the model errors for chloride concentration at various monitoring stations on the San Joaquin River. The model slightly under predicted the chloride concentration in general, but absolute error was under 20% at 5 of 6 stations. Assumptions about individual ion concentrations in irrigation water affect the predicted shallow groundwater and are important factors in simulated chloride concentration.

Table 1.15
Model Errors for Chloride Concentration in the San Joaquin River

Monitoring Station	Relative Error	Absolute Error
Stevinson	+0%	3%
Crows Landing	+16%	19%
Patterson	-13%	20%
Maze Road	-13%	19%
Vernalis	-12%	23%
Mossdale	+1%	17%

Conservative EC

Figure 1.25 through Figure 1.29 compare the predicted and observed time series of "Conservative EC" at various stations along the San Joaquin River. Although observed data obscured the simulation results in some of the graphs below, the simulation results generally tracked the observed data closely.

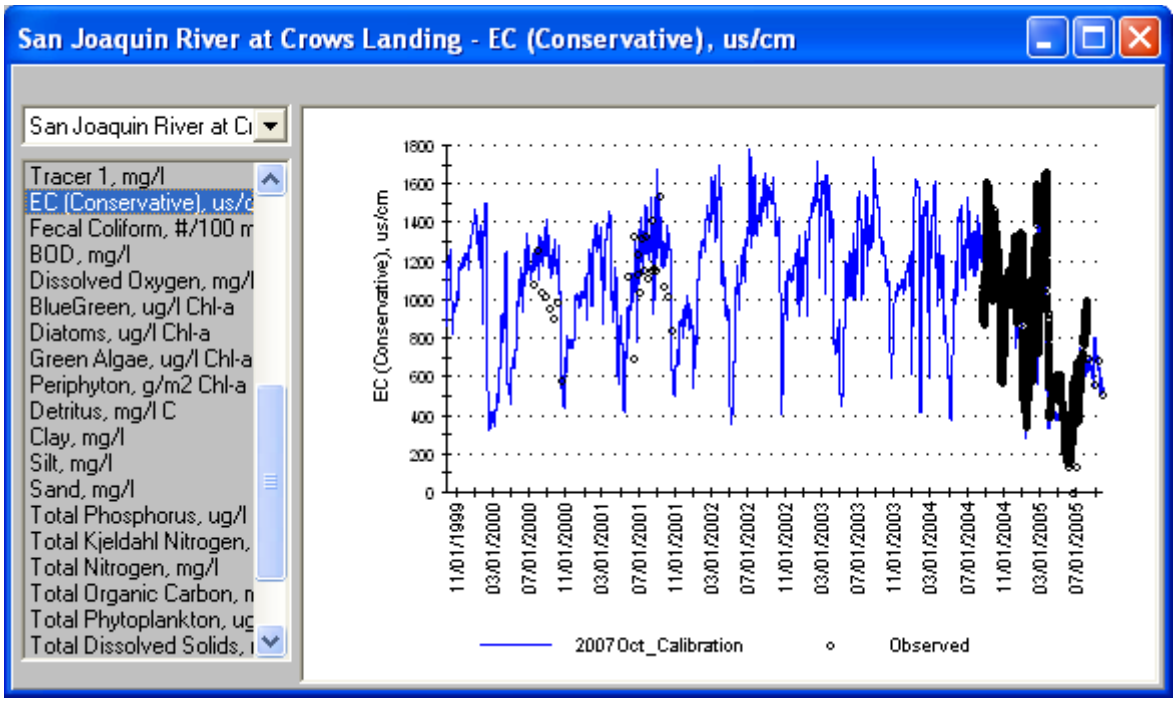

Figure 1.55 Simulated vs Observed "Conservative EC" at Crows Landing

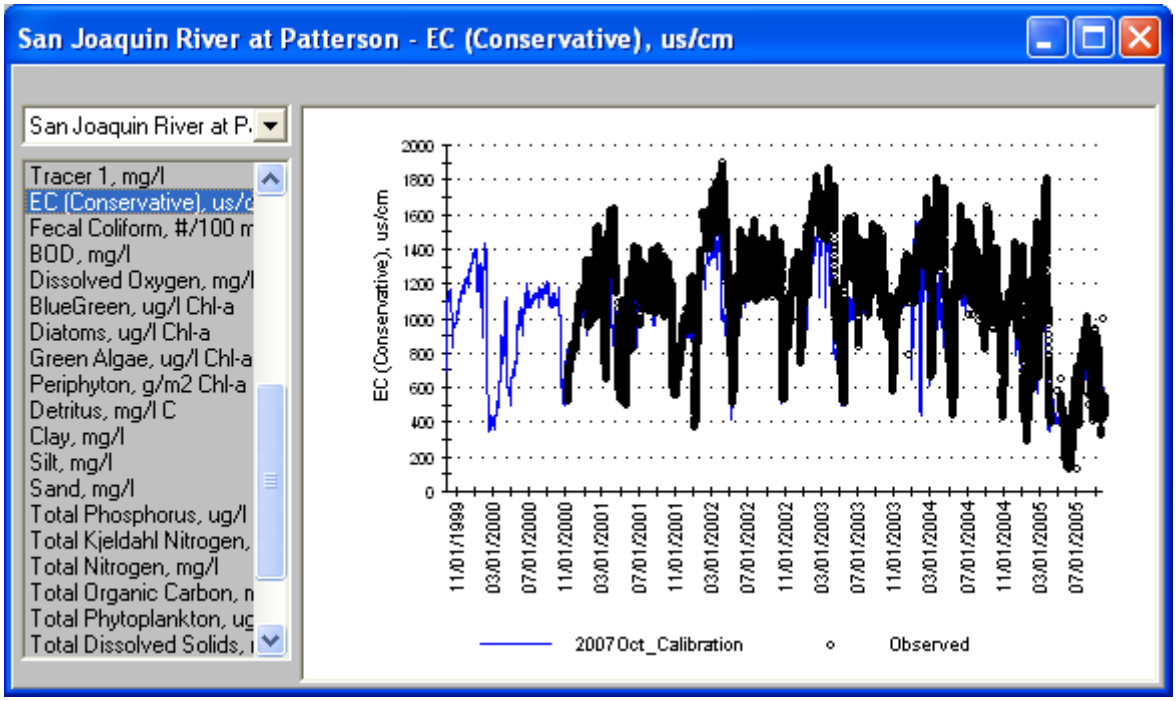

Figure 1.56 Simulated vs Observed "Conservative EC" at Patterson

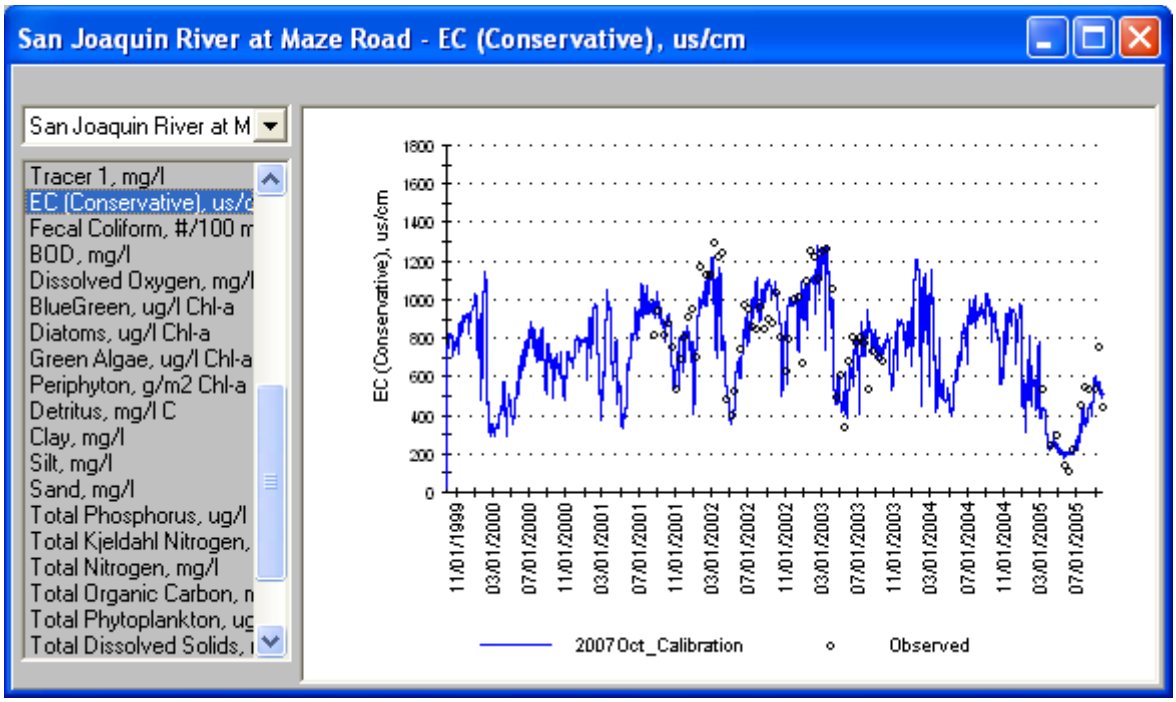

Figure 1.57 Simulated vs Observed "Conservative EC" at Maze Road

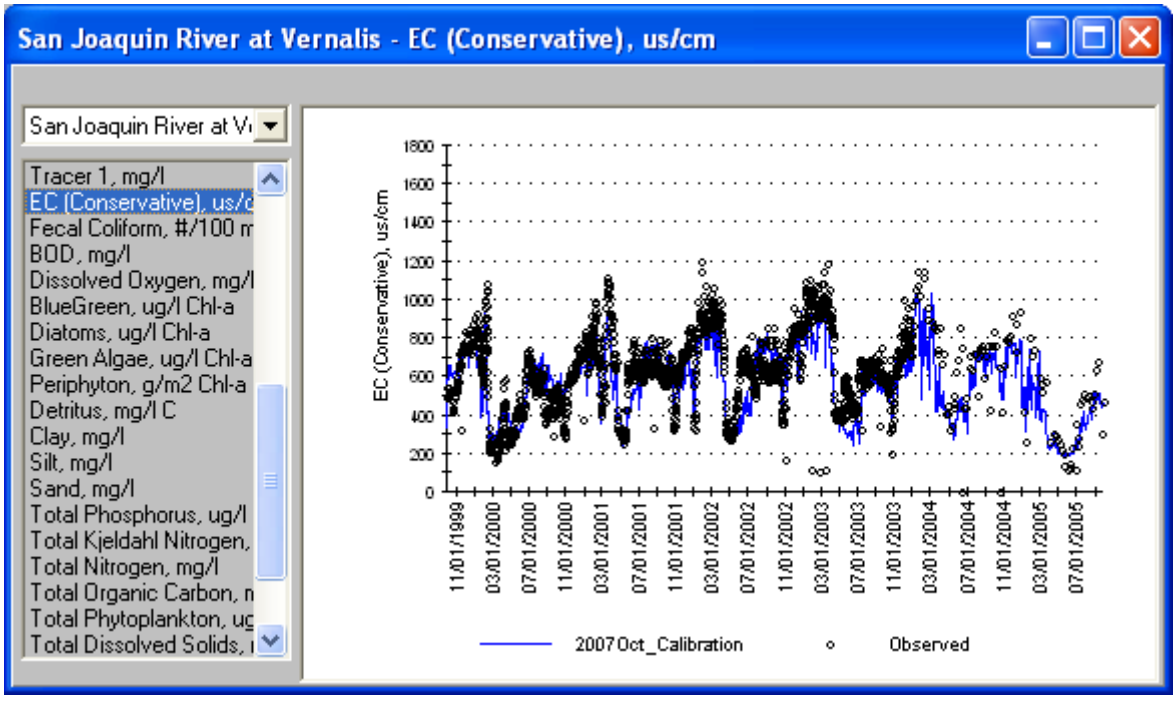

Figure 1.58 Simulated vs Observed "Conservative EC" at Vernalis

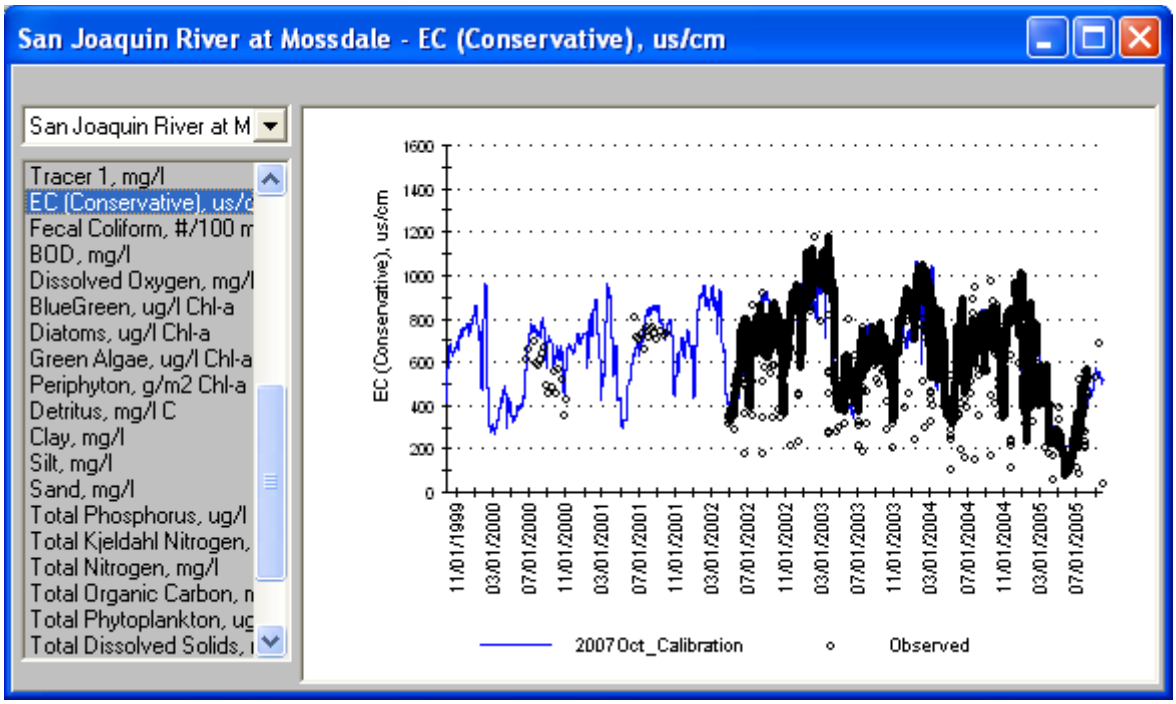

Figure 1.59 Simulated vs Observed "Conservative EC" at Mossdale

Table 1.10 shows the model errors for "Conservative EC" at various monitoring stations on the San Joaquin River. The model slightly under predicted "Conservative EC" at all stations, although relative error was within 10% and absolute error is under 20% at all stations.

Table 1.16
Model Errors for "Conservative EC" in the San Joaquin River

Monitoring Station	Relative Error	Absolute Error
Stevinson	-1%	5%
Crows Landing	-7%	15%
Patterson	-10%	14%
Maze Road	-3%	14%
Vernalis	-6%	16%
Mossdale	-4%	13%

Non Conservative EC

Figure 1.60 through Figure 1.65 compared the predicted and observed time series of "non conservative EC" at various stations along the San Joaquin River. Unlike "conservative EC", "non-conservative EC" reflected processes which can affect ions as they are transported throughout the watershed, including adsorption, settling, and equilibration of inorganic carbon with the atmosphere. In general, the predicted "non conservative EC" tracked the seasonal patterns of observed EC. The "non conservative EC" concentrations were systematically somewhat higher than the observed EC, although the pattern of observed data is followed closely.

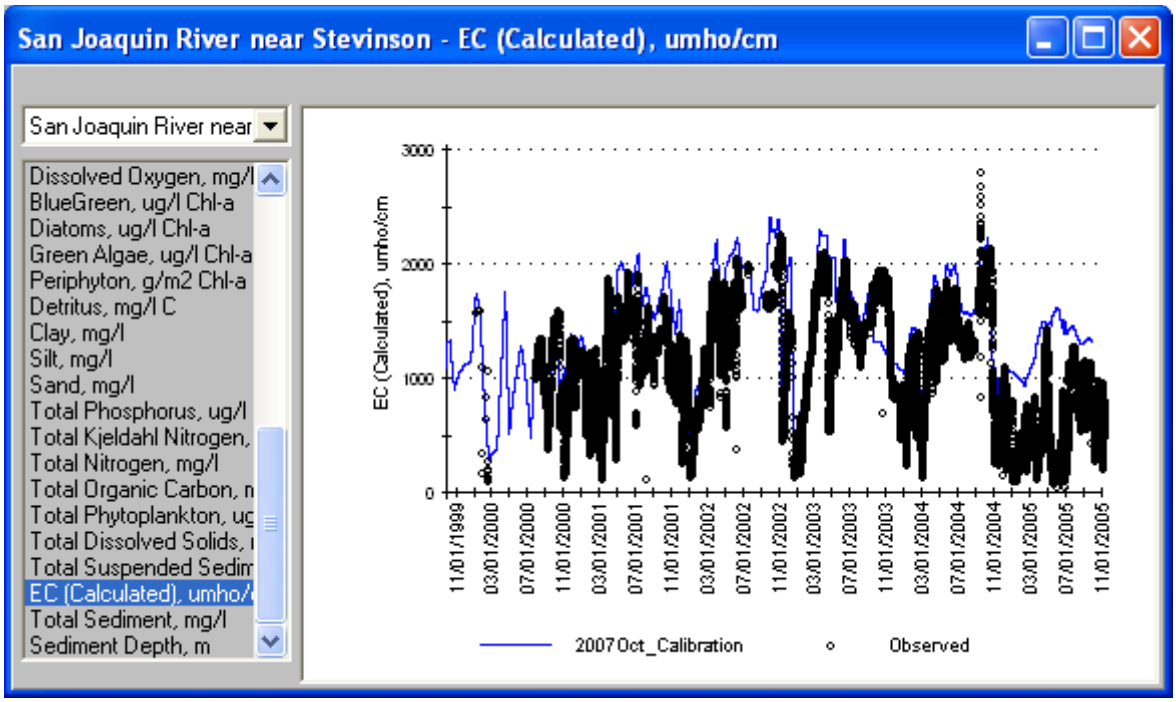

Figure 1.60 Simulated vs Observed "Non conservative EC" at Stevinson (Lander Ave.)

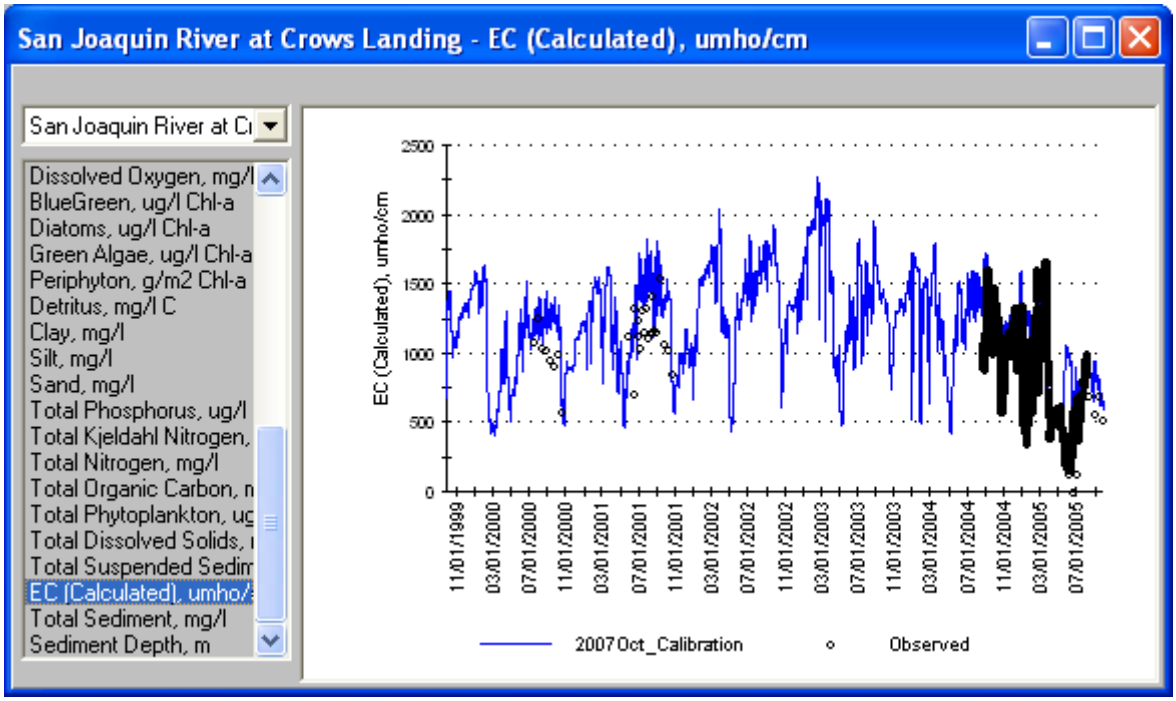

Figure 1.61 Simulated vs Observed "Non conservative EC" at Crows Landing

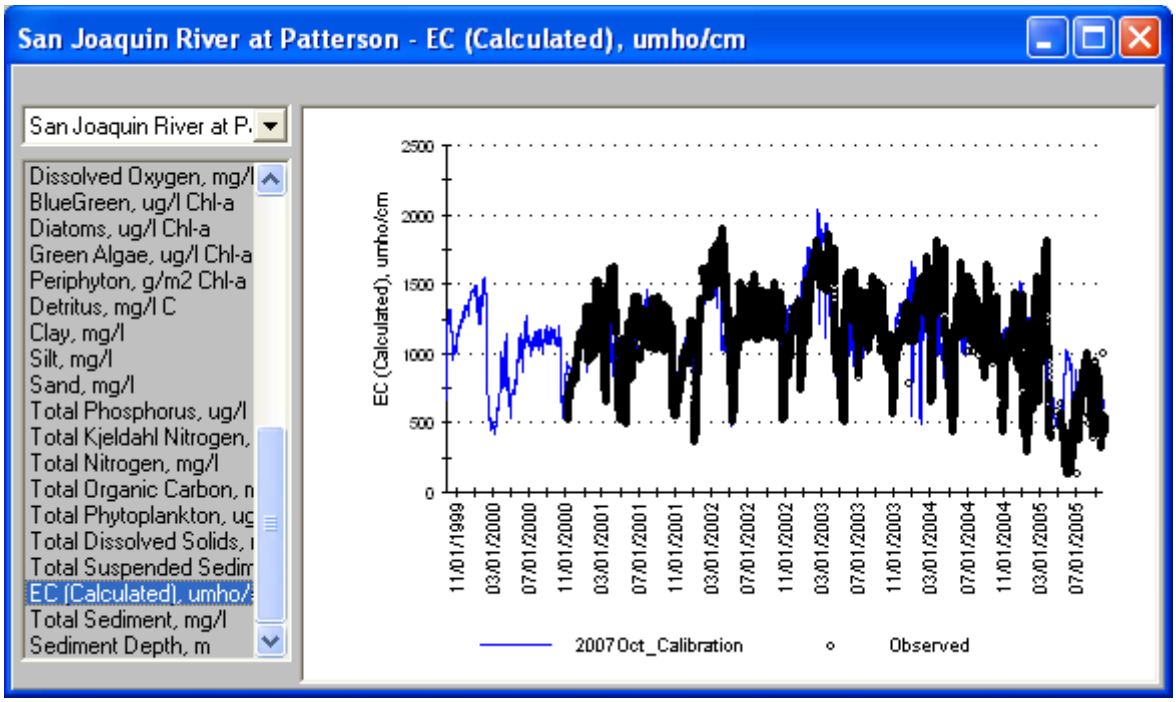

Figure 1.62 Simulated vs Observed "Non conservative EC" at Patterson

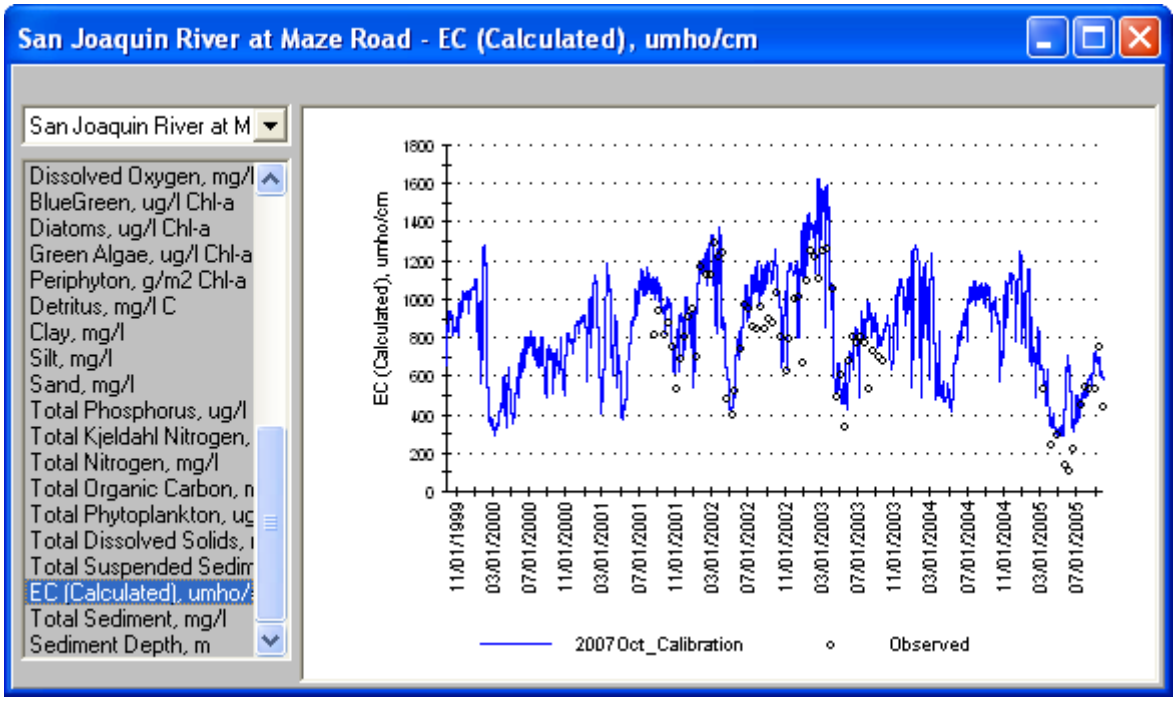

Figure 1.63 Simulated vs Observed "Non conservative EC" at Maze Road

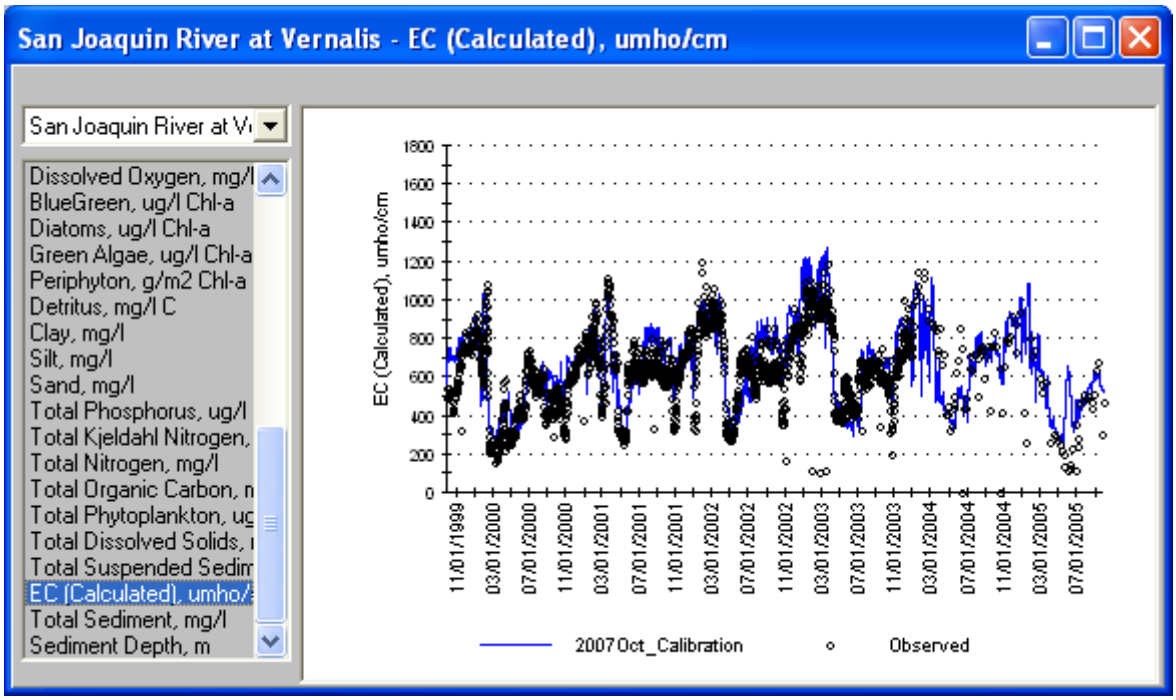

Figure 1.64 Simulated vs Observed "Non conservative EC" at Vernalis

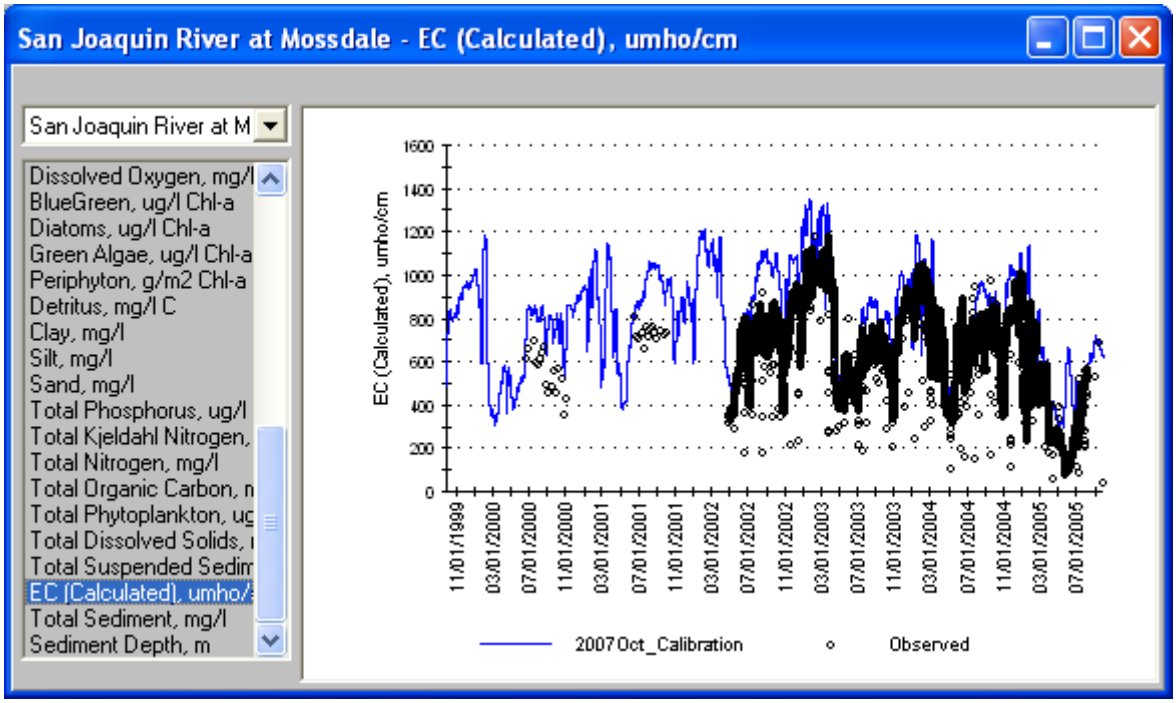

Figure 1.65 Simulated vs Observed "Non conservative EC" at Mossdale

Table 1.17 shows the model errors for "non conservative EC" at various monitoring stations on the San Joaquin River. The table shows that the over predictions of "non conservative EC" actually started at the most upstream stations (Stevinson and Crows Landing stations). These errors propagated to the downstream stations. The error is caused largely by the model's

underprediction of anion concentrations. This leads to high bicarbonate concentration to balance the charge and maintain pH equilibrium. Bicarbonate ion above neutral pH is included in calculation of TDS and "non-conservative EC".

Table 1.17
Model Errors for "Non conservative EC" in the San Joaquin River

Monitoring Station	Relative Error	Absolute Error
Stevinson	26%	31%
Crows Landing	25%	29%
Patterson	1%	15%
Maze Road	14%	20%
Vernalis	8%	17%
Mossdale	21%	24%

Inorganic Carbon

Figure 1.66 through Figure 1.69 compare the predicted and observed time series of inorganic carbon at various stations along the San Joaquin River. The model followed the seasonal patterns of observed inorganic carbon concentration, which is basically the alkalinity. The model over predicted the inorganic carbon concentration during the irrigation seasons.

WARMF performs complete simulation of pH, alkalinity, and carbonate and bicarbonate equilibrium. The water quality of the boundary river inflows were set up to match ion concentrations, not pH. The pH is theoretically defined by the ion concentrations. The model calculates pH by equilibrium, which is subject to errors in interpolation. River inflows are assumed to have inorganic carbon in equilibrium with the atmosphere. Measured alkalinity of boundary inflows often did not agree with the theoretical alkalinity, calculated by the sum of cations minus the sum of anions. All these make it difficult to match the calculated inorganic carbon concentration to the measured alkalinity concentration.

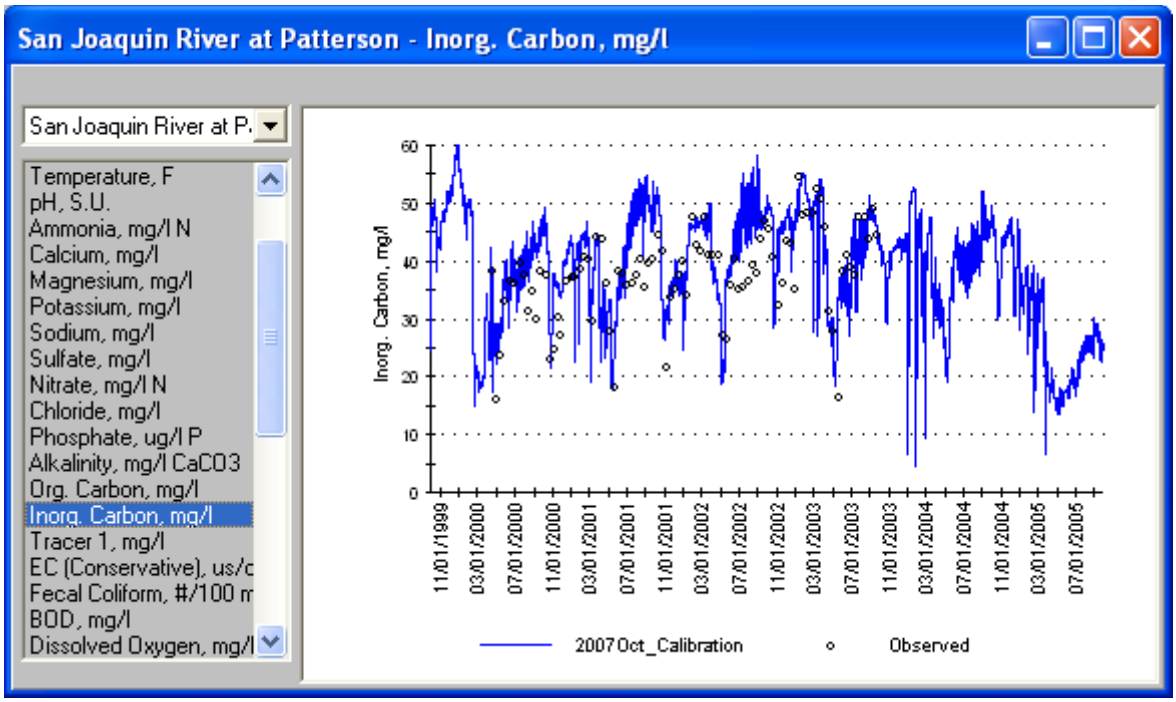

Figure 1.66 Simulated vs Observed Inorganic Carbon at Patterson

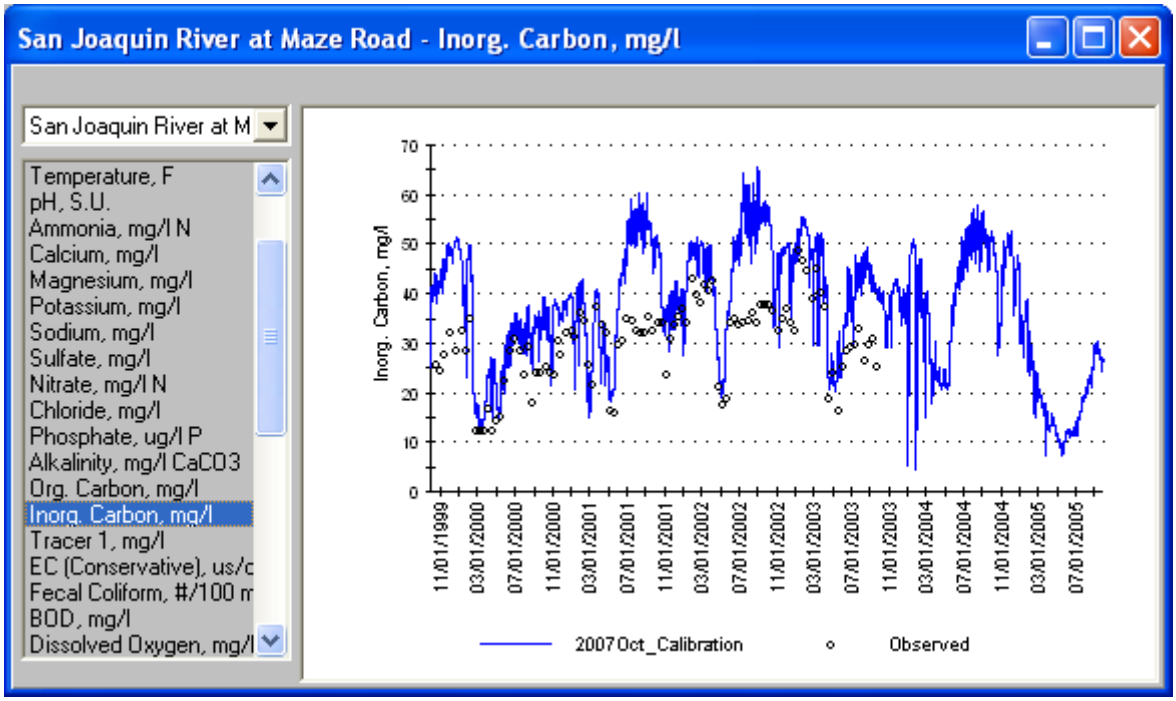

Figure 1.67 Simulated vs Observed Inorganic Carbon at Maze Road

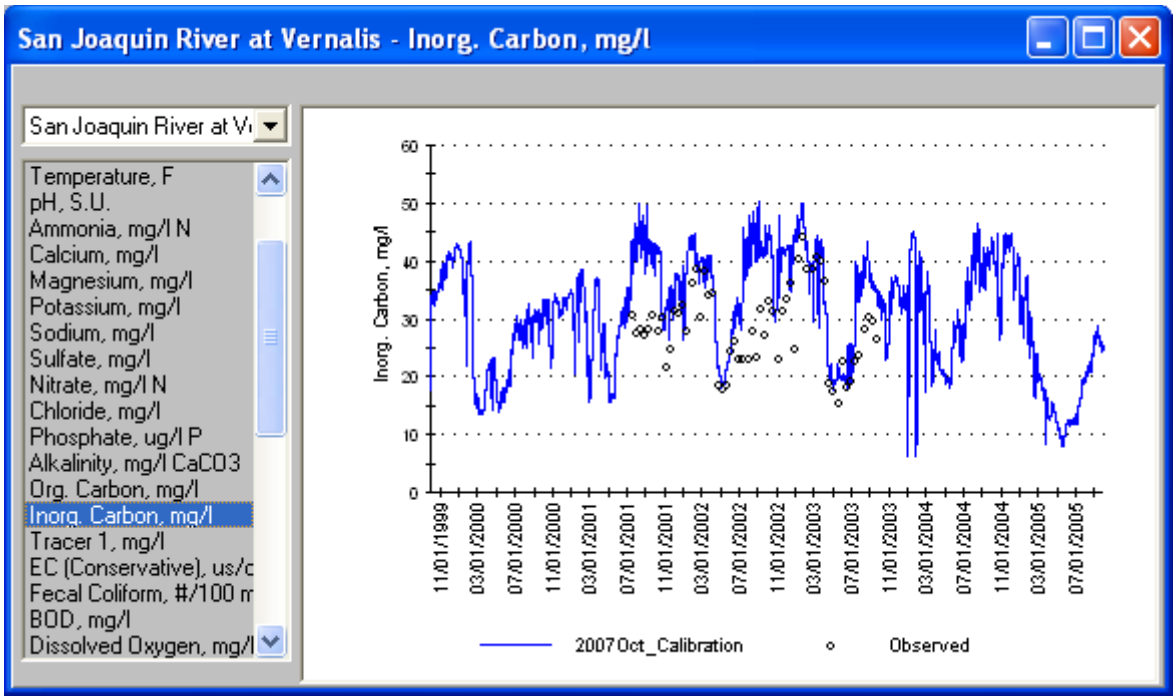

Figure 1.68 Simulated vs Observed Inorganic Carbon at Vernalis

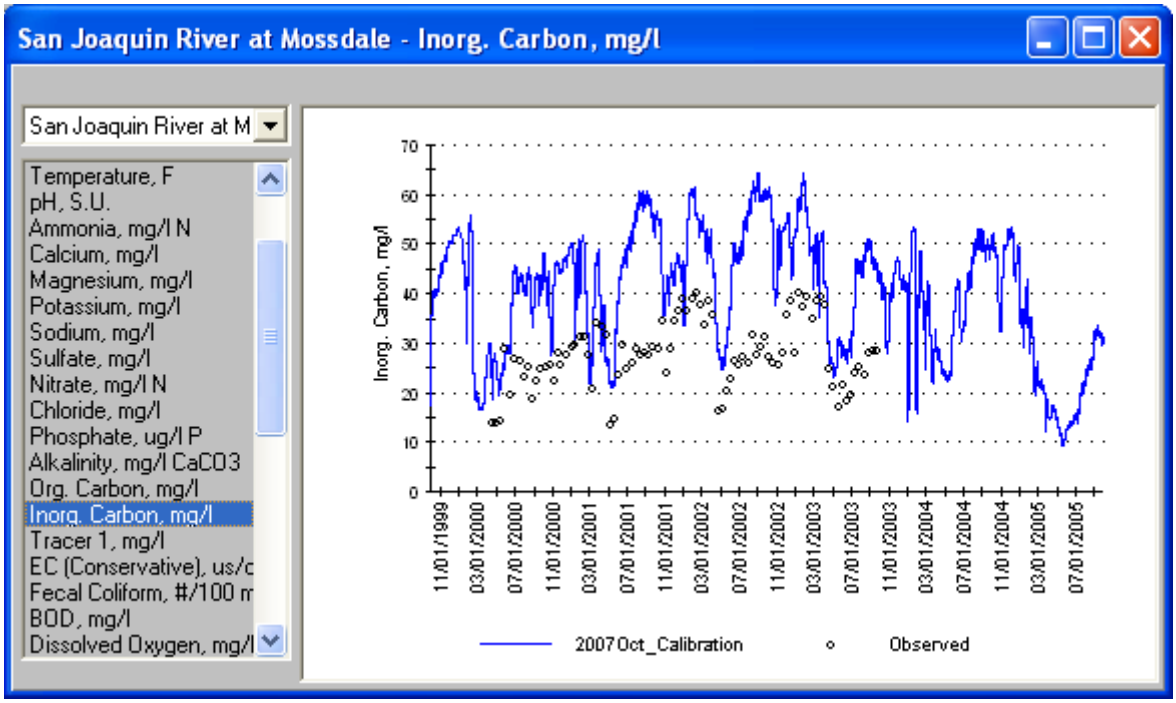

Figure 1.69 Simulated vs Observed Inorganic Carbon at Mossdale

Table 1.18 shows the model error for inorganic carbon concentration at various monitoring stations on the San Joaquin River. The over predictions of inorganic carbon concentration could be improved by better calibration of anions (sulfate and chloride), which the model

underpredicted. That would shift the pH equilibrium and reduce the amount of predicted inorganic carbon.

Table 1.18
Model Errors for Inorganic Carbon Concentration in the San Joaquin River

Monitoring Station	Relative Error	Absolute Error
Stevinson	+0%	4%
Crows Landing	No data	No data
Patterson	7%	13%
Maze Road	30%	30%
Vernalis	24%	25%
Mossdale	57%	58%

Ammonia

Figure 1.70 through Figure 1.76 compare the time series of predicted and observed ammonia concentration at various stations along the San Joaquin River. The results for Buckley Cove (Station R6) are based on the Link-Node model.

Several observations can be made. The observed ammonia concentrations were very low, generally below 1 mg/l, mostly below 0.5 mg/l. Observed ammonia concentrations were lowest in summer. The expanded scale led to the impression that ammonia concentrations varied a lot within a short range. The hourly simulated ammonia concentrations showed great diurnal variation during the summer due to high algal growth and nutrient uptake. While simulated ammonia fluctuated, observed data is consistently very low in summer. In winter, observed data shows higher concentrations than in simulation results.

The algorithm used to calculate phytoplankton uptake of nitrogen in WARMF favors ammonia. For example, if the ammonia concentration in the water were 0.1 mg/l while nitrate was 2 mg/l, the model still assumed that 90% of the nitrogen uptake is in the form of ammonia. When the phytoplankton respires, the model assumed that the ammonia is then released to the water column in dissolved form. Instead, the released ammonia may be in a form not measured in the dissolved ammonia measurements.

The observed ammonia concentrations for 2000 to 2003 at Mossdale Station and Patterson Station were much higher than the predicted values. The observed concentrations for 2004 to 2005 were lower and closer to the simulated results. We were not certain whether there was a change of sampling procedure to account for the difference. The river morphology changes significantly between Vernalis and Mossdale, which could affect biological processes. Although the model assumed that the tidal zone extends only as far upstream as the Old River, under low flow conditions the tidal influence can go upstream of the monitoring station at Mossdale. Under these conditions, ammonia discharged by the Stockton wastewater treatment plant could be influencing measurements at Mossdale, but this was not accounted for in the model.

The Garwood Bridge station is in the tidal reach of the San Joaquin River between the Old River and the DWSC. The Buckley Cove Station (R6) is located further down stream in the DWSC.

The good match between the predicted and observed values again proved the predictive power of the Link-Node model.

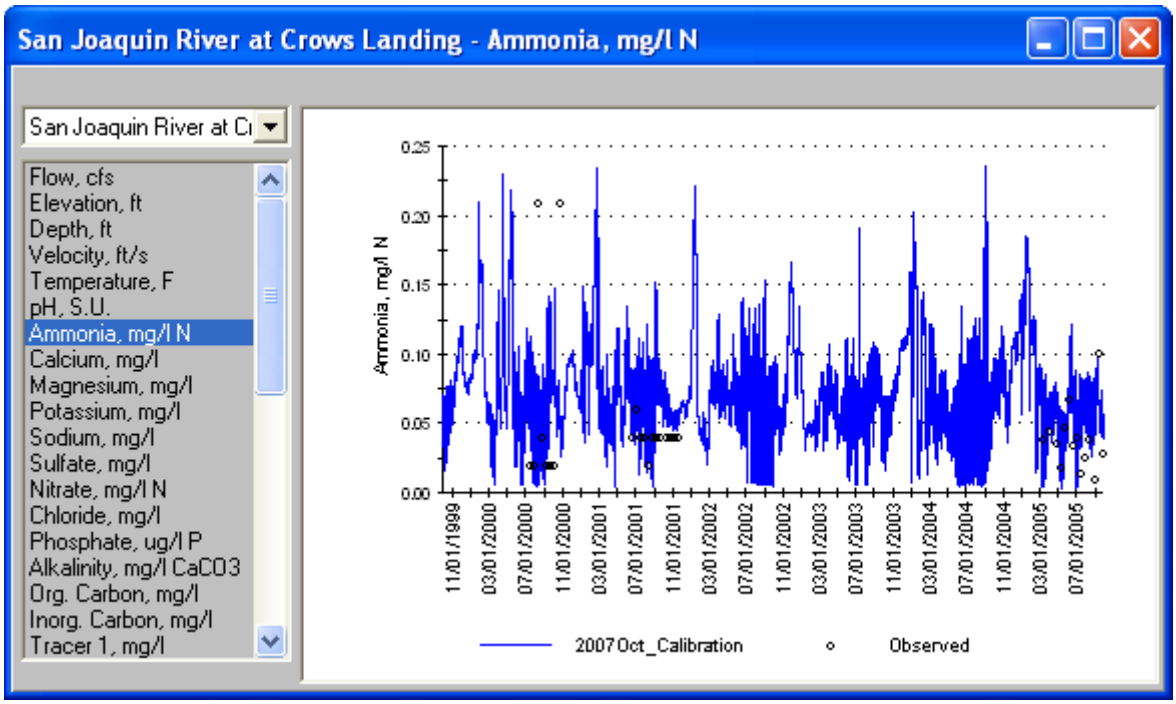

Figure 1.70 Simulated vs Observed Ammonia at Crows Landing

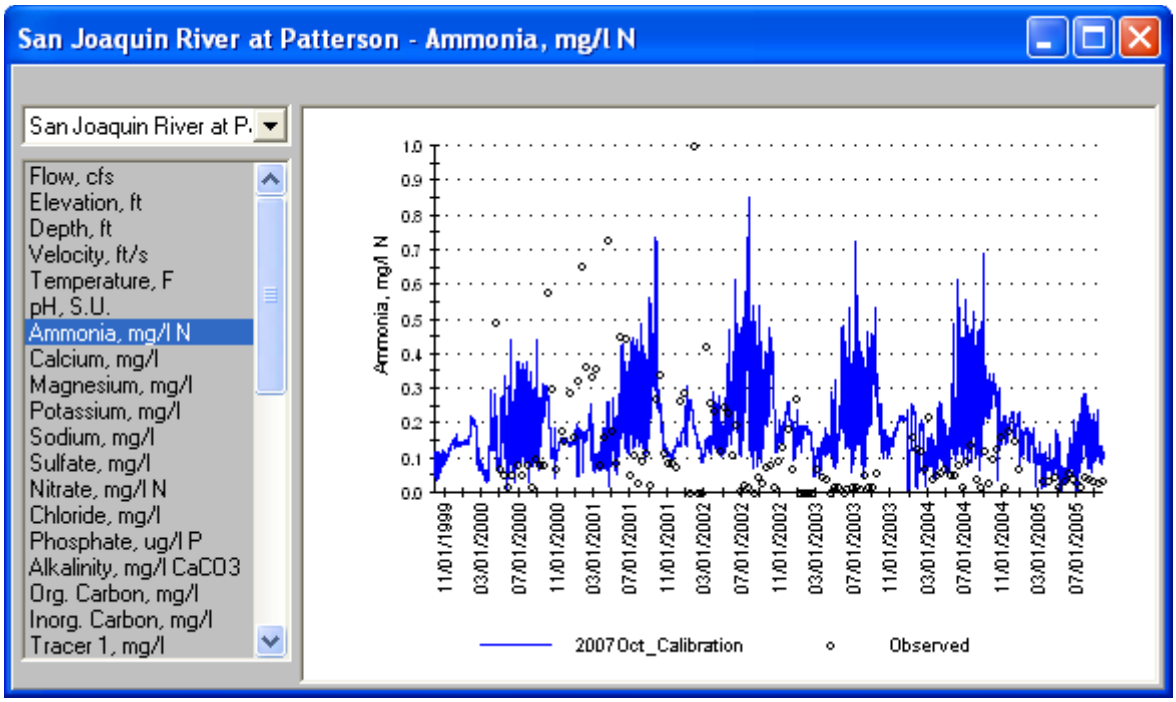

Figure 1.71 Simulated vs Observed Ammonia at Patterson

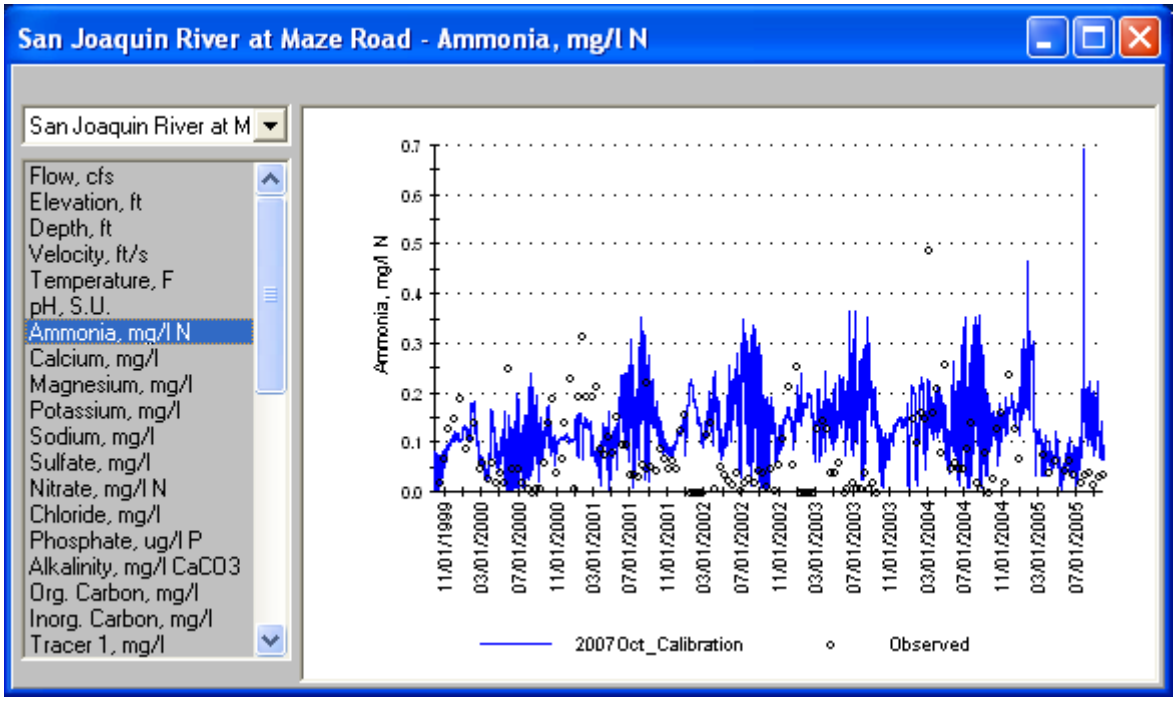

Figure 1.72 Simulated vs Observed Ammonia at Maze Road

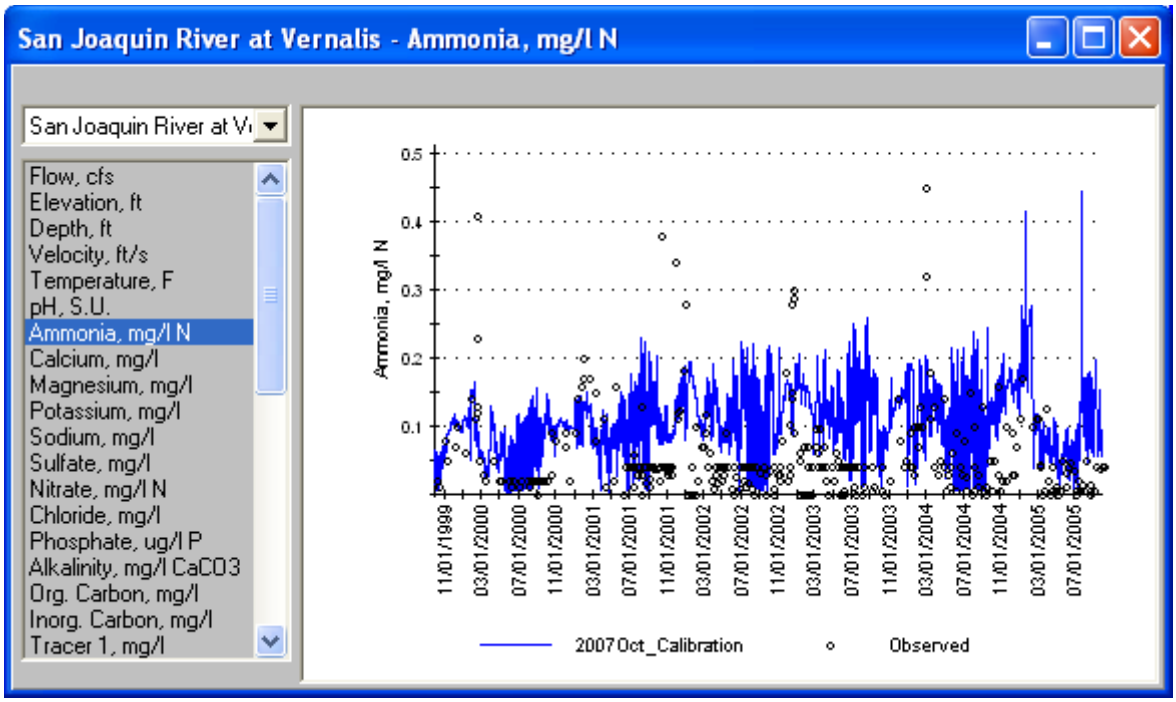

Figure 1.73 Simulated vs Observed Ammonia at Vernalis

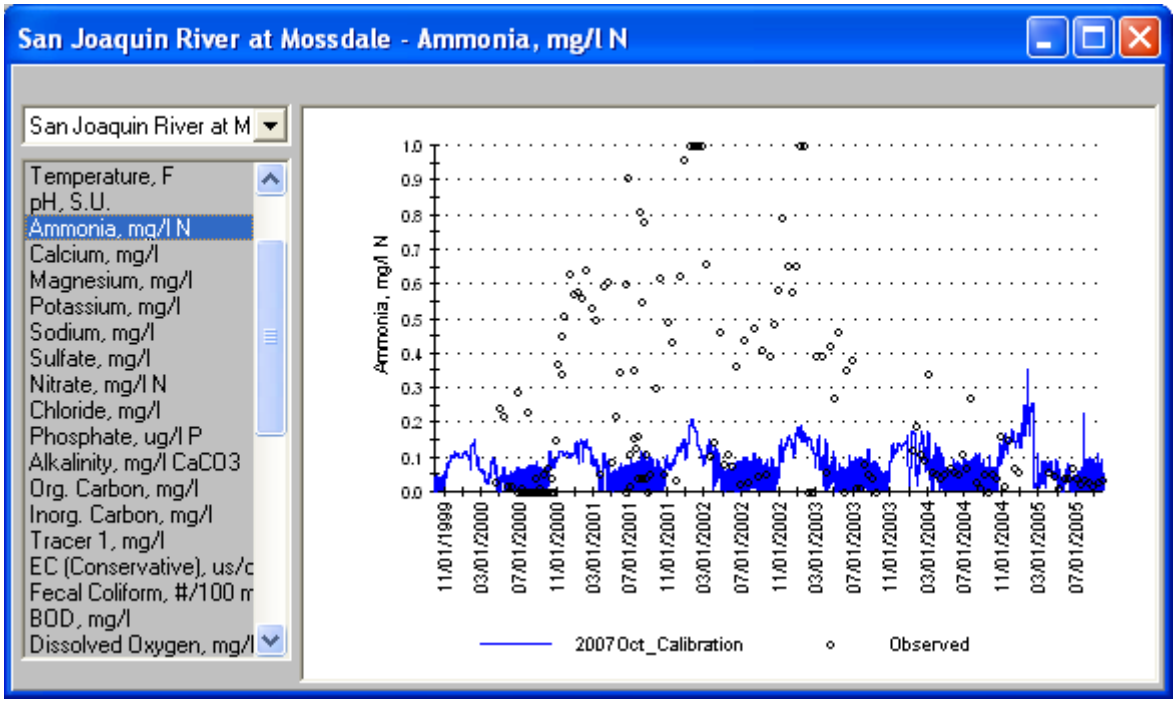

Figure 1.74 Simulated vs Observed Ammonia at Mossdale

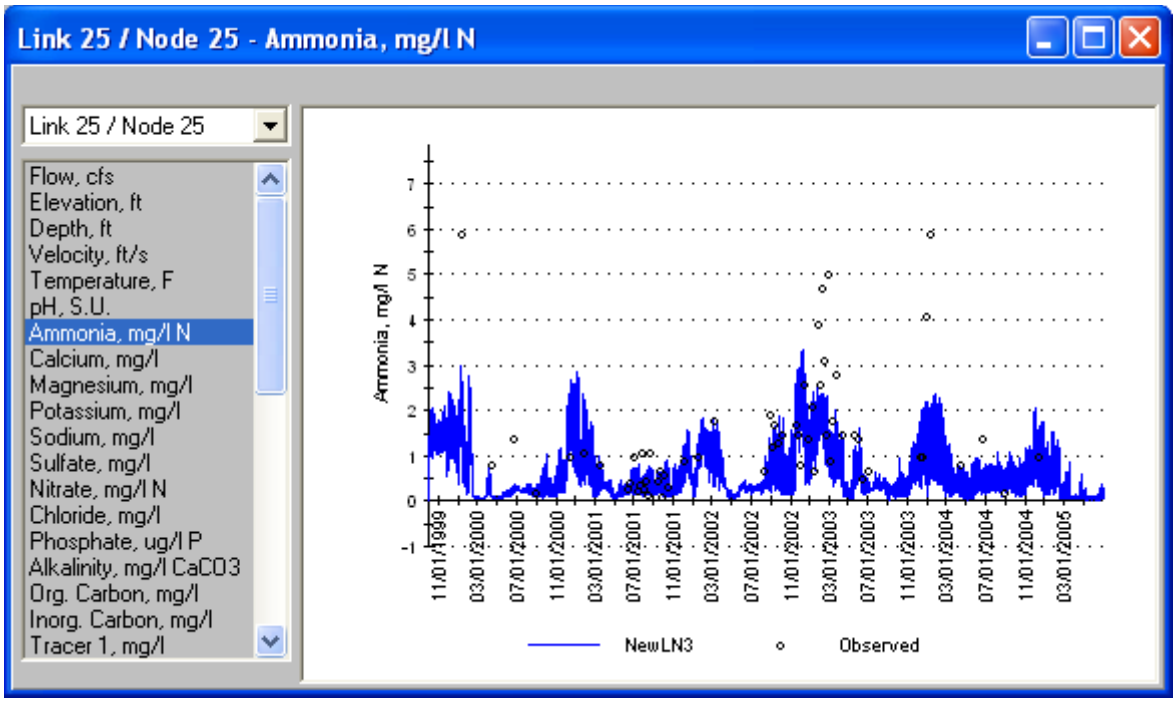

Figure 1.75 Simulated vs Observed Ammonia at Garwood Bridge

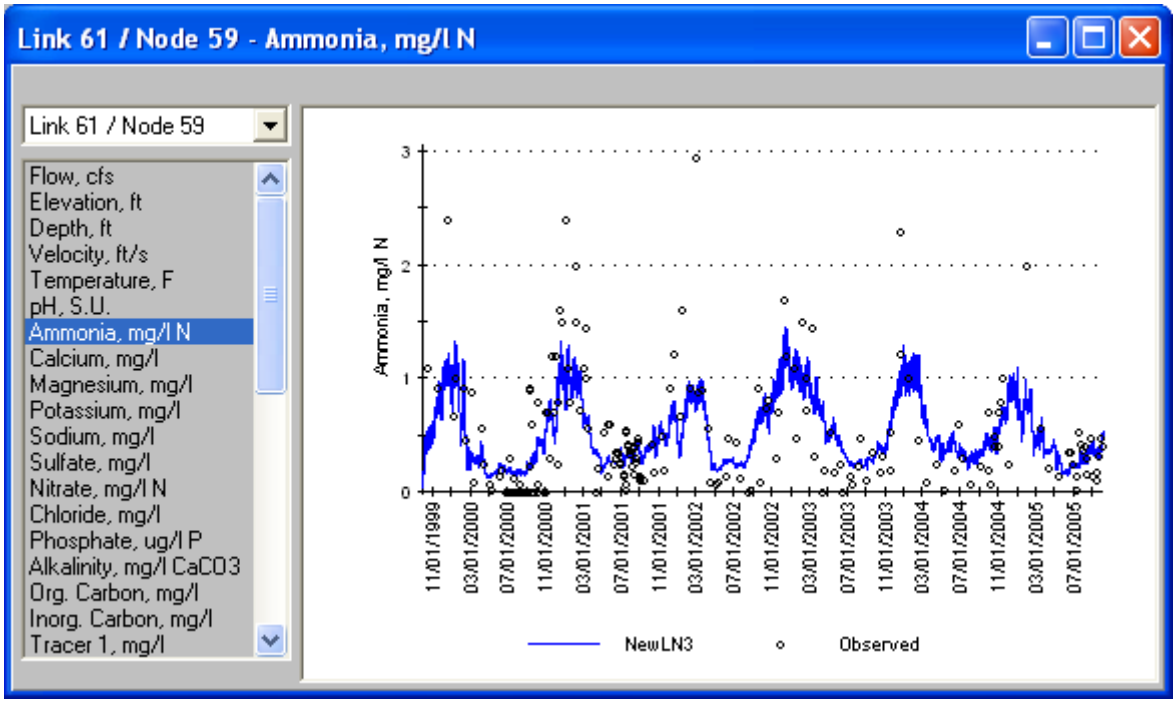

Figure 1.76 Simulated vs Observed Ammonia at Buckley Cove (Station R6)

The measured data at Mossdale appears to have concentrations in excess of 0.3 mg/l much more frequently than other stations. This means either there is a chemical/physical process occurring near Mossdale which is unique in the upstream San Joaquin River or there is a data measurement error. The observed data compiled in WARMF comes from a variety of sources, as shown in

Figure 1.77. Note that data collected for the San Joaquin River Dissolved Oxygen TMDL, shown in blue, and Bay Delta and Tributaries Project C7A in magenta recorded concentrations which never exceeded 0.1 mg/l from 2005 through 2007. Data collected from multiple sources into the San Joaquin River Data Atlas shows many measured values greater than 0.2 mg/l from 2000-2004 but few points that high from 1984 through 1995. Differences in analytical methods could account for the spread in concentrations seen at Mossdale.

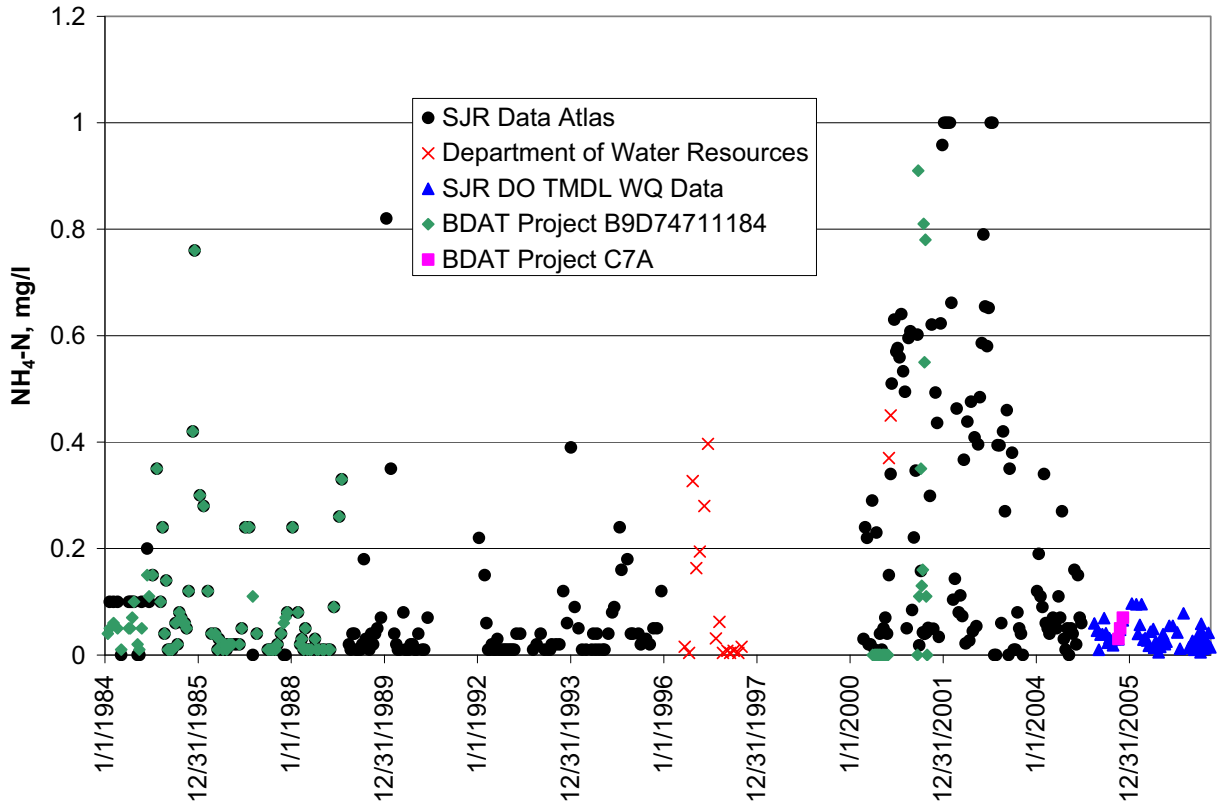

Figure 1.77 Sources of Observed Ammonia Data at Mossdale

Table 1.19 shows the model errors for ammonia at various monitoring stations on the San Joaquin River. The predicted concentrations were much greater than observed. The simulation does not have large relative error at Buckley Cove because the source of ammonia from the Stockton wastewater treatment plant is a major source of loading in the DWSC.

Table 1.19
Model Errors for Ammonia Concentration in the San Joaquin River

Monitoring Station	Relative Error	Absolute Error
Stevinson	3%	18%
Crows Landing	45%	90%
Patterson	60%	127%
Maze Road	96%	133%
Vernalis	111%	148%
Mossdale	-69%	85%
Garwood Bridge	-33%	56%
Buckley Cove (Stockton R6)	+1%	54%

Nitrate

Figure 1.78 through Figure 1.84 compare the time series of simulated and observed nitrate at various stations along the San Joaquin River. The results for Buckley Cove (R6) in the DWSC were from the Link-Node model. The match for predicted and observed nitrate concentration was very good for all stations.

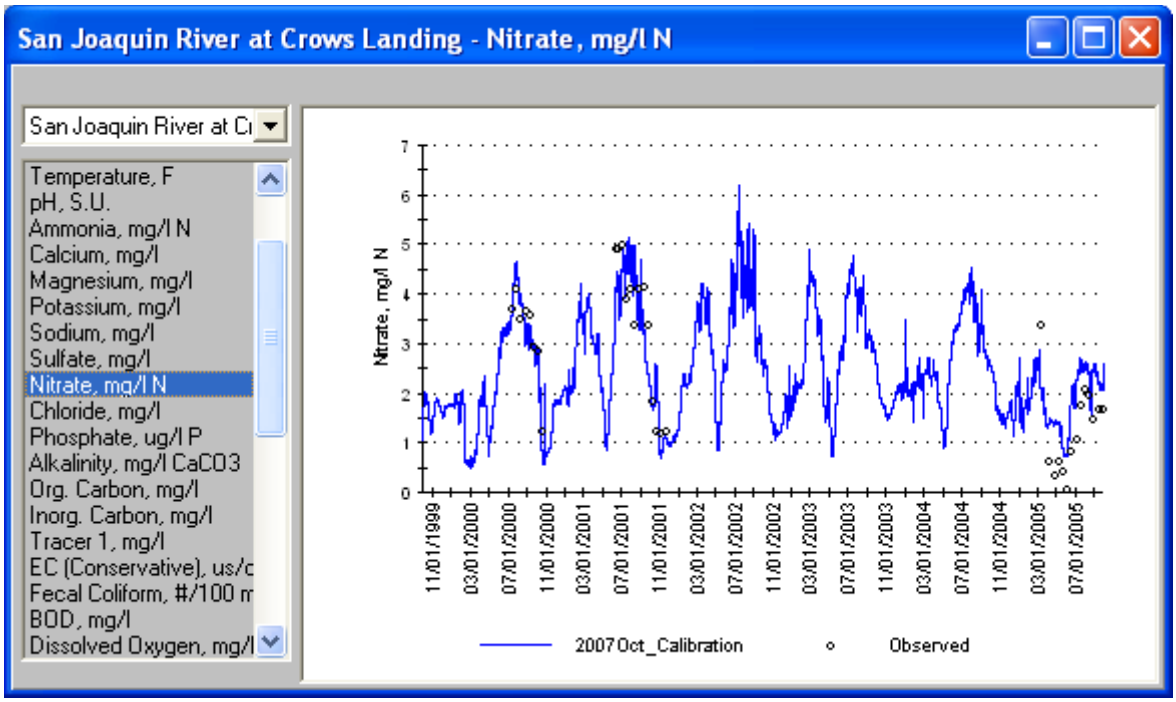

Figure 1.78 Simulated vs Observed Nitrate at Crows Landing

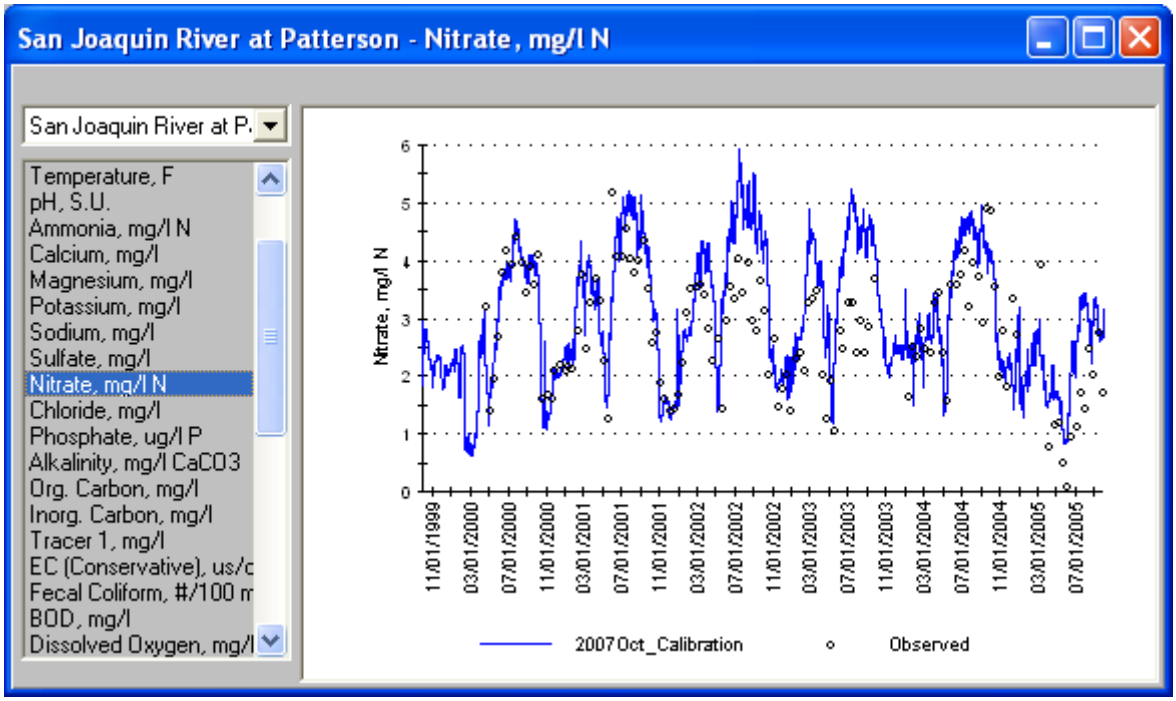

Figure 1.79 Simulated vs Observed Nitrate at Patterson

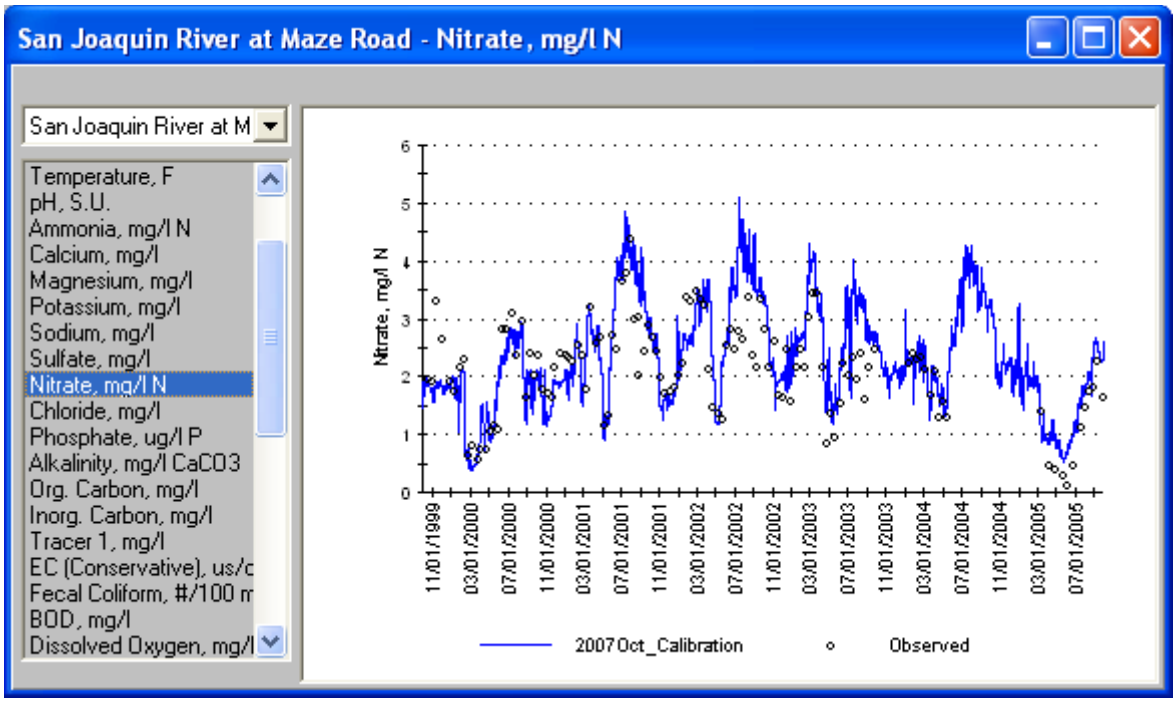

Figure 1.80 Simulated vs Observed Nitrate at Maze Road

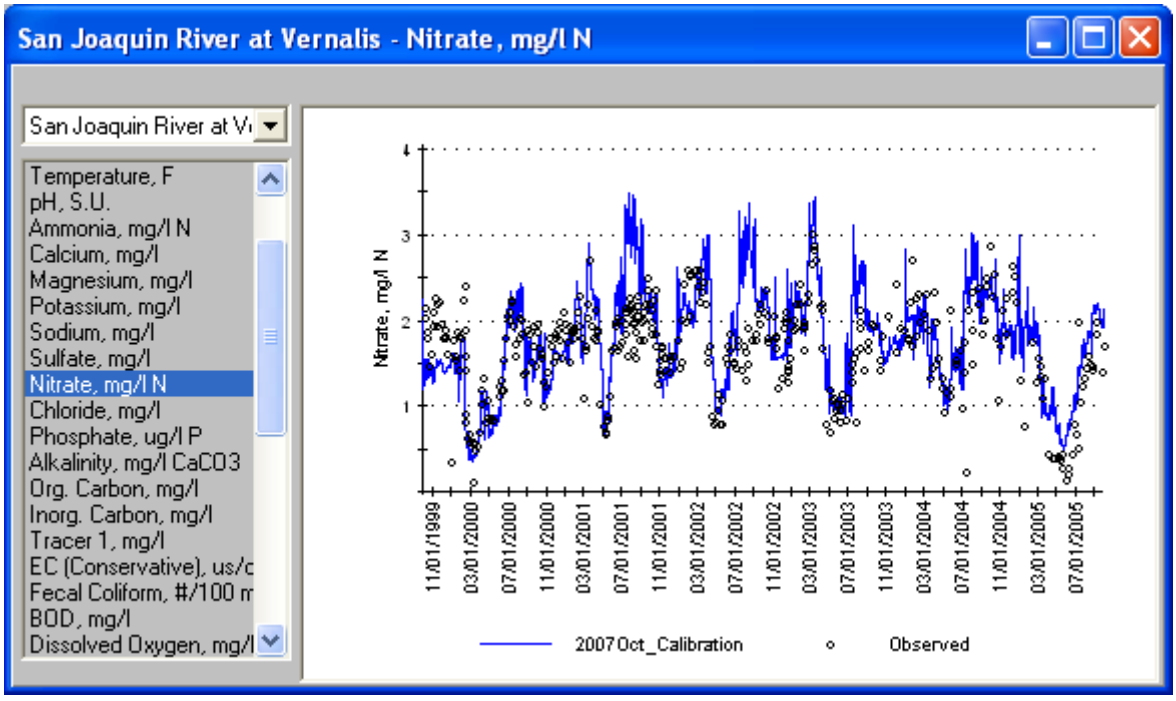

Figure 1.81 Simulated vs Observed Nitrate at Vernalis

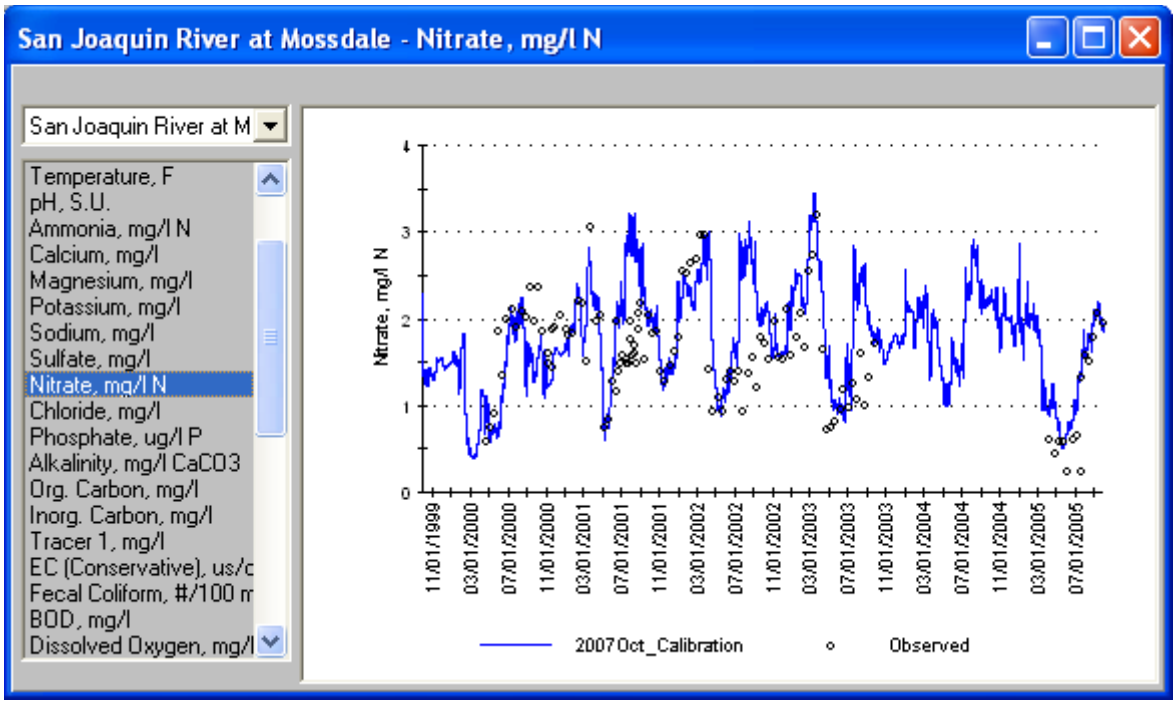

Figure 1.82 Simulated vs Observed Nitrate at Mossdale

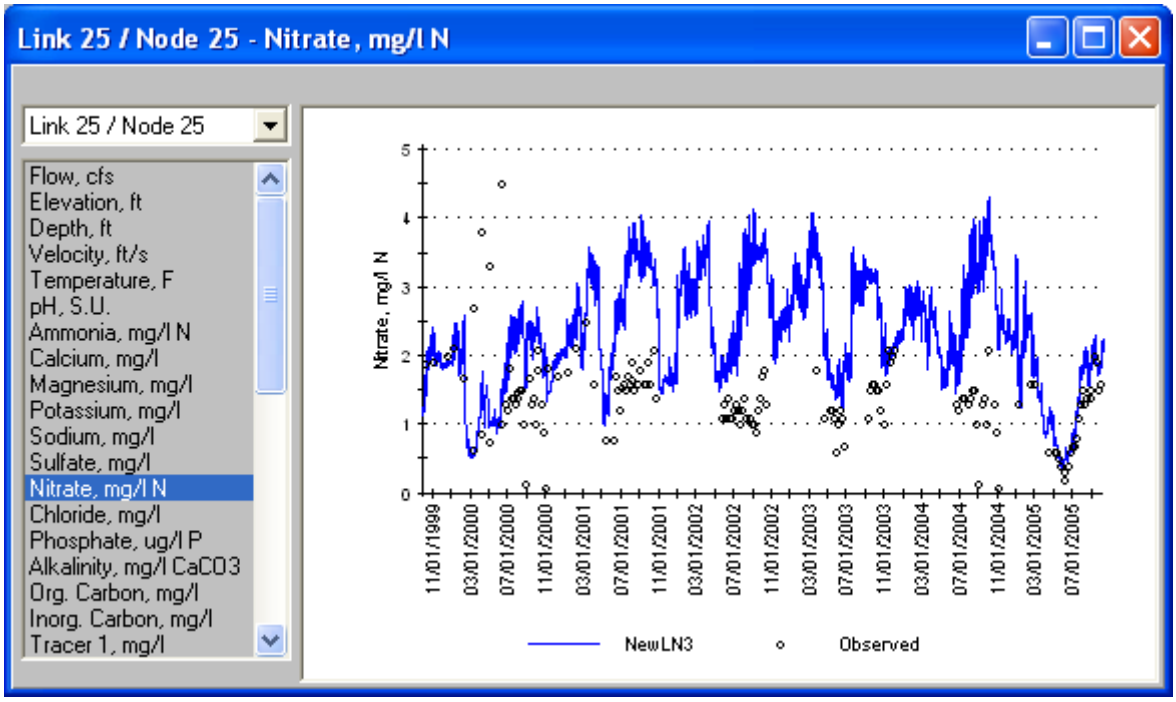

Figure 1.83 Simulated vs Observed Nitrate at Garwood Bridge

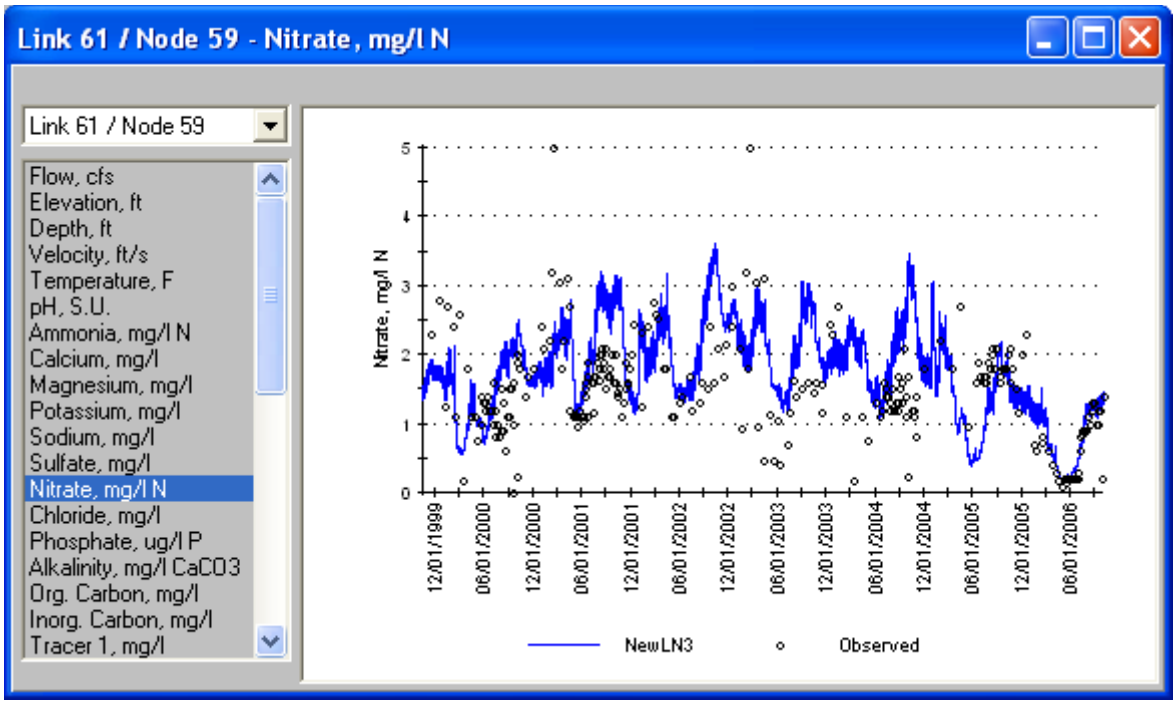

Figure 1.84 Simulated vs Observed Nitrate at Buckley Cove (Station R6)

Table 1.20 shows the model errors of nitrate at various monitoring stations on the San Joaquin River. Low statistical model errors are consistent with the good match shown in the graphical outputs. Overall, the WARMF model shows no bias to over or under predict nitrate concentration, and no station had greater than 10% relative error. The absolute error was below 30% for all stations upstream of the tidal zone. Nitrate was overpredicted within the Link-Node model domain, especially upstream of the DWSC.

Table 1.20
Model Errors of Nitrate Concentration in the San Joaquin River

Monitoring Station	Relative Error	Absolute Error
Stevinson	+8%	14%
Crows Landing	+8%	23%
Patterson	+16%	24%
Maze Road	+9%	20%
Vernalis	+8%	24%
Mossdale	+15%	29%
Garwood Bridge	+74%	77%
Buckley Cove / City of Stockton R6	+18%	42%

Total Nitrogen

Figure 1.85 through Figure 1.90 compare the time series of predicted and observed total nitrogen concentration at various stations along the San Joaquin River. Total nitrogen includes ammonia,

nitrate, adsorbed ammonia, and organic nitrogen. It is evident that the match between simulated results and observed data was good.

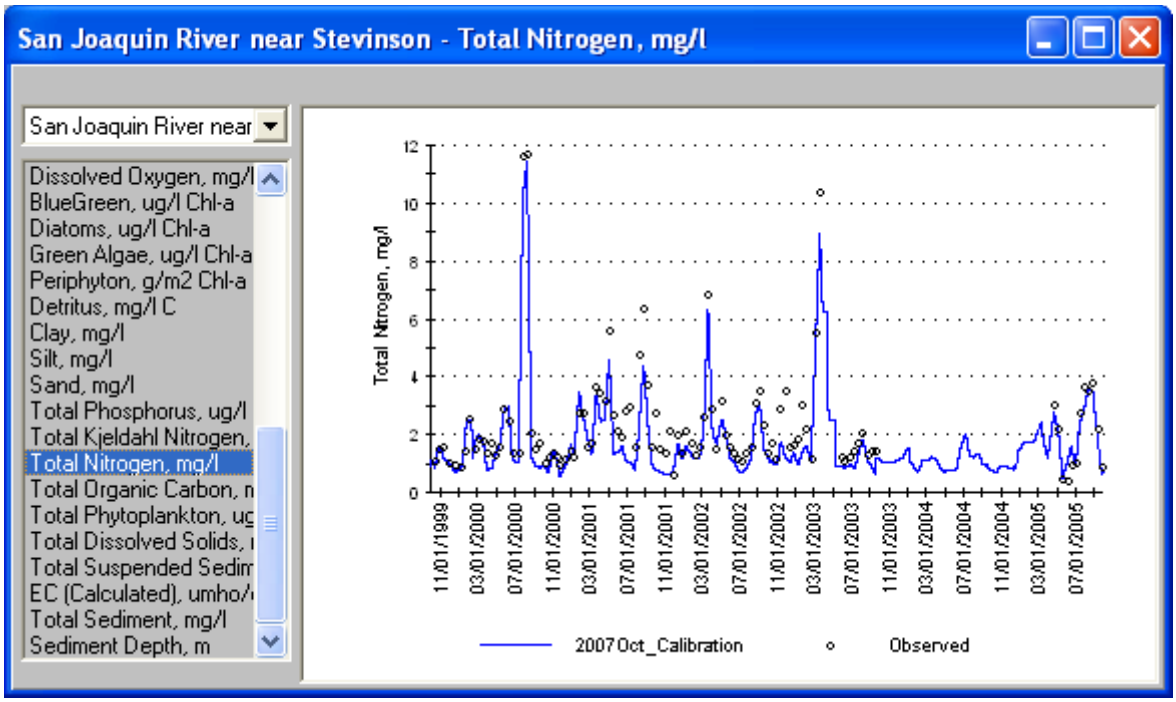

Figure 1.85 Simulated vs Observed Total Nitrogen at Stevinson (Lander Ave.)

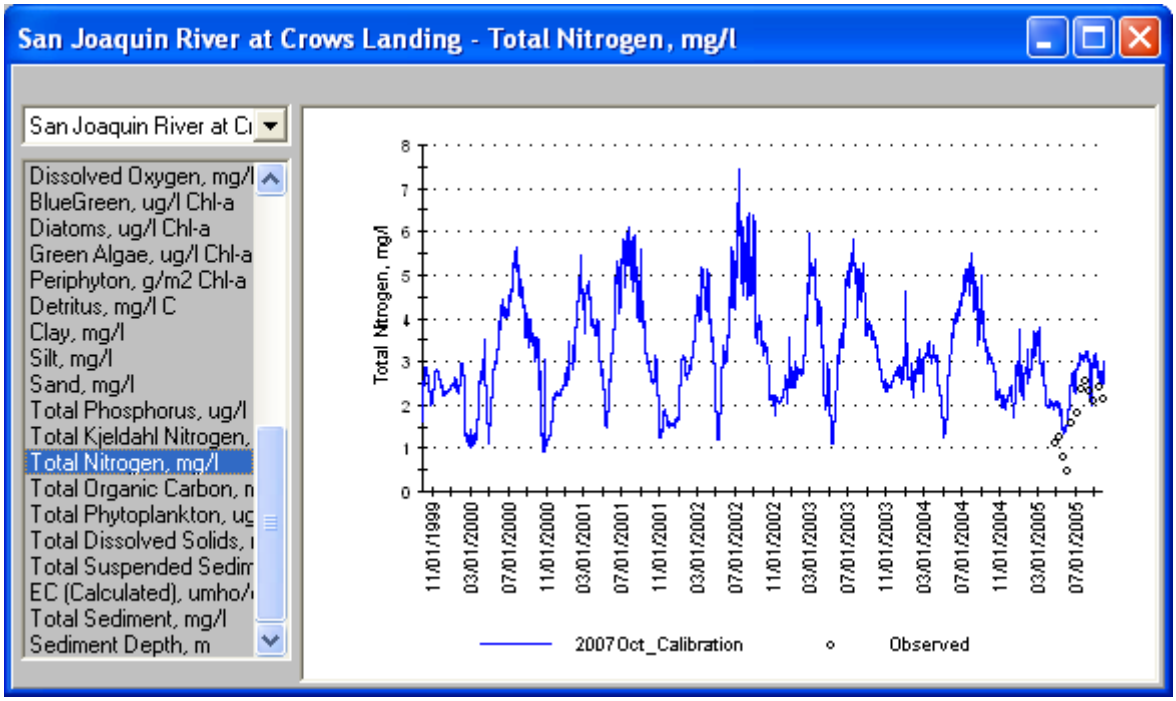

Figure 1.86 Simulated vs Observed Total Nitrogen at Crows Landing

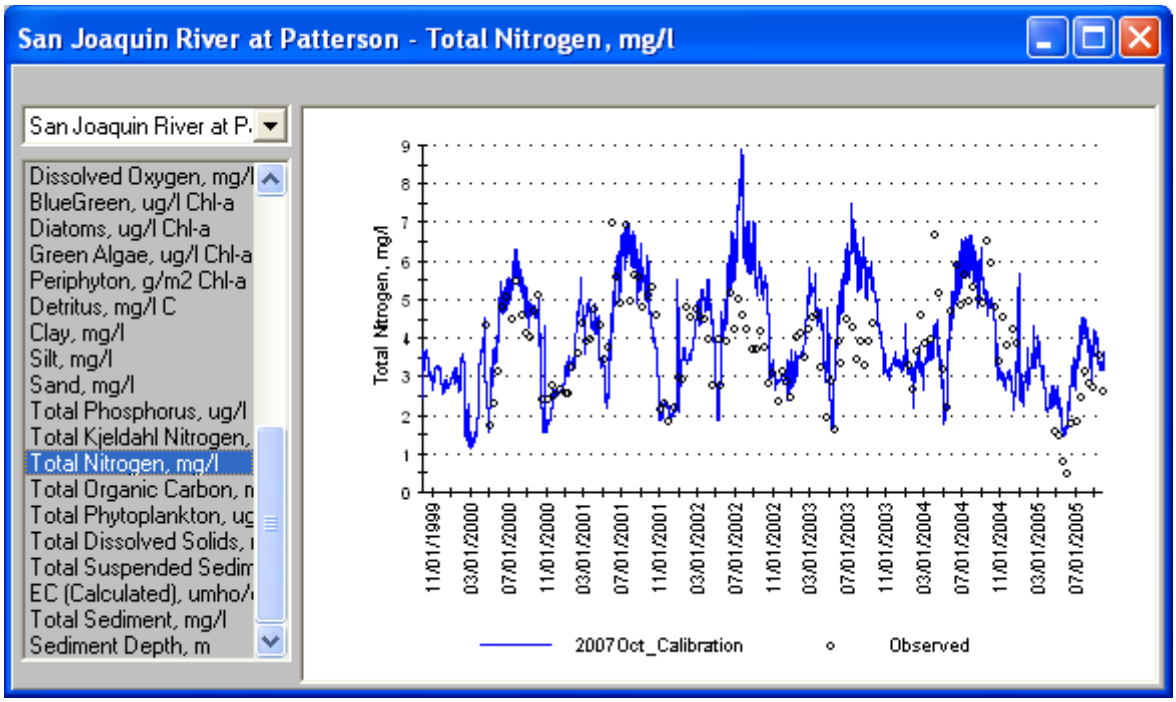

Figure 1.87 Simulated vs Observed Total Nitrogen at Patterson

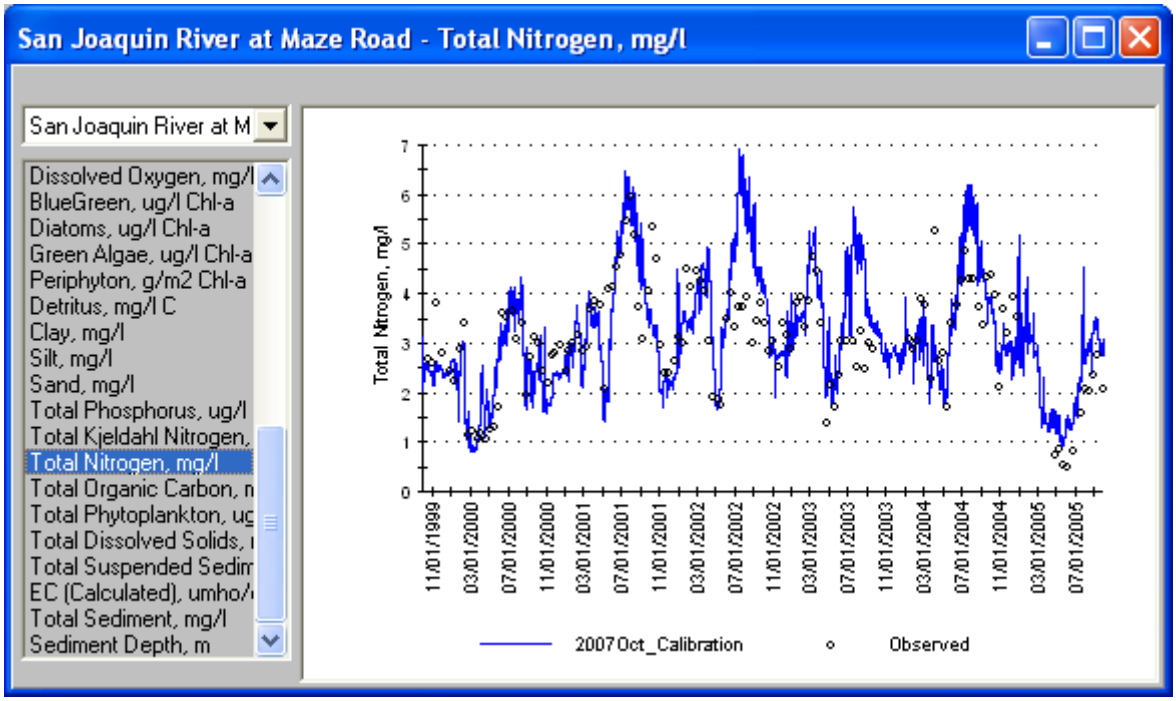

Figure 1.88 Simulated vs Observed Total Nitrogen at Maze Road

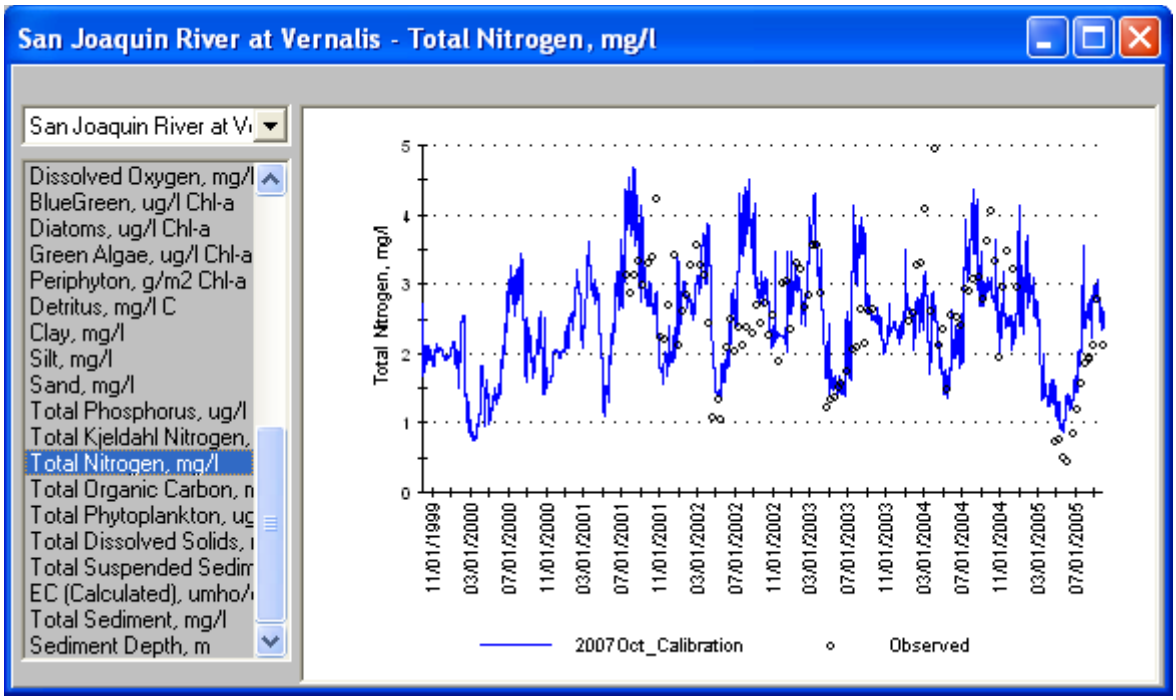

Figure 1.89 Simulated vs Observed Total Nitrogen at Vernalis

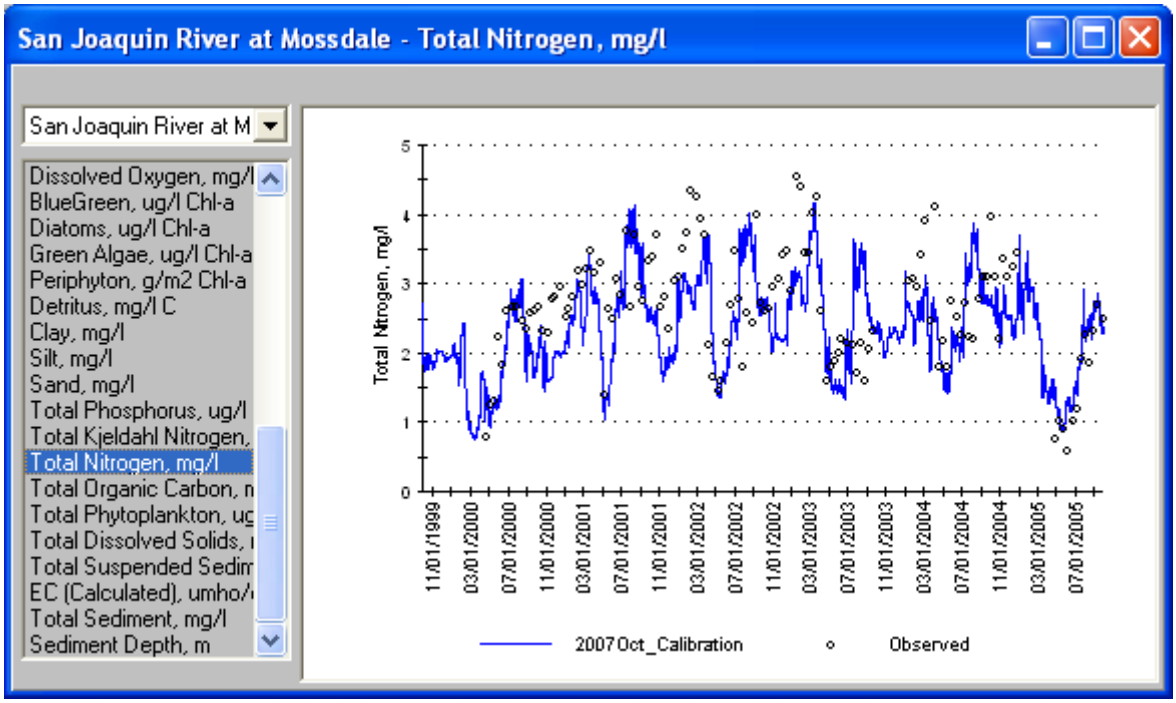

Figure 1.90 Simulated vs Observed Total Nitrogen at Mossdale

Table 1.21 shows the model errors for total nitrogen at various monitoring stations on the San Joaquin River. The absolute error was slightly greater than the target of 20%. The error at Crows Landing was higher because that location only has a few measured data points from 2005.

Table 1.21
Model Errors for Total Nitrogen in the San Joaquin River

Monitoring Station	Relative Error	Absolute Error
Stevinson	-21%	24%
Crows Landing	39%	39%
Patterson	8%	22%
Maze Road	5%	21%
Vernalis	3%	24%
Mossdale	-10%	23%

Phosphate

Figure 1.91 through Figure 1.97 compare the time series of predicted and observed concentrations of phosphate concentration at various stations along the San Joaquin River. The comparison is also made for Buckley Cove in the DWSC, which is based on the Link-Node model.

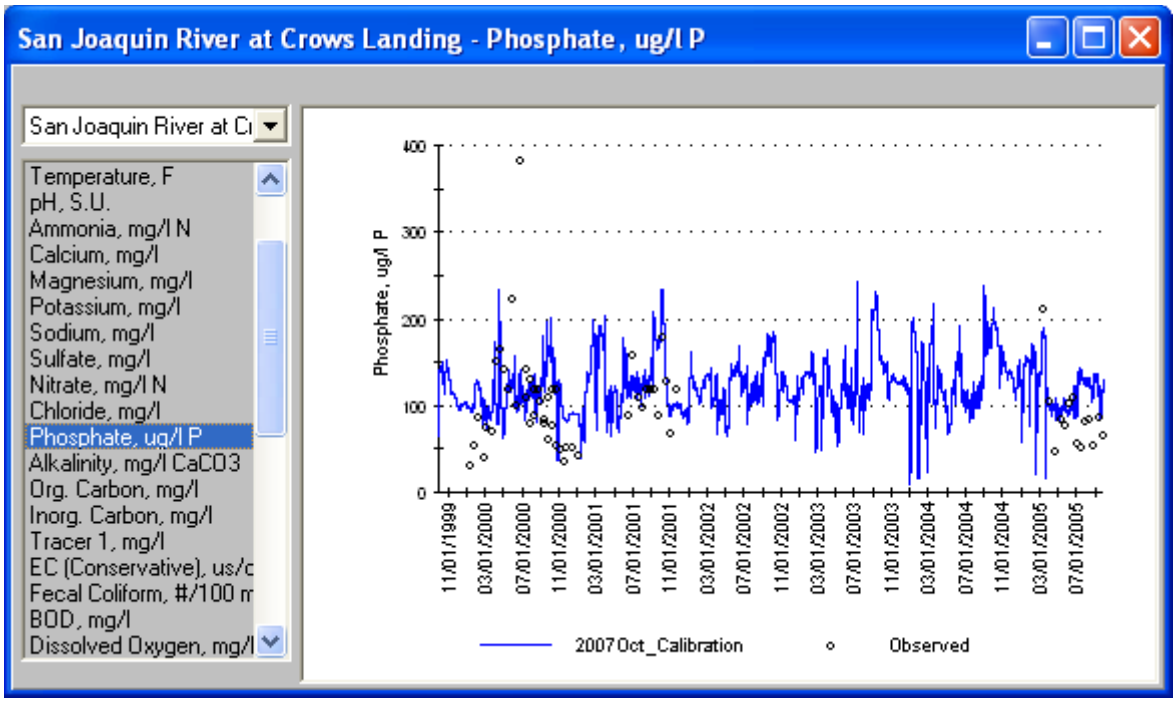

Figure 1.91 Simulated vs Observed Phosphate at Crows Landing

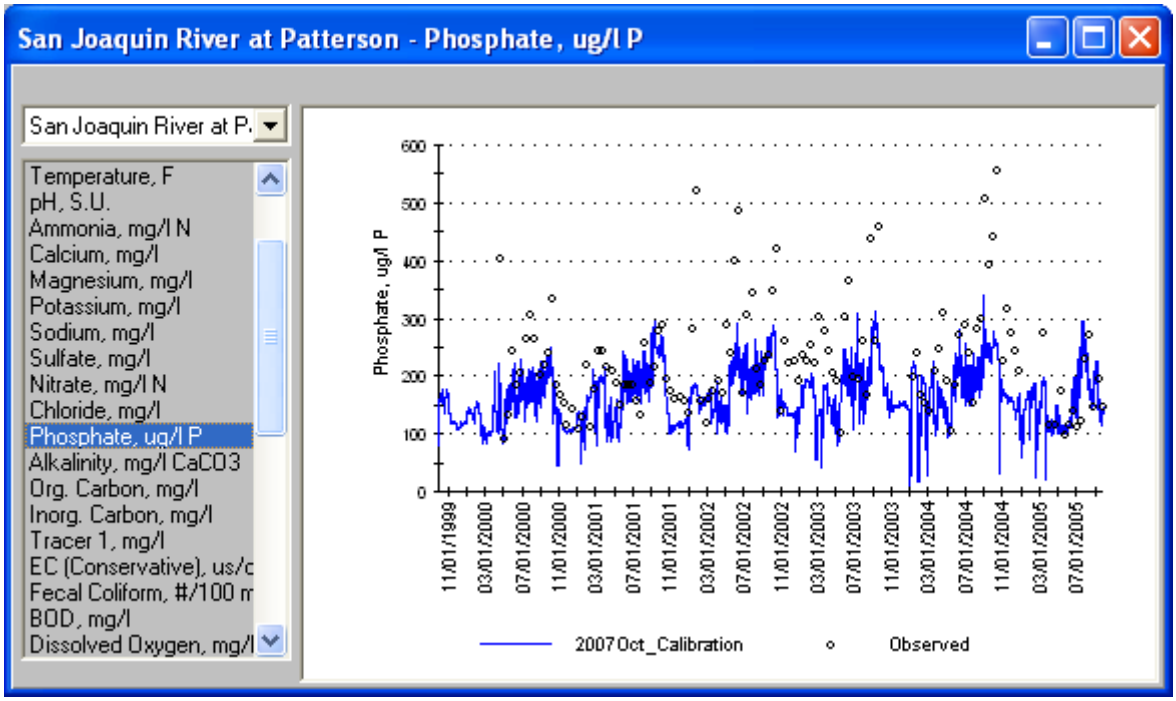

Figure 1.92 Simulated vs Observed Phosphate at Patterson

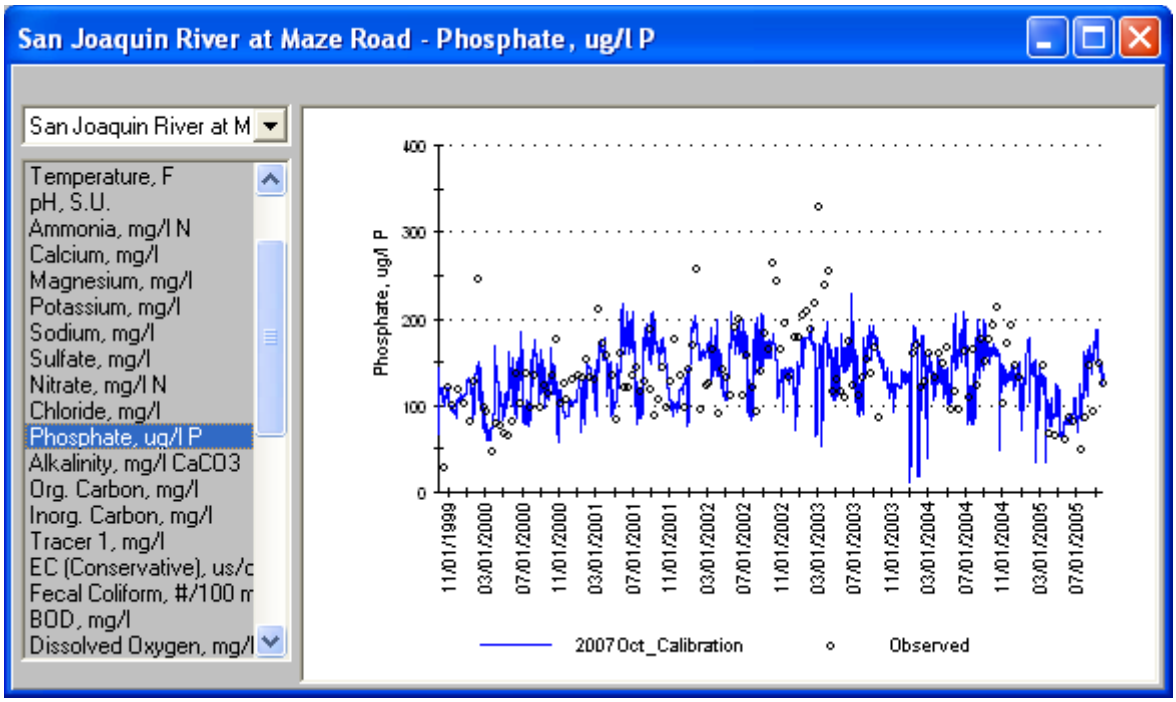

Figure 1.93 Simulated vs Observed Phosphate at Maze Road

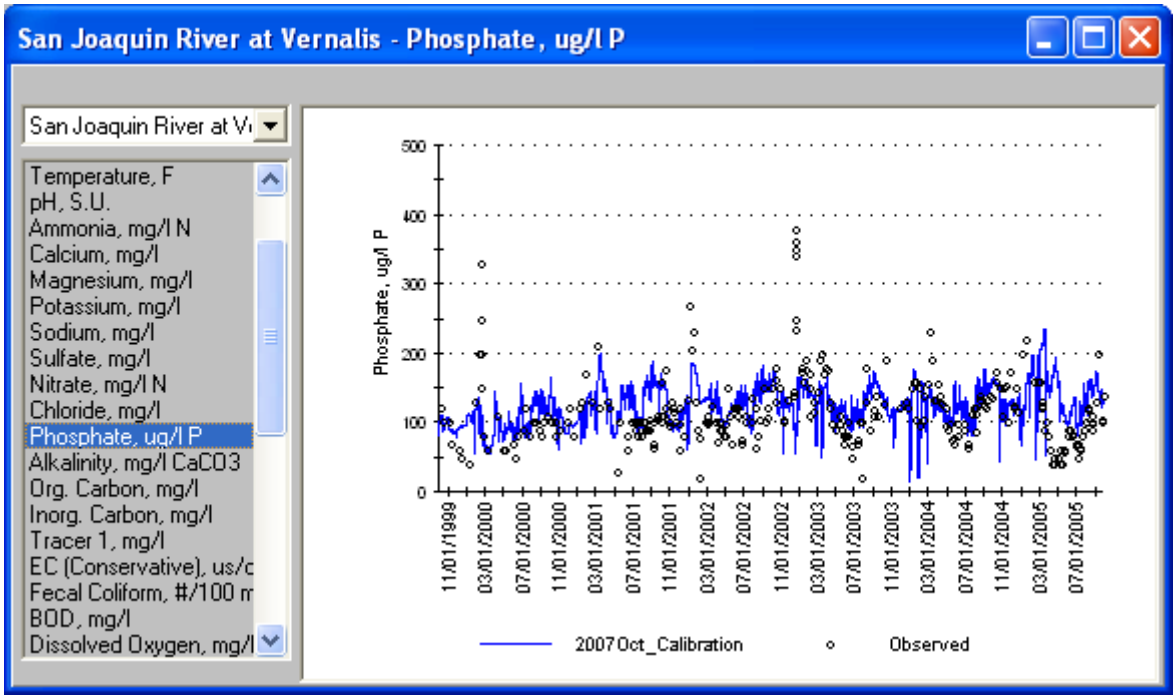

Figure 1.94 Simulated vs Observed Phosphate at Vernalis

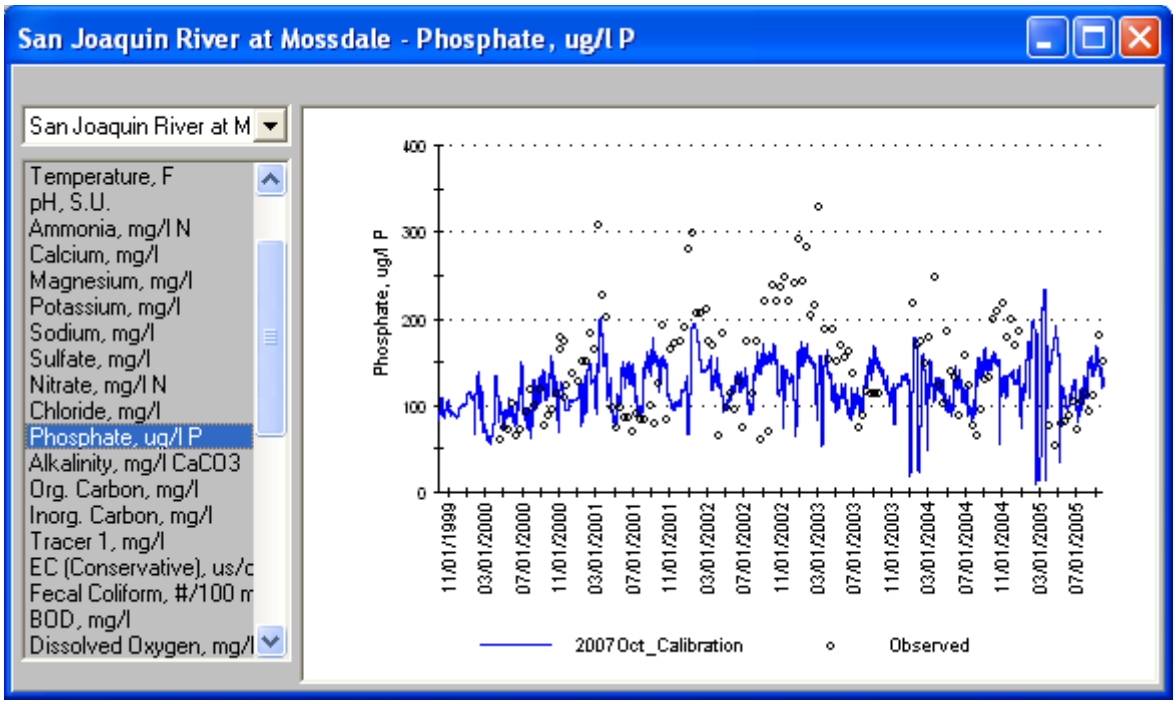

Figure 1.95 Simulated vs Observed Phosphate at Mossdale

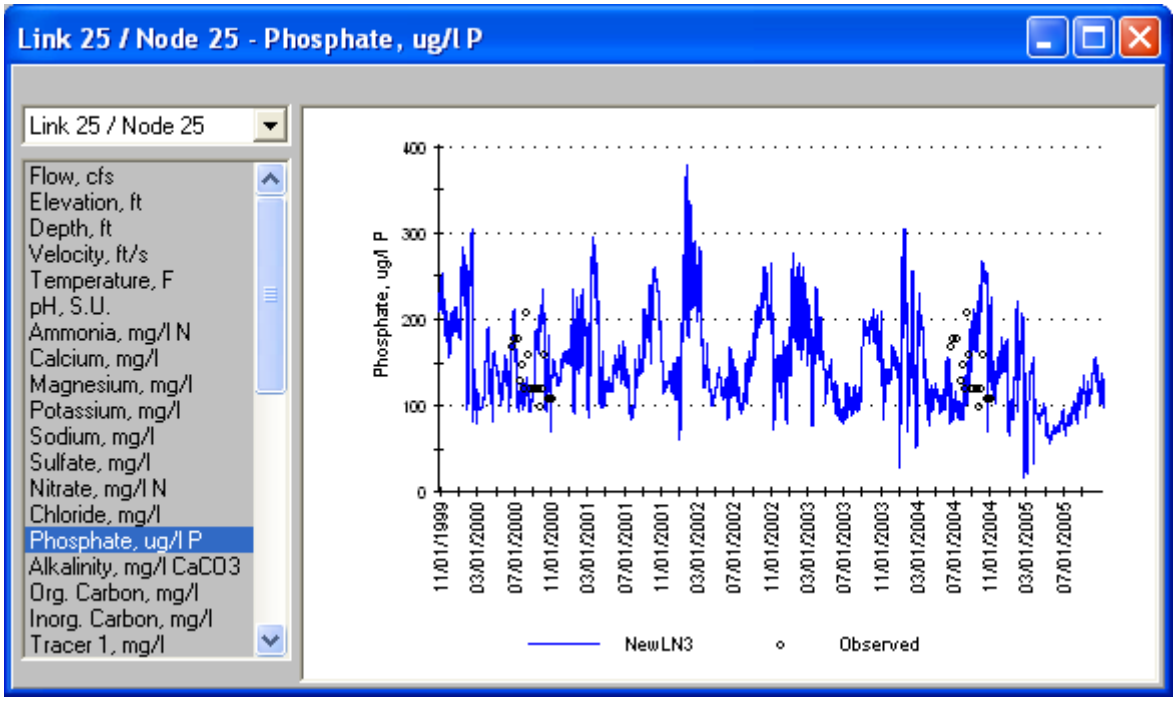

Figure 1.96 Simulated vs Observed Phosphate at Garwood Bridge

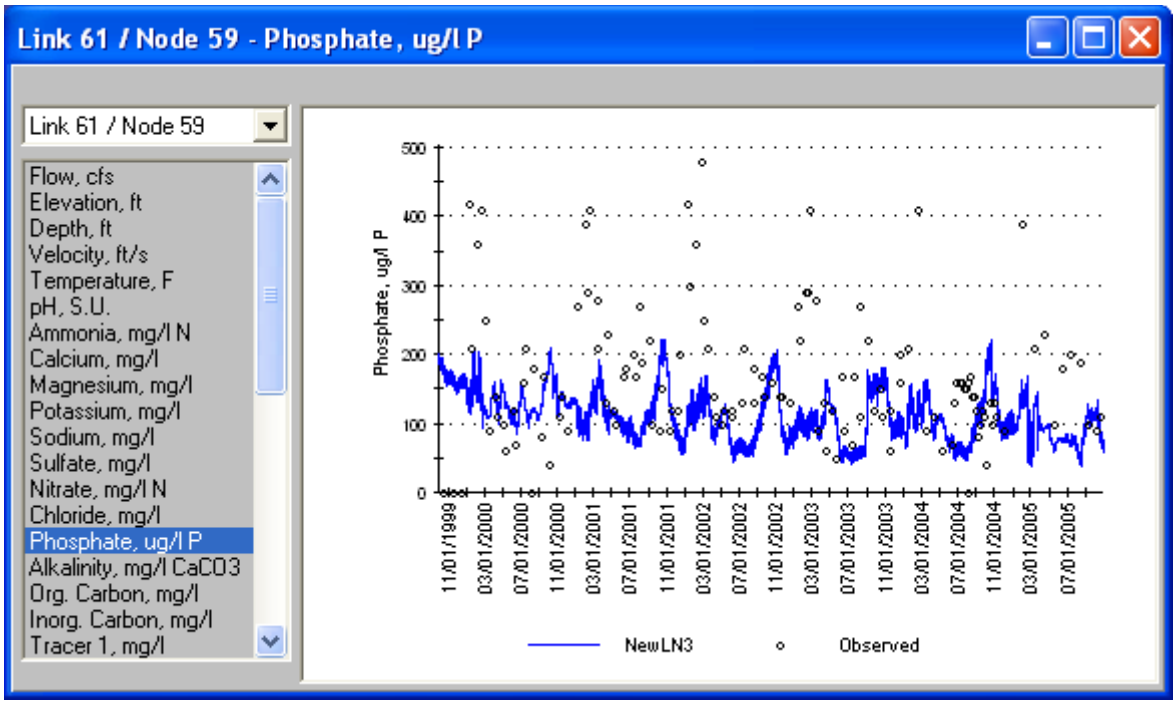

Figure 1.97 Simulated vs Observed Phosphate at Buckley Cove (Station R6)

Table 1.22 shows the model errors at various monitoring stations on the San Joaquin River. The model did not have an overall bias, although it under predicted phosphate concentrations at Patterson and Mossdale while over predicting phosphate at Crows Landing. The Link-Node model is predicting phosphate well at Garwood Bridge, but under predicting phosphate at Buckley Cove (Station R6).

Table 1.22
Model Errors for Phosphate Concentration in the San Joaquin River

Monitoring Station	Relative Error	Absolute Error
Stevinson	1%	8%
Crows Landing	16%	39%
Patterson	-27%	31%
Maze Road	-1%	24%
Vernalis	7%	34%
Mossdale	-15%	35%
Garwood Bridge	+3%	38%
Buckley Cove (station R6)	-32%	53%

Total Phosphorus

Figure 1.98 through Figure 1.103 compare the predicted and observed time series of total phosphorus concentrations at various stations along the San Joaquin River. Both simulated and observed showed a seasonal pattern with higher phosphorus concentration in summer. Observed

data showed particularly high concentration in the dry years of 2002 and 2003 which were not matched in simulation results.

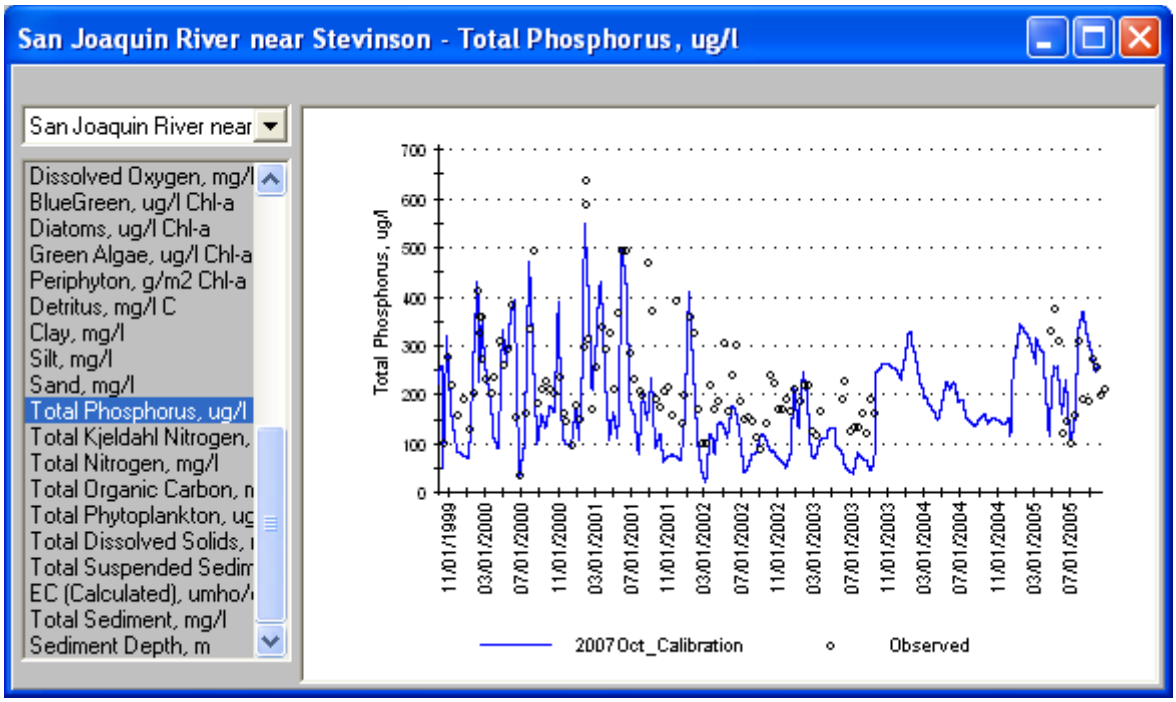

Figure 1.98 Simulated vs Observed Total Phosphorus at Stevinson (Lander Ave.)

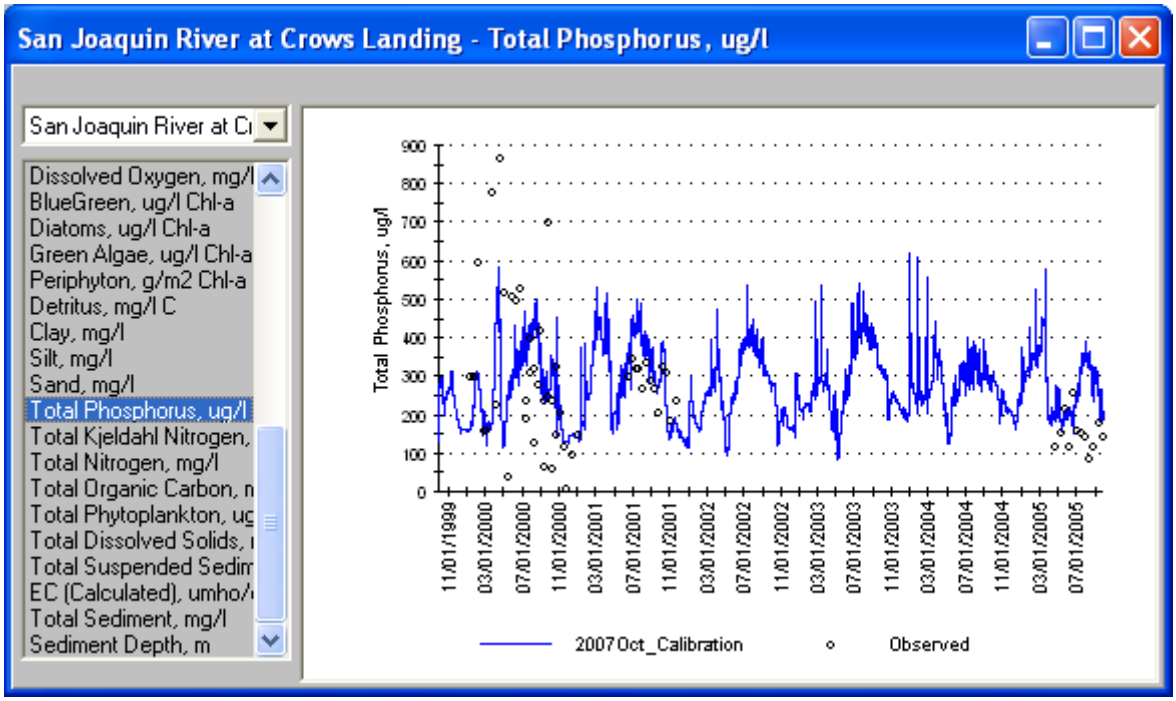

Figure 1.99 Simulated vs Observed Total Phosphorus at Crows Landing

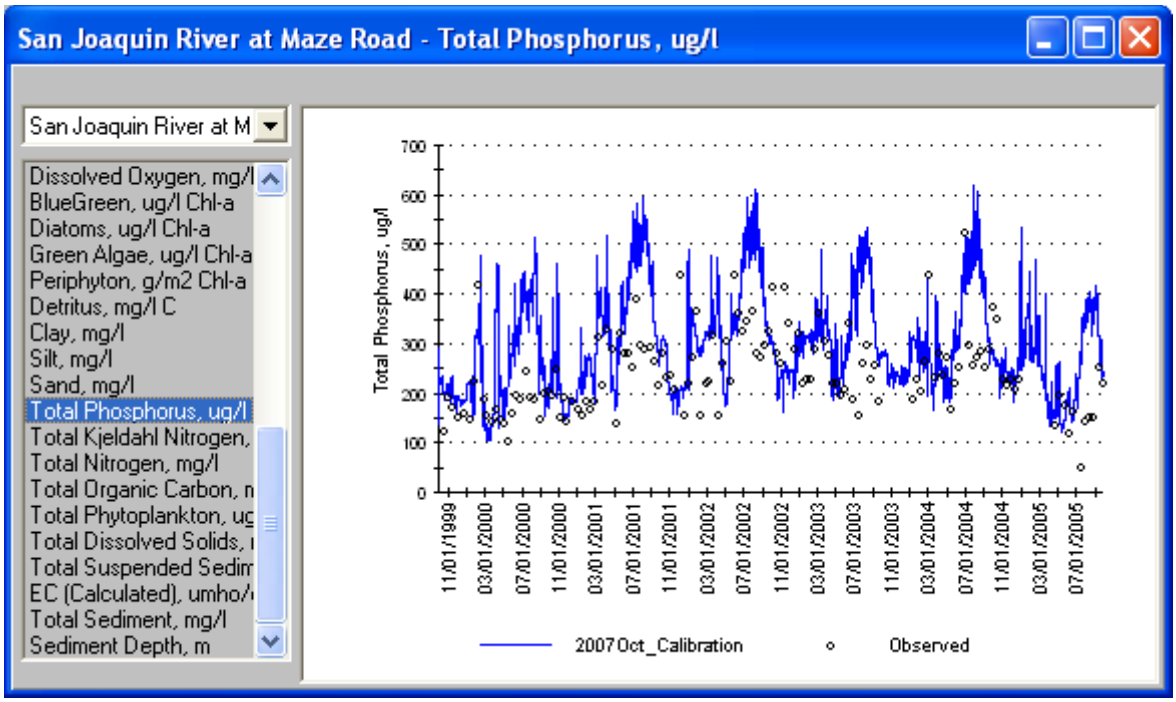

Figure 1.100 Simulated vs Observed Total Phosphorus at Patterson

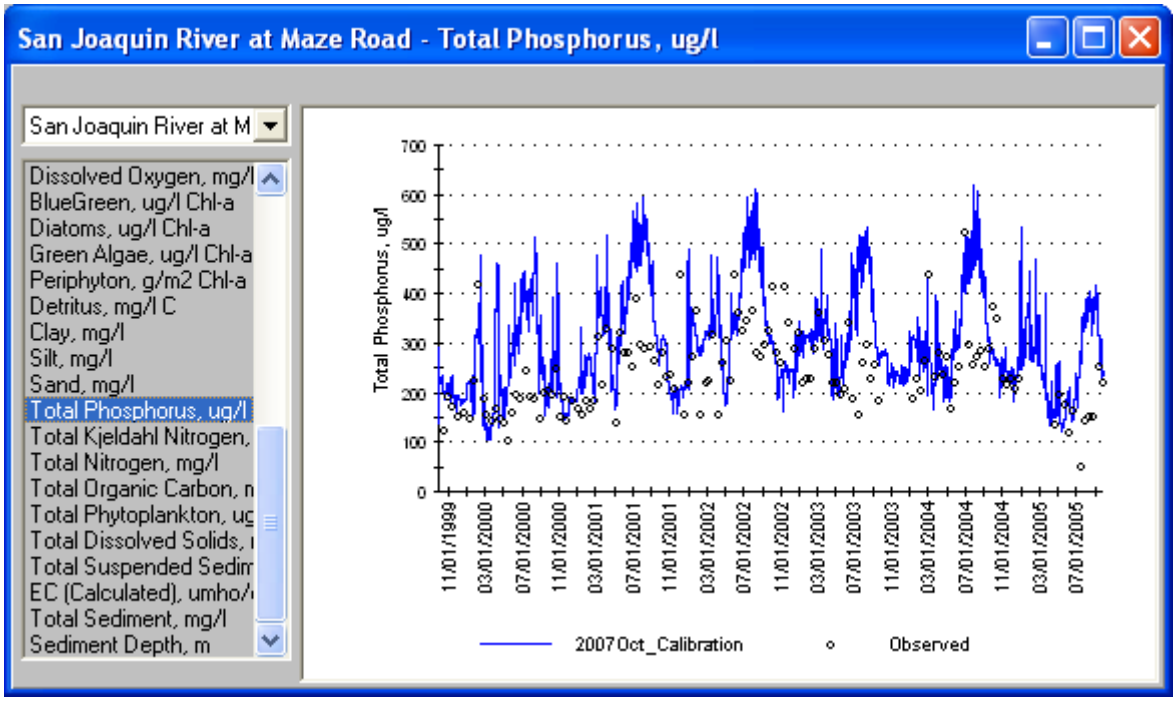

Figure 1.101 Simulated vs Observed Total Phosphorus at Maze Road

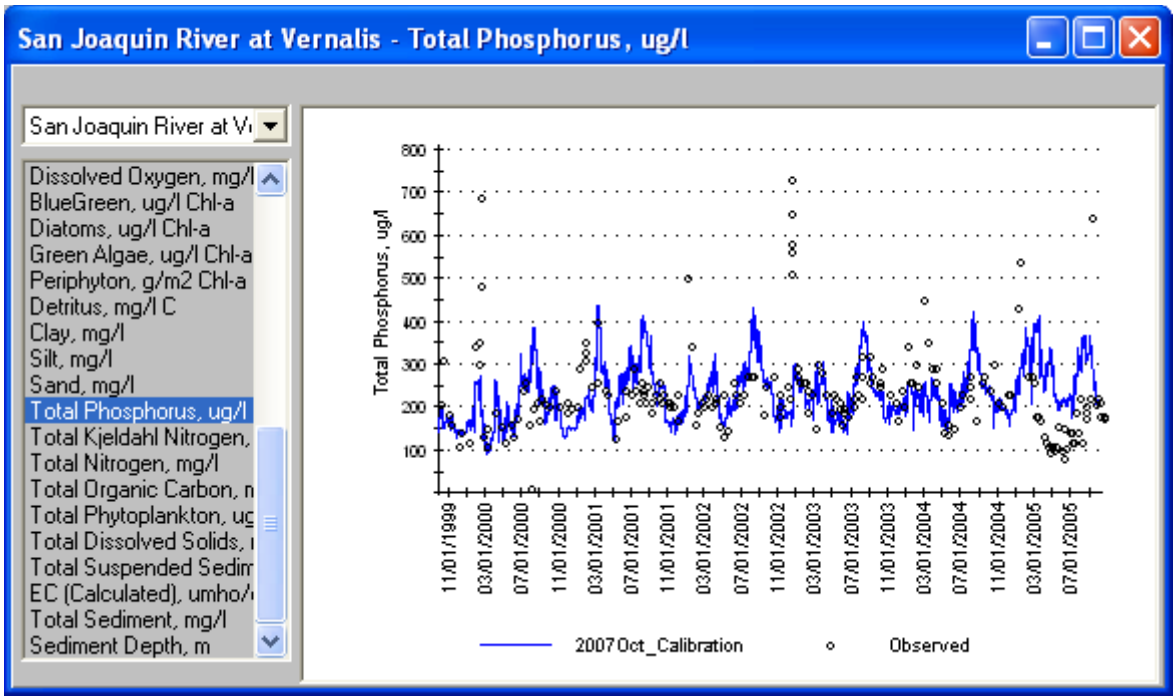

Figure 1.102 Simulated vs Observed Total Phosphorus at Vernalis

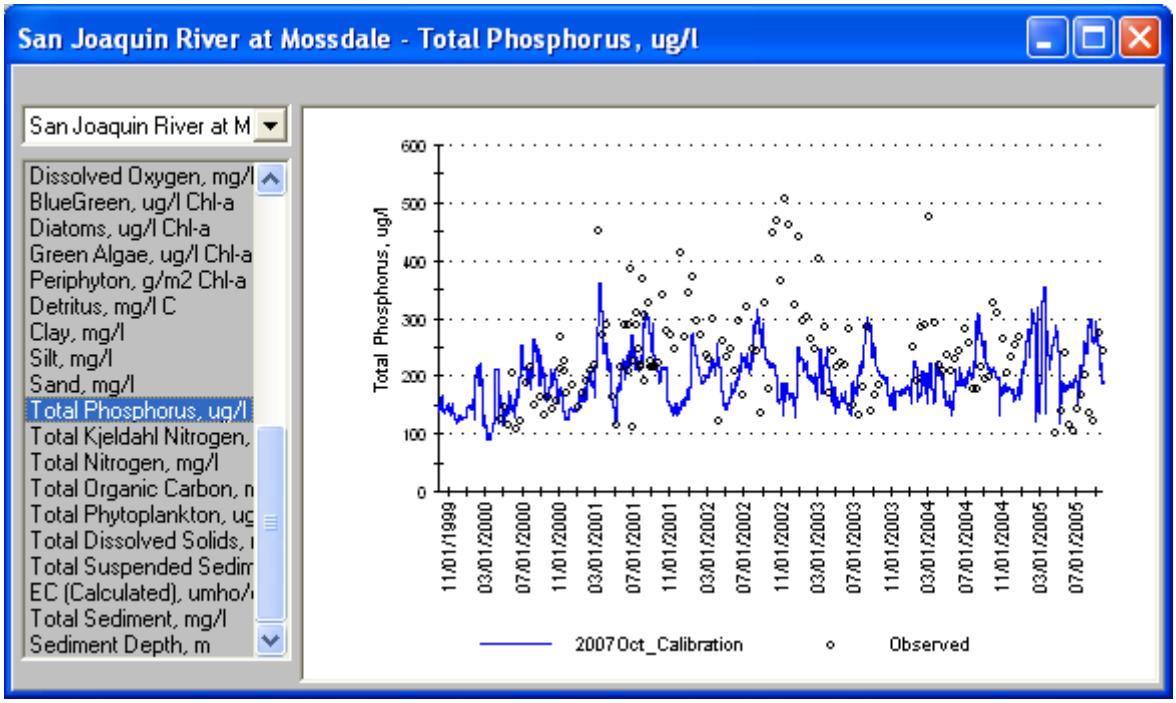

Figure 1.103 Simulated vs Observed Total Phosphorus at Mossdale

Table 1.23 shows the model errors for total phosphorus at various monitoring stations on the San Joaquin River. The relative error was under 10% at 4 of the 6 stations. The error at Mossdale for both total phosphorus and phosphate (Table 1.22) implies that there is a significant source of

phosphorus between Vernalis and Mossdale or tidal influence at Mossdale which was not represented by the model.

Table 1.23
Model Errors for Total Phosphorus in the San Joaquin River

Monitoring Station	Relative Error	Absolute Error
Stevinson	-23%	36%
Crows Landing	2%	44%
Patterson	-5%	28%
Maze Road	22%	35%
Vernalis	1%	33%
Mossdale	-15%	33%

Phytoplankton

WARMF simulated the biomass for three species of phytoplankton (greens, blue-greens, and diatoms). The biomass was converted to chlorophyll concentration according to a species specific factor, which was a model input. The chlorophyll concentrations of the three species of algae were summed for total chlorophyll concentration.

The field studies of algal composition determined that diatoms dominate in the San Joaquin River. For the input data, the phytoplankton concentrations in the boundary river inflows were assumed to be diatoms. High algal seeds in the inflows and lower half saturation constant for light intensity lead WARMF to predict high concentration of diatoms in the San Joaquin River. WARMF simulated little growth of green and blue-green algae for most of the simulation period.

Although diatoms can settle relatively rapidly in quiescent water, it was assumed that there was enough turbulence in most of the river to keep the diatoms in suspension in the water column. Downstream of the Stanislaus River, however, the river is much deeper (10-14 feet) and the river's velocity decreases, so a settling velocity of 1 m/d was used in that reach and further downstream in the Link-Node model domain.

Figure 1.104 through Figure 1.110 compare the time series of predicted and observed chlorophyll-a concentrations at various stations along the San Joaquin River. The model results showed large fluctuations of chlorophyll-a concentration within a day. For that reason, the daily minimum and maximum values are shown in the plots for both predicted and observed values.

The predicted chlorophyll-a concentration followed the same seasonal pattern of high concentration in summer and low concentration in winter. The predicted values match the observed well for most years at all station, as most measured concentrations fall between the simulated maximum and minimum daily concentration curves. WARMF under-predicted the peak algae concentrations in 2003 and 2004 at Patterson and Mossdale in particular.

The Link-Node model predicted chlorophyll-a concentration at Buckley Cove station reasonably well. The correct seasonal pattern was simulated. The maximum observed chlorophyll-a concentration was below 60 μg/l, the highest value observed in 2000. The observed data showed

much more scatter than simulation results, which may indicate water with low algae concentration coming upstream through the DWSC on the flood tide.

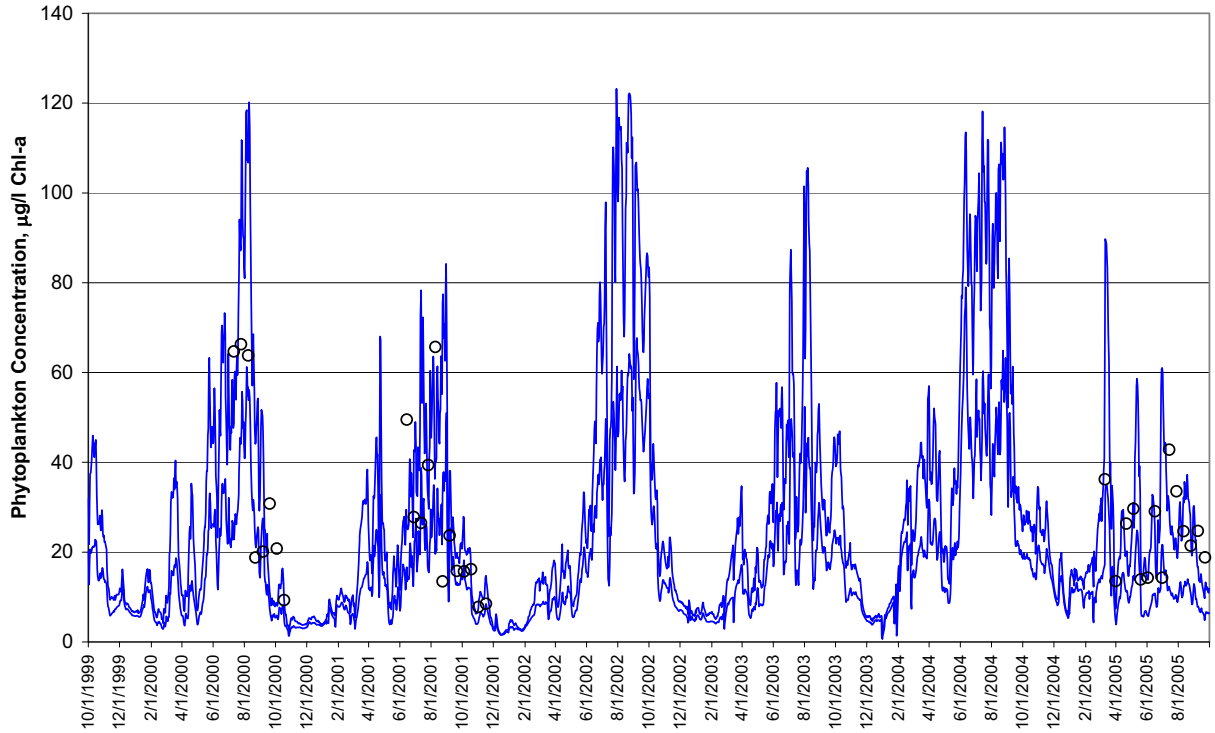

Figure 1.104 Simulated vs Observed Phytoplankton at Crows Landing

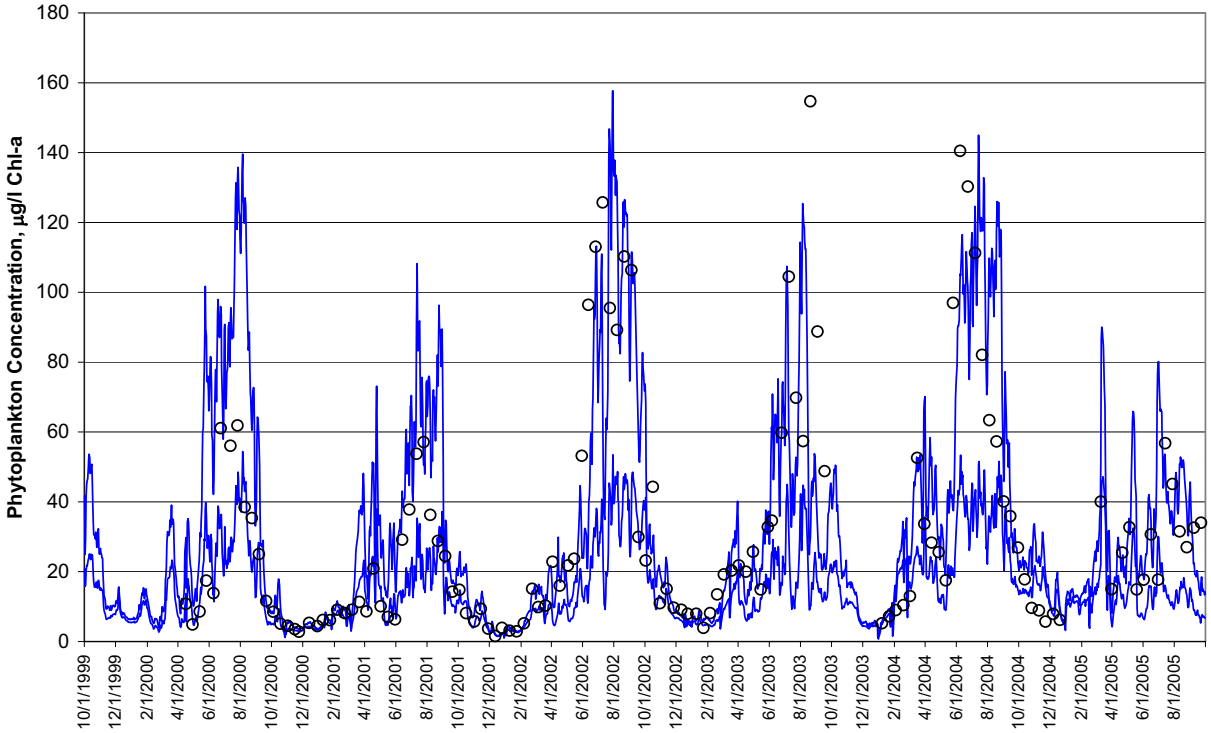

Figure 1.105 Simulated vs Observed Phytoplankton at Patterson

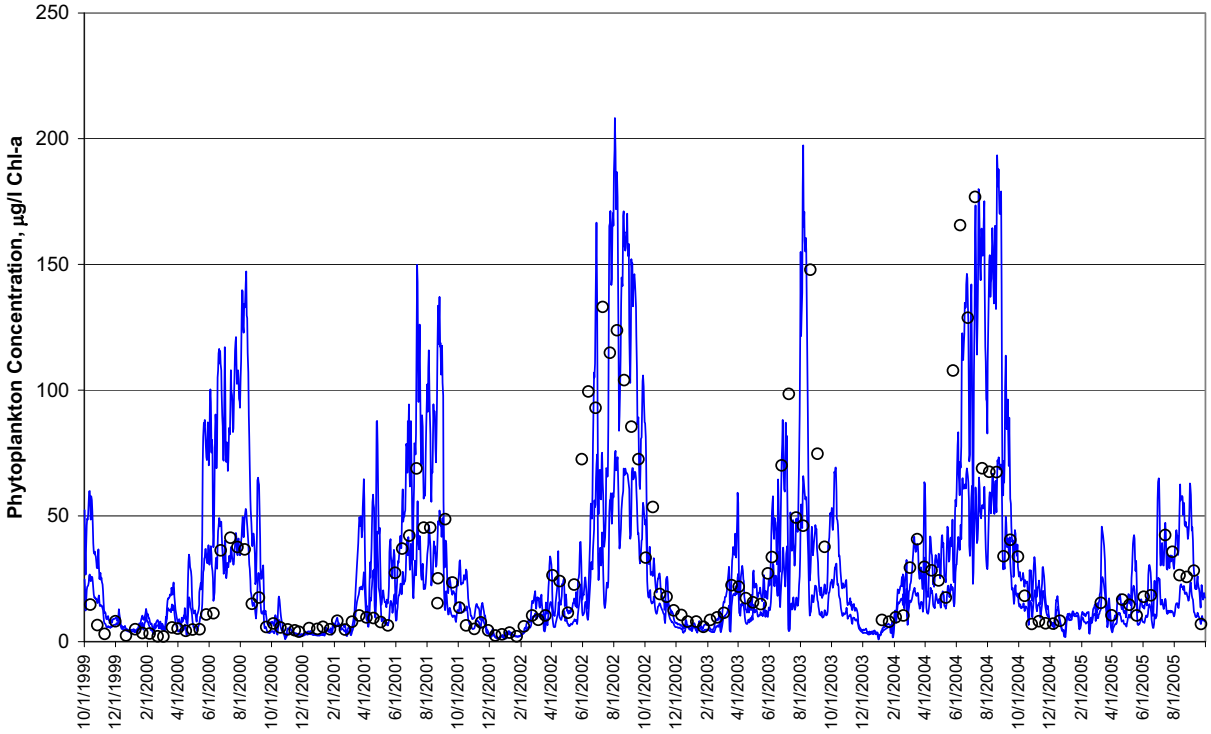

Figure 1.106 Simulated vs Observed Phytoplankton at Maze Road

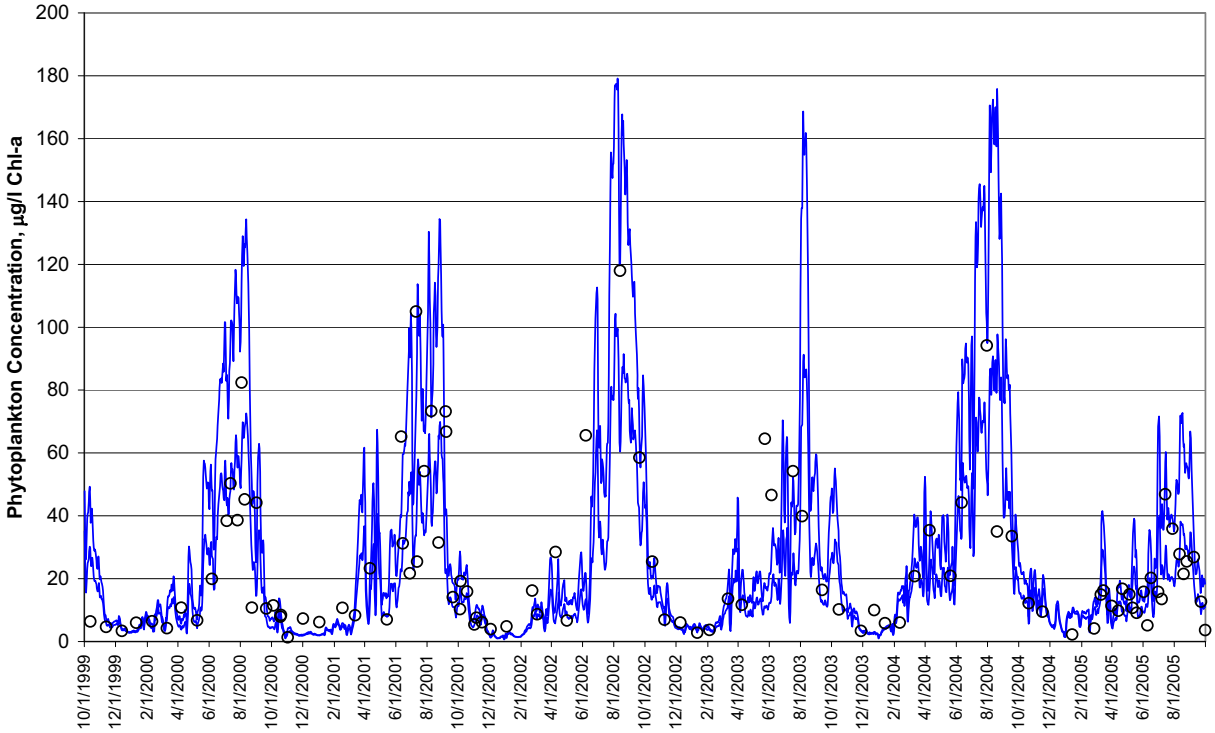

Figure 1.107 Simulated vs Observed Phytoplankton at Vernalis

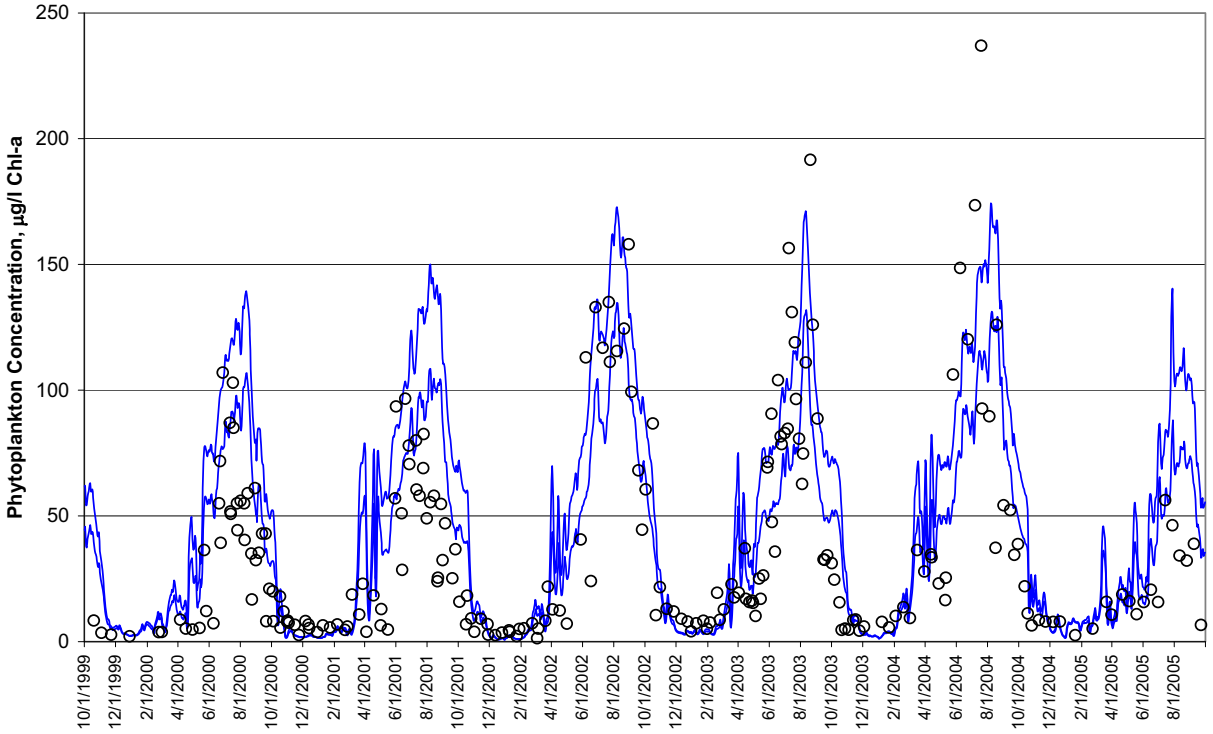

Figure 1.108 Simulated vs Observed Phytoplankton at Mossdale

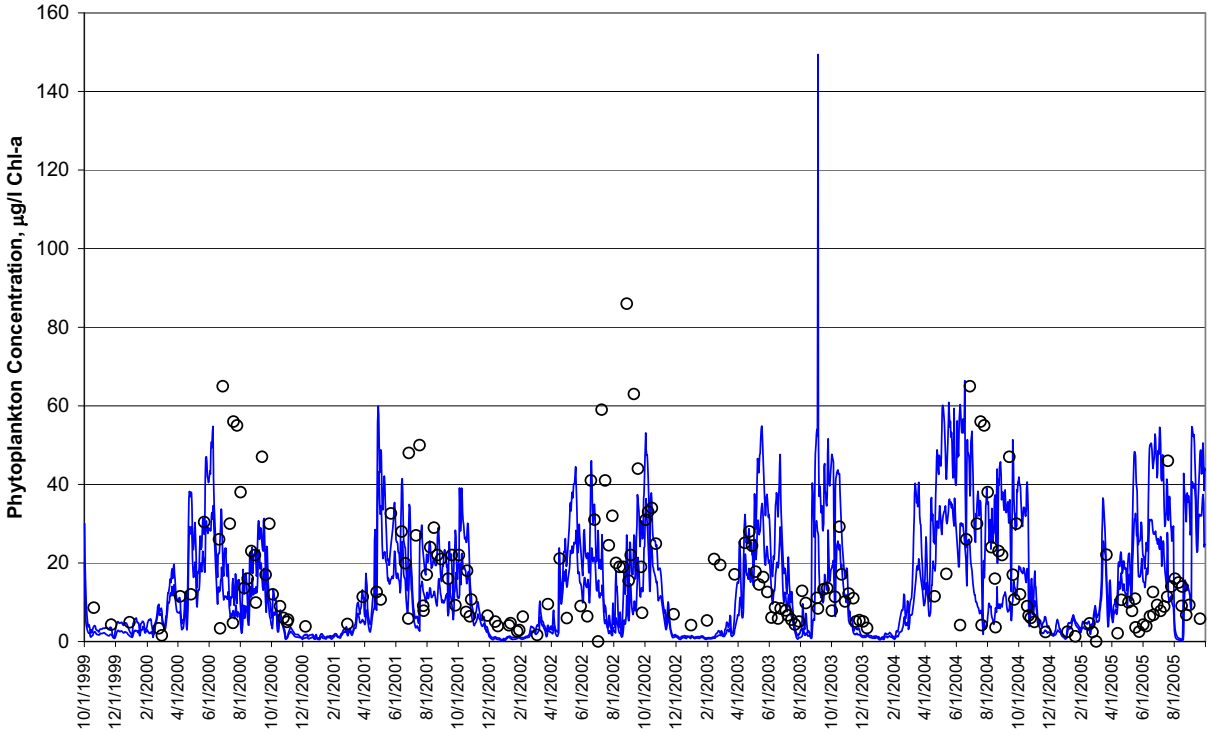

Figure 1.109 Simulated vs Observed Phytoplankton at Garwood Bridge

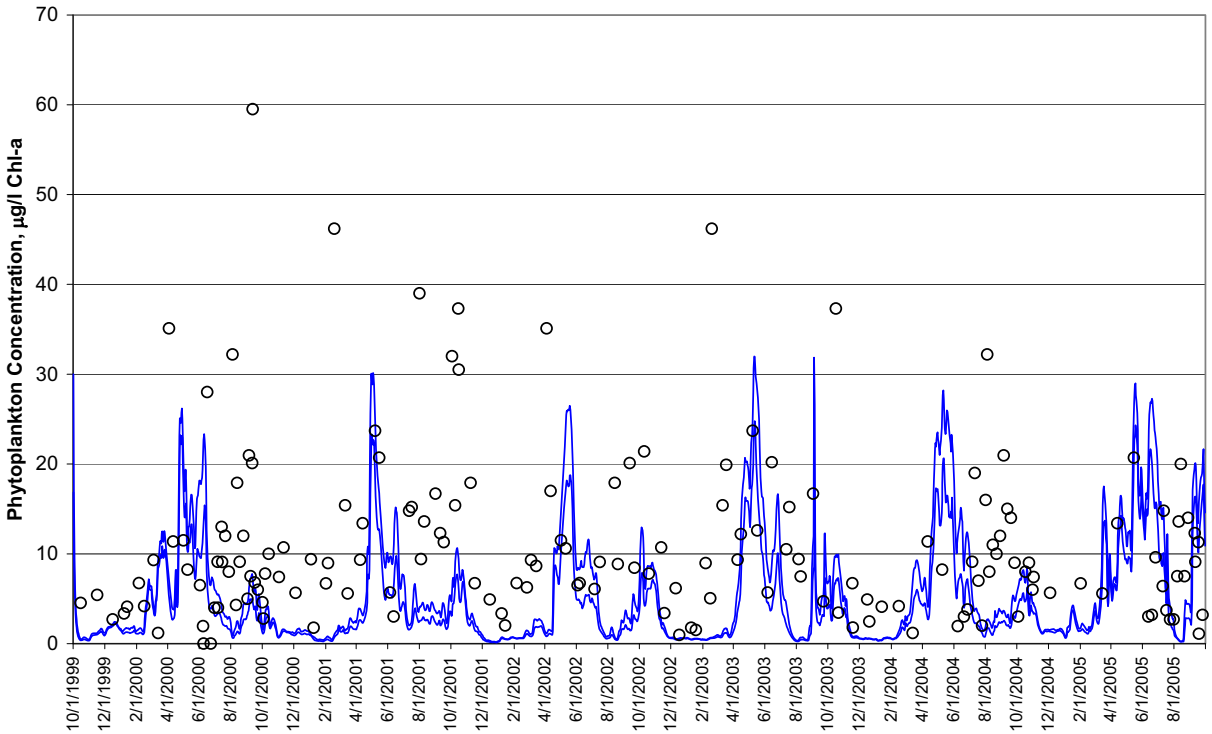

Figure 1.110 Simulated vs Observed Phytoplankton at Buckley Cove (Station R6)

Table 1.24 shows the model errors for chlorophyll-a concentration at various monitoring stations on the San Joaquin River. The goal of calibration was for the simulation results to bracket the observed data points. The model predicted large daily swings in chlorophyll-a concentration. The maximum concentrations were up to twice the minimum concentration. The calibration goal for phytoplankton is within 20% relative error and 50% absolute error because of the dramatic swings in concentration and complex interactions between phytoplankton and their environment. Observed data for Buckley Cove had significantly higher concentrations than those simulated by Link-Node.

Table 1.24
Model Errors for Phytoplankton in the San Joaquin River

Monitoring Station	Relative Error	Absolute Error
Stevinson	-3%	9%
Crows Landing	-12%	41%
Patterson	-27%	46%
Maze Road	-14%	49%
Vernalis	+8%	57%
Mossdale	+41%	65%
Garwood Bridge	-1%	75%
Buckley Cove / City of Stockton R6	-41%	85%

Phytoplankton (algae) growth is impacted by nutrients, light, temperature, and intrinsic growth rate. Channel geometry is also important, as it impacts the travel time and light penetration. The algae were assumed well mixed, so the light is calculated for each foot and averaged for representative light intensity. The large diurnal fluctuations of algae predicted by WARMF was consistent with Dahlgren's observation (personal communication 2006) that the peak concentration could be as much as twice the minimum concentration..

Phytoplankton Growth Pattern

There was much discussion about whether phytoplankton in the Upper San Joaquin River has a rate limited growth or rate unlimited growth. It has been argued that it would most likely be unlimited growth due to abundance of nutrients. If that is the case, the control strategy would be to reduce phytoplankton seed in the tributary inflows including the agricultural drains.

WARMF provided dynamic simulation of algae concentration subject to growth, respiration, settling, advection to the downstream, and dilution from upstream. There was no presumption of whether the algae has a limited or unlimited growth pattern. The growth rate was adjusted dynamically at each time step as a function of temperature, sunlight, and nutrient availability. At night, WARMF predicted no growth due to darkness. If the nutrients were truly unlimited, WARMF would only restrict growth based on suboptimal light and/or temperature conditions.

Figure 1.111 shows the longitudinal phytoplankton concentration profiles along the 54 model river segments of the San Joaquin River from Lander Avenue to the Old River. The figure shows snapshots in time of simulated phytoplankton along the river at midnight (dark blue), 6 AM (magenta), noon (green), 6 PM (orange), and the following midnight (purple). Note that

concentrations were at their daily minimum at 6 AM and at their maximum at 6 PM. The daily cycle of concentration is the vertical difference between the magenta and orange lines.

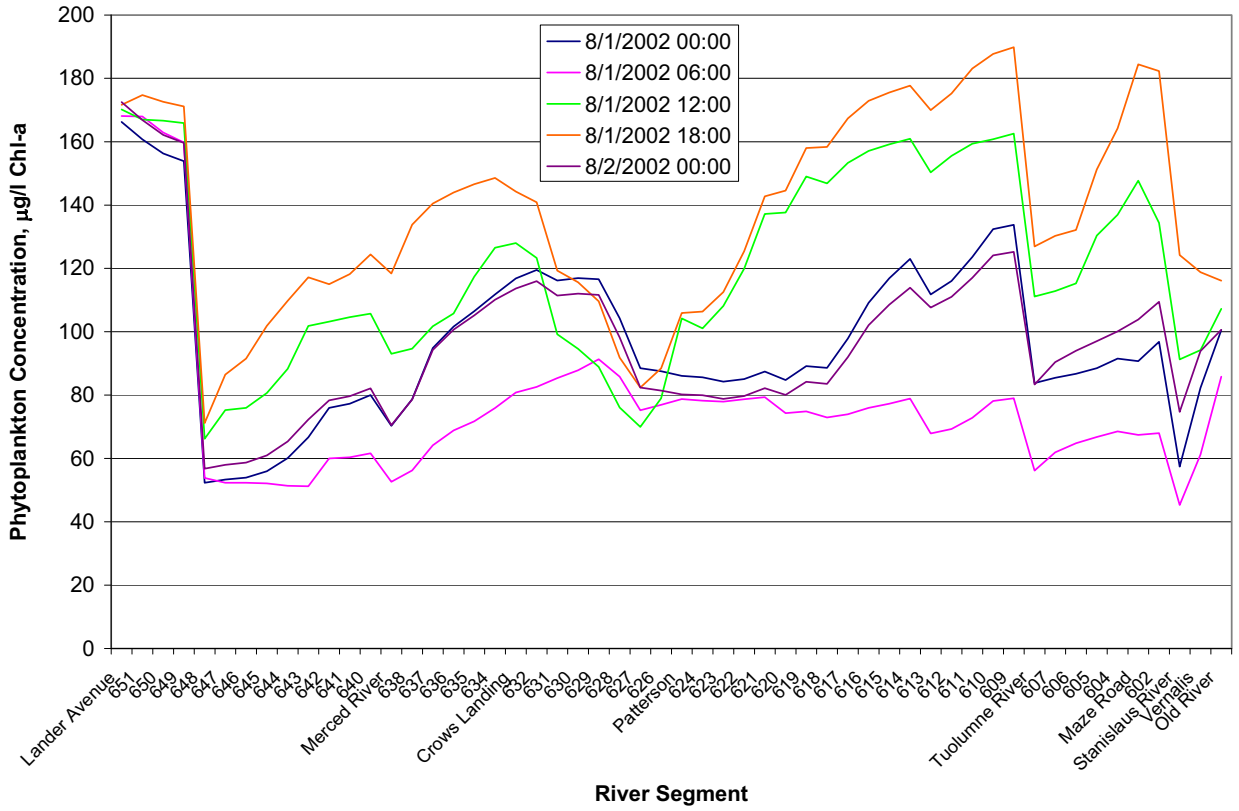

Figure 1.111 Phytoplankton Concentration Profile from Lander Avenue to Old River

The plots show that phytoplankton concentrations decrease at the confluences of tributary inflows, including Salt Slough (segment 648), agricultural drains between Crows Landing and Patterson, the Tuolumne River, and the Stanislaus River. These were caused by dilution where the inflows have lower phytoplankton concentrations than in the San Joaquin River. After the dilutions, phytoplankton concentration increased downstream along the river due to growth.

Figure 1.112 shows the phytoplankton load carried by the San Joaquin River along its entire length from Lander Avenue to the Old River. The decreases in load downstream of Patterson were caused by agricultural diversions. Just upstream of Patterson, an interesting phenomenon occurred: the peak phytoplankton concentration was at midnight and the minimum concentration was at noon. In this case, the concentration is controlled by advection of phytoplankton grown upstream rather than local growth.

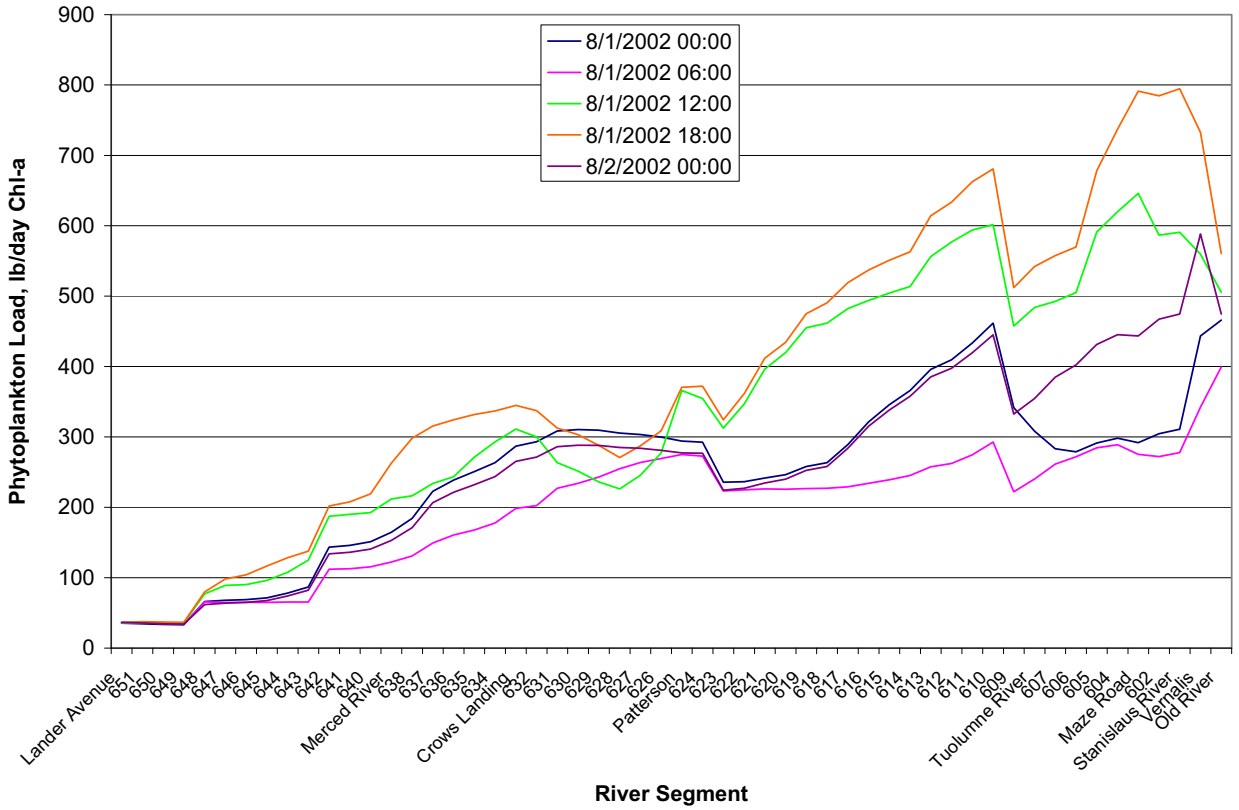

Figure 1.112 Phytoplankton Load Profile from Lander Avenue to Old River

Dissolved Oxygen

The dissolved oxygen concentration is a function of several reactions that take place simultaneously. For the San Joaquin River, the rapid growth of phytoplankton caused a large diurnal fluctuation of dissolved oxygen. As phytoplankton grew, dissolved oxygen concentrations were often well above saturation. At that point, dissolved oxygen could escape from water to the atmosphere. When phytoplankton respired and decayed at night, the dissolved oxygen concentration dropped.

Figure 1.113 through Figure 1.121 compare the time series of predicted and observed dissolved oxygen at various stations along the San Joaquin River. The daily minimum and maximum values for both simulated and observed are shown on the plots.

The simulated DO appear to pass through the median values of the observed DO at all stations upstream of Vernalis. Since the river inflow boundary condition at Lander Avenue did not include daily fluctuation of dissolved oxygen, the simulated DO did not cycle over the entire range shown in simulation results at Lander Avenue, Crows Landing, and Patterson. The observed data showed some over saturated DO as high as 19 mg/l at Stevinson, 14 mg/l at Patterson, 14 mg/l at Vernalis, and 16 mg/l at Mossdale. In general, however, the model over predicted the daily maximum and minimum DO values. This could have been caused in part by the re-aeration coefficient that was set too low to allow super saturated DO to escape from water

to the air. The model could also have been underestimating the various sources of oxygen demand.

The ability of the Link-Node model to predict DO in the DWSC is demonstrated in Figure 4.104 for Rough & Ready Island, where there was continuous monitoring of dissolved oxygen. The model matched the observed data well, although it did not predict the low DO below 1 mg/l observed in the spring of 2003. The other stations in the Link-Node model domain (Garwood Bridge and Buckley Cove) also show a good fit between simulated and observed dissolved oxygen.

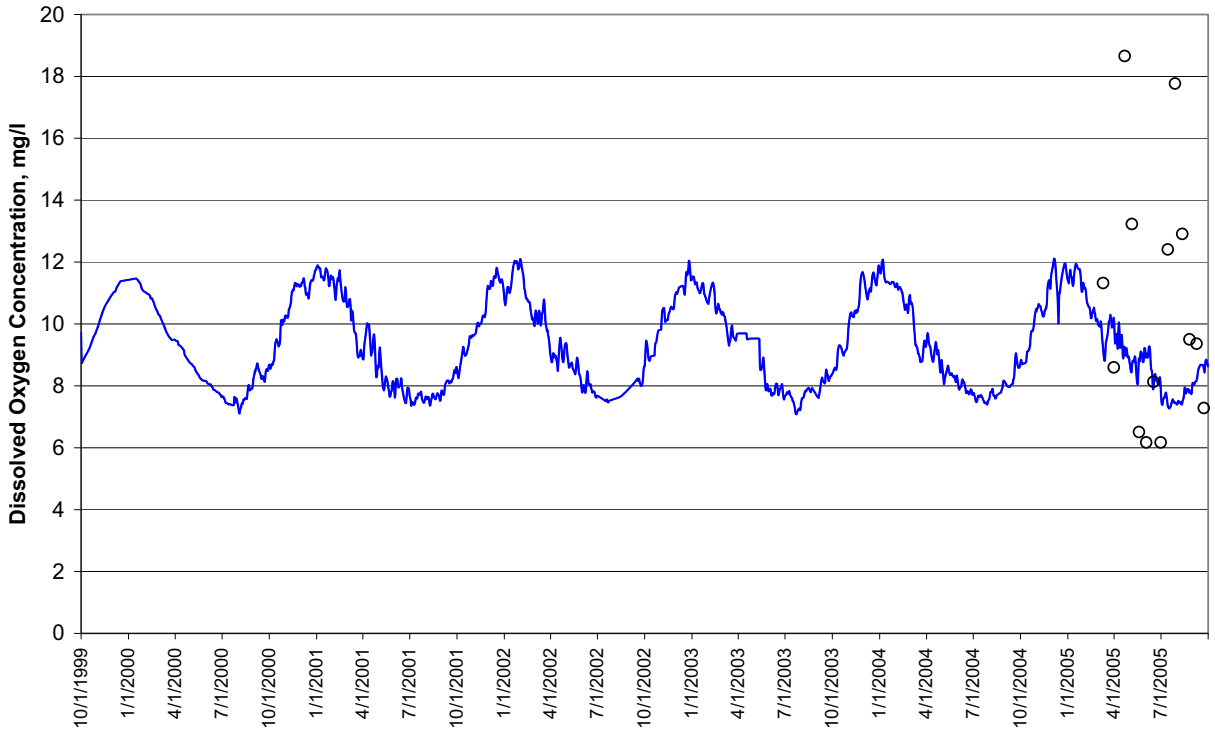

Figure 1.113 Simulated vs Observed Dissolved Oxygen at Stevinson (Lander Ave.)

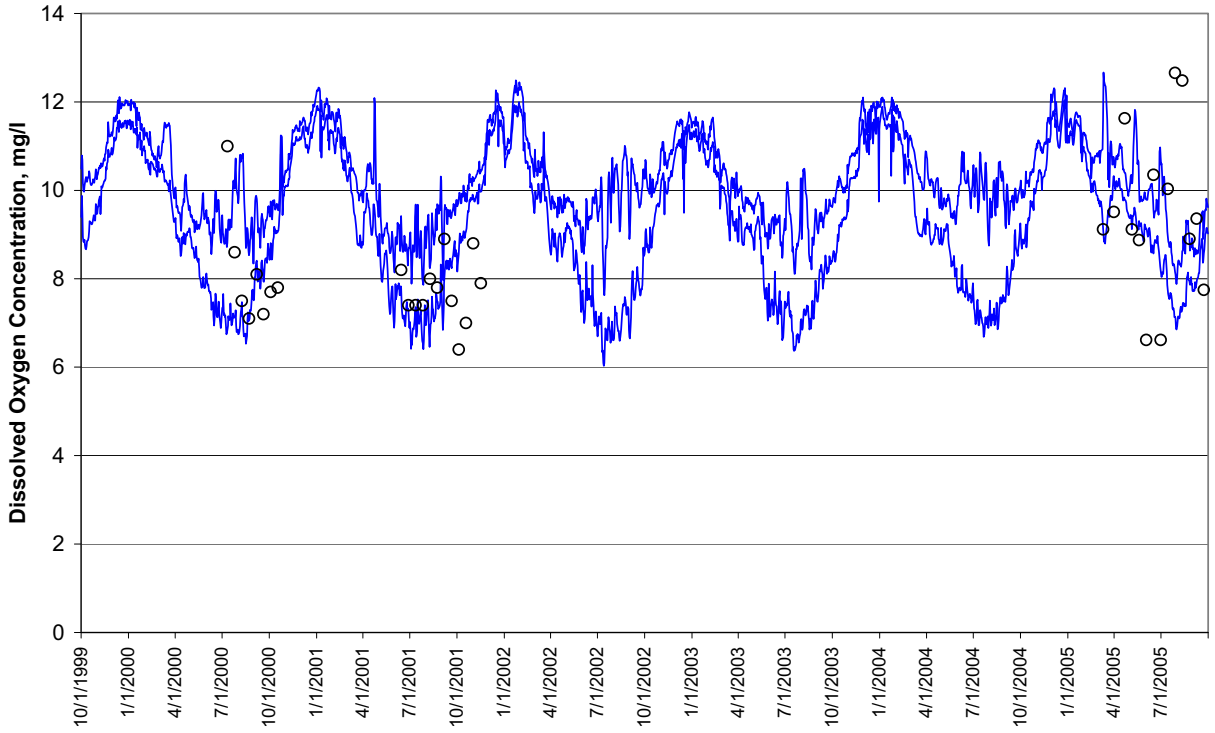

Figure 1.114 Simulated vs Observed Dissolved Oxygen at Crows Landing

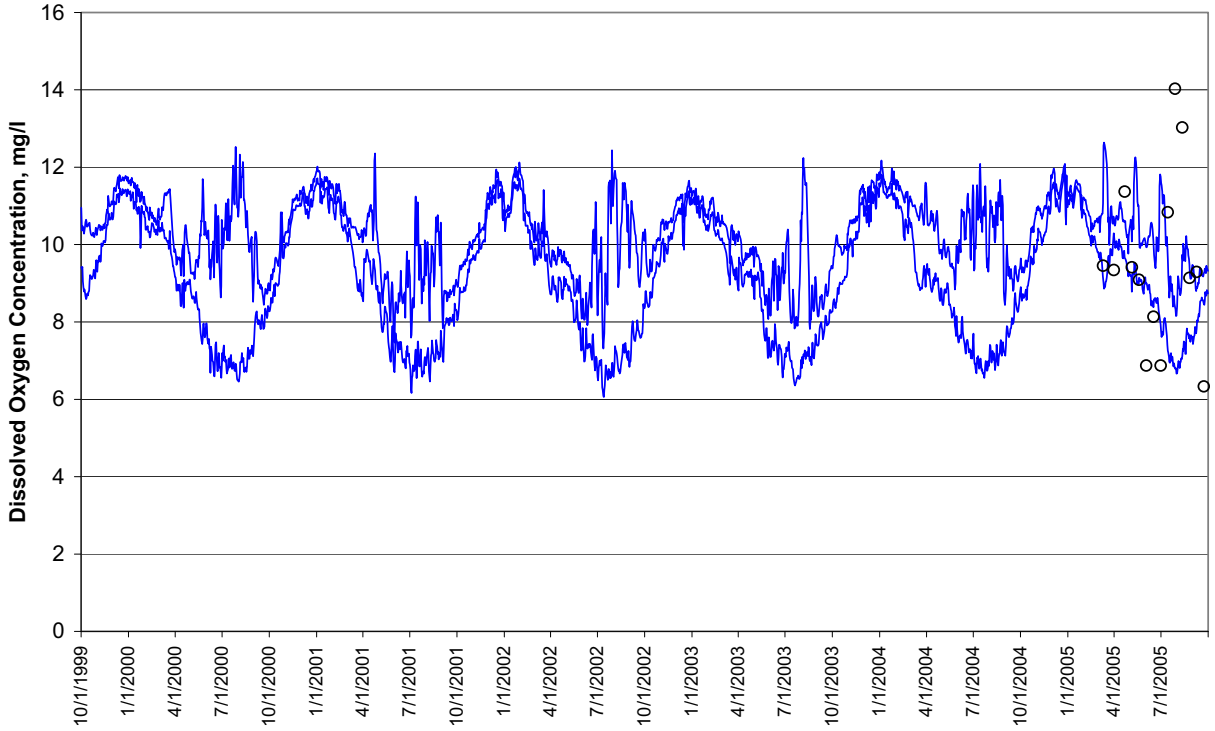

Figure 1.115 Simulated vs Observed Dissolved Oxygen at Patterson

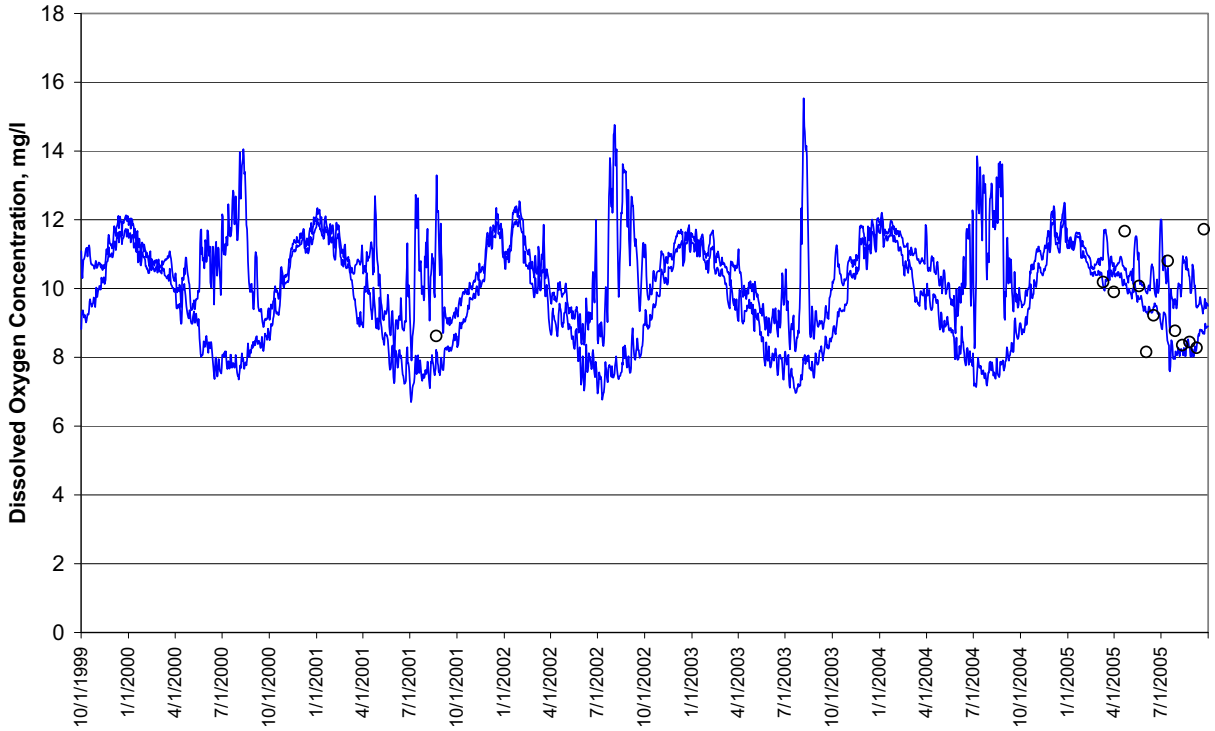

Figure 1.116 Simulated vs Observed Dissolved Oxygen at Maze Road

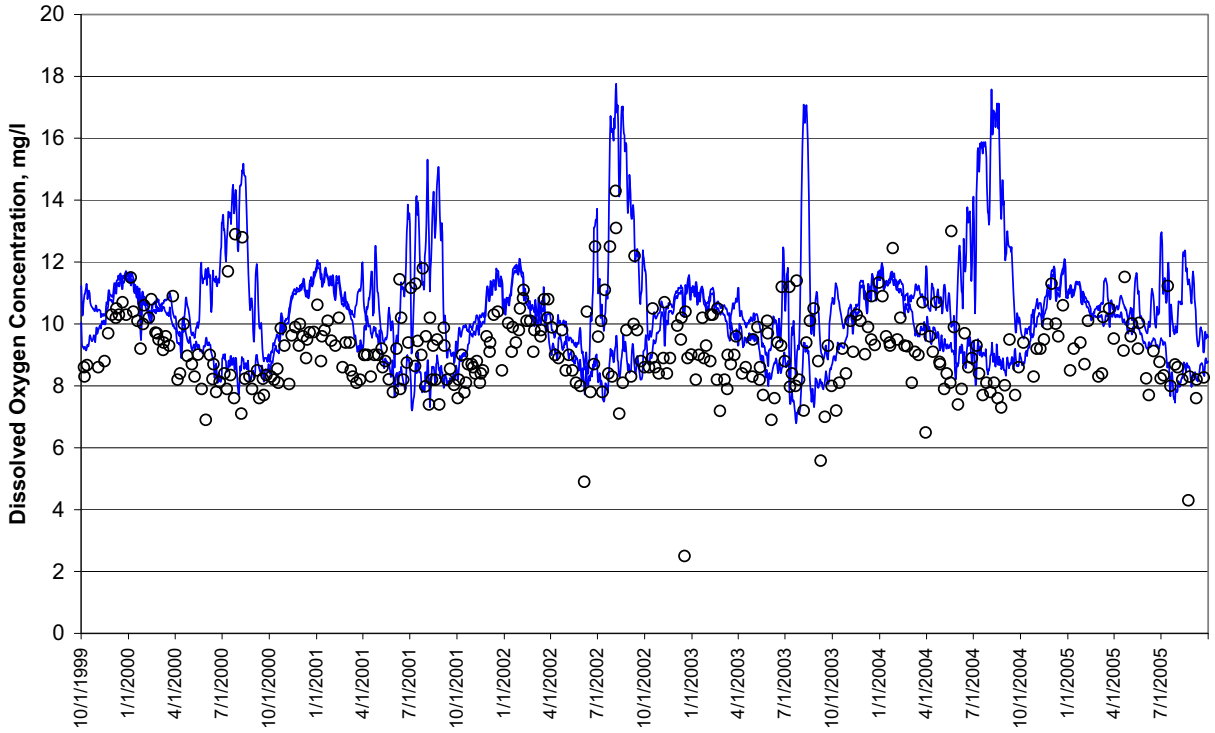

Figure 1.117 Simulated vs Observed Dissolved Oxygen at Vernalis

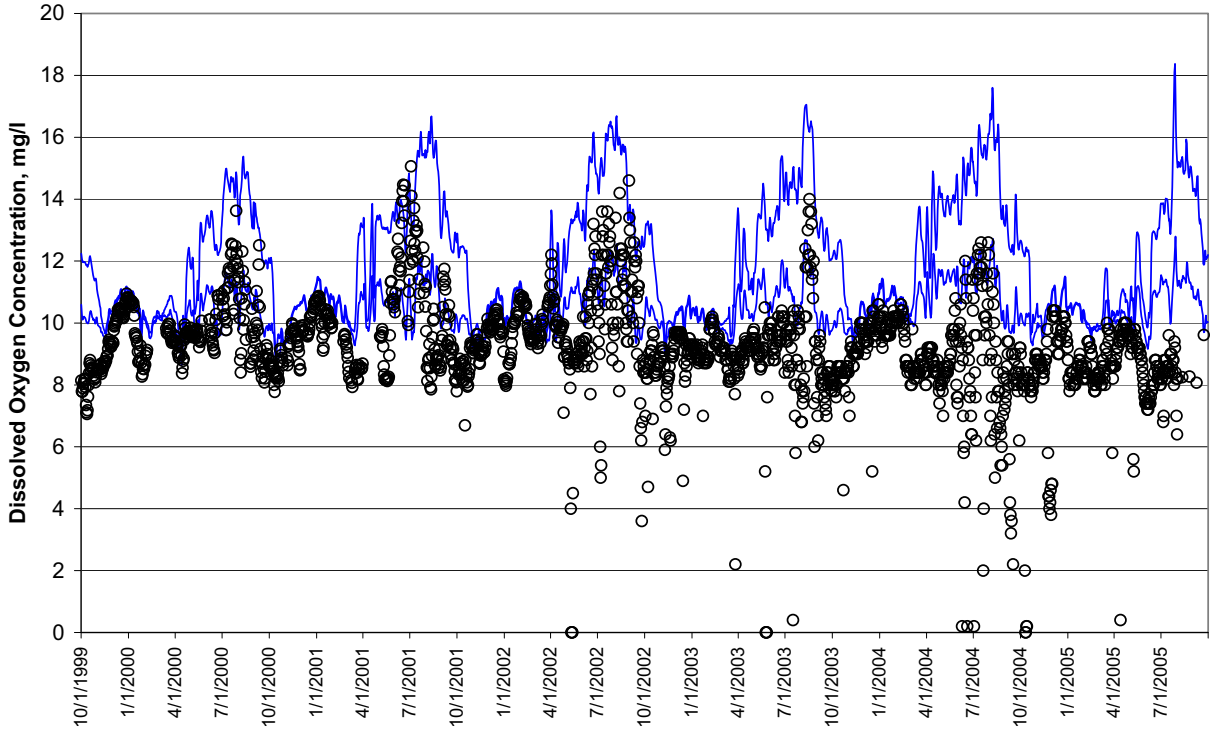

Figure 1.118 Simulated vs Observed Dissolved Oxygen at Mossdale

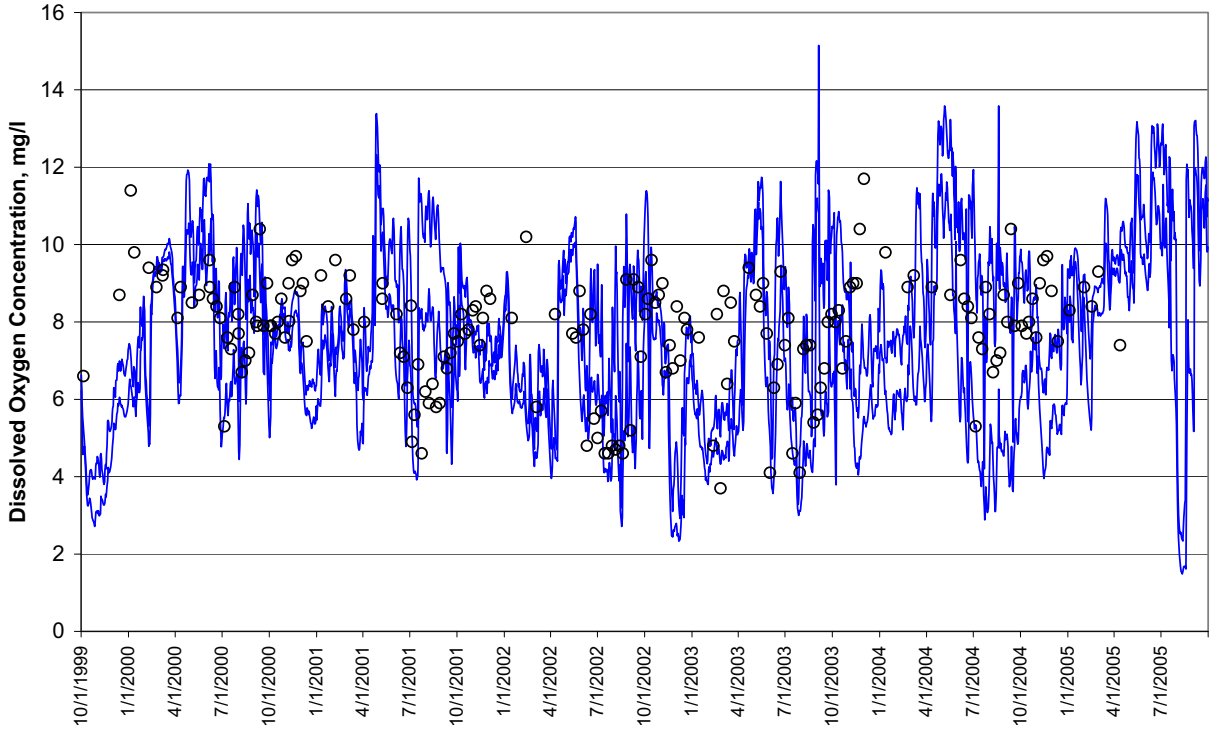

Figure 1.119 Simulated vs Observed Dissolved Oxygen at Garwood Bridge

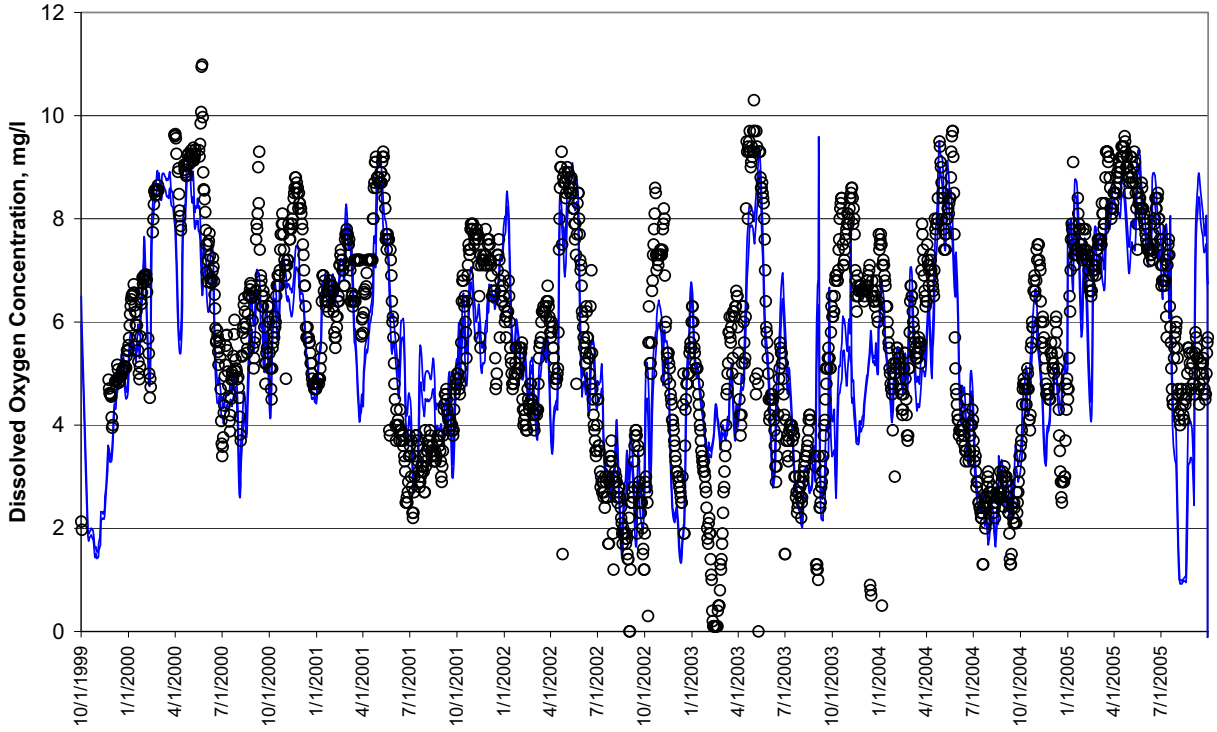

Figure 1.120 Simulated vs Observed Dissolved Oxygen at Rough & Ready Island

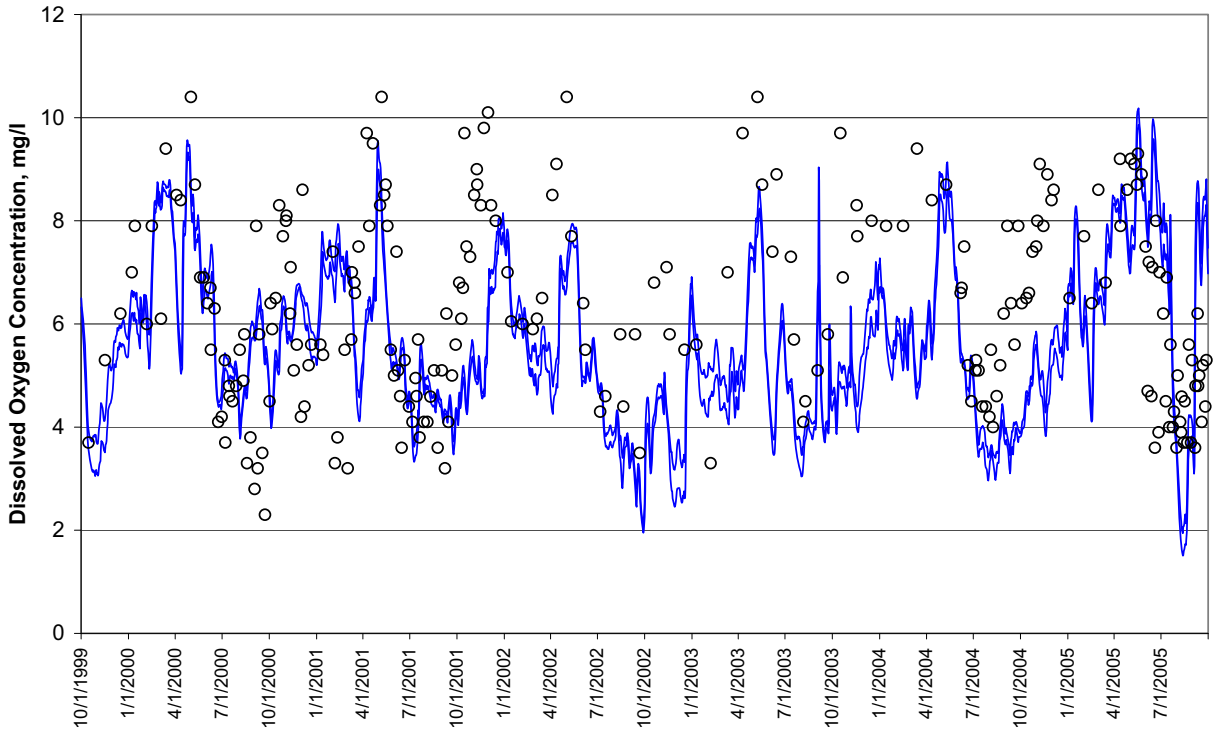

Figure 1.121 Simulated vs Observed Dissolved Oxygen at Buckley Cove

Table 1.25 shows the model errors for dissolved oxygen at various stations on San Joaquin River. Downstream of the boundary condition at Stevinson, the relative errors were small except at Vernalis and Mossdale. Absolute error was generally within 20% in spite of the large daily fluctuations. Observed data did not show the level of supersaturation at Vernalis and Mossdale predicted by the model. The model may have been underpredicting the reaeration rate, allowing more oxygen to stay in solution. The model simulates reaeration as a function of velocity, which is lower downstream of the Stanislaus River than elsewhere in the San Joaquin River, but there may be other mechanisms such as wind releasing supersaturated oxygen back to the atmosphere. The error at Mossdale did not propagate downstream through the Link-Node model to Rough & Ready Island, which implies that the dissolved oxygen concentration in the DWSC is not very sensitive to the dissolved oxygen concentration at Mossdale.

Table 1.25
Model Errors for Dissolved Oxygen in the San Joaquin River

Monitoring Station	Relative Error	Absolute Error
Stevinson	-20%	34%
Crows Landing	-3%	16%
Patterson	-10%	22%
Maze Road	-4%	8%
Vernalis	10%	15%
Mossdale	14%	16%
Garwood Bridge	-2%	24%
Rough & Ready Island	-12%	23%
Buckley Cove (Station R6)	-11%	28%

Summary

This report summarizes the calibration of the WARMF to the San Joaquin River as of May 2007. The comparisons of predicted and observed values were made for a large number of variables. The matches were generally good, although the WARMF model overpredicted the ammonia concentration in the San Joaquin River. Future investigators can continue to make improvements in the model.

SOURCE CONTRIBUTION

Introduction

The flow and water quality predictions discussed in Chapter 4 are useful for checking simulations against observed data. The model also provides information about source contribution of waters and pollutants useful to the understanding of watershed system behaviors, important to the formulation of management alternatives.

Source of Water

Figure 1.122 shows the locations of inflows to the model domain of the San Joaquin River. Red arrows are the boundary river inflows. Light blue is the point source discharge. Green arrows are agricultural return flows including spills and drains. Brown arrows are the nonpoint source flows of shallow groundwater. The orange arrows are for water diverted from the river.

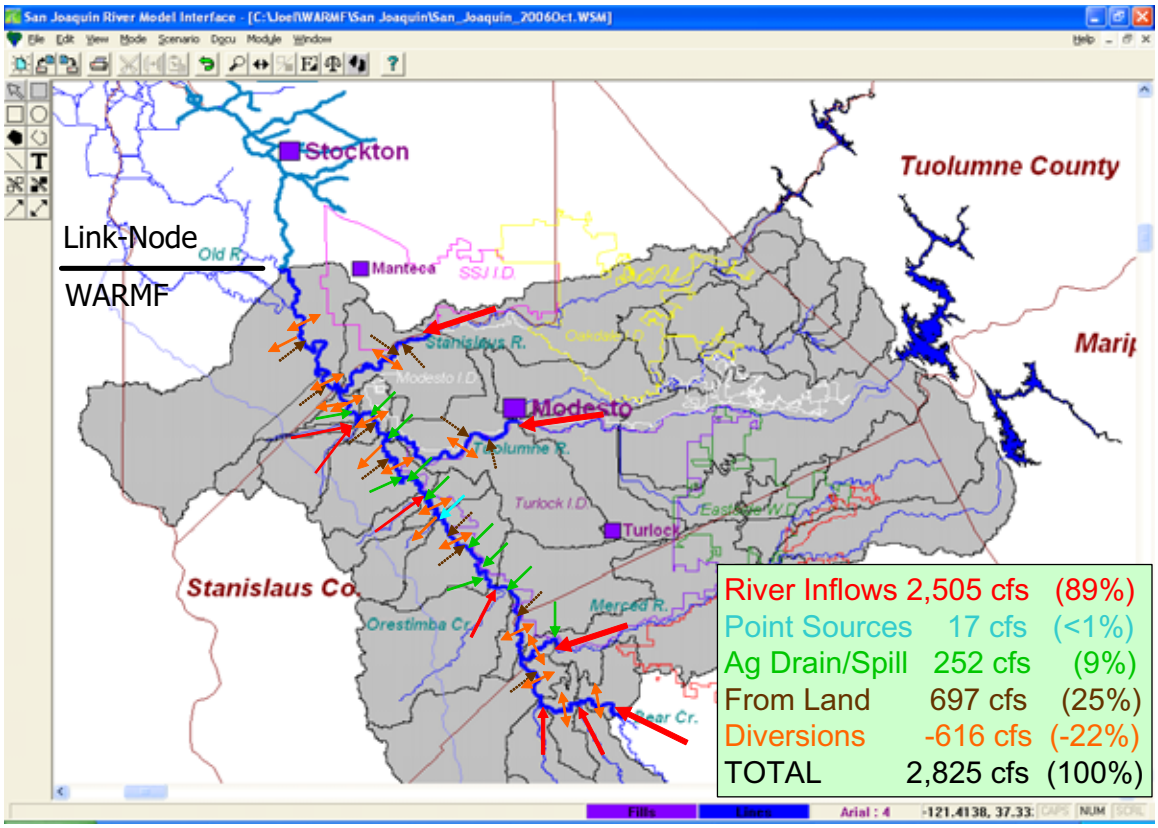

Figure 1.122 Locations of Inflows to the San Joaquin River

Table 5.1 shows the average flows of source waters to the San Joaquin River for the simulation period of 10/1/1999 to9/30/2005. Total boundary river inflow was 2,505 cfs, which was 89% of the San Joaquin River flow at Vernalis. The majority of inflows came from Stanislaus River, Tuolumne River, Merced River, and San Joaquin River upstream, which are generally referred to as the east side tributaries.

Table 1.26 Average Flows of Source Waters for the San Joaquin River

Item	Flow in cfs	Percent of Total, %
Boundary River Inflows	2,505	81
Tuolumne River	*880*	*29*
Stanislaus River	*566*	*18*
Merced River	*481*	*16*
San Joaquin River upstream	*184*	*6*
Salt Slough	*182*	*6*
Mud Slough	*127*	*4*
Los Banos Creek	*37*	*1*
Orestimba Creek	*27*	*1*
Ingram Creek	*12*	*<1*
Hospital Creek	*5*	*<1*
Del Puerto Creek	*4*	*<1*
Point Source Discharge	17	<1
Agricultural Drains	252	8
Shallow Groundwater	697	10
Total Inflows	***3,471***	***100***
Diversion within model domain	616	
Total Flow at Vernalis	***2,855***	
Water Sources Originating Outside of Model Domain		
Precipitation	578	
Irrigation Water Modesto Irrigation District	286	
Irrigation Water Turlock Irrigation District	503	
Delta Mendota Canal	287	
Irrigation & Precip. Water Reaching the San Joaquin R.		42%

The east side tributaries contributed high quality water to the San Joaquin River, with low nutrient, dissolved solids, and algae concentrations. The point source discharge (the Modesto Water Quality Control Facility) was 17 cfs, all of which is in the winter high flow season. Most of the pollutant load came from the west side river inflows and agricultural drainage.

For modeling, the flow and water quality of east side tributaries and west side tributaries (e.g. Salt Slough, Mud Slough, etc.) were prescribed inputs. The flow and water quality of agricultural canals and drains were also prescribed inputs. The agricultural canals and drains included 6 from the Turlock Irrigation District, 4 from Modesto Irrigation District, and 4 from west side irrigation districts. The preparation of this input data is described in Chapter 2.

The groundwater drainage from farmland was simulated by WARMF using the quantity and quality of irrigation water applied to the crops as input data, which varies by irrigation district. Chapter 2 documents the method to estimate and prepare the irrigation data.

Because agriculture drainage is seasonal, the relative amount of source waters to the San Joaquin River varied by season and year. Figure 1.123 shows the seasonal variations of source waters at

Vernalis. In winter, the water in the San Joaquin River was principally from the river inflows. In summer, the agricultural drainage in the form of groundwater accretion from farmland became important.

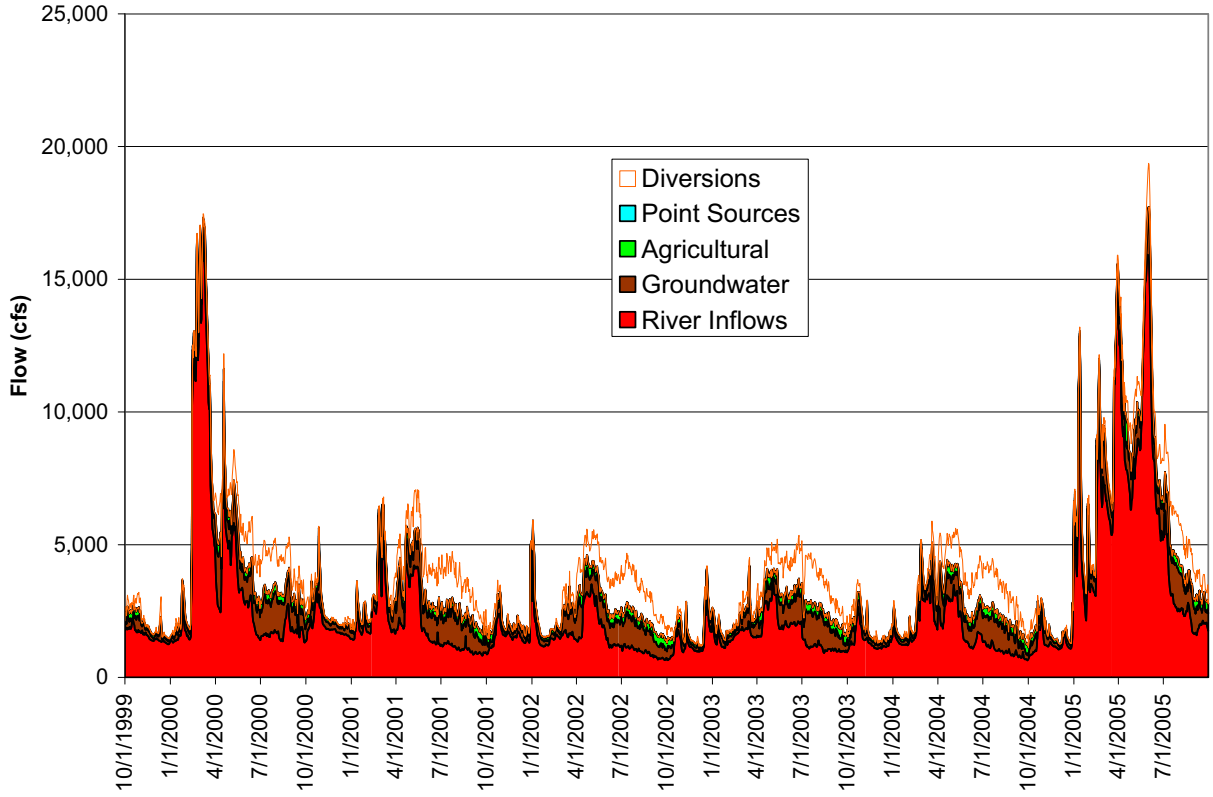

Figure 1.123 Seasonal Variations of Source Waters in the San Joaquin River

Sources of Total Dissolved Solids

The concentration of total dissolved solids (TDS) is a marker indicative of salty agricultural surface and subsurface drainage entering the San Joaquin River for the Upper San Joaquin River, where sea water intrusion is not important. TDS is highly correlated to electrical conductivity, which is easily measured and used to estimate the sources of TDS.

Table 1.27 summarizes the fluxes of TDS load to the San Joaquin River as estimated from conservative EC. Mud Slough, Salt Slough, agricultural drains and groundwater accretion from the land were the largest sources of TDS. Together, they accounted for 76% of the total source loads.

Diversions removed about 15% of the TDS load. Since two of the diversions are upstream of the Tuolumne River confluence and a third diversion is upstream of the Stanislaus River, the diverted water has high TDS. The salts removed from the river eventually return, however, as

irrigation water applied to the land and drains back to the San Joaquin River through agricultural facilities or groundwater seepage.

Table 1.27
Sources of Total Dissolved Solids to the San Joaquin River

Sources	Total Dissolved Solids (tons/day)
Stanislaus River	86
Tuolumne River	139
Merced River	110
San Joaquin River	113
Salt Slough	419
Mud Slough	510
Los Banos Creek	85
Orestimba Creek	23
Del Puerto Creek	3
Hospital & Ingram Creeks	23
Agricultural Spills / Drains + Modesto WQCF	232
Groundwater Accretion and Surface Runoff	1,467
Resuspension from River Bed	0
Sinks	
Settling to River Bed	0
Diversions	820
Net Load in San Joaquin at Old River	2,390

Figure 1.124 shows the relationship between TDS load and TDS concentration at Mossdale. High TDS loads led to high TDS concentration in the receiving water. From midsummer through midwinter, the TDS concentration increased with higher TDS loads from agricultural drainage, Mud Slough, and Salt Slough. In the spring, the TDS load to the San Joaquin River was relatively low while flow was high, producing the lowest seasonal TDS concentrations.

The relationship between TDS loads and TDS concentration has been distorted in 2005. The year 2005 was a wet year. Both TDS load and TDS concentration are dominated by the boundary river inflows in late winter and early spring. Although the load was high, the TDS concentration was not any higher than in a normal year.

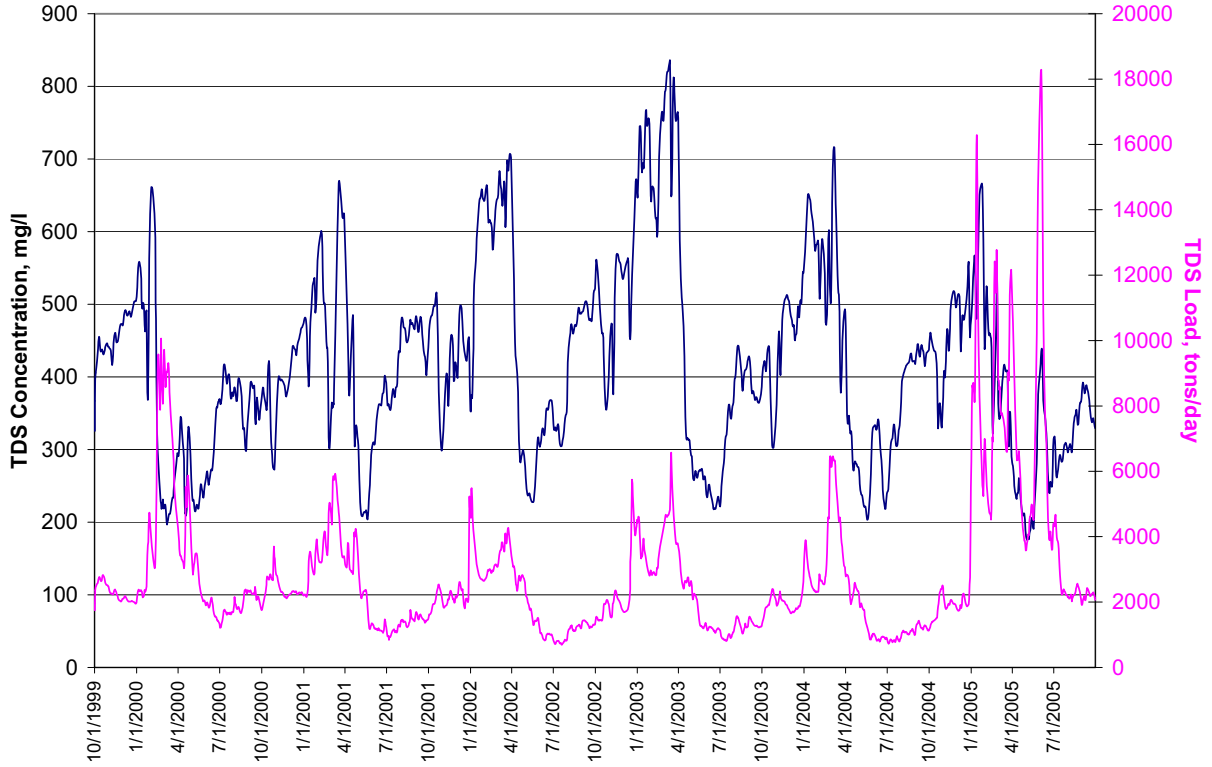

Figure 1.124 TDS Load (Pink Line) vs. TDS Concentration (Black Line) at Mossdale

Sources of Nitrogen

Table 5.3 summarizes the sources of nitrogen load to the San Joaquin River. The boundary river inflows contributed two third of the total nitrogen loaded to the San Joaquin River. Another third was contributed by agricultural drains and spills. Most of the nitrogen load was in the form of nitrate.

Figure 1.125 shows the relationship between total nitrogen load and total nitrogen concentration at Mossdale. High total nitrogen load led to high total nitrogen concentration except in early 2005, when high flow made high load possible without high concentration.

Table 1.28
Sources of Total Nitrogen to the San Joaquin River

Sources	Total Nitrogen (tons/day)
Stanislaus River	0.94
Tuolumne River	2.13
Merced River	2.06
San Joaquin River	0.77
Salt Slough	1.46
Mud Slough	2.07
Los Banos Creek	0.15
Orestimba Creek	0.25
Del Puerto Creek	0.04
Hospital & Ingram Creeks	0.55
Agricultural Spills / Drains + Modesto WQCF	3.73
Groundwater Accretion and Surface Runoff	8.78
Resuspension from River Bed	0.28
Sinks	
Settling to River Bed	1.49
Diversions	5.53
TOTAL	16.18

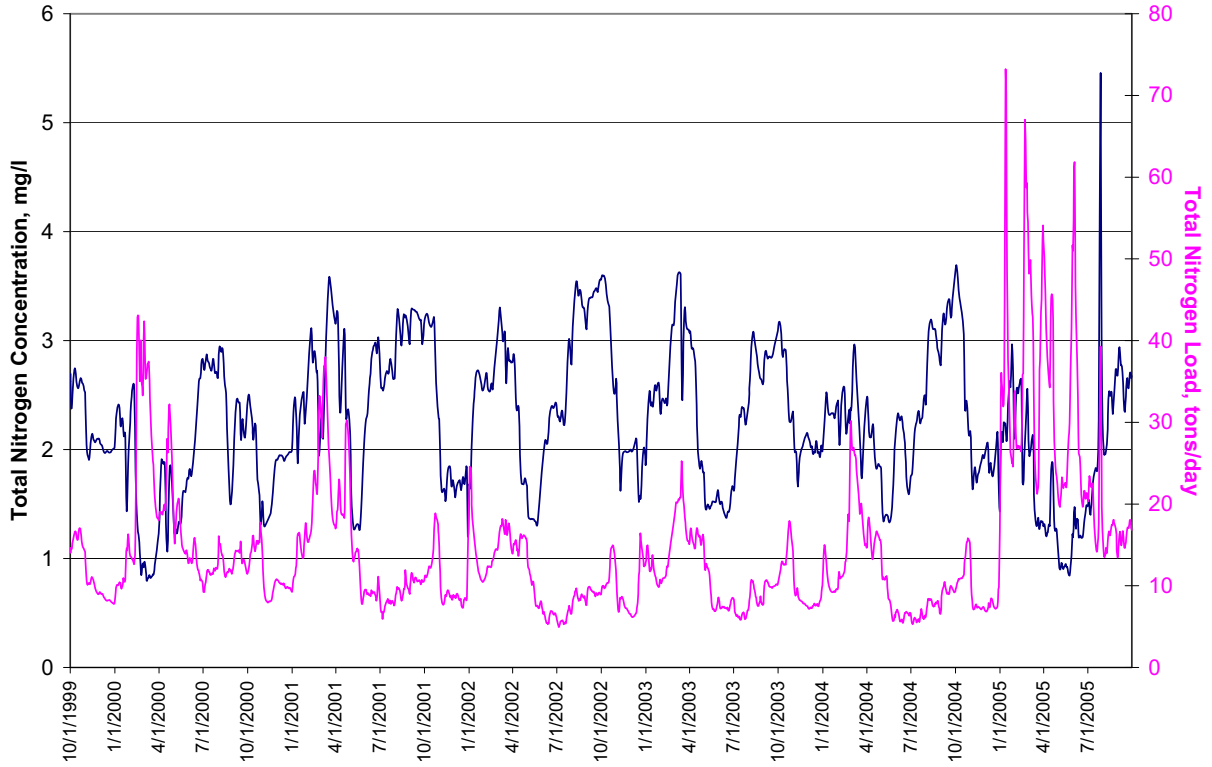

Figure 1.125 Total Nitrogen Load (Pink Line) vs. Total Nitrogen Concentration at Mossdale

Sources of Phosphorus

Table 1.29 summarizes the sources of phosphorus load to the San Joaquin River. The east side tributaries, Salt Slough, Mud Slough, and Los Banos Creek were major contributors of phosphorus load to the San Joaquin River. However, the largest source simulated by the model was from farmlands, both in groundwater accretion and in overland flow during storms.

Because phosphorus adsorbs strongly to suspended sediment, the model predicted that much of the phosphorus load to the San Joaquin River settles with sediment to the river bottom. The model also predicted that about a third of the settled phosphorus was re-suspended back to the water column.

Table 1.29
Sources of Total Phosphorus to the San Joaquin River

Sources	Total Phosphorus (lb/day)
Stanislaus River	568
Tuolumne River	359
Merced River	216
San Joaquin River	249
Salt Slough	364
Mud Slough	165
Los Banos Creek	174
Orestimba Creek	50
Del Puerto Creek	3
Hospital & Ingram Creeks	120
Agricultural Spills / Drains + Modesto WQCF	642
Groundwater Accretion and Surface Runoff	2,546
Resuspension from River Bed	702
Sinks	
Settling to River Bed	2,078
Diversions	1,024
TOTAL	3,056

Figure 1.126 shows the relationship between loading and concentration of phosphorus. High loading is associated with high concentration for most years. As with TDS and nitrogen, high flow in early 2005 produced high loads but normal concentrations.

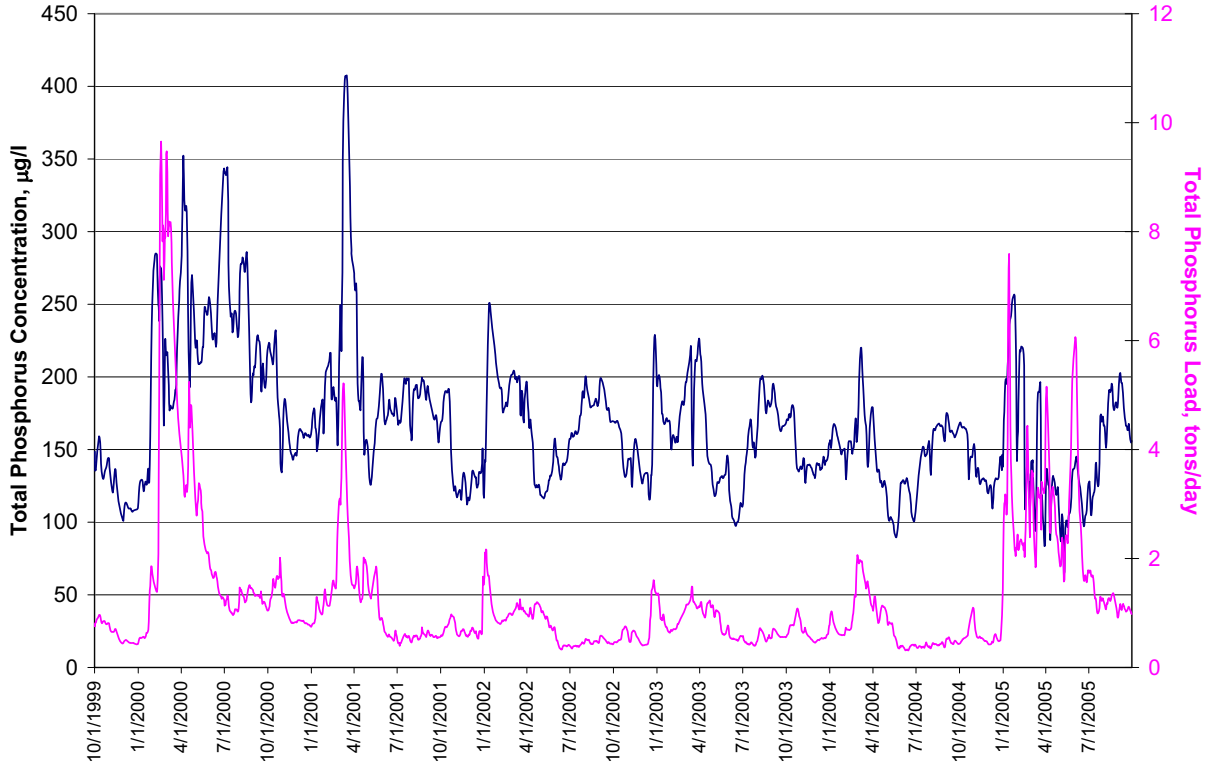

Figure 1.126 Total Phosphorus Load (pink line) vs. Phosphorus Concentration at Mossdale

Sources of Sediment

Table 1.30 summarizes the sources of suspended sediment load to the San Joaquin River. The soil erosion from farmlands was simulated to be a major contributor of total suspended sediment to the river. Most of the suspended sediment was predicted to settle to the river bed. About 30% of the settled sediment was predicted to be scoured back to the water column.

Figure 1.127 shows the relationship between loading and concentration of suspended sediment. High loading again led to high concentration, including during the high flow of early 2005.

The scales of the plot happen to show the curve for suspended sediment loading above the suspended sediment concentration. It may give an impression that settling has occurred in the river. This is strictly coincidental, because the scales can be adjusted to have the curve for concentration above the curve for loading.

Table 1.30
Sources of Total Suspended Sediment to the San Joaquin River

Sources	Total Suspended Sediment (tons/day)
Stanislaus River	18
Tuolumne River	26
Merced River	23
San Joaquin River	24
Salt Slough	49
Mud Slough	16
Los Banos Creek	9
Orestimba Creek	10
Del Puerto Creek	0
Hospital & Ingram Creeks	14
Agricultural Spills / Drains + Modesto WQCF	8
Surface Runoff	605
Resuspension from River Bed	177
Sinks	
Settling to River Bed	528
Diversions	94
TOTAL	**357**

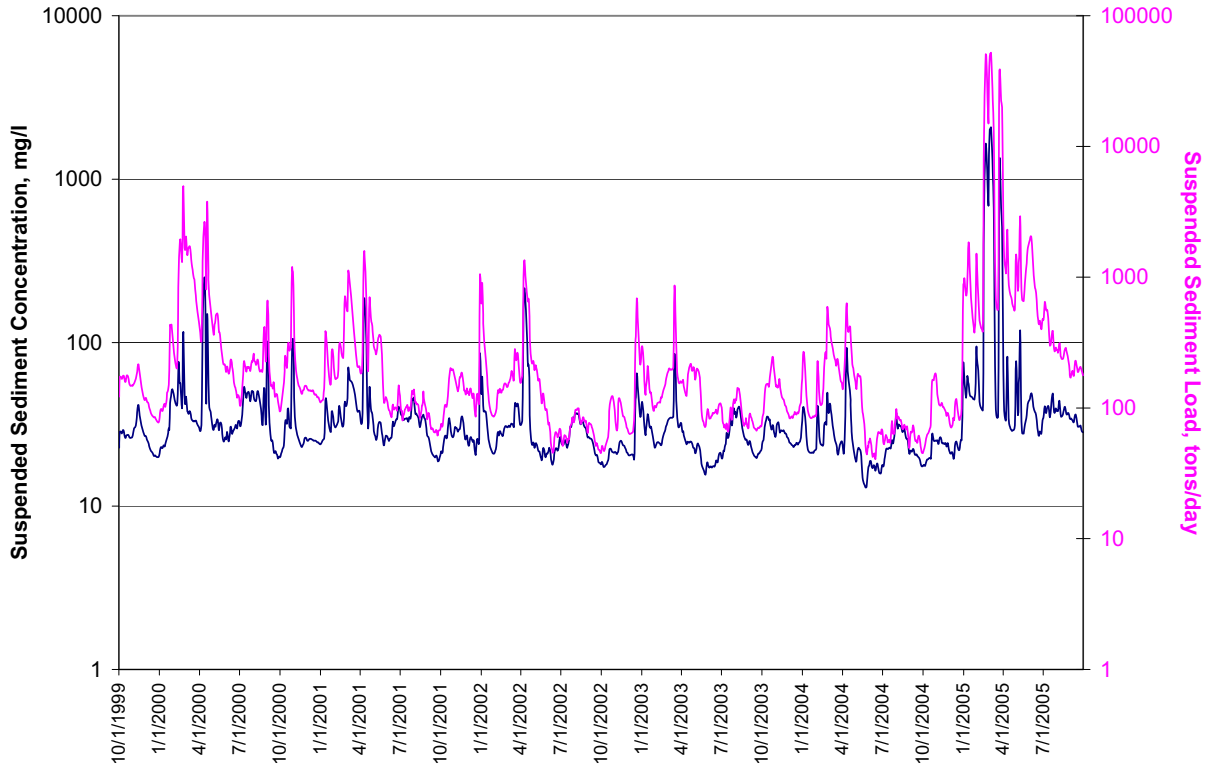

Figure 1.127 Total Suspended Sediment Load (pink line) vs. Concentration at Mossdale

Sources of Phytoplankton

Table 1.31 summarizes the sources and sinks of phytoplankton and the amount produced by growth and destroyed by mortality and respiration. The model predicted that about 80% of phytoplankton at Mossdale grew within the Upper San Joaquin River.

Table 1.31
Sources of Phytoplankton to the San Joaquin River

Sources	Total Phytoplankton (lb/day Chl-a)
Stanislaus River	8
Tuolumne River	11
Merced River	4
San Joaquin River	25
Salt Slough	17
Mud Slough	21
Los Banos Creek	3
Orestimba Creek	1
Del Puerto Creek	1
Hospital & Ingram Creeks	2
Agricultural Spills / Drains + Modesto WQCF	5
Groundwater Accretion and Surface Runoff	0
Growth	927
Sinks	
Mortality, Respiration, and Settling to River Bed	410
Diversions	171
TOTAL	**444**

Figure 1.128 shows the relationship between the net phytoplankton source and phytoplankton concentration at Mossdale. The primary source of phytoplankton was the blooms which typically occur from June through August when optimum temperature and light conditions are combined with low flow. In the winters, there was little growth, which led to little phytoplankton load and concentration.

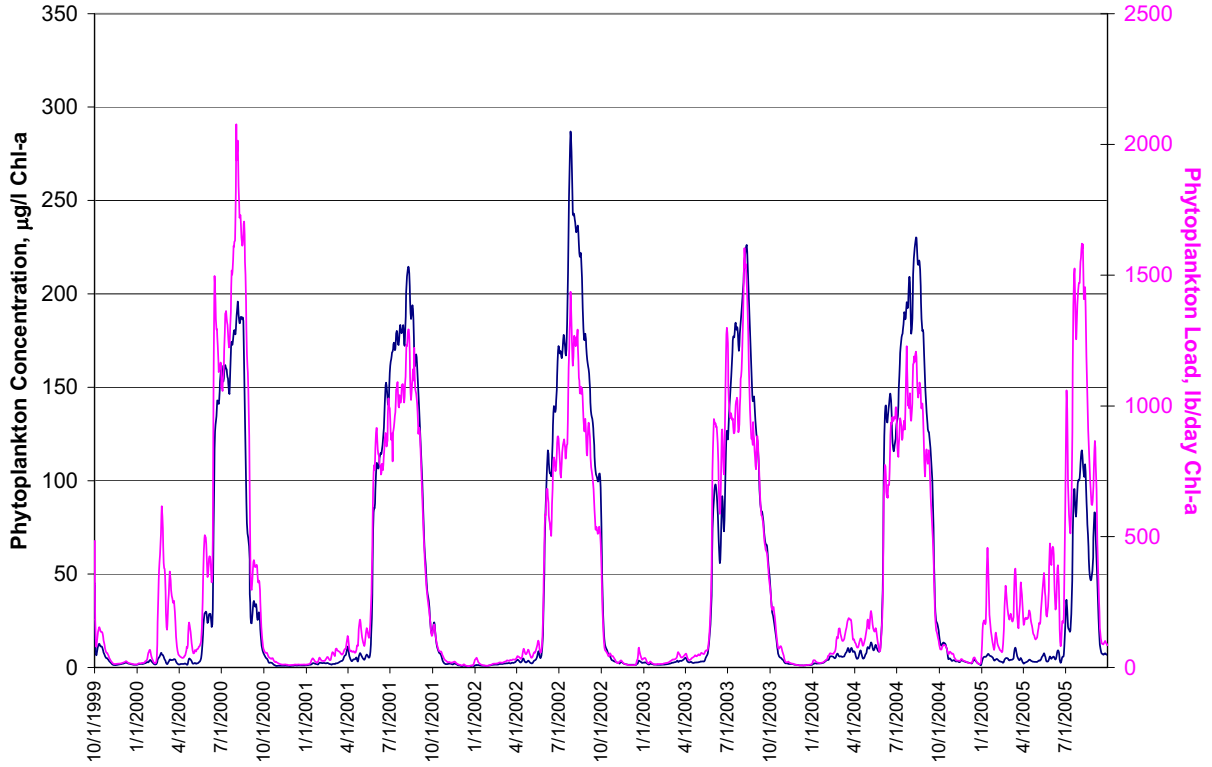

Figure 1.128 Total Phytoplankton Load (pink line) vs Concentration at Mossdale

SENSITIVITY ANALYSIS

Introduction

A sensitivity analysis with the San Joaquin River Model could help determine if the model error of a specific pollutant is likely to affect the DO of DWSC. A sensitivity analysis could quantify the potential error that can arise from the uncertainty of model coefficients used in the model input. A sensitivity analysis could identify sensitive parameters or coefficients that may affect the management strategy to increase DO in DWSC. These coefficients needed to be measured accurately by field and laboratory investigators.

There are thousands of model coefficients, so it was not practical to run a sensitivity analysis on all of them. Users of the San Joaquin River Model are free to perform any simulation to determine model sensitivity. Included here are three examples to demonstrate the methodology and highlight key insights about the model and the San Joaquin River system.

Effect of Simulation Time Step

WARMF may be run on a daily or shorter time step. A daily time step requires less time for a model run and less disk space to store results. A daily time step is adequate for water quality parameters not affected by sunlight and algal growth dynamics. There are certain cases that require a higher temporal resolution of an hourly time step. These include storm hydrology, suspended sediment, and algae.

The run time for a 6 year simulation of the San Joaquin River watershed on an hourly time step was about 12 hours using a fast computer. There was a practical benefit to reducing the run time, so more simulations could be done. One alternative was to run the model on a 6 hour time step. The 6 hourly time steps were from midnight to 6 AM, 6 AM to noon, noon to 6 PM, and 6 PM to midnight. The two time steps in the middle of the day captured phytoplankton growth, while all time steps could simulate phytoplankton respiration and mortality.

A sensitivity analysis was performed to determine the difference between hourly time step and 6 hours time step. To choose the time step for simulation, click on Scenario / Run dialog shown below in Figure 1.129. Note that the number of time steps per day is entered, not the time step length.

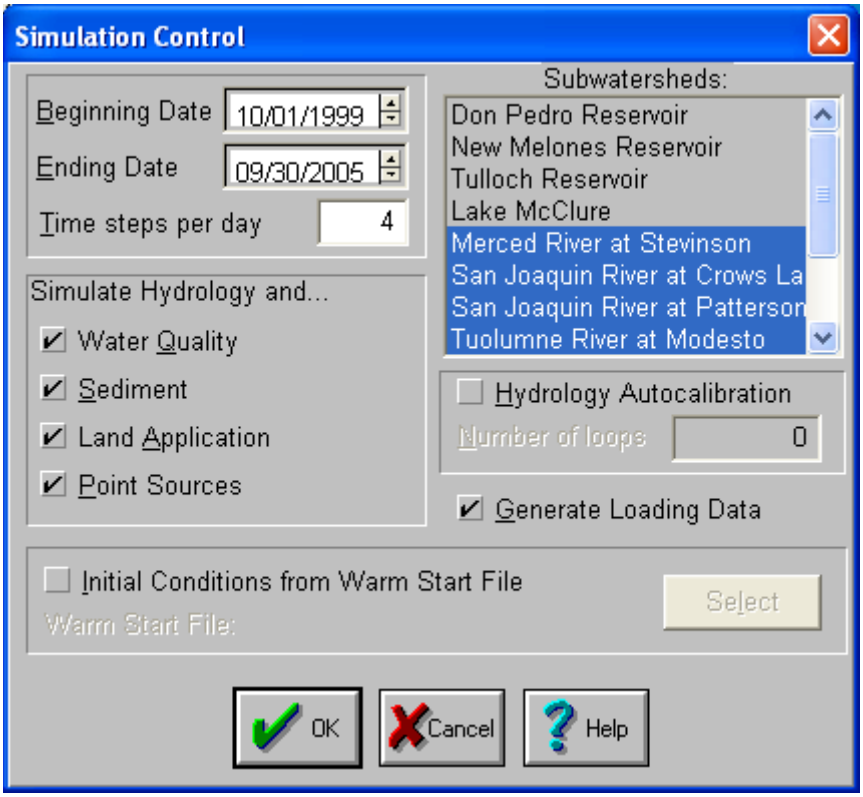

Figure 1.129 Dialog for Selection of Time Step

Figure 1.130 through Figure 1.132 compare the results of hourly time step vs. 6 hour time step for flow, conservative EC, and phytoplankton at Vernalis. The result of hourly time step

simulation is shown in blue and the result of 6 hour time step simulation is shown in green. The black circles are observed data

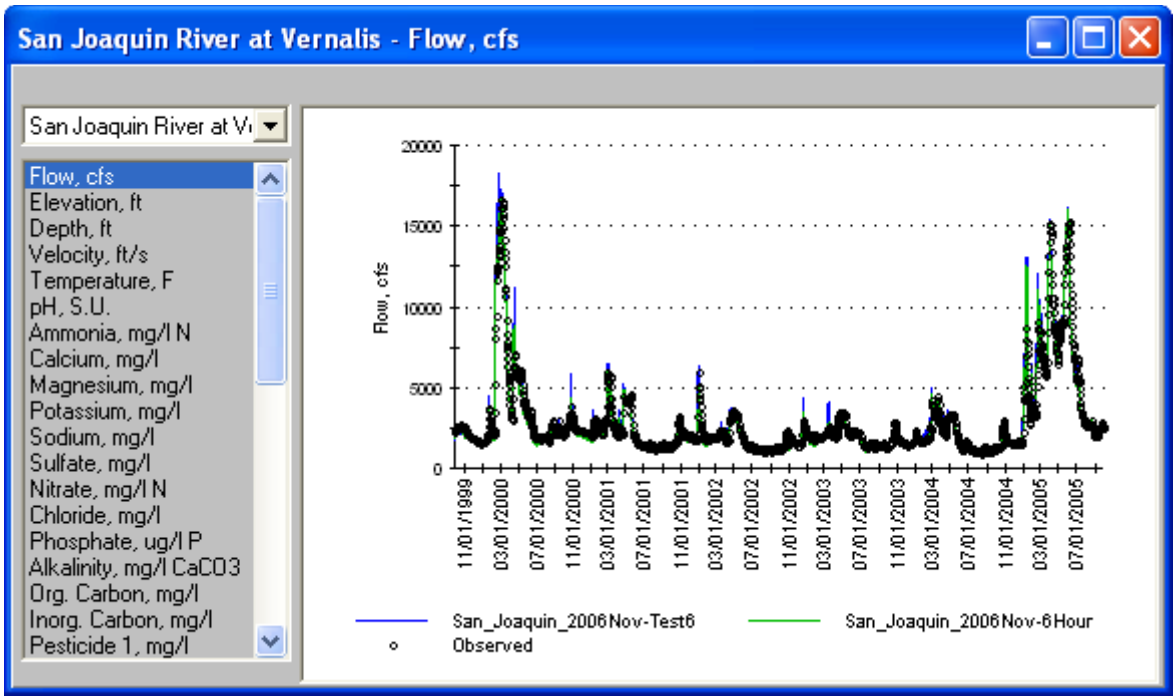

Figure 1.130 Flow at Vernalis: 1 Hour Time Step vs 6 Hour Time Step

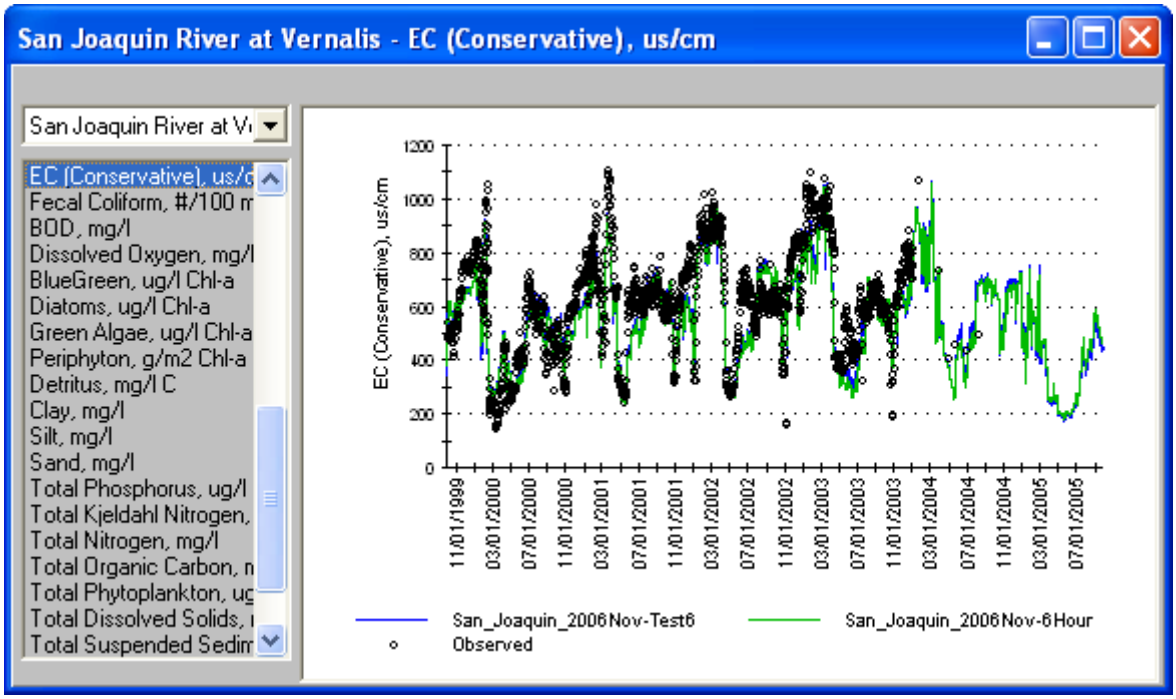

Figure 1.131 Conservative EC at Vernalis: 1 Hour Time Step vs 6 Hour Time Step

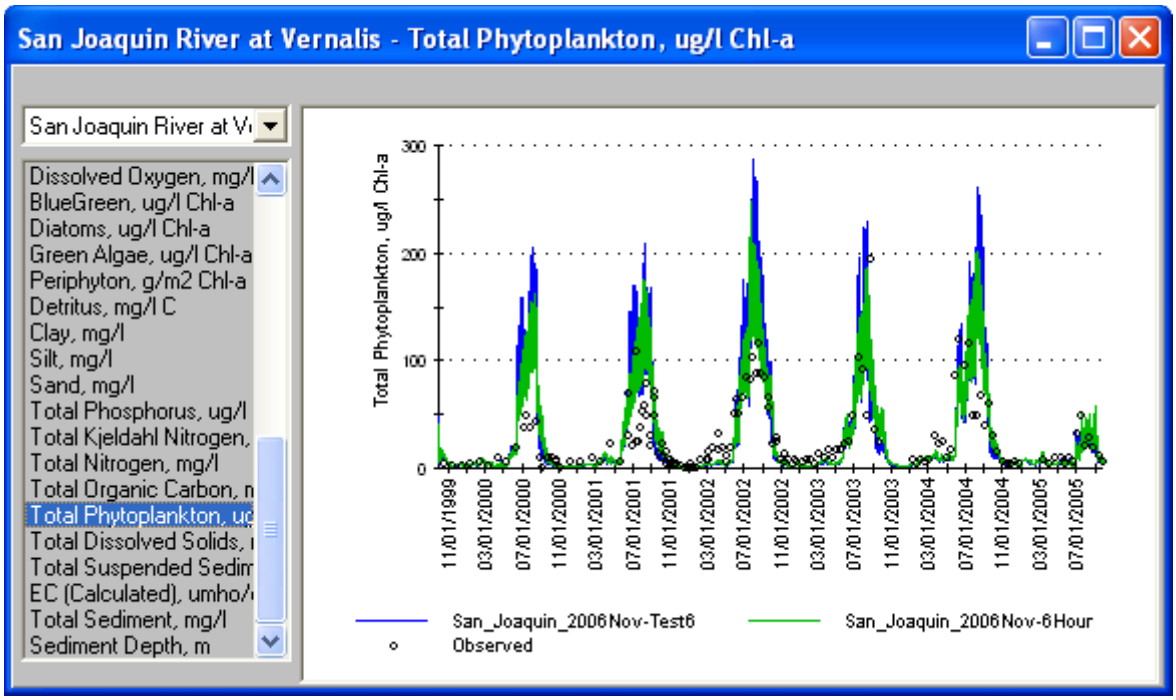

Figure 1.132 Phytoplankton at Vernalis: 1 Hour Time Step vs 6 Hour Time Step

The flow and conservative EC showed small differences using two different time steps. The time step difference for phytoplankton is substantial. The phytoplankton concentration was 20% lower when running with the 6 hour time step. To save run time, it could be appropriate to use 6 hourly time step for screening level runs. An hourly time step should be used in the final run to evaluate the effectiveness of a proposed watershed management plan.

Effect of Nutrients on Phytoplankton

This sensitivity analysis was performed to test the hypothesis that nutrients in the San Joaquin River were over abundant and that halving nutrient inputs would not affect the phytoplankton concentration. To test the hypothesis, a simulation was run by halving the ammonia, nitrate, and phosphate in river inflows, agricultural drains & spills, and point sources.

The WARMF Consensus Module was used to modify the pollution loads quickly. It is accessed through Module / Consensus in the WARMF menu. Figure 1.133 shows the Consensus Module. In step 5 of the Consensus Module, a global change can be made to all model point sources. Clicking on the Edit button produces a smaller dialog box as shown in Figure 1.133. The first column lists the water quality constituents and second column list the multiplication factors to use. To test the sensitivity of algae to nutrient concentration, the factors for ammonia, nitrate, and phosphate were changed from 1 to 0.5. The change affected everything treated as point sources by the model, including river inflows and agricultural drains.

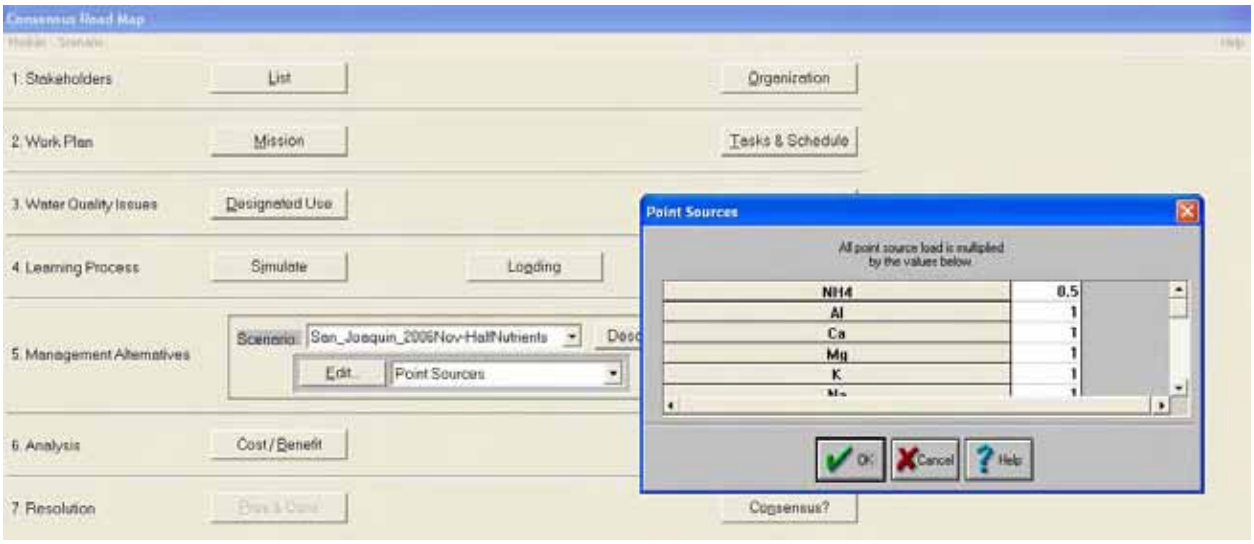

Figure 1.133 Point Source Load Multipliers in the Consensus Module

Figure 1.134 through Figure 1.137 show the response of ammonia, nitrate, phosphate, and phytoplankton to the nutrient load reduction. The base case is in blue, which represents no reduction in nutrient inputs. The nutrient reduction case is in green. The observed data is in black circles.

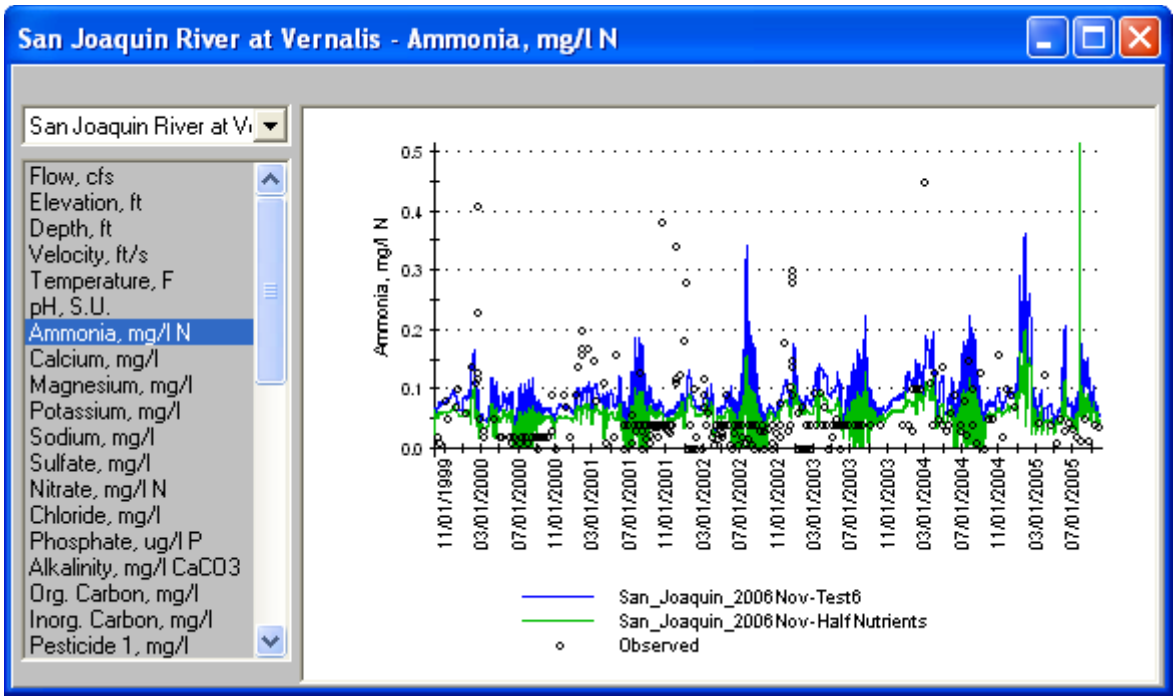

Figure 1.134 Response of Ammonia to Nutrient Load Reduction at Vernalis
No Load Reduction (Blue Line) and Load Reduction (Green Line)

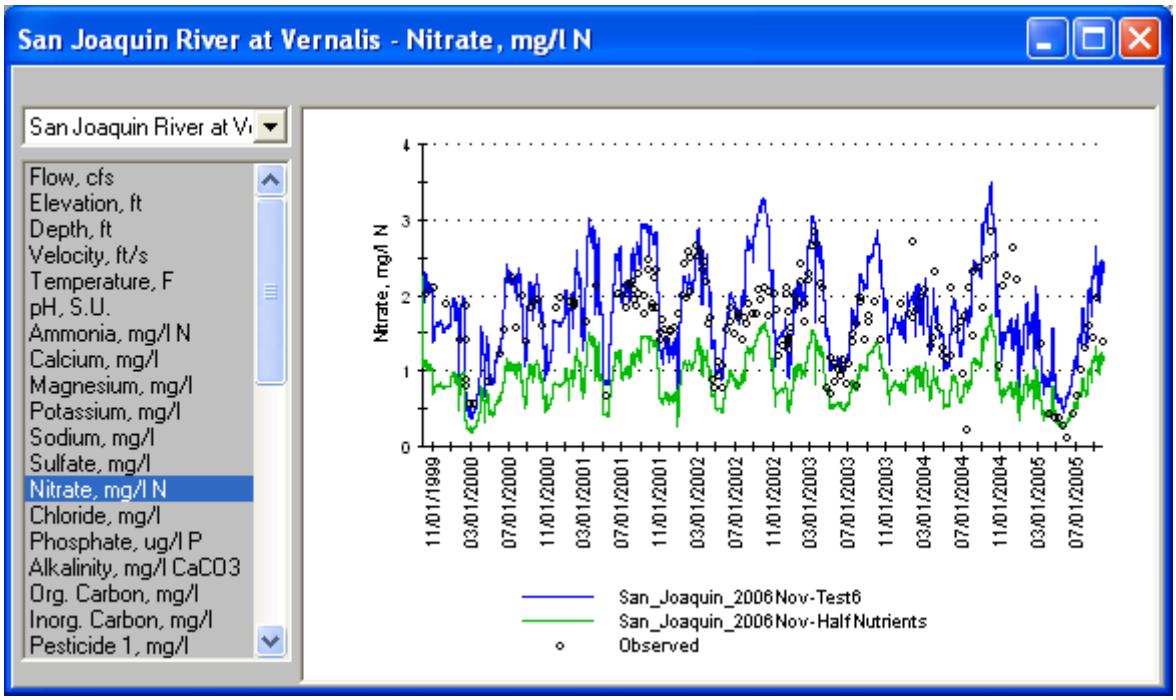

Figure 1.135 Response of Nitrate to Nutrient Load Reduction at Vernalis
No Load Reduction (Blue Line) and Load Reduction (Green Line)

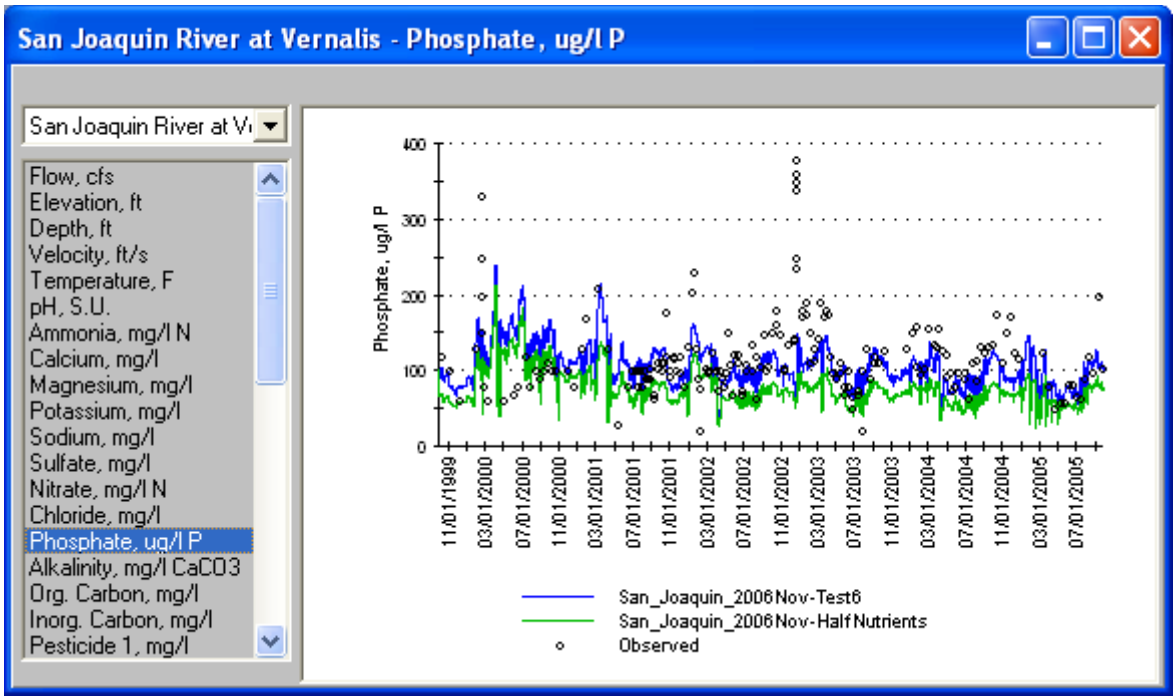

Figure 1.136 Response of Phosphate to Nutrient Load Reduction at Vernalis No Load Reduction (Blue Line) and Load Reduction (Green Line)

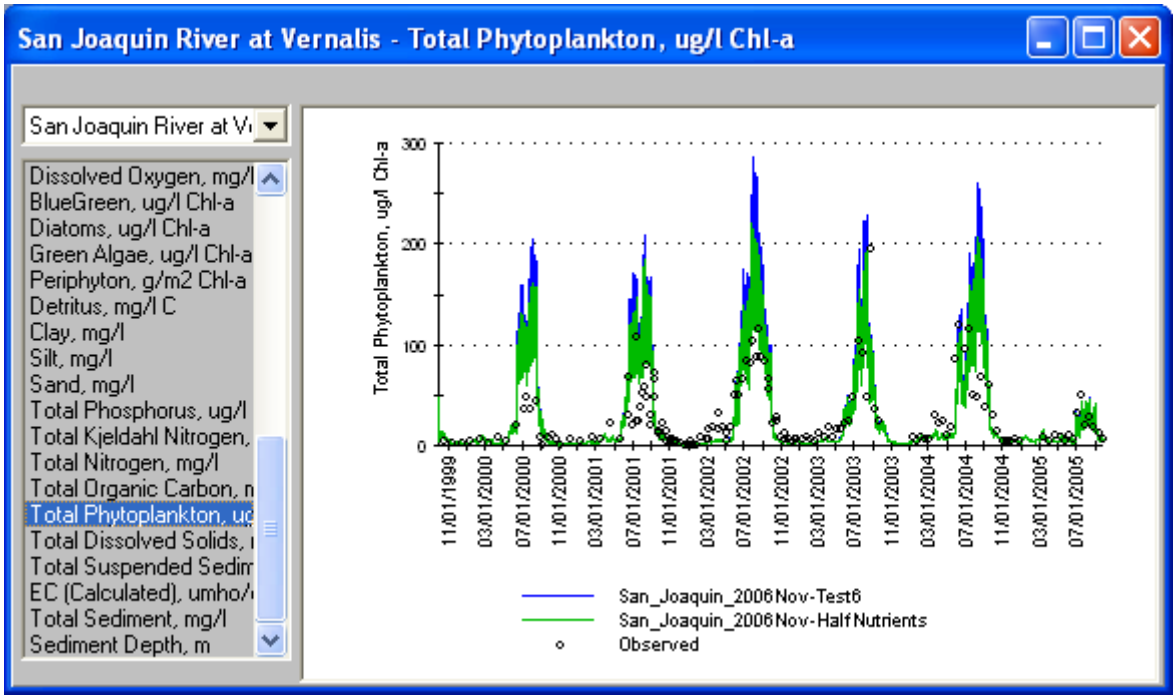

Figure 1.137 Response of Phytoplankton to Nutrient Load Reduction at Vernalis No Load Reduction (Blue Line) and Load Reduction (Green Line)

The results show that nutrient concentrations in the river responded to point source load reduction: 33% for ammonia, 51% for nitrate, and 27% for phosphate. The reduction in

phytoplankton concentration was only 9%, much less than the reduction in nutrients but nevertheless a decrease. Additional reduction of phytoplankton could be achieved by the reduction of nonpoint loads of nutrients in the drainage from farmlands, which was simulated by WARMF but was not included in this sensitivity analysis. The small reduction of phytoplankton means that although nutrient reduction would reduce phytoplankton growth somewhat, a comprehensive solution to excess phytoplankton at Mossdale may require other management actions as well.

The finding of this analysis was consistent with the current understanding about the over abundance of nutrients in the Upper San Joaquin River. Nevertheless, it is significant for the model to have confirmed it. The relatively small change in phytoplankton upon a drastic change in nutrients means that the calibration errors of nutrients may not affect the accurate calibration of phytoplankton.

Effect of Light on Phytoplankton

This sensitivity analysis tested the hypothesis that light is limiting algal growth more so than nutrients in the San Joaquin River. Light penetration into the water column is a function of the water's clarity. In WARMF, the light extinction coefficient was calculated as a function of phytoplankton, detritus, and suspended sediment concentrations similar to the equation used by Di Toro (1978):

$$K_e = \alpha_S S + \alpha_D D + \alpha_P P$$

K_e is the extinction coefficient in m^{-1}, S is suspended sediment concentration in mg/l, D is detritus concentration in mg/l, and P is the phytoplankton concentration in μg/l Chl-a. Coefficients α_S, α_D, and α_P represent the light attenuation properties of sediment, detritus, and phytoplankton respectively.

To test the hypothesis, the model coefficients were set to double the sediment loads in the boundary river inflows, agricultural drains & spills, and point sources. The procedure was the same as the sensitivity analysis for the load reduction of nutrients discussed earlier. In this case, the multipliers for suspended sediment loads were set at 2.

Figure 1.138 shows the response of suspended sediment concentration to the doubling of "point source" suspended sediment loads to the San Joaquin River. All loading sources treated as point sources by the model were affected equally, including river inflows and agricultural drains. The blue line is for the base case. The green line is for the case in which the sediment loads were doubled. The suspended sediment concentration increased 44% by the doubling sediment loads in the boundary inflows. The nonpoint load of sediment eroded from farmlands was simulated by WARMF and was not increased in this sensitivity analysis.

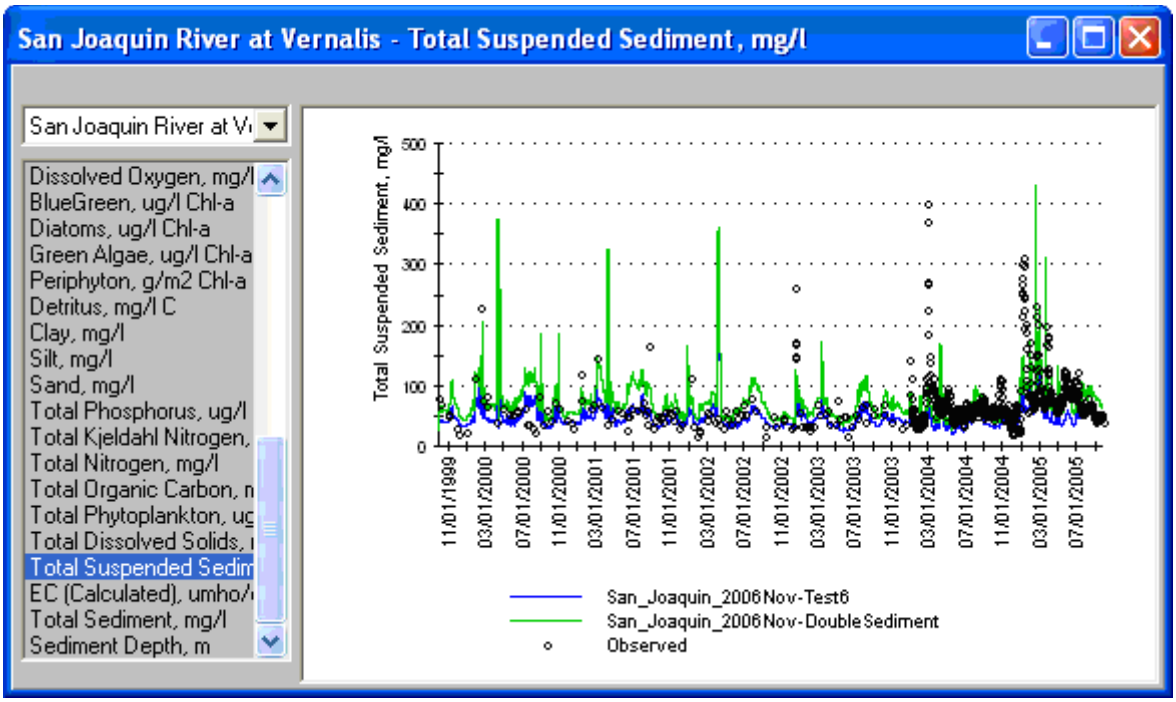

Figure 1.138 Response of Suspended Sediment to Doubling of Sediment Load at Vernalis No Load Increase (Blue Line) and Load Increase (Green Line)

Figure 1.139 shows the response of phytoplankton concentration to the doubling of sediment loads at Vernalis. The doubling of sediment loads was shown to have very little effect on the phytoplankton concentration.

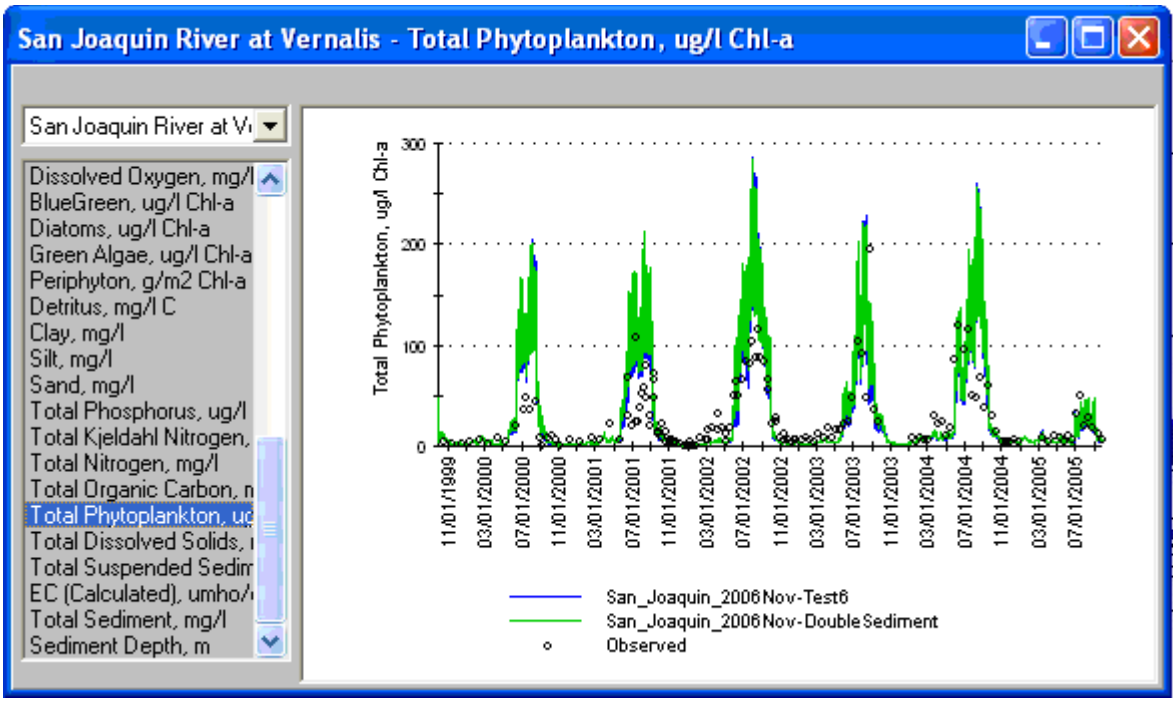

Figure 1.139 Response of Phytoplankton to Doubling of Sediment Load at Vernalis No Load Increase (Blue Line) and Load Increase (Green Line)

A more detailed analysis of the results determined that phytoplankton concentration was actually slightly higher with more sediment. The model calculates the light intensity as a function of depth and sediment concentration. Diatoms have an optimum light intensity for its growth, meaning too much light may bleach chlorophyll-a while too little light cannot support photosynthesis. At higher sediment concentration, the model calculated a thicker zone of water depth favored by diatoms and therefore a higher phytoplankton concentration.

The calculated difference was insignificantly small. The results of this test and the nutrient reduction test indicated that phytoplankton follows an unlimited growth pattern in the San Joaquin River, which has important implications for management of the watershed to control phytoplankton.

Management Implication

The results of the source contribution analysis in the previous section and the sensitivity analysis have implications for the management of the San Joaquin River. The sources of pollutants were identified, along with the loading from each source. This gave an indication of where reduction strategies should be focused.

The sensitivity analysis revealed that nutrient loading reduction would have only limited benefit, as phytoplankton growth does not appear to be limited by nutrient concentration. Further sensitivity analyses, such as a reduction in seed algae loaded to the San Joaquin River, could be run by investigators to determine the potential effectiveness of different management

alternatives. The model links the pollutant loads to the water quality concentration and can thus calculate load reduction needed to meet the water quality standard.

An effective control strategy may not be to rely on a single solution, but rather a combination of incremental changes. These may include some control of algae seed, some control of fertilizer application, some change of crops, some alteration of irrigation practices, and some river aeration. These changes might be identified through the involvement of stakeholders. A combination of load reductions and best management practices can be simulated by the model to determine the resultant reduction of algae concentration at Mossdale.

Since it usually only takes a few days for water to travel along the San Joaquin River from Lander Avenue to Mossdale, the system can respond quickly to changes. Although salts may be stored in the soil of land adjacent to the San Joaquin River, the system has relatively little storage of oxygen consuming materials. A management action which reduces oxygen consuming materials will have quick impact upon dissolved oxygen in the DWSC.

STAKEHOLDER INVOLVEMENT

The San Joaquin River Model was developed to provide a robust simulation tool which could be used by investigators and stakeholders. For investigators, we made presentations at the San Joaquin River DO TMDL Working Group meetings. In October 2006, we gave presentation at the CALFED Science Conference in Sacramento.

We involved stakeholders in the model development process as well. We benefited from stakeholders' knowledge of irrigation system. They provided useful data for the model not available elsewhere. Stakeholders, who contribute their knowledge and data, have "buy-in" to the model. This gave the model more credibility and increased the opportunity for the model to be used. The goal is for the stakeholders to use the model as a decision support system. They can use the model to learn about the San Joaquin River System, to formulate alternatives, to evaluate their effectiveness, and to build a consensus on a watershed management plan which is scientifically feasible, cost effective, and politically acceptable.

To achieve that goal, we placed the model and its data base on an FTP site to distribute it to interested parties. We encouraged the investigators to download the model and test it at their own leisure. We participated in outreach workshops and wished to invite the stakeholders to also download the program and test it. Representatives of the Modesto and Turlock Irrigation Districts have reviewed the model and offered information regarding riparian diversions (List and Paulsen 2008). The response to the review is in Appendix B of this report.

The model can be used to formulate and evaluate control strategies for the DO TMDL of DWSC. Because the San Joaquin River is a multiple variable model, it can be used to develop TMDLs for other pollutants. The model can also integrate the effects of divergent studies, such as reduction in TDS load or investigating the impact of the recent court settlement restoring flow to the length of the San Joaquin River.

CONCLUSIONS AND RECOMMENDATIONS

Conclusions

The calibration of the WARMF model showed reasonable results. Predicted flow and electrical conductivity matched the observed data very well. The model predicted the water quality concentrations for a large number constituents including major cations, anions, ammonia, nitrate, phosphate, total suspended sediment, dissolved oxygen, temperature among others at various stations along the San Joaquin River. Predicted values matched the seasonable patterns and magnitude of the observed data reasonably well, as presented in the report.

The output of the WARMF model to the Upper San Joaquin River Watershed was linked to the downstream estuary model by a graphical user interface. The Interface allowed us to run both the upstream watershed model and the downstream estuary model without manually transferring the output of the upstream model to the input of downstream model. The downstream estuary model is the Link-Node, which was developed in 1990s, recalibrated and verified in 2001. The database for the Link-Node model was updated to 2007, and re-calibration was performed using the data collected since 2000. The simulation results for Buckley Cove (Station R6) and Rough & Ready Island demonstrate that the Link-Node model maintained its predictive power.

WARMF was demonstrated to be capable of simulating nonpoint loads of pollutants from farmlands based on natural precipitation and irrigation waters that fall on them. The model not only predicted total pollution loads but also their source contributions. The model provided a tight link between pollution loads and water quality in the receiving water. This tight link allows the model to calculate the load reduction needed for the receiving water quality concentration to meet the water quality standard. The source contributions output provided stakeholders information about which source terms are largest and what management alternative to reduce them. The analysis of source contributions output suggest that the water quality problem of the San Joaquin River cannot be solved by a single solution. The water quality management plan should include a combination of small changes for incremental improvements that may have a cumulative compound benefit.

The computer run time was 6 hours for a 6 year simulation of the San Joaquin River watershed on an hourly time step using a PC with a fast processor. A sensitivity analysis showed that run time with 6 hourly time step may be more practical and may yield reasonable results. Simulation of many parameters is accurate with a daily time step. The sensitivity analysis showed that the model errors for the concentrations of ammonia, nitrate, and phosphate had little effect on the accuracy of simulation for phytoplankton because there was little nutrient limitation to growth. The sensitivity analysis for increasing sediment loads to the San Joaquin River led to an insignificant increase in phytoplankton concentration. The model offered an explanation of why diatoms dominate in the turbid San Joaquin River.

Recommendations

The model domain of the San Joaquin River watershed should be expanded. On the east side, the model domain should be extended to the dams of the east side tributaries. WARMF should be used to simulate irrigation return flow and groundwater accretion from farmlands to the east side tributaries. On the west side, the model domain should be extended to include drainage areas contributing flow, nutrients, and algae to the west side tributaries. The expansion of the model domain will simplify the model input procedure. In stead of preparing the flow and water quality of east side tributaries as input to the model, WARMF would simulate them based on the agriculture practices of irrigation water and fertilizer application. WARMF could then be used to evaluate agriculture practices that may be employed to reduce algae loads to the Lower San Joaquin River.

WARMF model should be used to manage not only the algae load but also the salt load for the San Joaquin River. This is consistent with the recommendations of stakeholders who wish to have a multiple parameter model during their review of the original proposal for the project. Management of phytoplankton load can affect salt load and vice versa. Management of salt loads and algae loads can be coordinated to benefit each other.

Further model calibration should continue with the help of field investigators and stakeholders. Investigators could provide better estimate of model coefficients for process rates. Stakeholders from irrigation districts could furnish better data for the quantity and quality of irrigation waters applied to their farmlands in their irrigation districts. It may be possible to get better estimates of fertilizer application rates and refined land use shape files for the model.

Stakeholder involvement should be emphasized. The ultimate goal of the San Joaquin River Model was to serve as a decision support tool for the stakeholders to learn about the river system. The more knowledge the stakeholders have the more they can formulate management strategies. The model can evaluate the effectiveness of those management strategies and help stakeholders reach a consensus the best way to meet the need of DO TMDL.

2 FORECASTING PROCEDURE

INTRODUCTION

Model Forecasting

The San Joaquin River has many constraints upon it: it is vitally important for agricultural and municipal water supply, as a conduit to assimilate agricultural drainage, and as an important corridor for wildlife and fish. The extension of the San Joaquin River into the Delta has been dredged to form the Stockton Deep Water Ship Channel (DWSC). Dissolved oxygen in the DWSC frequently does not meet its criterion for the passage of salmon. The San Joaquin River Basin Plan Amendment places controls on salinity and boron loading to meet water quality objectives at Vernalis (SWQCB 2004).

San Joaquin River flows are controlled by dam releases on all three of the San Joaquin's east side tributaries, diversions removing water from the river, and agricultural return flows. This management of the river can cause water quality problems, but it also provides opportunities to use coordinated management to mitigate or alleviate poor water quality on a near real-time basis. By manipulating the various flows which combine in the San Joaquin River, the resulting water quality can be improved.

One of the challenges of managing the river for water quality is the delayed feedback. During the low flow season, it takes about 4 days for water to travel from Lander Avenue down to Mossdale, with additional time required to get to the Stockton Deep Water Ship Channel (DWSC). Along the way, many chemical reactions take place which make it difficult to predict the water quality with or without any management action. To manage the river for water quality, it would be necessary to have a tool which can predict far enough into the future to identify how today's river inflows affect water quality at Vernalis and in the Stockton DWSC a week later. The tool would also have to facilitate coordination between multiple organizations which would need to act in concert for effective real-time management.

Efforts to Date

Creating a coordinated forecasting system requires automated data collection with centralized distribution. A network of monitoring stations has been established with data available near real-time through the Internet at the California Data Exchange Center (CDEC) (Quinn 2003). This data has been used to drive a model called San Joaquin River Input-Output (SJRIO) which simulates flow, total dissolved solids, selenium and boron from Lander Avenue to Vernalis. The

model was upgraded to run on a daily time step (SJRIO-DAY) and used to simulate a forecast two weeks into the future to predict water quality.

A Windows based graphical user interface was developed to run SJRIO-DAY and display its results. The San Joaquin River Real-Time Water Quality Interface provided graphic map-based displays to facilitate cooperative management (Chen et al. 1996). Figure 2.1 shows the program displaying spatial output from the SJRIO-DAY model. Clicking on individual locations on the map produced plots of flow and water quality presented as either concentration or load as shown in Figure 2.2.

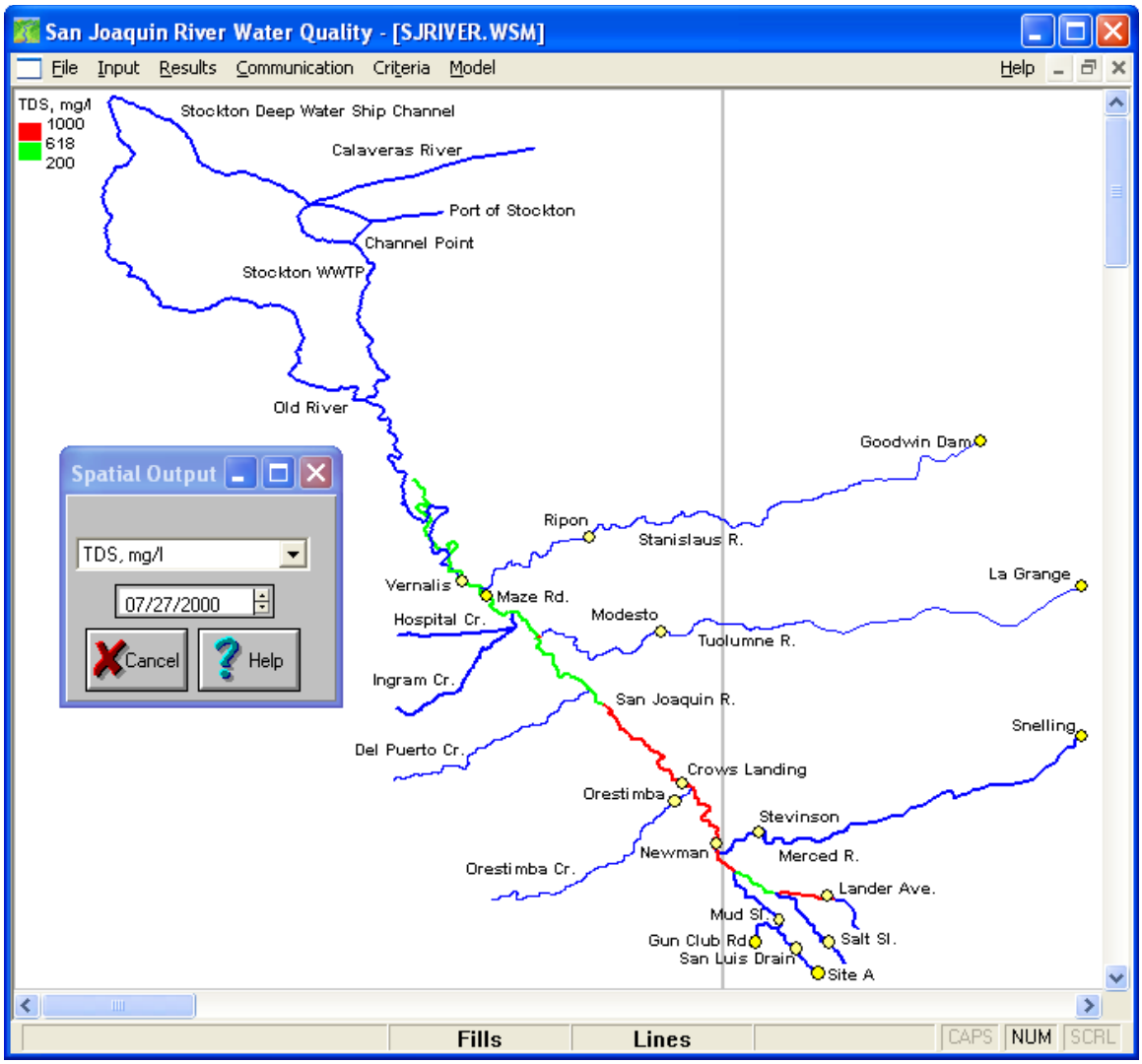

Figure 2.1 San Joaquin River Real-Time Water Quality Interface Spatial TDS Output

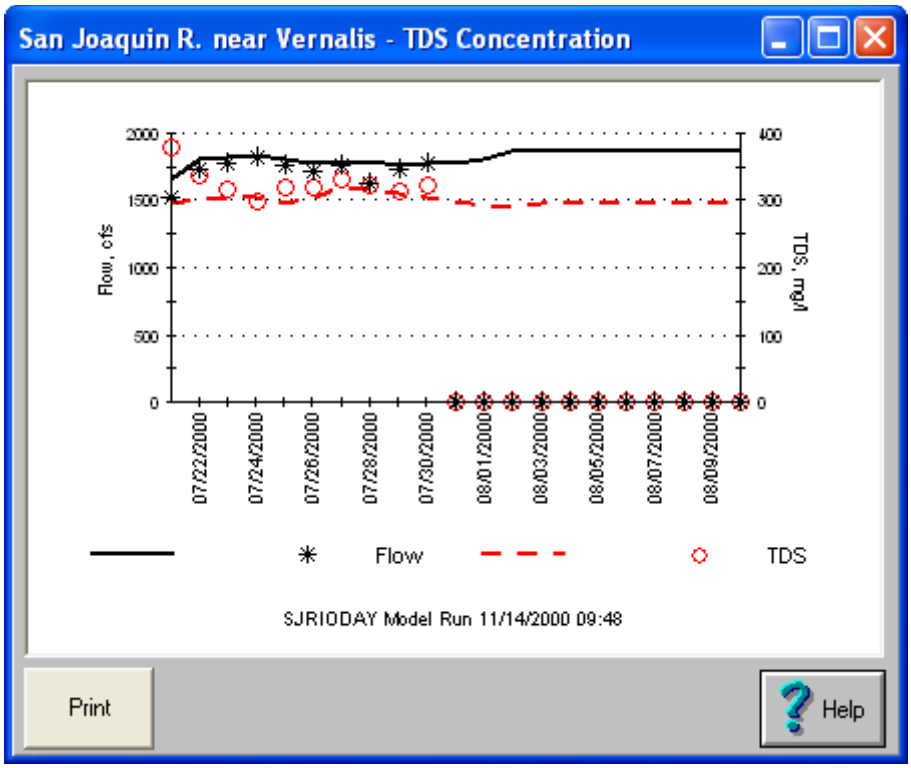

Figure 2.2 San Joaquin River Real-Time Water Quality Interface Time Series TDS Output

The California Department of Water Resources maintains a website dedicated to real-time water quality management of the San Joaquin River (http://www.sjd.water.ca.gov/waterquality/realtime/). SJRIO-DAY is used to hindcast for one week to compare simulations with monitoring data and then two weeks into the future using projected flows. The projected flow and electrical conductivity is displayed on the website as shown in Figure 2.3. Management options for control of total dissolved solids concentration at Vernalis include timing discharges from wetlands and the Grasslands Bypass Channel, and release of pulse flows from the dams on the east side tributaries.

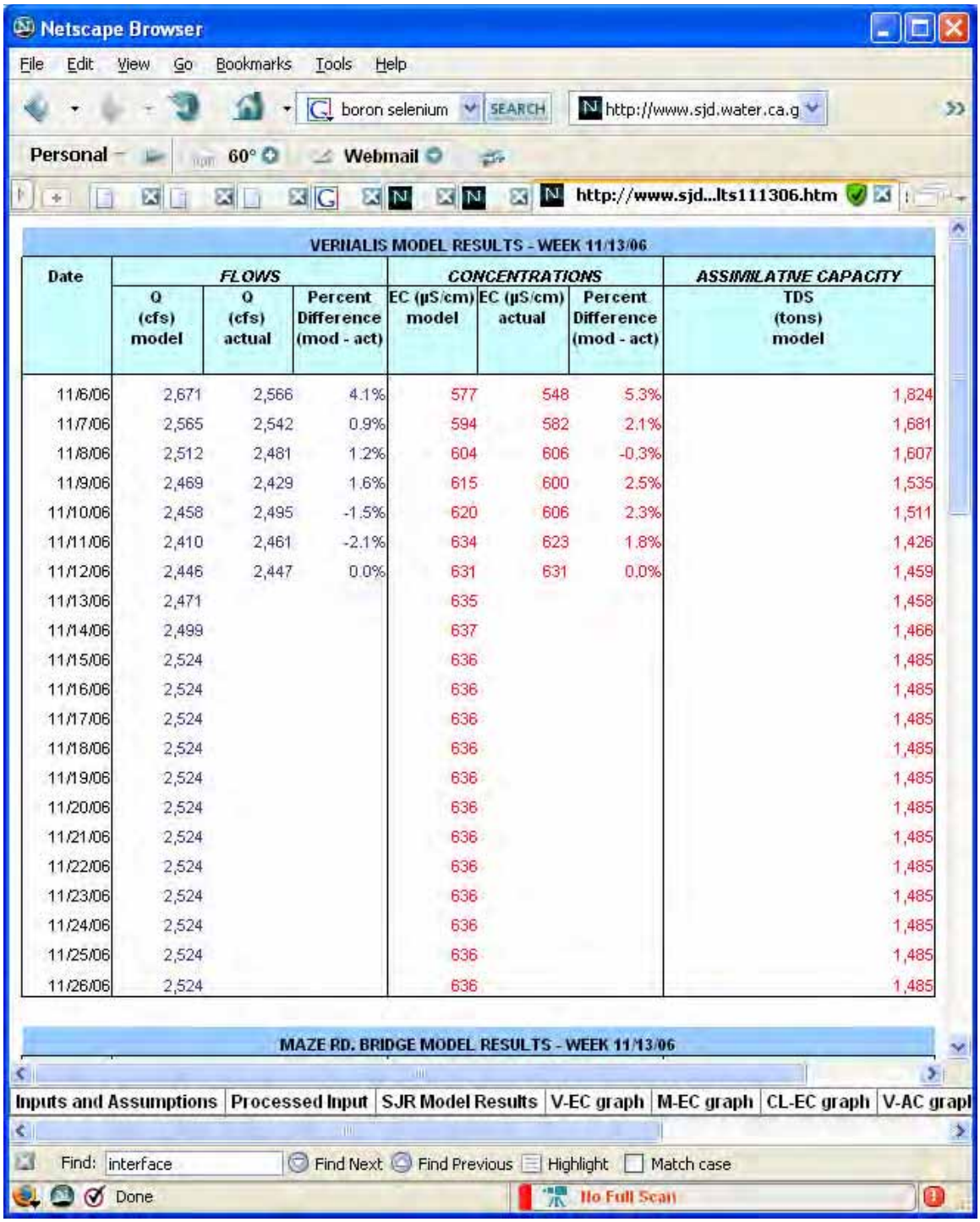

Figure 2.3 California Department of Water Resources Real-Time Water Quality Projection

Forecasting Dissolved Oxygen Demand

Background

The SJRIO-DAY model is designed to simulate conservative substances which do not transform within the San Joaquin River. A major component of impairment of the Stockton DWSC is oxygen demand from decaying algae produced in the riverine portion San Joaquin River between its gages at Lander Avenue near Stevinson and the Old River junction near Mossdale. To meet the dissolved oxygen criteria in the Stockton DWSC of 5 mg/l December through August and 6 mg/l September through November, the goal is to control the loading of algae entering the tidal portion of the San Joaquin River at the Old River.

San Joaquin River Model Interface

The San Joaquin River Model Interface was developed to simulate the phytoplankton in the San Joaquin River and its effect on water quality in the Stockton DWSC (Herr et. al. 2006). It used inflows and water quality from rivers, agricultural drainage, and groundwater to calculate phytoplankton growth along the length of the San Joaquin River. It included two simulation models: a watershed model called WARMF which simulated the riverine portion of the river from Lander Avenue to the Old River and an estuary model called Link-Node which simulated the San Joaquin River from the Old River through the Stockton DWSC. The models were linked together and calibrated to measured flow and water quality monitoring data along the San Joaquin River.

Forecasting Current Conditions

The first step in real-time management of phytoplankton load to the Stockton DWSC was to predict the water quality under the existing conditions with no management action. Using data collected by real-time monitoring stations, the time series inputs of the San Joaquin River Model Interface could be updated to the day when the simulation is run. Projected flows could be entered into the Interface so that it could simulate two weeks into the future. The week previous to the simulation would be simulated as well to compare simulation results against monitored flow and electrical conductivity. There was no real-time collection of phytoplankton concentration available to compare with model results. The model would be pre-run with a simulation of a time period ending a week before the day of the simulation in order to provide initial conditions not available from real-time data, such as groundwater flow, nutrient, and algae concentrations. The ending results of the pre-run would then be fed into the forecasting run. The model would be run on an hourly time step to simulate the daily growth cycle of phytoplankton. Simulation results would show the projected phytoplankton concentration at various locations, including at the Old River. Since the simulation would also include the Stockton DWSC, the projected dissolved oxygen will be calculated and a violation of the criterion for passage of salmon could be anticipated.

Forecasting Management Options

Upon projecting a violation of the dissolved oxygen criterion in the Stockton DWSC, there were several potential management options which could be simulated. In 2007, it was not expected

that these options will be implemented, as some require infrastructure improvements. The model could predict whether the proposed improvements are likely to be effective in the future.

Flow Control at Head of Old River

It was anticipated that flow entering the Old River from the San Joaquin River may be controlled in the future. Having greater flow in the San Joaquin River past the Old River reduces the residence time in the Stockton DWSC, in effect flushing oxygen consuming materials through the Delta. Higher flows also dilute the effluent discharged from the City of Stockton wastewater treatment facility. Diverting more San Joaquin River flow down the Old River, however, would decrease the load of phytoplankton from the San Joaquin River to the Stockton DWSC. Lower flow would also increase the incremental change in dissolved oxygen concentration achievable by the Port of Stockton and new Department of Water Resources aeration facilities.

Delta-Mendota Canal Recirculation

The Delta-Mendota Canal delivers water from the Delta at the Clifton Court Forebay to irrigators west and south of the San Joaquin River. Some water in the canal indirectly reaches the San Joaquin River by percolating through the soil of irrigated lands and arriving at the river through groundwater exfiltration. It is proposed to divert 125 to 500 cfs of water from the canal through the Newman Wasteway directly to the San Joaquin River to improve water quality in the San Joaquin River on a real-time basis. This would dilute the high nutrient and salinity flows from Mud and Salt Slough and decrease the residence time of the San Joaquin River. This would be expected to reduce the salinity and phytoplankton concentration along the San Joaquin River as a result.

San Joaquin River Restoration Flow

The court settlement announced June 30, 2006 between the Friant Water Users Authority, Natural Resources Defense Council, and the federal government will apply minimum flow requirements on the order of 50-150 cfs to the San Joaquin River from Friant Dam to Lander Avenue. It is expected that this water will have low salinity to provide dilution flow to the San Joaquin River downstream of Lander Avenue. It is not currently known if the phytoplankton in the settlement water at Lander Avenue will be low from a lack of nutrients or high from the potentially long travel time from Friant Dam to Lander Avenue. Assumptions can be made about the water quality of this additional water so simulations can be run projecting how it would affect phytoplankton concentration at the Old River. It is not known at this time whether the additional water would be at a constant flow rate or if it would be subject to real-time management.

Load Reduction from Grasslands Drainage Authority

Another potential source of water quality improvement is reduction of load originating from the Grasslands Drainage Authority, which enters the San Joaquin River via Mud Slough. Recycling of agricultural drainage water may reduce the load of salinity, nutrients, and phytoplankton to the San Joaquin River. It would also reduce the flow entering the San Joaquin River. Although this benefit is expected to be a long-term impact and not necessarily part of real-time management, its effect upon predicted salinity and phytoplankton in the lower San Joaquin River could be simulated in model forecasting simulations.

Aeration of the Stockton DWSC

The new Department of Water Resources aeration facility is expected to be operational in 2008. The impact of adding 10,000 lb/day of oxygen directly to the river could be evaluated using model simulations under various management scenarios.

Forecasting Procedure

A test of the San Joaquin River Model Interface forecasting procedure would be done in summer 2007. Using real time data, model inputs would be updated to simulate three weeks, one week of hindcasting and two weeks of forecasting. Depending on what potential management options would be available at that time, simulations would also be made of potential methods used to reduce salinity and phytoplankton load in the San Joaquin River. Although none of the management options will be implemented based in the results produced by the San Joaquin River Model Interface in summer 2007, the actual water quality in the river would be compared against the simulated forecast after the fact to determine how well the model performed under a "do nothing" management scenario.

CONCLUSION

The San Joaquin River Model Interface was ready to be implemented to evaluate the water quality effect of both long-term and short-term management strategies. The short-term management using the modeling system would be tested in summer 2007 to determine its accuracy and potential benefit toward meeting the dissolved oxygen criterion in the Stockton DWSC. Simulation results would also provide insight which can guide management strategies not yet implemented, such as settlement flows from Friant Dam.

3 FORECASTING RESULTS

INTRODUCTION

The Forecasting Procedure Report of December 2006 (Herr and Chen 2006b) outlined the procedure for forecasting dissolved oxygen in the Stockton Deep Water Ship Channel (DWSC). This report describes the results of forecasting which took place in summer 2007.

The usefulness of a model can be judged by its capability to make predictions. Given the input data of meteorology (daily precipitation, daily maximum and minimum ambient temperatures, wind speed, solar radiation, etc.) and operating conditions (flow releases from reservoirs, irrigation diversions, irrigation applications, waste discharges, aerator operation, etc.), the model should accurately predict the stream flows and water quality at various stations along the river system.

The predictive capability of the model could be tested in different stages of model development and application. For model calibration, the actual meteorological and operating data for the field sampling period were used to drive the model. The model predicted the stream flows and water quality which were compared to the observed values for confirmation. If they did not match, the model coefficients were adjusted to reduce the initial uncertainties of model coefficients to yield improved simulations.

For application to real time water quality management in the future, the anticipated meteorological and operating data would be used to drive the model. The model forecasted the stream flows and water quality, which were compared to the water quality objectives. If the predicted water quality did not satisfy the objectives, the model could be used to design an operational plan to meet water quality objectives by exploring various operational changes or remedial measures to improve the water quality.

Forecasting was performed in July 2007 based on an anticipated action to shut off flow from the San Luis Drain. This section describes the procedure used, predictions made, and how the projected model inputs and model predictions compare to measured data.

Real Time Water Quality Management of Dissolved Oxygen

The methods used for model forecasting were demonstrated in an existing system. California Department of Water Resources (DWR) in cooperation with US Bureau of Reclamation (Reclamation) had previously developed a real time water quality management system of total dissolved solids (TDS) for the Upper San Joaquin River. The general concepts for the water quality management system have been described by Quinn et al. (1997). The purpose was to

create a framework for various water resource managers to coordinate their flow releases to meet the EC objectives for the San Joaquin River at Vernalis.

The real time water quality management of dissolved oxygen would follow the same concepts and procedures for the real time water quality management of TDS. However, it would be more complex, because it required two models to make the forecasts instead of one, and there were several more water quality parameters requiring model inputs.

The dissolved oxygen criterion was sometimes violated at the DWSC, which is located in the Lower San Joaquin River near Stockton. It was caused in part by the large river loads (i.e., high concentrations) of algae from upstream (Chen and Tsai 2000). The forecasting model needed to include the DWSC and the upstream San Joaquin River segments.

The San Joaquin River downstream of Vernalis is influenced by tides, which required an estuary model. The non-tidal San Joaquin River, on the other hand, is strongly influenced by agricultural practices, which required a watershed model.

An estuary model had already been developed for the tidal portion of the San Joaquin River, extending from Mossdale to the Stockton DWSC at Venice Island (Schanz and Chen 1993, and Chen and Tsai 2002). The WARMF watershed model was developed and calibrated for the San Joaquin River Basin upstream of Mossdale, which is the interface point for the two models.

To link the two models together, a graphical user interface was developed as shown in Figure 3.1. The interface automatically transferred the output from the Upper San Joaquin River Basin model to the input of the estuary model of the Lower San Joaquin River. One could, therefore, run both models through the interface.

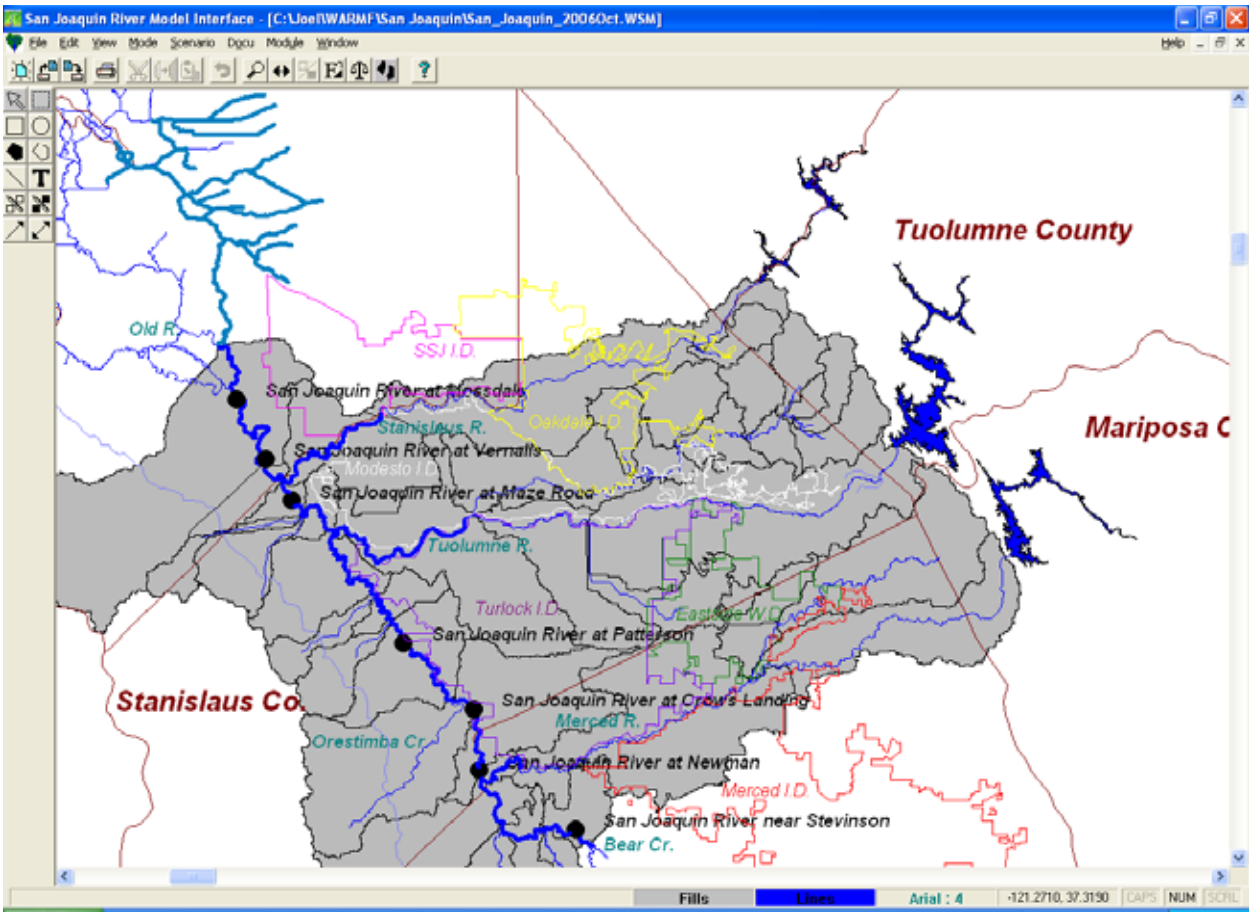

Figure 3.1 Graphical User Interface for the Upper San Joaquin River Basin Model and the Estuary Model of the Lower San Joaquin River and DWSC

The WARMF San Joaquin River Basin Model was calibrated (Herr and Chen 2006a). For the calibration, the meteorology and river flow data was compiled for the period of water years 2000 to 2005, when bi-weekly river water quality data were collected. With this data, the model predicted stream flow and water quality at various locations where the data has been monitored. The calibrated model could then predict the future conditions given projected model inputs and determine the effectiveness of measures designed to reduce the organic loading to the DWSC.

Testing Organic Load Reduction Strategies

Multiple strategies have been proposed to reduce the organic loading to the DWSC and increase the dissolved oxygen concentration. The strategies involved alterations of the flow regime, a reduction in phytoplankton loading to the San Joaquin River, and direct injection of oxygen into the DWSC. Two proposed methods were tested in WARMF: recirculation of Delta-Mendota Canal water to the San Joaquin River via the Newman Wasteway and temporary shutoff of the San Luis Drain. The first strategy had two potential positive effects: dilution of phytoplankton and decrease in travel time down the river to reduce phytoplankton growth. The benefit of shutting off San Luis Drain was to remove a large source of phytoplankton seed to the upper part

of the river so that exponential growth of the reduced phytoplankton seed would result in less phytoplankton entering the DWSC.

To test these strategies, the historical simulation period of water years 2000-2005 was used. Each strategy was put into operation in WARMF one week before dissolved oxygen concentrations in the DWSC dropped below 5 mg/l and remained in operation until the dissolved oxygen concentration recovered. Figure 3.2 shows the time series results at Vernalis for summer of 2002. Blue represents the base case simulation with no action taken; green is recirculation of 250 cfs of Delta-Mendota Canal water; red is shutting off the San Luis Drain.

The figure shows that the changes don't always result in a reduction of phytoplankton loading at Vernalis. The Delta-Mendota Canal recirculation strategy results in higher predicted phytoplankton loading in early July. Over the entire period from May 15 – October 15, 2002, however, the simulated Delta-Mendota Canal recirculation strategy had 3% less phytoplankton loading at Vernalis than the do nothing case. The shutoff of the San Luis Drain reduced phytoplankton loading by 6% on average.

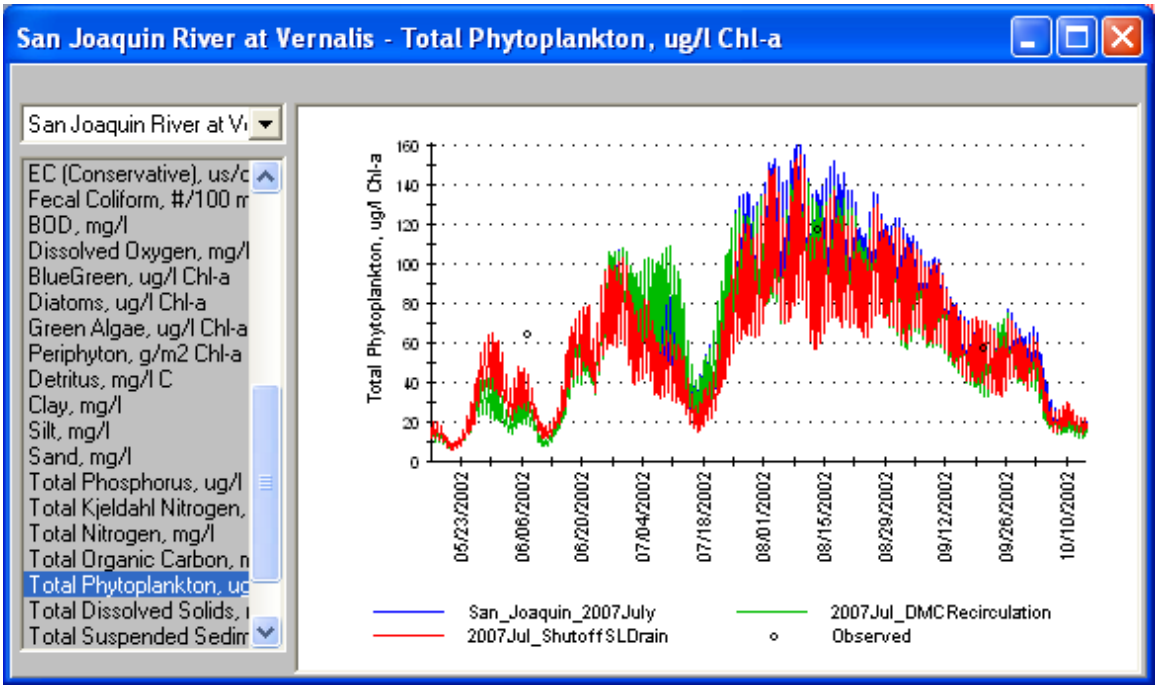

Figure 3.2: Predicted phytoplankton concentrations at Vernalis for organic load reduction strategies

The predicted change to phytoplankton concentration at Vernalis, however, had almost no effect on predicted dissolved oxygen in the DWSC as shown in Figure 3.3. A more thorough examination of the Link-Node model would be required to determine why the changes to organic loading appeared to have little effect on dissolved oxygen concentration in the DWSC.

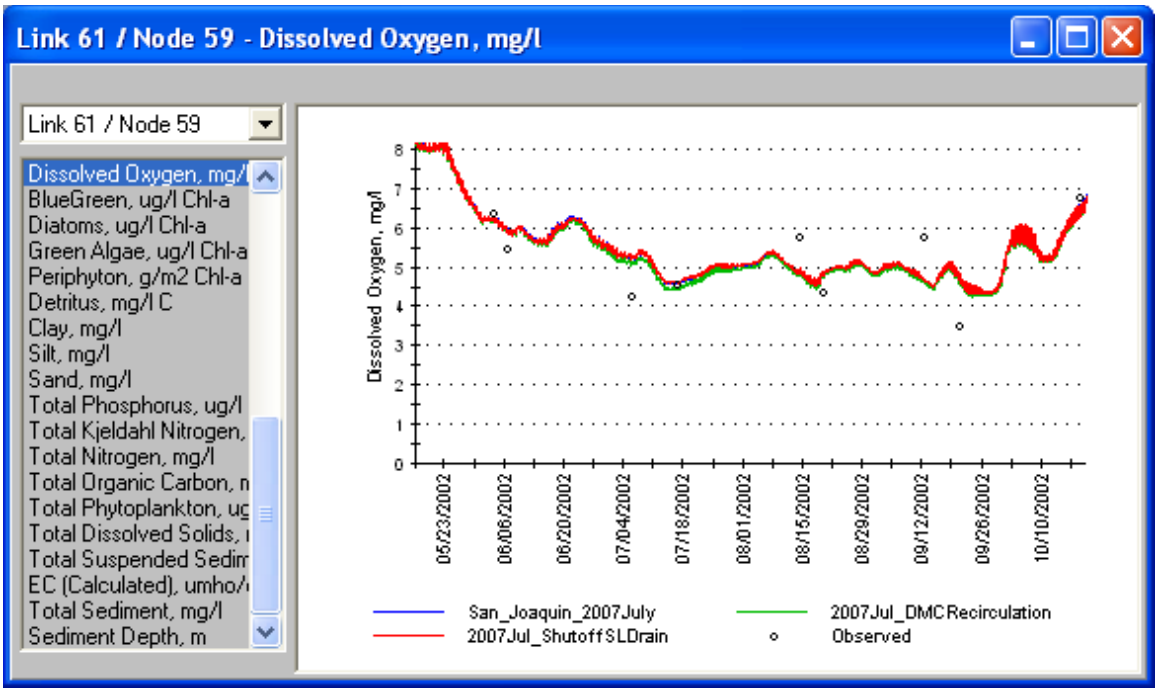

Figure 3.3: Predicted dissolved oxygen concentrations at Buckley Cove (DWSC) for organic load reduction strategies

Real-time Forecasting Simulation

A field test to confirm the effectiveness of the strategy to shut off the San Luis Drain was scheduled for July 23, 2007 to last for up to one week. This provided the opportunity to test the application of WARMF as a forecasting tool.

There were many time series inputs required to run WARMF including tributary inflows, agricultural drains, and diversions. For diversions, only flow data was required. Tributary inflows and agricultural drains require flow, temperature, EC, and all other water quality constituents. Of particular importance were those water quality constituents impacting phytoplankton growth: nutrients, sediment, and phytoplankton concentration itself.

Real-time data sources provided some of these model inputs, but most required estimation. To get estimates, an analogous time period was used. Since 2007 is a dry year, a similar year is needed within the 2000-2005 water years for which model time series data is complete. To find an analogous year, the river flow was analyzed for the first two weeks in July for each year as shown in Table 3.1.

Table 3.1: Average Flows, July 1-14

Year	Mud Slough	Salt Slough	SJR at Lander	Merced River	Tuolumne River	Stanislaus River	SJR at Vernalis
2000	73	221	97	194	509	423	1884
2001	74	167	41	147	204	555	1396
2002	73	143	30	96	228	528	1275
2003	56	136	11	115	352	612	1630
2004	91	150	14	101	246	601	1199
2005	91	225	174	1267	2934	323	5446
2007	**24**	**147**	**31**	**173**	**257**	**451**	**1076**

Either 2002 or 2004, both drier than average years with low flow at Vernalis, could be used as an analog for 2007. The combined tributary flows in 2002 are 15 cfs greater than those observed in 2007 and the flow at Vernalis is 199 cfs greater. 2004 tributary flows combined are 120 cfs more than in 2007 but the flow at Vernalis was just 124 cfs greater than in 2007. 2002 was chosen as the analog year because of the closer match of its tributary flows, although a match of tributary flows was not necessarily more important than a match of Vernalis flow in finding a suitable analog year.

Table 3.2 shows the sources of data used for the forecasting simulation. Real-time flow data was available up until the time the simulation was run on July 19th for the major tributaries. Temperature and EC data were available for most of the tributary inflows, but there was no real-time data available for phytoplankton or other water quality parameters. All 14 simulated agricultural drains and all 18 simulated diversions used 2002 data because no real-time data was available.

Table 3.2: Sources of tributary inflow data for 2007 forecasting simulation

Tributary Inflow	Flow	Temperature	EC	Phytoplankton	Other WQ
Stanislaus River	Real-time	2002 data	2002 data	2002 data	2002 data
Tuolumne River	Real-time	Real-time	Real-time	2002 data	2002 data
Merced River	Real-time	Real-time	Real-time	2002 data	2002 data
San Joaquin River	Real-time	Real-time	Real-time	2002 data	2002 data
Salt Slough	Real-time	Real-time	Real-time	2002 data	2002 data
Mud Slough	Real-time	Real-time	Real-time	2002 data	2002 data
Los Banos Creek	2002 data	2002 data	2002 data	2002 data	2002 data
Orestimba Creek	Real-time	Real-time	Real-time	2002 data	2002 data
Del Puerto Creek	2002 data	Real-time	Real-time	2002 data	2002 data
Hospital Creek	2002 data	Real-time	Real-time	2002 data	2002 data
Ingram Creek	2002 data	Real-time	Real-time	2002 data	2002 data
Delta-Mendota Canal	2002 data	Real-time	Real-time	2002 data	2002 data
Modesto Canal	Real-time	2002 data	2002 data	2002 data	2002 data
Turlock Canal	2002 data	2002 data	2002 data	2002 data	2002 data

Real-time flow data was projected into the future by first comparing the data at each tributary inflow between July 1-14, 2007 and July 1-14, 2002. A ratio of the flows between 2007 and 2002 was calculated for each tributary based on the average flows shown in Table 3.1 and then 2002 flows from July 15-August 6 2002 were modified based on those ratios to represent July 15-August 6, 2007.

A similar method was used to calculate projected EC from 2002 and 2007 data for the Merced and Tuolumne Rivers. The Stanislaus River has no real-time EC monitoring, so 2002 data was used unaltered. Mud Slough and the San Joaquin River at Lander Avenue showed strong decreasing trends in measured EC leading up to the date the simulation was run, so for those locations a constant EC was used representing the end of the trend in the data. Salt Slough showed a relatively constant EC (916-2020 μs/cm) for the weeks leading up to the simulation, so an average value was used for the forecasted EC.

The model was run from July 1 through August 6 using the hybrid data from 2007 and 2002. A base case simulation was run assuming no action was taken. Then the tributary inflow file for Mud Slough was modified to simulate the elimination of the contribution from San Luis Drain from July 23 through July 30. Historical data was examined to determine the proportion of Mud Slough flow, EC, phytoplankton, and other water quality constituents contributed by the San Luis Drain under summer conditions. The data indicated that San Luis Drain would represent essentially all the flow in Mud Slough, so the assumption was made that the shutoff would reduce the Mud Slough flow and loading to zero.

Forecasting Inputs

The tributary flow and phytoplankton concentrations were the model inputs to which the forecasts of phytoplankton concentration at Vernalis were most sensitive. Flow inputs affected travel time down the San Joaquin River, which in turn controlled how much phytoplankton is able to grow. Phytoplankton inputs were the amount of seed phytoplankton available in the upper part of the San Joaquin River for exponential growth as it flowed downstream.

Flow Inputs

Real-time flow data through July 18, 2007 was included in the forecasting simulation, but flow had to be forecasted for July 19 through August 6. Real-time monitoring data was subsequently collected after the conclusion of the forecast period. Figure 3.4 shows the forecast and measured flow for Mud Slough, Salt Slough, and the San Joaquin River at Lander Avenue. Solid colors represent the forecasted flows and the discrete shapes are measured data. Mud Slough never went below 9 cfs, indicating either the assumption that all Mud Slough flow came from the San Luis Drain was not valid or the Drain never reached zero flow. Measured flow in the San Joaquin River at Lander Avenue was less than the forecast. Forecasted flow for Salt Slough was accurate one week into the future, but was greatly overestimated for the second and third weeks.

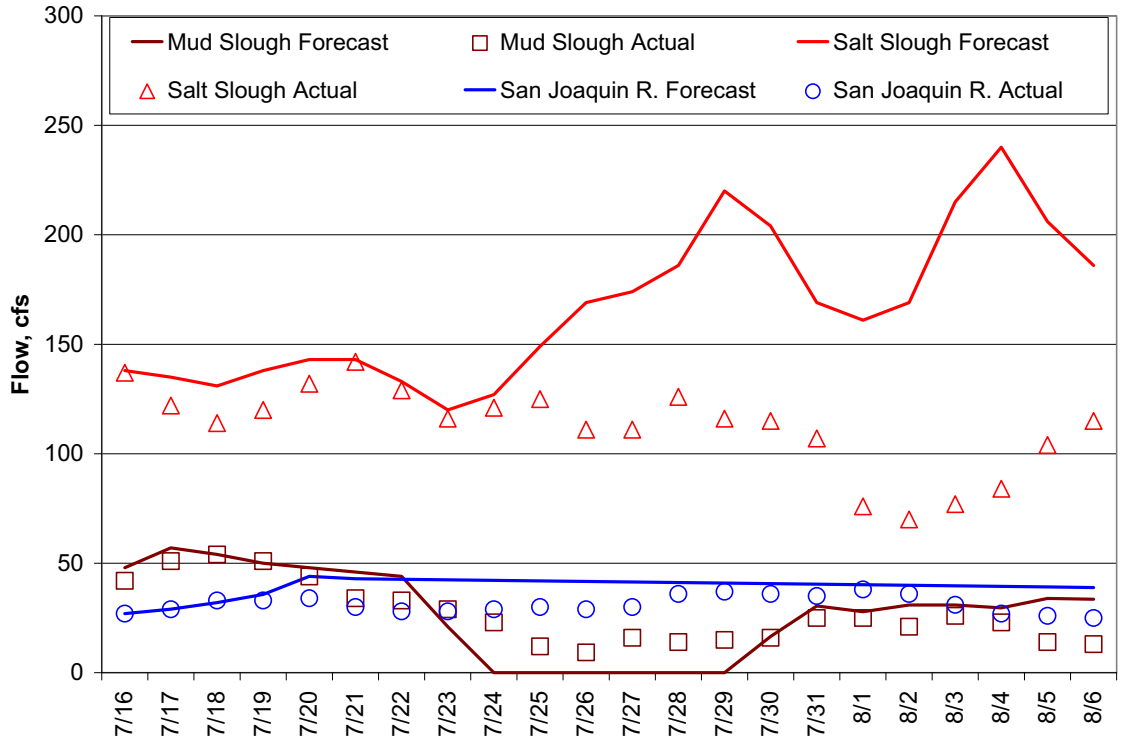

Figure 3.4: Forecast and actual flow inputs for Mud Slough, Salt Slough, and San Joaquin River at Lander Avenue

Figure 3.5 shows the forecasted flows (in solid lines) for the three major east side tributaries compared against the subsequently measured flows (discrete shapes). Forecasted flow for the Merced River and Stanislaus Rivers was too low. The measured Tuolumne River flow was close to the forecasted flow for two weeks, but the forecasted flow was too high in the final week of the simulation.

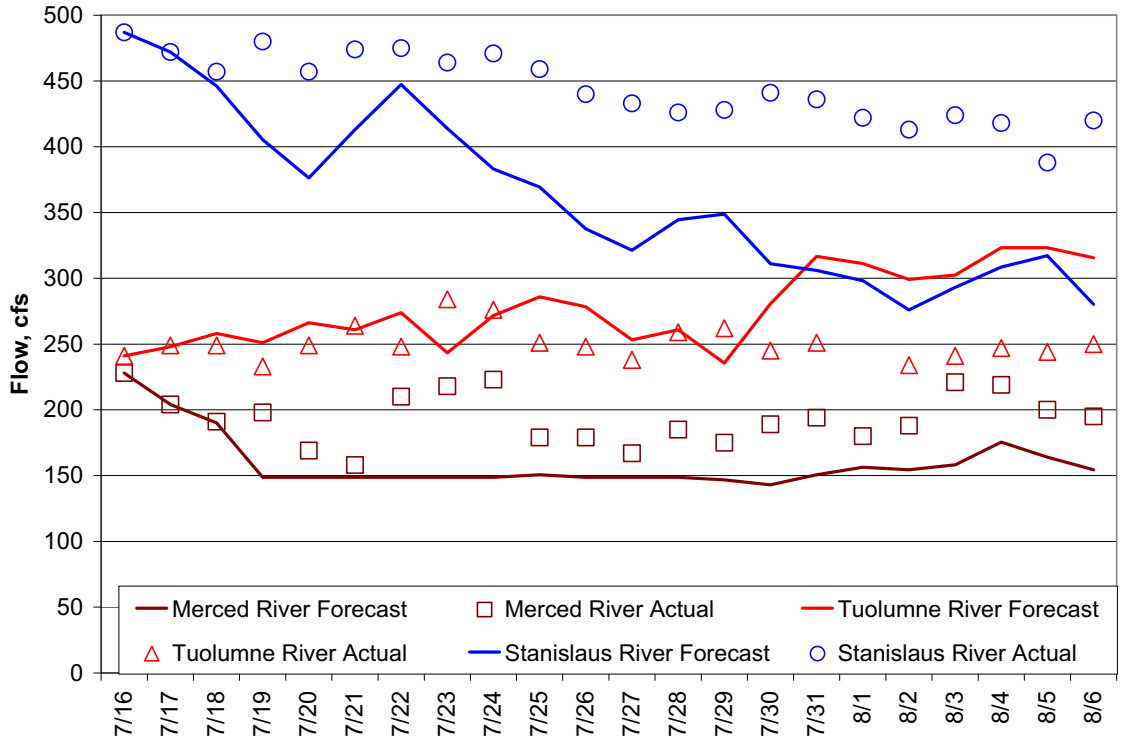

Figure 3.5: Forecast and actual flow inputs for Merced River, Tuolumne River, and Stanislaus River

The relative error of forecasted flows shown in Table 3.3 is the average forecasted flow minus the average observed flow, divided by observed flow. It is a measure of bias in the forecast. Since there was significant error in most of the flow forecasts, alternate methods of forecasting future flows should be explored to find methods with greater accuracy.

Table 3.3: Relative error of forecasted flows, July 19 – August 6, 2007

	Mud Slough	Salt Slough	San Joaquin River	Merced River	Tuolumne River	Stanislaus River
Forecast	0%	+55%	+30%	-21%	+12%	-22%

Phytoplankton Inputs

No real-time data was available for phytoplankton concentrations, so the concentrations from 2002 were used for all model inputs when running the forecasting simulations. Collection of phytoplankton data during the forecasting period allowed us to check the assumptions made in the model inputs to determine the error in the forecasts used to drive the model. Figure 3.6 shows the forecasted phytoplankton concentrations in solid lines and the measured data in discrete shapes. The 2002 phytoplankton concentrations used for 2007 forecasts were much higher than actual 2007 data for Mud Slough. Forecasted phytoplankton concentrations for the San Joaquin River at Lander Avenue were lower than measured data in the first week of the forecast and then higher than actual concentrations for the remaining two weeks of the

simulation. The 2002 phytoplankton data used to forecast Salt Slough concentrations in 2007 were relatively accurate.

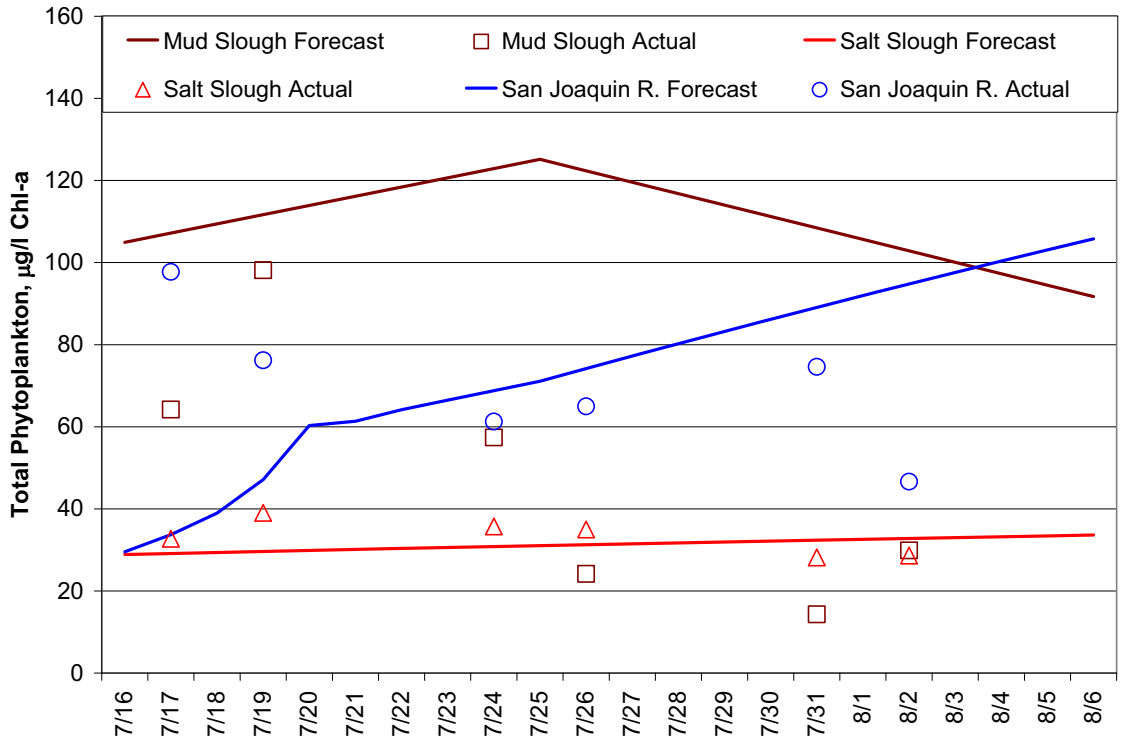

Figure 3.6: Forecast and actual phytoplankton concentration inputs for Mud Slough, Salt Slough, and San Joaquin River at Lander Avenue

The model inputs and measured phytoplankton concentrations for the major east side tributaries are shown in Figure 3.7. Although the phytoplankton concentrations of both model inputs and measured data were very low, the model input concentrations were much higher than the observed for all three rivers.

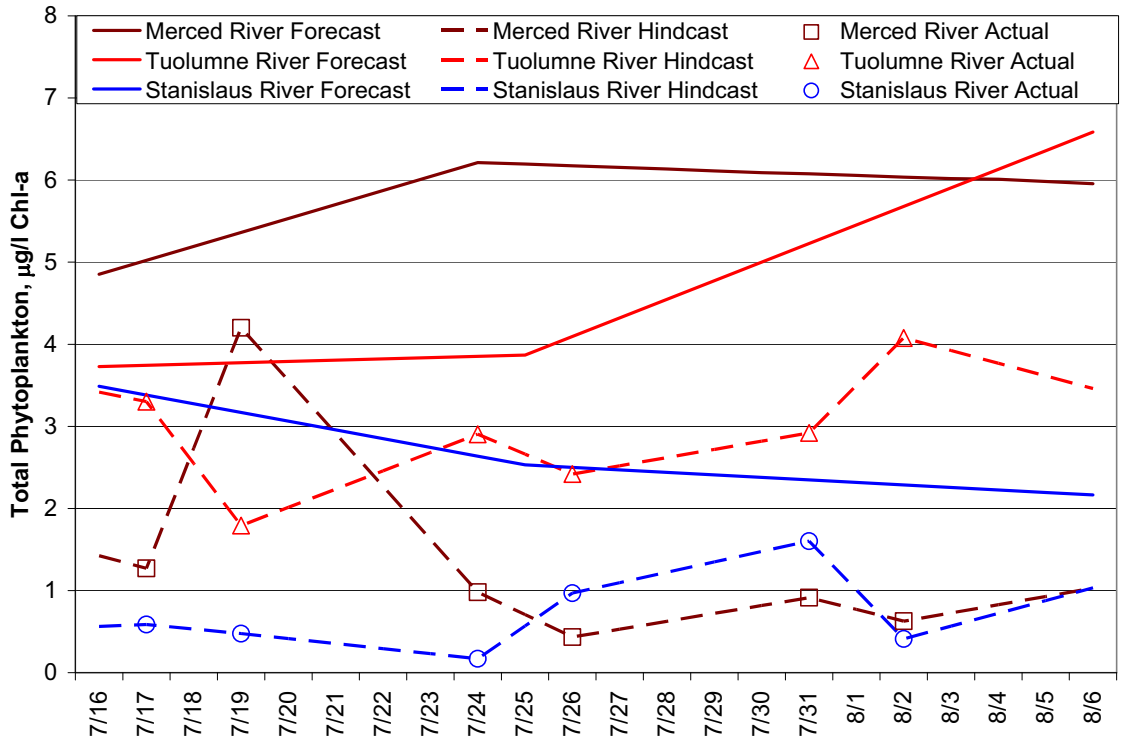

Figure 3.7: Forecast and actual phytoplankton concentration inputs for Merced River, Tuolumne River, and Stanislaus River

The relative error of forecasted phytoplankton shown in Table 3.4 is the average forecasted phytoplankton minus the average observed values, divided by observed. The use of 2002 phytoplankton data for the model forecast caused large errors in the model inputs for Mud Slough, Merced River, Tuolumne River, and Stanislaus River.

Table 3.4: Relative error of forecasted phytoplankton, July 16 – August 6, 2007

	Mud Slough	Salt Slough	San Joaquin River	Merced River	Tuolumne River	Stanislaus River
Forecast	+250%	-5%	+8%	+601%	+57%	+525%

Electrical Conductivity Inputs

Although EC has no direct bearing on the phytoplankton concentration of the San Joaquin River where it enters the DWSC, it is a measure determining whether the proportion of fresh and saline flow sources used by the model is accurate. Real-time EC data through July 18, 2007 was included in the forecasting simulation, but EC had to be forecasted for July 19 through August 6. Real-time monitoring data was subsequently collected after the conclusion of the forecast period. Figure 3.8 shows the forecast and measured EC for Mud Slough, Salt Slough, and the San Joaquin River at Lander Avenue. Solid colors represent the forecasted EC and the discrete shapes are measured data. The Mud Slough, Salt Slough, and San Joaquin River at Lander Avenue EC forecast all assumed a constant concentration. Mud Slough and San Joaquin River

both recorded rapidly decreasing EC leading up to the simulation, so the forecasted values assumed a value at the end of the trend. Measured EC at Salt Slough was very constant (913-1020 µs/cm) in the two weeks leading up to the simulation, so the average over that time period was used in the forecast. Forecasted EC was usually less than subsequently observed for all three locations as shown in Figure 3.8. Solid lines are the forecasted EC and discrete shapes are the observed for each location.

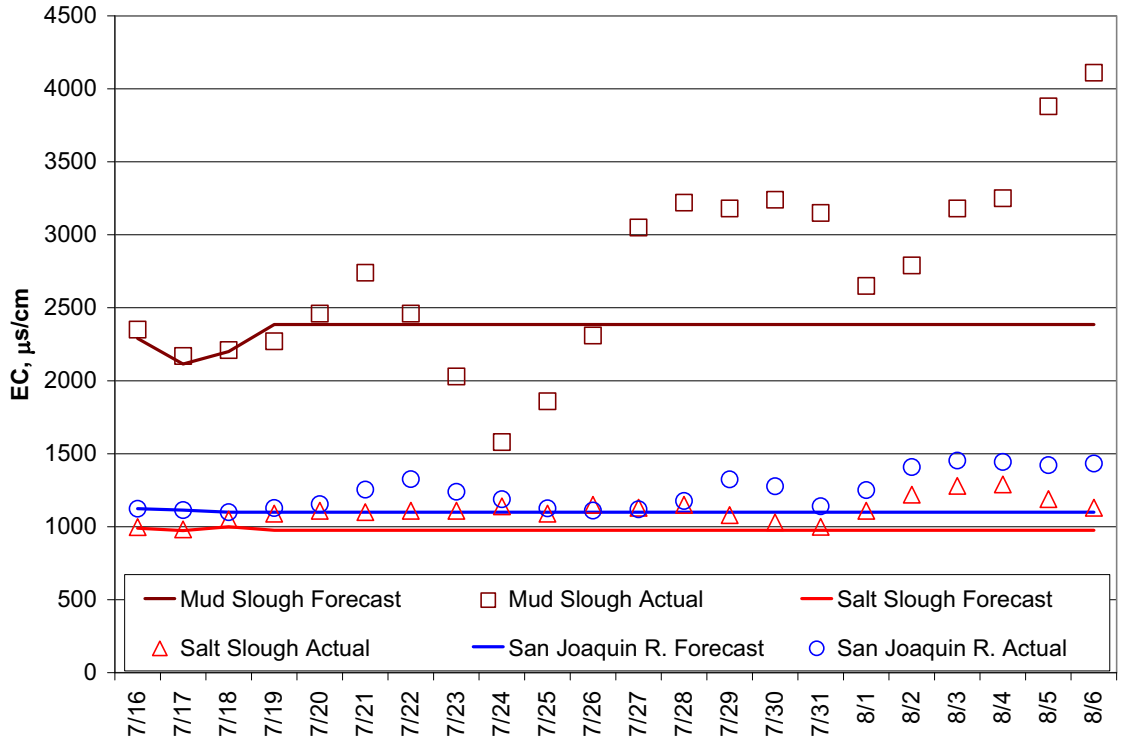

Figure 3.8: Forecast and actual EC inputs for Mud Slough, Salt Slough, and San Joaquin River at Lander Avenue

Figure 3.9 shows the forecasted EC (in solid lines) for the three major east side tributaries compared against the subsequently measured EC (discrete shapes). The forecasted EC for the Merced River was reasonably good, but for Tuolumne River it was higher than measured. Grab samples measuring EC for the Stanislaus River recorded slightly higher values than those used as model inputs.

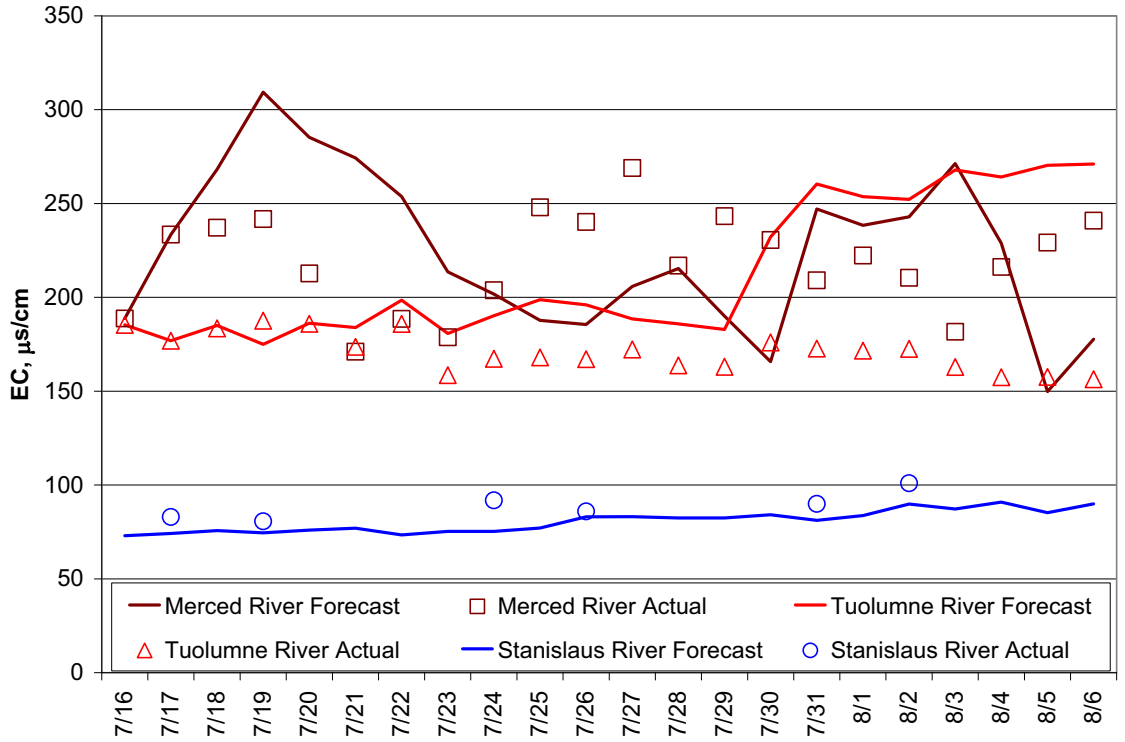

Figure 3.9: Forecast and actual EC inputs for Merced River, Tuolumne River, and Stanislaus River

The relative error of EC shown in Table 3.5 is the average forecasted EC minus the average observed EC, divided by observed EC. Having real-time data for EC provided a good basis for forecasting and produced much better accuracy than the forecasted phytoplankton.

Table 3.5: Relative error of forecasted EC, July 19 – August 6, 2007

	Mud Slough	Salt Slough	San Joaquin River	Merced River	Tuolumne River	Stanislaus River
Forecast	-15%	-14%	-13%	+2%	+29%	-10%

Forecasting Outputs

The simulated flow, EC, and phytoplankton of a forecasting simulation could be compared against subsequently measured data. The comparison tells us if the combination of forecasting technique, data available for forecasting, and calibrated model can predict water quality accurately.

Simulated and observed flow at Vernalis is shown in Figure 3.10. The simulated flow was initially 35% greater than the observed data, but overall averages 20% more than measured values. The chosen analog year of 2002 used for diversions, agricultural drains, and smaller tributary inflows had higher flow at Vernalis than was observed in 2007. The effects of that discrepancy are embedded in the forecasted flow.

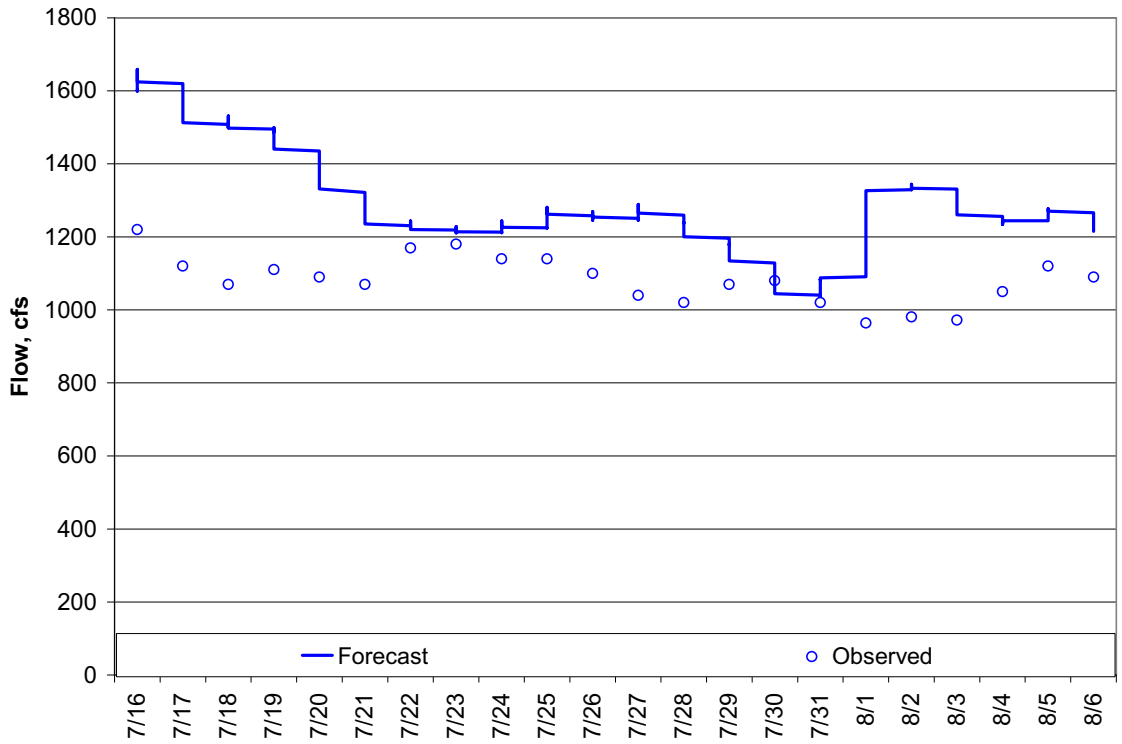

Figure 3.10: Forecasted vs measured flow, San Joaquin River at Vernalis

Figure 3.11 shows the model prediction and subsequent measurements of the phytoplankton concentration at Vernalis under the forecasted base (do nothing) scenario and with implementation of the San Luis Drain shutoff strategy. The base case is in blue; the simulated effect of the San Luis Drain shutoff is shown in green, subsequently measured data is in black circles, and the model predicted percent reduction is in red using the scale on the right. There was a predicted time lag in the effectiveness of the shutoff, with no effect noticed until two days after the shutoff and peak reduction of phytoplankton concentration reached after about 6 days. After the San Luis Drain resumed discharging, there was a similar time lag and little residual benefit left after one week. The peak forecasted reduction of phytoplankton was 19%. The three measured data points from before and one day after the shutoff average 68 µg/l Chl-a, while the measured phytoplankton starting 3 days after the shutoff average 54 µg/l Chl-a, 20% less. Data from Mud Slough indicates that the phytoplankton concentration in its discharge remained much lower than before the San Luis Drain was shut off even after flow resumed in the drain. Although it is not clear why the phytoplankton concentration in Mud Slough did not increase after flow resumed in the San Luis Drain, the data implies that reduction of loading from Mud Slough does have a significant impact upon the loading in the San Joaquin River at Vernalis.

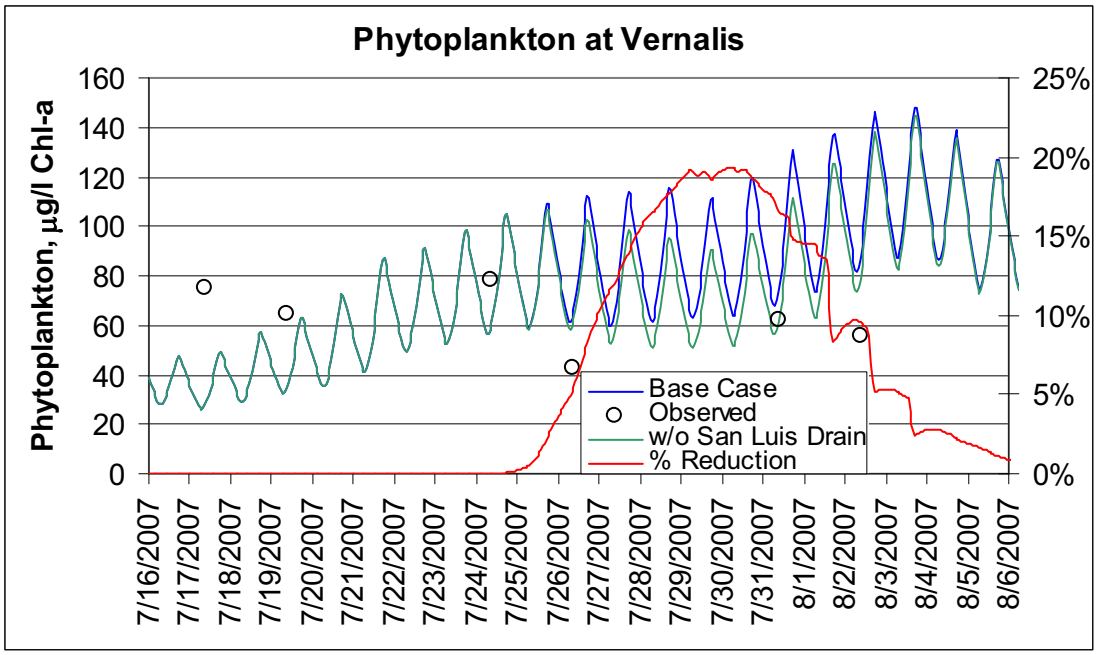

Figure 3.11: Forecasted reduction of phytoplankton concentration at Vernalis, San Luis Drain load eliminated

The San Luis Drain and Mud Slough is a major source of EC to the San Joaquin River. The forecasted Mud Slough EC for this simulation period was over 2000 µs/cm. Since EC does not grow exponentially like phytoplankton, however, reducing EC from Mud Slough does not have a similar impact to reducing phytoplankton loading. Figure 3.12 shows the reduction of EC at Vernalis resulting from shutting down the San Luis Drain. The peak reduction was less than 4%. The pattern of the reduction is similar to that for phytoplankton, taking a week to see the full effects of the drain being shut off and then opened again. The EC monitoring data is similar to the forecast. The small reduction in EC predicted in the forecast can not be discerned in the measured data.

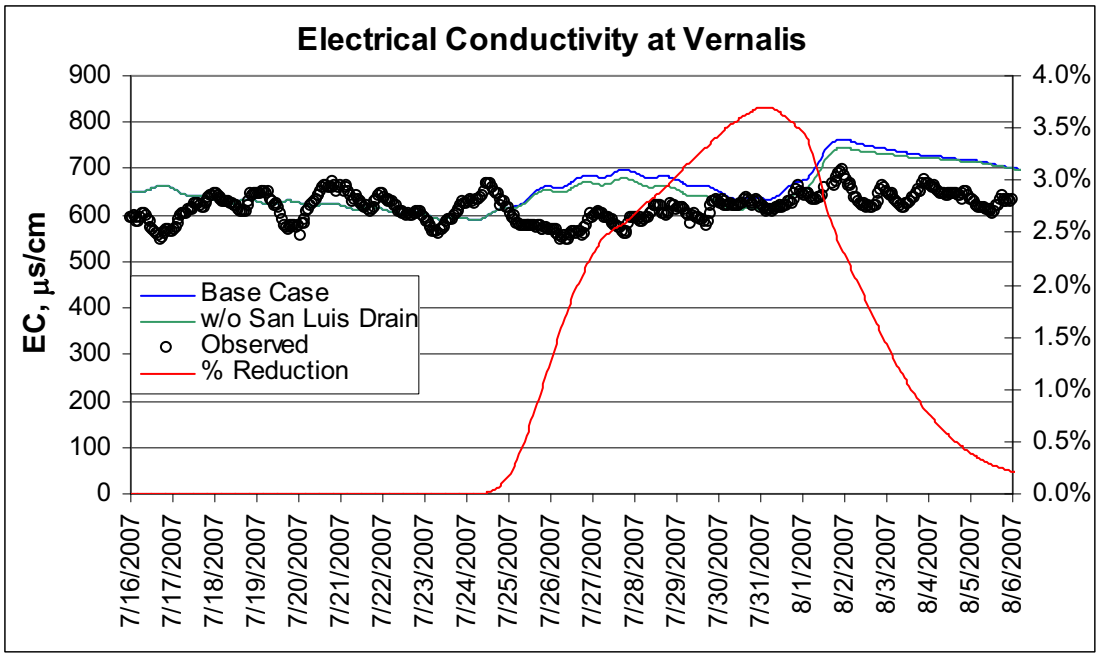

Figure 3.12: Forecasted reduction of EC at Vernalis, San Luis Drain load eliminated

It was not known at the time of the simulation whether the shutoff of the San Luis Drain would result in a net reduction of loading to the San Joaquin River or just a shift of loading to the time periods immediately before and/or after the shutoff. To estimate the effect of a shift in loading, an additional simulation was run. The loading which would have been discharged from the San Luis Drain under a do-nothing scenario was added to the week prior to the scheduled shutoff. The simulation results are shown in Figure 3.13. In this case, the base case shown in blue represents even flow and loading throughout the simulation. The simulation of the San Luis Drain shutoff case in green includes an increase in flow and loading in the week of July 16 through 23 and a corresponding decrease from July 23 through 30. As before, the phytoplankton load shows a delayed response. With the shift in load, however, the phytoplankton load increased at Vernalis by a similar amount to the subsequent decrease. The change is shown in red.

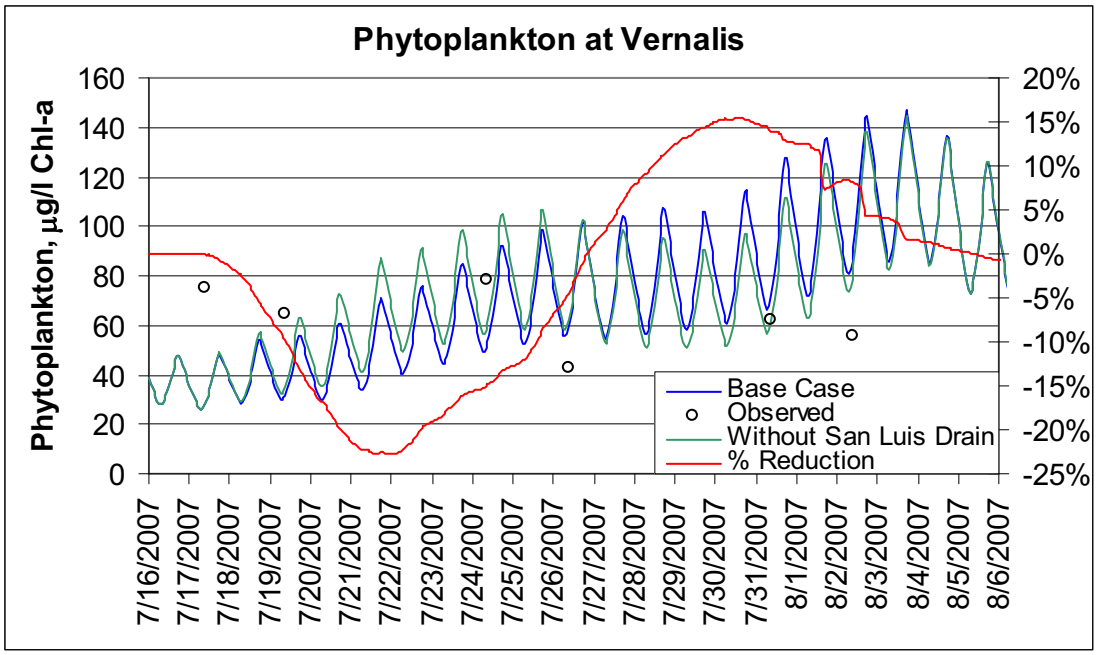

Figure 3.13: Forecasted reduction of phytoplankton concentration at Vernalis, San Luis Drain load shifted

Figure 3.14 shows the changes in simulated EC at Vernalis resulting from shifting the load of the San Luis Drain. Like phytoplankton, there was an increase in EC during the week with extra loading and a decrease when the San Luis Drain was shut off.

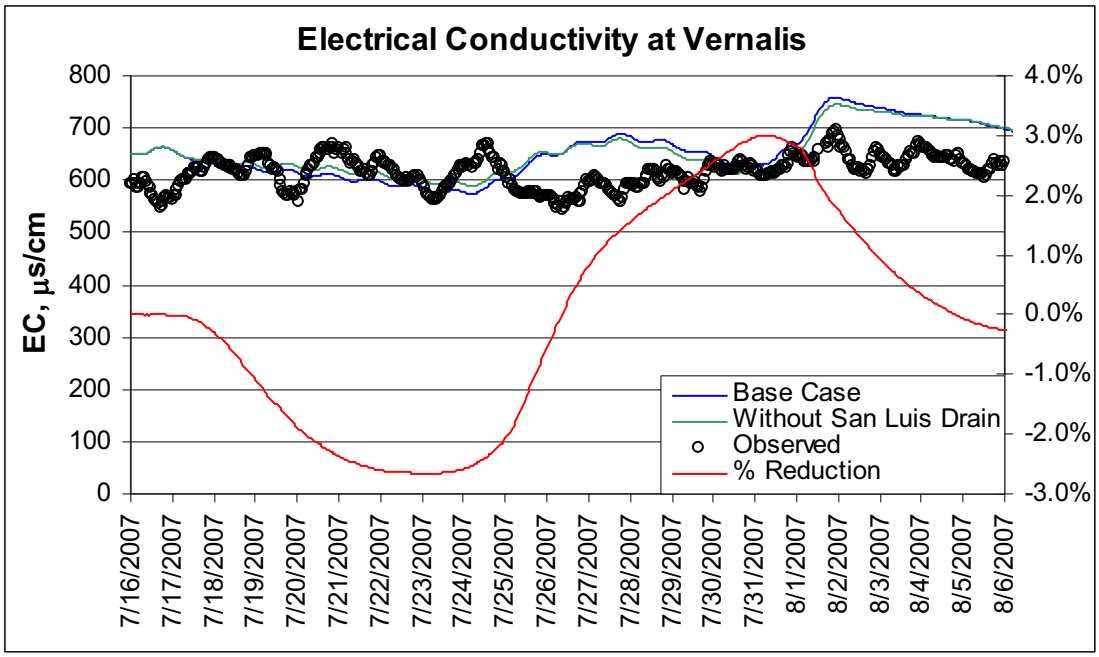

Figure 3.14: Forecasted reduction of EC at Vernalis, San Luis Drain load shifted

The ultimate goal of the forecasting model runs was to predict dissolved oxygen concentration in the DWSC. WARMF was linked to the Link-Node model, which simulated the estuarine part of the San Joaquin River downstream of the Old River junction. The Link-Node input file for the boundary condition at the Old River includes the WARMF model output for water quality constituents such as phytoplankton, dissolved oxygen, and nutrients. The DO in the DWSC as simulated by the Link-Node model was not sensitive to changes in organic loading at the Old River during test simulations. Causes of this insensitivity included diversion of organic loading to the Old River and diffusion / dispersion of loading once within the tidal zone.

The WARMF simulations in forecasting mode were posted on Systech Water Resources' FTP site prior to the actual shutoff of the San Luis Drain for analysis by other interested parties. The forecast could then be evaluated after the event to determine the accuracy of the forecast and how the assumptions of the simulation could be improved for future forecasting.

SUMMARY

The calibrated WARMF model of Upper San Joaquin River Watershed was applied to perform forecasting 3 weeks into the future. By comparing a "do nothing" scenario with a planned temporary shut off of the San Luis Drain, a phytoplankton concentration reduction of 19% at Vernalis was predicted. The predicted reduction in EC was only 3%. Monitoring data from before, during, and after the San Luis Drain shutoff showed a similar decrease in phytoplankton concentration after the load from San Luis Drain was stopped, but the concentration in Mud

Slough and at Vernalis did not increase back to its original level when the drainage flow resumed.

The forecasted flow and water quality of tributary inflows to the model were calculated using a combination of 2002 data and real-time data from the two weeks immediately prior to the forecast simulation. The error between forecast and measured flows ranged from -21% to +55% and the simulated flow at Vernalis was 20% greater than observed. Alternate techniques should be tested using historical data to determine a better method of estimating future flows. The error of forecasted EC was -15% to 29% with only a 6% average error in simulated EC. This suggested that the model and forecasting methodology could produce reasonable predictions of EC. With no real-time data collected for phytoplankton, all model inputs relied upon data from a similar time period in 2002. In practice, the measured concentrations in 2002 differed markedly from those later measured in 2007. This introduced a major source of error in the model forecasts. If reliable real-time data became available for phytoplankton, that could provide important guidance in predicting phytoplankton load to the San Joaquin River.

4 REFERENCES

Brown, R. 2002. "Evaluation of Stockton Deep Water Ship Channel Water Quality Model Simulation of 2001 Conditions: Loading Estimates and Model Sensitivity", Prepared for San Joaquin River Dissolved Oxygen TMDL Technical Advisory Committee and CALFED Water Quality Program, Jones and Stokes, Sacramento, CA.

Brown, R.. 2005. "San Joaquin River Water Quality Data Atlas", a CD containing the available historic data for the San Joaquin River, Jones and Stokes, Sacramento, CA.

Brown, R. and A. Huber. 2005: "Initial Simulation of 2000-2003 Flows and Water Quality in San Joaquin River Using DSM2-SJR Model", Jones and Stokes, Sacramento, CA

Chen, C.W., Herr, J., Gomez, L.E., Quinn, N.W.T., Kipps, J., Landis, P.J., Cummings E.W., 1996. "Design and Development of a Graphic User Interface for Real-Time Water Quality Management of the San Joaquin River," prepared for California Department of Water Resources, San Joaquin District.

Chen, C.W. and W. Tsai. 1996. "Effects of Bay-Delta Operations on Dissolved Oxygen in San Joaquin River" Report to the City of Stockton, Systech Engineering, Inc., San Ramon, CA.

Chen, C.W. and W. Tsai, 1997a. "Evaluation of Alternatives to Meet the Dissolved Oxygen Objectives of the Lower San Joaquin River," prepared for City of Stockton Municipal Utilities Department.

Chen, C. W. and W. Tsai, 1997b. "Draft Evaluation of Alternatives to Meet the Dissolved Oxygen Objectives of the Lower San Joaquin River " Report to State Water Resources Control Board and Central Valley Regional Water Quality Control Board, Sacramento, CA

Chen, C.W. and W. Tsai. 2000. "Rough Loading Calculation for Dissolved Oxygen Sinks in Lower San Joaquin River", Systech Engineering, Inc., San Ramon, CA.

Chen, C.W., Herr, J., and Weintraub, L.H.Z. 2001. "Watershed Analysis Risk Management Framework: Update One: A Decision Support System for Watershed Analysis and Total Maximum Daily Load Calculation, Allocation, and Implementation," EPRI, Palo Alto, CA. Topical Report 1005181.

Chen C. W. and W. Tsai. 2002. "Improvements and Calibrations of Lower San Joaquin River DO Model" Final Report for CALFED Grant 99-B16, and DWR 4600000989, Systech Engineering, Inc., San Ramon, CA 94583

Chen, C.W. and W. Tsai, 2002. "User's Manual: San Joaquin River Dissolved Oxygen Model," prepared for California Department of Water Resources, Systech Engineering, Inc. San Ramon, CA 94583.

Di Toro, D.M., 1978. "Optics of Turbid Estuarine Waters: Approximations and Applications", Water Research 12: 1059-1068.

Foe, C., M. Gowdy, M. McCarthy. 2002. "Strawman Load Allocation of Responsibility Report", Draft, Central Valley Regional Water Quality Control Board, Sacramento, CA.
Jones & Stokes. 1998. "Potential Solutions for Achieving the San Joaquin Dissolved Oxygen Objectives", Prepared for City of Stockton, Jones & Stokes, Sacramento, CA

Driscoll, Jr. C. T., R.A. Bodaly, O.R. Bullock, Jr., D.P. Krabbenhoft, R.P. Mason, C.D. Pollman, and T. A. Wool. 2004. "Report of The Peer Review Panel on the Development of the Watershed Analysis Rish Management Framework (WARMF) Model to Assess Mercury in the Western Lake Superior Basin, Minnesota", University of Minnesota Sea Grant Program, Duluth, Minnesota, Publication No. CT 15.

Herr, J., Weintraub, L.H.Z., and Chen, C.W. 2001. "User's Guide to WARMF: Documentation of Graphical User Interface," EPRI, Palo Alto, CA. Topical Report.

Herr, J., and C. W. Chen 2006 (a). "Calibration Report": a deliverable report for the CALFED Project ERP-02D-P63, Monitoring and Investigation of the San Joaquin River and Tributataries Related to Dissolved Oxygen, Task 6 Model Calibration and Forecasting. Systech Engineering, Inc. San Ramon, California.

Herr, J., and C. W. Chen 2006 (b). "Forecasting Procedure Report": a deliverable report for the CALFED Project ERP-02D-P63, Monitoring and Investigation of the San Joaquin River and Tributataries Related to Dissolved Oxygen, Task 6 Model Calibration and Forecasting. Systech Engineering, Inc. San Ramon, California.

Herr, J., and C. W. Chen 2007. "Forecasting Results Report": a deliverable report for the CALFED Project ERP-02D-P63, Monitoring and Investigation of the San Joaquin River and Tributataries Related to Dissolved Oxygen, Task 6 Model Calibration and Forecasting. Systech Engineering, Inc. San Ramon, California.

Huckelbridge, K. 2006. "Stockton DO Project LBNL Modeling Report", Draft, Lawrence Berkeley National Laboratory, Berkeley, CA

Jones & Stokes. 2005. "San Joaquin River Deep Water Ship Channel Demonstration Dissolved Oxygen Aeration Facility Initial Study/Mitigated Negative Declaration". Prepared for California Department of Water Resources.

Keller A., 2000 “Peer review of the watershed analysis risk management framework (WARMF): an evaluation of WARMF for TMDL applications by independent experts using USEPA guidelines”, Electric Power Research Institute, Palo Alto, CA. Technical Report 1000252.

Keller A. 2001. “Peer Review of the Acid Mine Drainage Module of the Watershed Analysis Risk Management Framework (WARMF) – An evaluation of WARMF/AMD using EPA Guidelines”, Electric Power Research Institute, Palo Alto, CA. Technical Report 1005182.

Kratzer, C.R., P.J. Pickett, E.A. Rashimawi, C.L. Cross, and K.D. Bergerson. 1987. An Input-Output Model of the San Joaquin River from the Lander Avenue Bridge to the Airport Way Bridge”, Technical Committee Report No. N.Q. 85-1. California Water Resources Control Board, Sacramento, CA

Kratzer, C.R., P.D. Dileanis, C. Zamora, S. R. Silva, C. Kendall, B.A. Bergamaschi, and R. A Dahlgren. 2004. “Sources and Transport of Nutrients, Organic Carbon, and Chlorophyll-a in the San Joaquin River Upstream of Vernalis, California, during Summer and Fall, 2000 and 2001”, Water Resources Investigations Report 03-4127, US Geological Survey, Sacramento, CA.

Kratzer, C.R. and J.L. Shelton. 1998. “Water Quality Assessment of the San Joaquin-Tulare Basins, California: Analysis of Available Data on Nutrients and Suspended Sediment in Surface Water 1972-1990”, US Geological Survey, Professional Paper 1587.

Lee, G.F., and A.J. Lee. 2000. “Synopsis of Issues in Developing the San Joaquin River Deep Water Ship Channel DO TMDL” available from http://www.gfredlee.com/SJRsynopsis.pdf.

Lehman, P.W., J. Sevier, J. Giulianotti, and M. Johnson. 2004. “Sources of Oxygen Demand in the Lower San Joaquin River, California”, Estuaries, Vol. 27, No. 3, pp 405-418.

List, E.J. and S.C. Paulsen, 2008. “Peer Review of San Joaquin River Watershed Modeling” Final Draft, Flow Science Incorporated, Pasadena, CA.

Pate, T. 2001. “DSM2 San Joaquin Boundary Extension” in Chapter 5 of Methodology for Flow and Salinity Estimates in the Sacramento-San Joaquin Delta and Suisun Marsh, 22nd Annual Progress Report to the State Water Resources Control Board in Accordance with Water Right Decision 1485, Order 9, Department of Water Resources, Sacramento, CA.

Quinn, N.W.T., L. F. Grober, Jo-Anne Kipps, C. W. Chen, and E. Cummings. 1997. “Computer Model Improves Real-Time Management of Water Quality”, California Agriculture, Vol. 51, No. 5, pp. 14-20.

Quinn, N.W.T, 2003. “Concept Paper for Real-Time Temperature and Water Quality Management for San Joaquin River Riparian Habitat Restoration,” prepared for U.S. Bureau of Reclamation, Mid Pacific Region.

Regional Water Quality Control Board Central Valley Region, 1999. “Regional Toxic Hot Spot Cleanup Plan” Central Valley Regional Water Quality Control Board, Sacramento, CA April 1999.

Schanz, R. and C. W. Chen. 1993 “City of Stockton Water Quality Model, Volume 1: Model Development and Calibration”, Final Report to the City of Stockton, PWA, San Francisco and Systech Engineering, Inc. San Ramon, CA.

Wilde, J. and B. Suits. 2004. “DSM2 San Joaquin River Extension Simulation Over the 1990-1999 Period”, Technical Memorandum, Department of Water Resources Bay-Delta Office, Sacramento, CA.

Wilde, J. 2005. “Using Dye-Injection Study to Revise DSM2-SJR Geometry” in Chapter 2 of Methodology for Flow and Salinity Estimates in the Sacramento-San Joaquin Delta and Suisun Marsh, 26th Annual Progress Report to the State Water Resources Control Board in Accordance with Water Right Decision 1485, Order 9, Department of Water Resources, Sacramento, CA

APPENDIX A: CALIBRATION SUPPLEMENT

The time series inputs and results of the calibration of the WARMF model are shown in Section 1 of this report. That section describes the methods used to create the time series input files for meteorology, air/rain chemistry, point sources, tributary inflows, and diversions. It also describes how the geometric data and land use coefficients, which are key model coefficients, were entered into WARMF. This appendix lists the values of model coefficients for which specific values are not readily available.

Since the submission of the calibration report, WARMF was modified further. Changes included the addition of riparian diversions, splitting of land catchments which straddled the San Joaquin River, and subdivision of the river segments between the Stanislaus River and the Old River. Modest changes in model coefficients were made to maintain the model calibration, especially in response to the significant additional diverted water and irrigation, and subsurface flow resulting from the riparian diversions. The original model calibration period was water years 2000 through 2005. Since the calibration was done, years 2006 and 2007 became available. The data for these last two years was compiled so that a verification run could be made using the model coefficients calibrated through 2005.

Recalibration of the Link-Node model was also performed after submission of the original Calibration Report. The Link-Node database was expanded through the 2007 water year. The Link-Node code was upgraded to allow for different reaction rates in different nodes of the model domain instead of single values for each reaction applicable everywhere.

Model Calibration Coefficients

There are thousands of model coefficients in the San Joaquin River WARMF model. Some apply throughout the watershed, some apply to individual land uses while other coefficients apply to individual catchments and river segments. The model was not very sensitive to the values of a majority of the coefficients, so those could be safely be left at default literature values unless there was specific information to enter.

System Coefficients

The systemwide coefficients can be viewed by double-clicking on the white space on the WARMF map. Following in Table A-1 are the system coefficients used in calibration of the San Joaquin River model. The range is the typical range within which the coefficient varies. The column on the right has the value used for the San Joaquin River calibration.

Table A-1: Calibrated System Coefficients

Coefficient	Units	Description	Range	Value
Evaporation Magnitude	None	Multiplier of potential evapotranspiration calculated from temperature, humidity, and latitude	0.6 – 1.4	0.775
Evaporation Skewness	None	Seasonal adjustment of evapotranspiration calculations	0.6 – 1.4	0.794
Diatom Nitrogen Half-Saturation	mg/l	Half-saturation concentration for nitrogen growth limitation	0.01-0.03	0.01
Diatom Phosphorus Half-Saturation	mg/l	Half-saturation concentration for phosphorus growth limitation	0.001-0.005	0.001
Diatom Light Half-Saturation	W/m^2	Optimum light intensity for growth	40-200	42
Diatom Chl-a/C ratio	None	Cholorphyll content relative to carbon content	0.015-0.03	0.025
Diatom N/C ratio	None	Nitrogen content relative to carbon content	0.05-0.15	0.15
Diatom P/C ratio	None	Phosphorus content relative to carbon content	0.01-0.03	0.01

There are a number of model system coefficients which have values for each land use. These coefficients define how the different land uses receive anthropogenic model inputs such as irrigation and respond to natural model inputs such as atmospheric deposition. These coefficients are accessed in WARMF the same way as the coefficients above, by double-clicking in the white space on the WARMF map. The land use coefficients are under the land use tab of the ensuing dialog box. The model is sensitive to the coefficients shown in Table A-2.

Table A-2: Calibrated System Land Use Coefficients

	Impervious Fraction	Cropping Factor	Productivity	Leaf Area Index
Units	none	none	$kg/m^2/yr$	none
Description	Portion of each land use which is paved	"C" factor of Universal Soil Loss Equation	Net creation of vegetation	Ratio of leaf area to land area (varies monthly)
Range	0 - 1	0 - 1	0 – 3	0-15
Deciduous	0	0.01	0.8	0-4.5
Coniferous	0	0.05	0.8	12-15
Mixed Forest	0	0.03	0.8	6-10
Orchard	0	0.1	0.8	0-4.5
Cropland / Pasture	0	0.5	0.1	1-1.5
Confined Feeding	0	1	0	0
Rangeland	0	0.1	0.1	1-1.5
Forested Wetland	0	0.01	0.8	0-4.5
Non-forested Wetland	0	0	0.1	1-1.5
Barren	0	1	0	0
Residential	0.3	0.2	0.2	0-1.8
Comm./Industrial	1	0	0	0
Water	0	0	0	0

Catchment Coefficients

Catchment coefficients are key for simulating shallow groundwater flow and nonpoint source load. The coefficients can be set differently for each catchment if they have different properties or lumped together with the same values. The coefficients for each individual catchment can be viewed and edited in WARMF by double-clicking on the catchments.

The catchment area, slope, and aspect were calculated from digital elevation models and are not subject to calibration. Meteorology coefficients are set automatically. The nearest station to each catchment is assigned to it. The precipitation weighting factor and temperature lapse are set using an inverse distance algorithm using multiple meteorology stations and have not been calibrated. Land uses are calculated by overlaying a land use shapefile with catchment boundaries. Fertilization and irrigation are estimated from data. The remaining calibrated coefficients are primarily reaction rates and soil properties. Reaction rates are shown in Table A-3. These rates are adjusted based on temperature. Reactions only occur under the proper dissolved oxygen concentration, for example nitrification under oxic conditions and denitrification when dissolved oxygen is near zero.

Table A-3: Calibrated Catchment Reaction Rate Coefficients

Reaction Rate	Units	Range	Value
BOD Decay	1/d	0.05-0.5	0.1
Nitrification	1/d	0-0.1	0.01
Denitrification	1/d	0-0.1	0.1
Sulfate Reduction	1/d	0-0.5	0.01

Table A-4 shows soil coefficients which are calibrated. Four soil layers were used in the San Joaquin River application. Although the soil is truly very deep in the San Joaquin Valley, the watershed modeling is concerned with those soil layers make up the shallow groundwater which interacts with surface waters. Flow calibration for the catchments used the difference between the gaged inflows and the measured flow at Vernalis. Since there wasn't a way to differentiate the catchments from each other, they were calibrated together with the same coefficients.

Table A-4: Calibrated Catchment Soil Coefficients

Coefficient	Units	Description	Range	Value
Soil Erosivity	none	"K" factor of Universal Soil Loss Equation	0.16 – 0.28	0.2
Layer 1 thickness	cm	thickness of the top soil layer	> 0	38.578
Layer 2 thickness	Cm	thickness of the second soil layer from the top	> 0	24.053
Layer 3 thickness	Cm	thickness of the third soil layer	> 0	20.628
Layer 4 thickness	Cm	thickness of the bottom soil layer	> 0	150
Layer 1 field capacity	none	field capacity of the top soil layer	0.1-0.3	0.24
Layer 2 field capacity	none	field capacity of the second soil layer from the top	0.1-0.3	0.24
Layer 3 field capacity	none	field capacity of the third soil layer	0.1-0.3	0.228
Layer 4 field capacity	none	field capacity of the bottom soil layer	0.1-0.3	0.15
Layer 1 saturation	cm	saturation of the top soil layer	0.2-0.5	0.4
Layer 2 saturation	cm	saturation of the second soil layer from the top	0.2-0.5	0.35
Layer 3 saturation	cm	saturation of the third soil layer	0.2-0.5	0.3
Layer 4 saturation	cm	saturation of the bottom soil layer	0.2-0.5	0.25
Layer 1 initial moisture	none	initial moisture of the top soil layer	0.1-0.5	0.24
Layer 2 initial moisture	none	initial moisture of the second soil layer from the top	0.1-0.5	0.24
Layer 3 initial moisture	none	initial moisture of the third soil layer	0.1-0.5	0.228
Layer 4 initial moisture	none	initial moisture of the bottom soil layer	0.1-0.5	0.2

The other important parameters for calibrating the water quality of the shallow groundwater is setting the initial concentrations of each chemical constituent in each soil layer of each catchment (Table A-5). The initial concentrations weren't calibrated, but were set based on a balance over the course of the simulation. The initial concentrations were set individually for each catchment and soil layer to match the ending concentrations of the simulation under the assumption that the actual soil chemistry in the San Joaquin valley is in relative equilibrium rather than undergoing a trend of increasing or decreasing concentration.

Table A-5: Calibrated Catchment Initial Soil Pore Water Concentrations

Constituent	Units	Values
Ammonia	mg/l as N	0.2-2
Calcium	mg/l	60-800
Magnesium	mg/l	20-300
Potassium	mg/l	5-40
Sodium	mg/l	70-750
Sulfate	mg/l	0.1-70
Nitrate	mg/l as N	0.01-1
Chloride	mg/l	500-1000
Phosphate	µg/l as P	100-1000
Organic Carbon	mg/l	4-8
EC (Conservative)	µs/cm	300-8000
Dissolved Oxygen	mg/l	0.1-8

River Coefficients

Physical data for river segments, including upstream and downstream elevations and lengths, comes from digital elevation model data. The stage-width curves representing the cross sections were taken from the DSM2 model of the San Joaquin River and its east side tributaries which in turn used measured data. Manning's n for each river segment was also taken verbatim from the DSM2 model. Calibrated coefficients include reaction rates, river bed scour coefficients, and adsorption isotherms. Table A-6 shows the reaction rates

Table A-6: Calibrated River Reaction Rate Coefficients

Reaction Rate	Units	Range	Value
BOD Decay	1/d	0.1-1	0.2
Organic Carbon Decay	1/d	0.01-0.1	0.07
Nitrification	1/d	0.01-1	0.5
Denitrification	1/d	0-1	0
Sulfate Reduction	1/d	0-0.5	0
Clay Settling	m/d	>0	0.000346*
Silt Settling	m/d	>0	8.64
Sand Settling	m/d	>0	1036.8
Diatom Growth	1/d	0.2-0.5	3.2
Diatom Respiration	1/d	0.1-0.5	0.15
Diatom Mortality	1/d	0.1-0.5	0.05**
Diatom Settling	m/d	0-1	0*
Detritus Decay	1/d	0-1	0.2
Detritus Settling	m/d	0-1	0*
Settled Detritus Decay	1/d	0-0.1	0.2

* Settling rates are assumed to be minimal throughout the watershed except for the reach of the San Joaquin River at Mossdale. The Mossdale reach has settling rates of 1 m/d for clay, 0.5 m/d for diatoms, and 0.5 m/d for detritus.
** The diatom mortality rate was set to 0.15/d in the Mossdale reach due to higher zooplankton activity.

Sediment transport in rivers is affected by the settling rates shown above but also scour from the river bed. Scour is controlled by the shear velocity of the water next to the river bed. Above the critical shear velocity, scour is calculated in the form aV^b where a is the multiplier and b is the exponent. For all river segments, $a=1.0x10^{-6}$ and b=2.0.

Adsorption coefficients control the partioning between the dissolved phase of each constituent and the portion adsorbed to suspended sediment. For ammonia, phosphate, and organic carbon the adsorption isotherms were calculated using concurrent data of suspended sediment with ammonia, nitrate, and total nitrogen; phosphate and total phosphorus; and dissolved organic carbon with total organic carbon. Although calculated values varied greatly based on location and sample date, average values were determined and applied uniformly to all river segments.

Table A-7: Calibrated River Adsorption Isotherm Coefficients

Constituent	Units	Values
Ammonia	L/kg	27000
Calcium	L/kg	472.552
Magnesium	L/kg	404.556
Potassium	L/kg	197.971
Sodium	L/kg	20.7365
Sulfate	L/kg	16.2596
Nitrate	L/kg	0
Chloride	L/kg	0
Phosphate	L/kg	17000
Organic Carbon	L/kg	107.184
EC (Conservative)	L/kg	0

Model Verification

The WARMF model was calibrated using water years 2000-2005. Since the model was calibrated, data for water years 2006 and 2007 have become available to determine how well the model performs simulating a time period for which it has not been calibrated. 2006 was the second wettest year in 24 years – not a critical year for water quality in the San Joaquin River but a good test for the performance of WARMF under high flow and high water table conditions. 2007 was a drier than average year, at the 39th percentile of water years 1984 through 2007.

Data Compilation

Data was collected for 2006 and 2007 to create a complete set of input time series for the model and measured data to evaluate the model calibration. The data was collected from the same data sources as for years 2000-2005 as described in section 1 of this report. Meteorology data collected from CIMIS was appended to the original data files. Air quality data from CASTNET and rain chemistry from NADP was added to the existing data from Yosemite. Point source data for the City of Modesto WQCF was collected from the US EPA Pollution Control System.

Tributary inflows and agricultural drains require complete time series of flow and water quality data. These data sets are generally as complete for 2006 and 2007 as for previous years. Data gaps for those two years include the following:

- There is no 2007 data for the Merced River at Stevinson, which is used for the Merced River tributary inflows. The Merced River flow is estimated using a correlation with data from the Merced River station upriver at Cressy.
- Diversion data is not yet available for the Patterson Water District, El Solyo Water District, and Banta-Carbona Irrigation District for 2007. Data is copied from 2002, a similar hydrologic year, to fill in the missing 2007 data.
- There is no monitoring data for the major cations and anions (Ca, Mg, K, Na, SO_4, Cl) and inorganic carbon to provide information for agricultural drains, tributary inflows, or for calibration data. The boundary inflows use determined average concentrations from previous years for each inflow.

Model Verification Simulation of 2006-2007

For the model verification simulation, the calibrated model was initially run for years 2000-2005. The end point of that simulation was used to establish the initial conditions of a verification simulation running from October 1, 2005 through September 30, 2007. The second simulation was run using the same model coefficients as the first. To evaluate the performance of the model, simulation results at Vernalis were compared to measured data. The statistical measures of the verification simulation were then compared against the statistics from the calibration simulation.

Flow

Figure A-1 shows the calibration simulation in blue, the verification simulation in green, and measured data in black circles. The simulations closely follow the measured data in both the calibration and verification periods, indicating that the model is accounting for the known flows and calculating shallow groundwater inflows correctly.

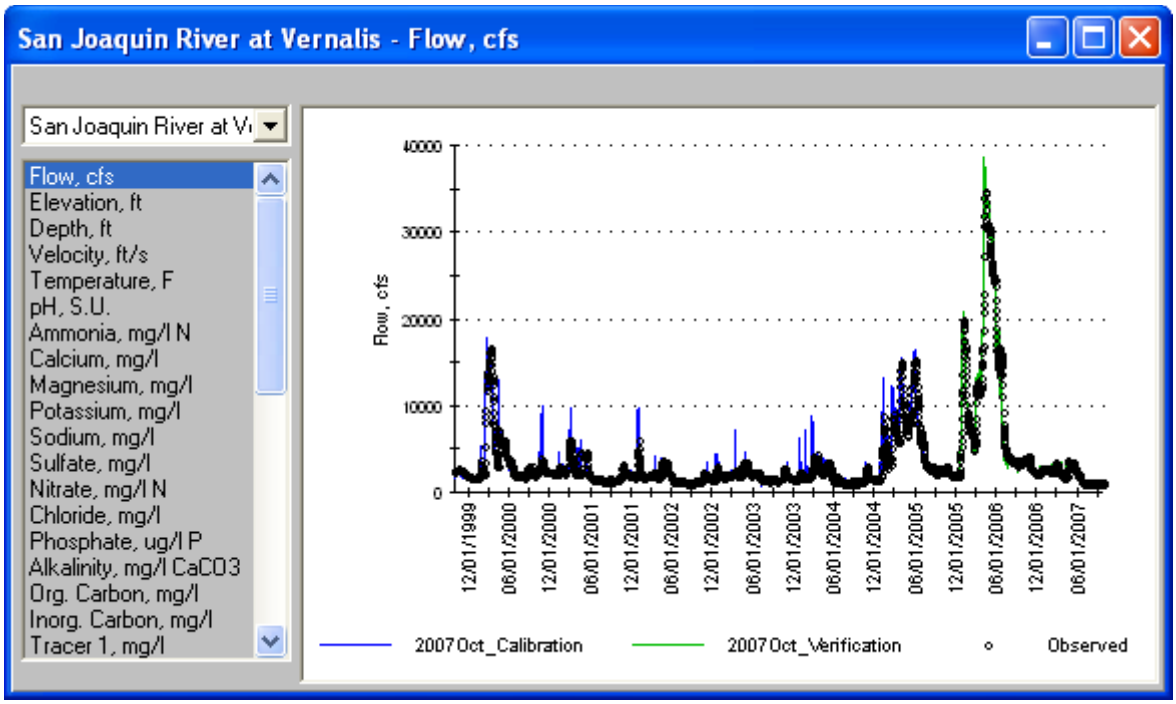

Figure A-1 Simulated vs Observed Flow at Vernalis

Table A-8 provides the summary statistics of model errors, assuming the measured flows are accurate. Relative error is the average of the deviations between simulated and observed. Absolute error is the average of the absolute differences between model predictions and observations. The goal of calibration is to have the relative error below 5% and the absolute error below 10%. These values are believed to be within the accuracy of instruments used to measure the flow.

Table A-8
Statistics of Model Calibration and Verification for Flow Simulation at Vernalis

Simulation	Relative Error	Absolute Error
Calibration (2000-2005)	-1%	13%
Verification (2006)	+3%	9%
Verification (2007)	-3%	8%

One of the key assumptions for the verification simulation is the estimation of Merced River flow. To test this assumption, we can use the flow gage in the San Joaquin River at Newman, which is just downstream of the confluence with the Merced River. As Figure A-2 shows, there is too little simulated flow at Newman from October 2006 through March 2007 indicating the estimated Merced River flow may be too low. From April through September of 2007, however, there is a close match between the simulated and observed flow.

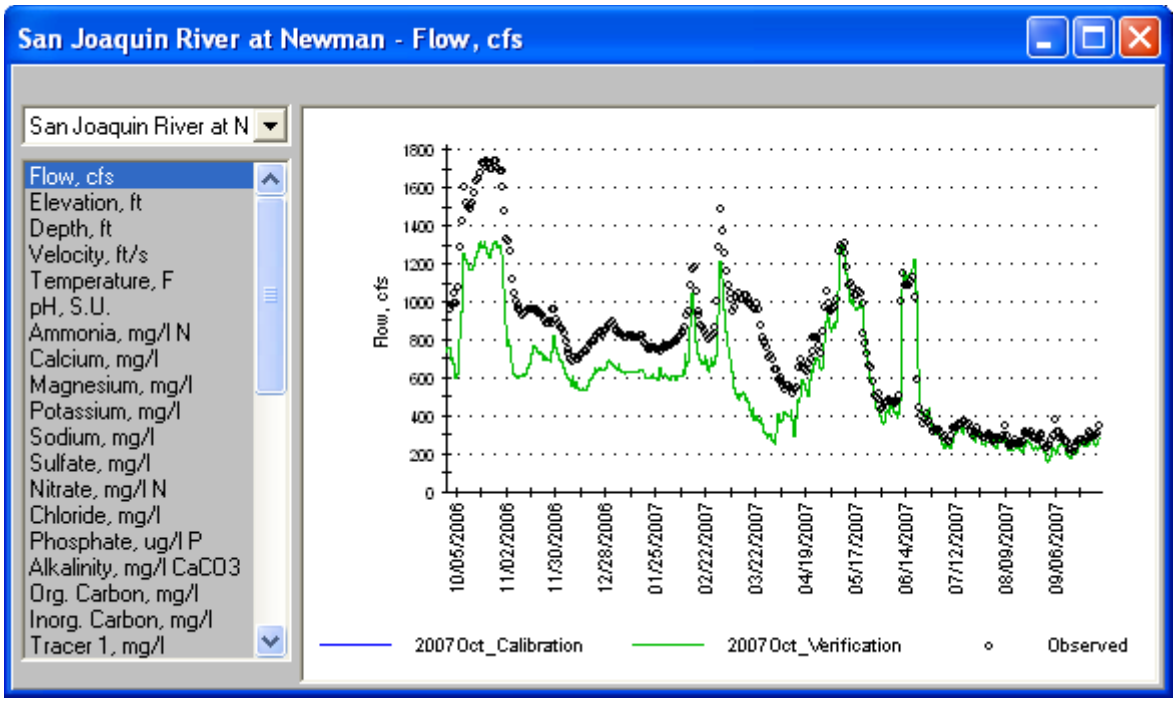

Figure A-2 Simulated vs Observed Flow at Newman

Temperature

The temperature simulations of 2006 and 2007 were quite consistent with 2000-2005, showing the same seasonal pattern as shown in Figure A-3. The calibration simulation is in blue and the 2006-2007 verification is in green.

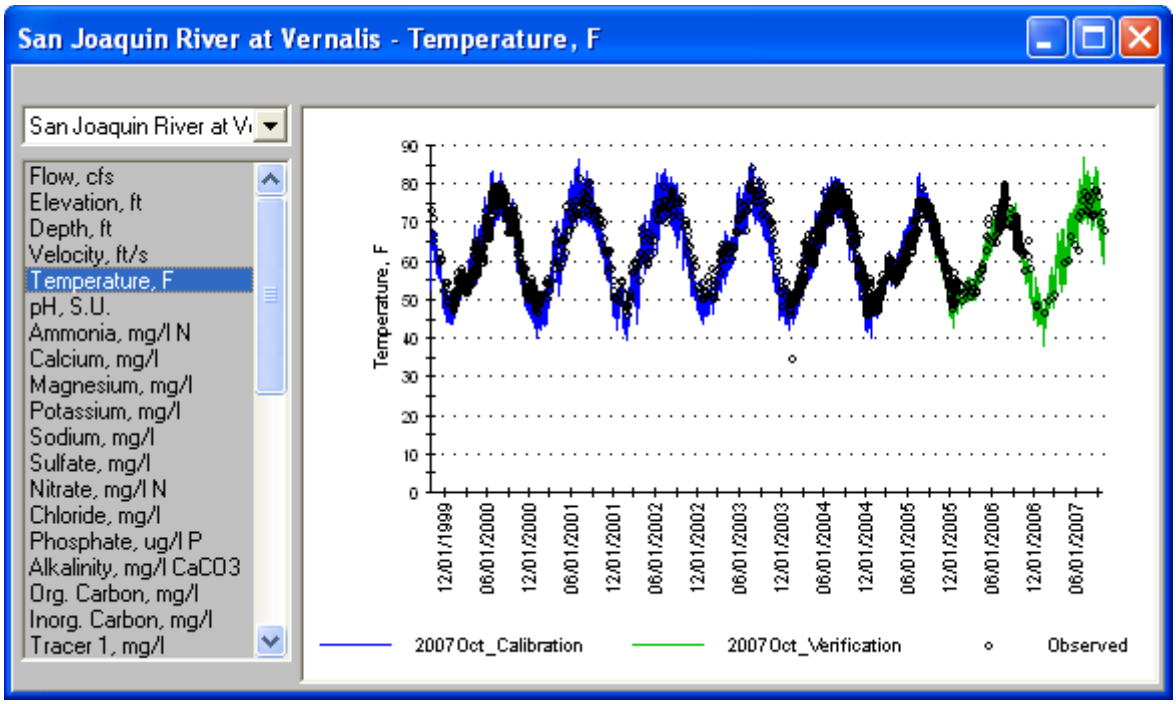

Figure A-3 Simulated vs Observed Temperature at Vernalis

Table A-9 provides a summary of model errors for the San Joaquin River at Vernalis, assuming that the observed data are accurate. The 2006 and 2007 relative errors were within the goal of 1 ^{o}C (1.8 ^{o}F).

Table A-9
Model Calibration and Verification Errors of Water Temperature at Vernalis

Simulation	Relative Error	Absolute Error
Calibration (2000-2005)	-0.5 ^{o}F	2.0 ^{o}F
Verification (2006)	-1.1 ^{o}F	1.7 ^{o}F
Verification (2007)	+0.4 ^{o}F	1.9 ^{o}F

Suspended Sediment

Figure A-4 shows the calibration (blue) and verification (green) simulations overlayed with monitoring data (black circles). Note that in 2006, there is daily data of suspended sediment collected by the USGS.

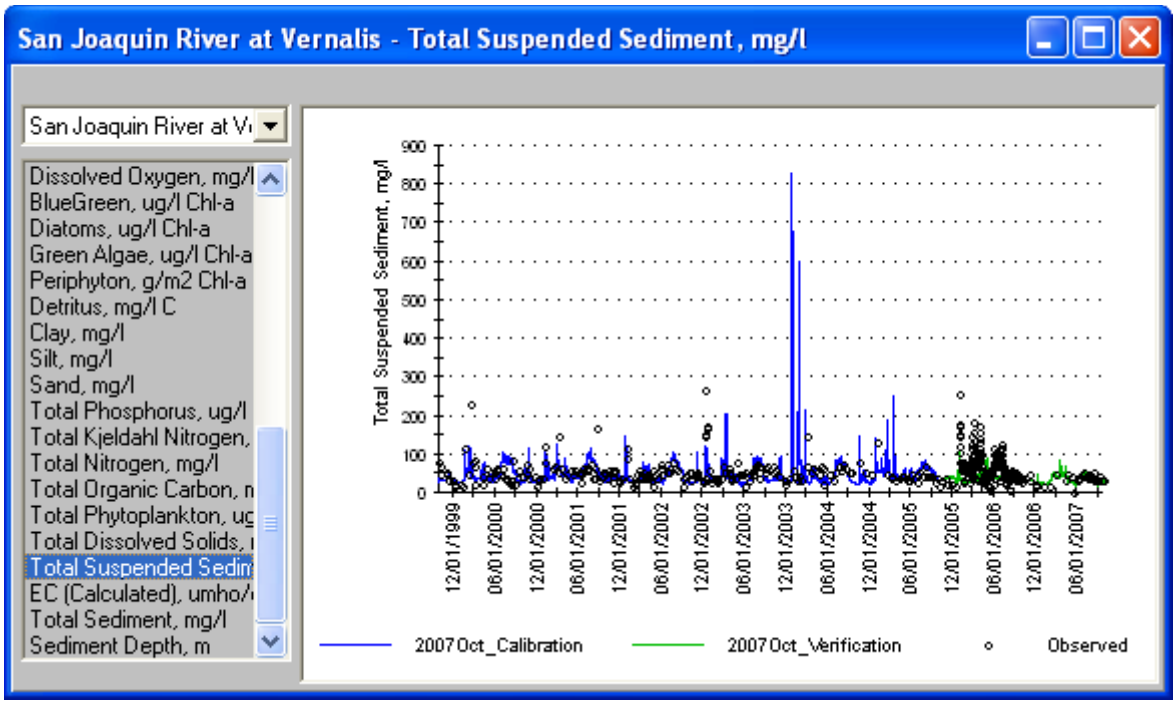

Figure A-4 Simulated vs Observed Suspended Sediment at Vernalis

If we zoom in on the year 2006, the differences between the simulation results, grab sample data, and USGS daily data become apparent as shown in Figure A-5. The lower row of measured data is biweekly grab sampling collected by the San Joaquin River DO TMDL monitoring program and the Bay Delta and Tributaries Project using the same methods as the data for which the model was calibrated in years 2000-2005. The suspended sediment concentrations reported by the USGS were considerably higher. On days when grab samples were taken, the measured USGS concentrations averaged 2.5 times the grab sample data. It needs to be determined which data set is correct, but for model calibration purposes it is assumed that the USGS values are not accurate and thus are excluded from the analysis.

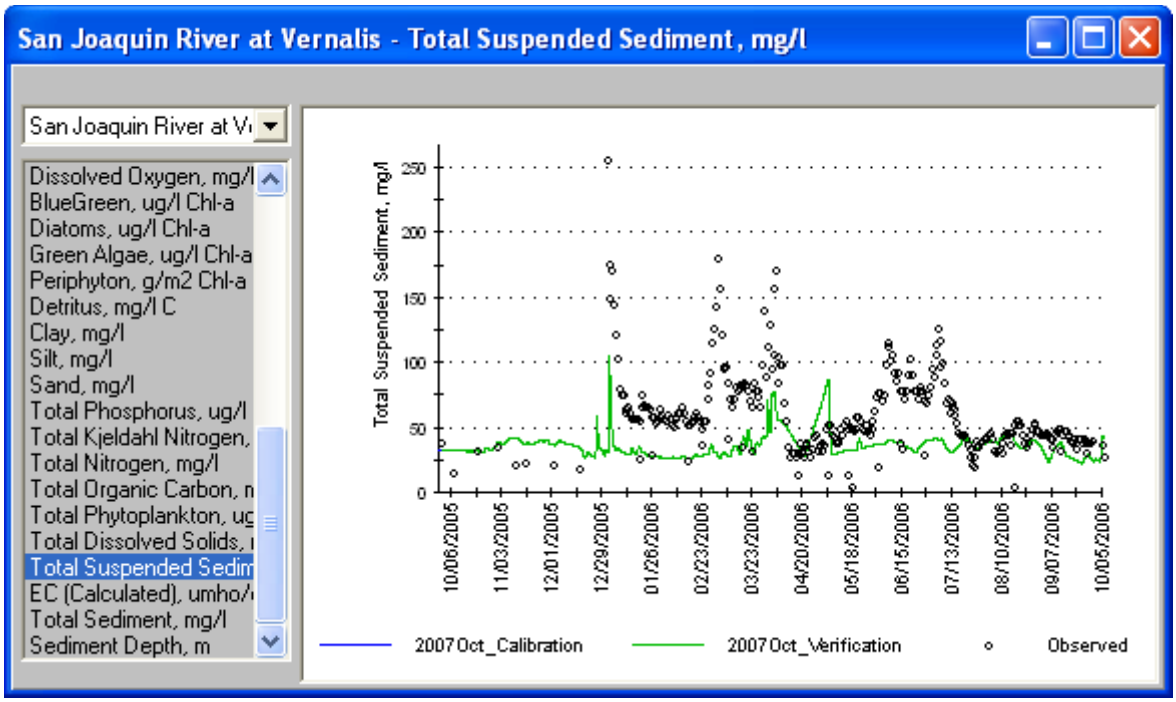

Figure A-5 Simulated vs Observed Suspended Sediment at Vernalis, Water Year 2006

Table A-10 shows the model errors for suspended sediment at Vernalis on the San Joaquin River. The errors in 2006 and 2007 were similar to the errors in the calibration and inline with the goal of 10% relative error and 50% absolute error for suspended sediment calibration.

Table A-10
Model Calibration and Verification Errors of Suspended Sediment at Vernalis

Simulation	Relative Error	Absolute Error
Calibration (2000-2005)	-10%	40%
Verification (2006)	+8%	45%
Verification (2007)	-13%	26%

Conservative EC

Figure A-6 shows the calibration (blue) and verification (green) simulations of "Conservative EC" at Vernalis overlayed with measured data in black circles. From the plot it is apparent that the model simulation of Conservative EC was significantly less than observed in 2007.

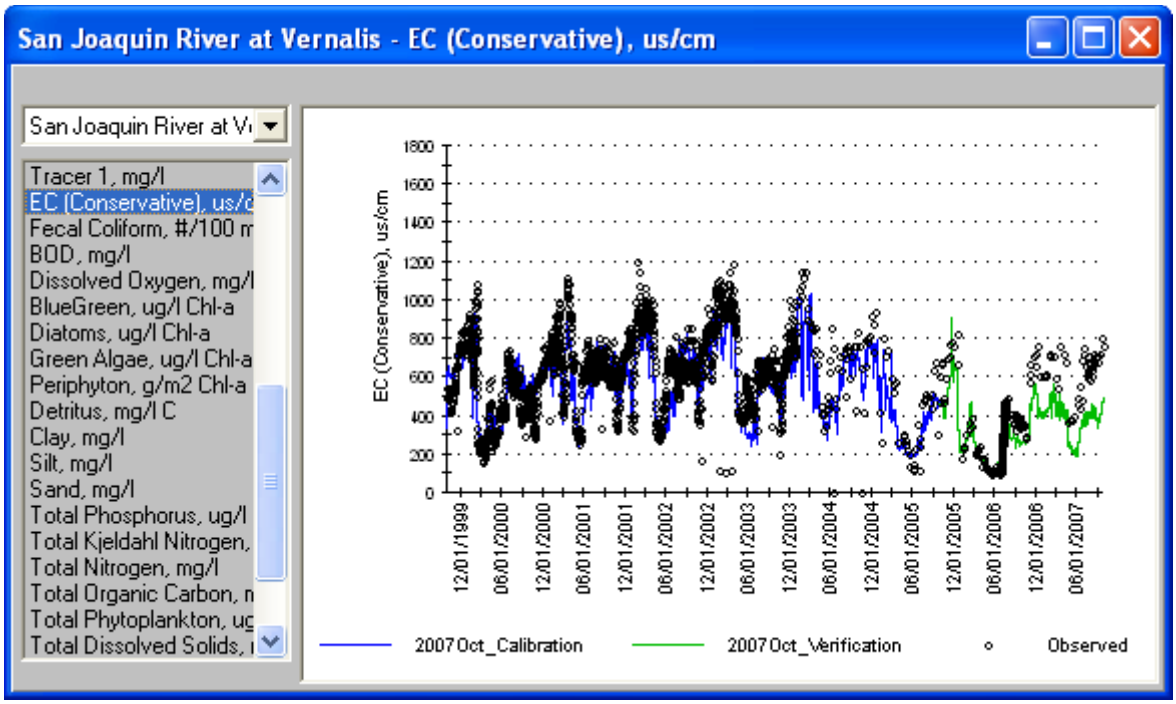

Figure A-6 Simulated vs Observed "Conservative EC" at Vernalis

Table A-11 shows the model errors for Conservative EC at Vernalis. The model under predicted Conservative EC in late 2005, in midsummer 2006, and throughout the 2007 water year.

Table A-11
Model Calibration and Verification Errors of Conservative EC at Vernalis

Simulation	Relative Error	Absolute Error
Calibration (2000-2005)	-6%	16%
Verification (2006)	-26%	27%
Verification (2007)	-36%	36%

Ammonia

Measured data of ammonia at Vernalis had very low concentrations in 2006 and 2007, similar to water years 2000-2005. Figure A-7 shows the calibration (blue) and verification (green) simulations of ammonia and the observed data. Visual inspection of the plot reveals that the model is simulating much more ammonia than was observed.

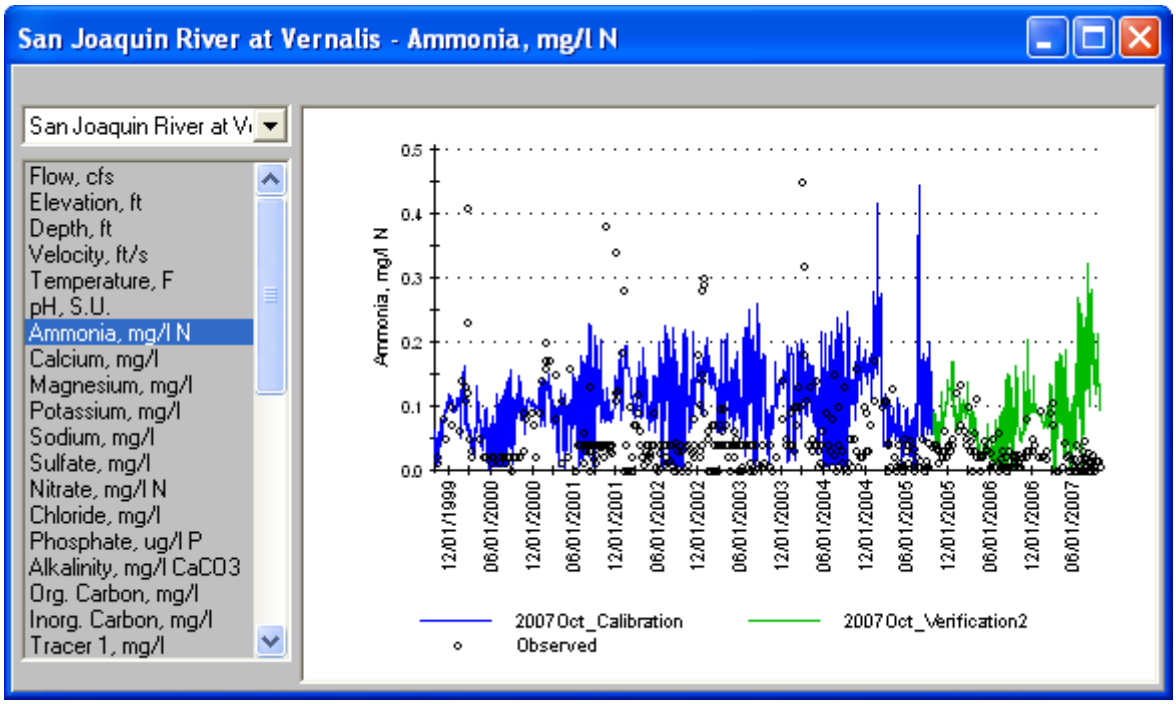

Figure A-7 Simulated vs Observed Ammonia at Vernalis

Table A-12 shows the model errors for ammonia at Vernalis. As with the calibration scenario, the model predicts much higher concentration of ammonia than was measured. Investigation is continuing as to the source of the model error.

Table A-12
Model Calibration and Verification Errors of Ammonia at Vernalis

Simulation	Relative Error	Absolute Error
Calibration (2000-2005)	+111%	148%
Verification (2006)	+91%	110%
Verification (2007)	+406%	411%

Nitrate

Figure A-8 shows the calibration (blue) and verification (green) simulations of nitrate at Vernalis. Measured data is shown in black circles. The graph shows the simulated nitrate closely following the observed data until summer of 2007.

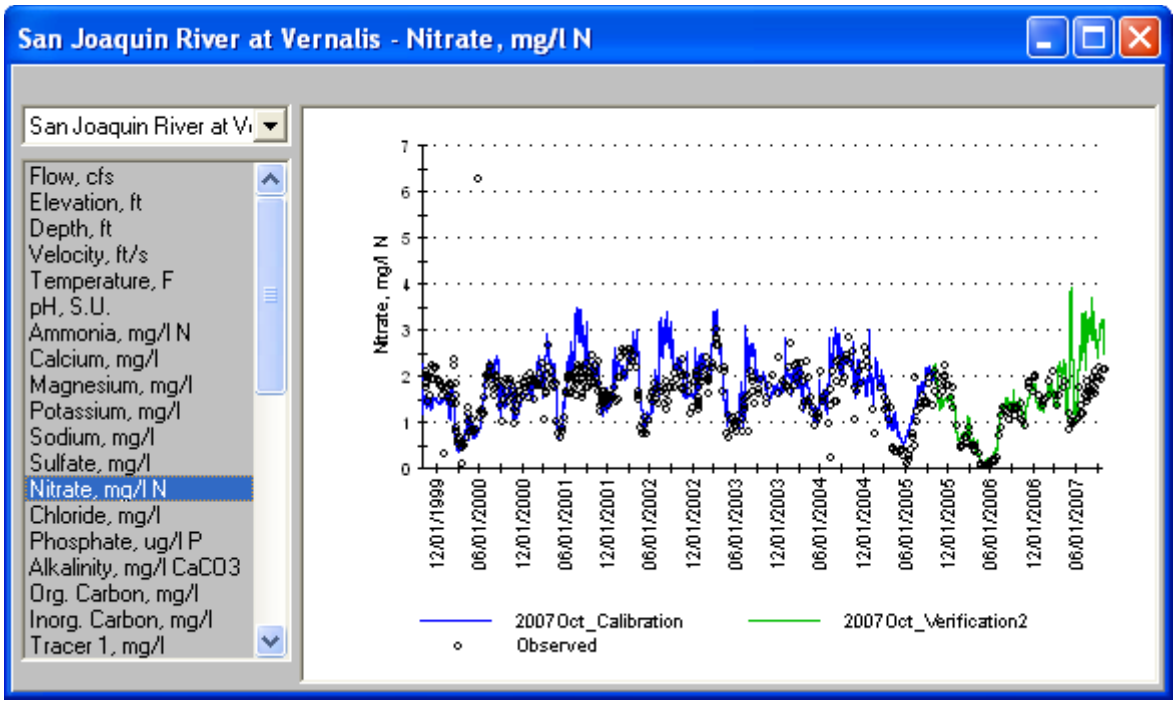

Figure A-8 Simulated vs Observed Nitrate at Vernalis

Table A-13 shows the model errors for nitrate at Vernalis. The model simulation was very good in 2006, but had large error in 2007.

Table A-13
Model Calibration and Verification Errors of Nitrate at Vernalis

Simulation	Relative Error	Absolute Error
Calibration (2000-2005)	+8%	24%
Verification (2006)	-1%	14%
Verification (2007)	32%	41%

Total Nitrogen

Figure A-9 shows the calibration simulation in blue and the verification in green for total nitrogen at Vernalis. The graph is similar to Figure A-8 of nitrate, since nitrate is the largest component of total nitrogen in the San Joaquin River. The measured data is followed closely by the simulation until summer 2007, when the simulated total nitrogen is significantly higher than the measured data.

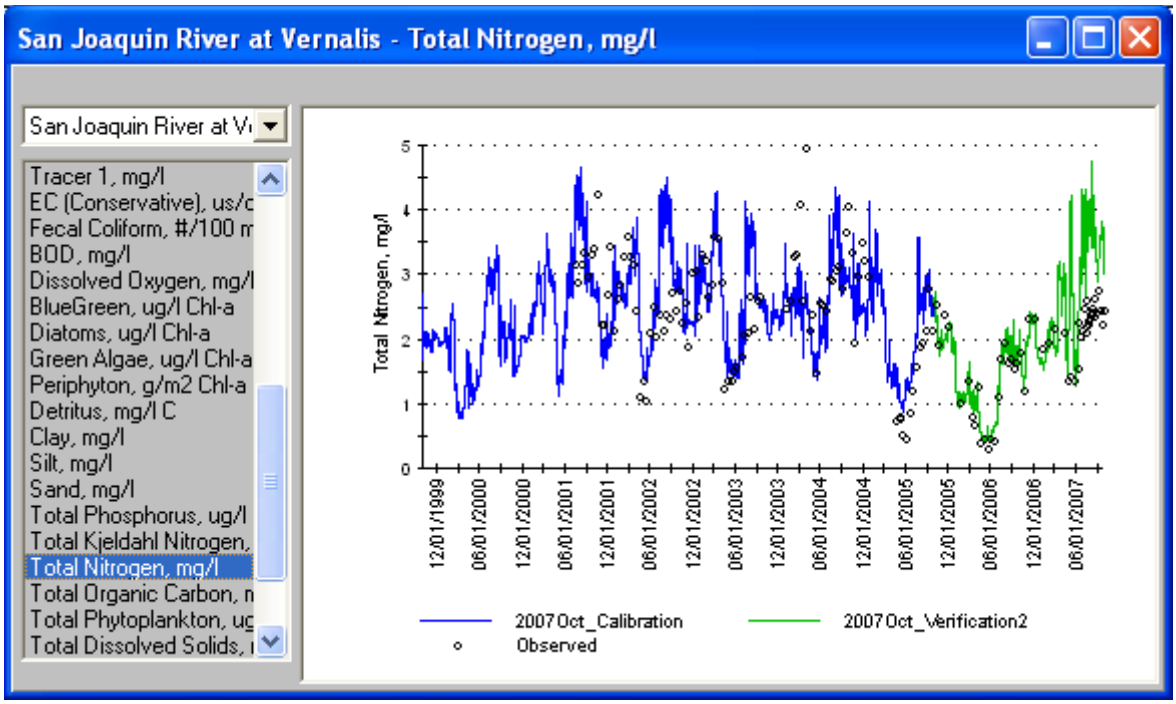

Figure A-9 Simulated vs Observed Total Nitrogen at Vernalis

Table A-14 shows the model errors for total nitrogen at Vernalis. The verification simulation of 2006 closely matches the observed data like in the calibration period. The simulation of 2007 had significant error.

Table A-14
Model Calibration and Verification Errors of Total Nitrogen at Vernalis

Simulation	Relative Error	Absolute Error
Calibration (2000-2005)	+3%	24%
Verification (2006)	+1%	13%
Verification (2007)	+35%	39%

Phosphate

The simulation of phosphate at Vernalis is shown in Figure A-10. The calibration simulation is in blue and the verification simulation is in green. Observed data is shown in black circles. The verification simulation tracks the observed data closely, but with increasing error through the verification simulation period.

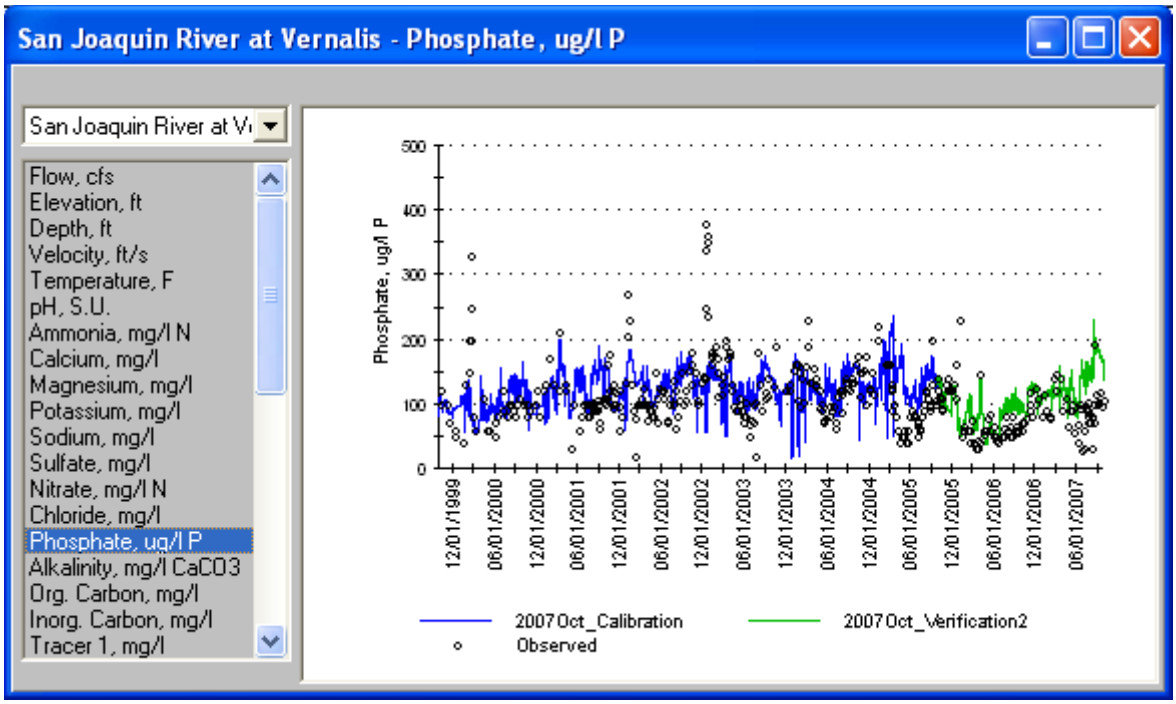

Figure A-10 Simulated vs Observed Phosphate at Vernalis

Table A-15 shows the model errors for phosphate at Vernalis. The model slightly over predicts phosphate concentration in 2006 with a greater error in 2007. A discussion of this error is included in the Total Phosphorus section.

Table A-15
Model Calibration and Verification Errors of Phosphate at Vernalis

Simulation	Relative Error	Absolute Error
Calibration (2000-2005)	+7%	34%
Verification (2006)	+12%	36%
Verification (2007)	+47%	49%

Total Phosphorus

Figure A-11 shows the results of the calibration simulation (blue), the verification (green), and observed data (black circles). The verification simulation is tracking the observed data well, although slightly higher than the observed.

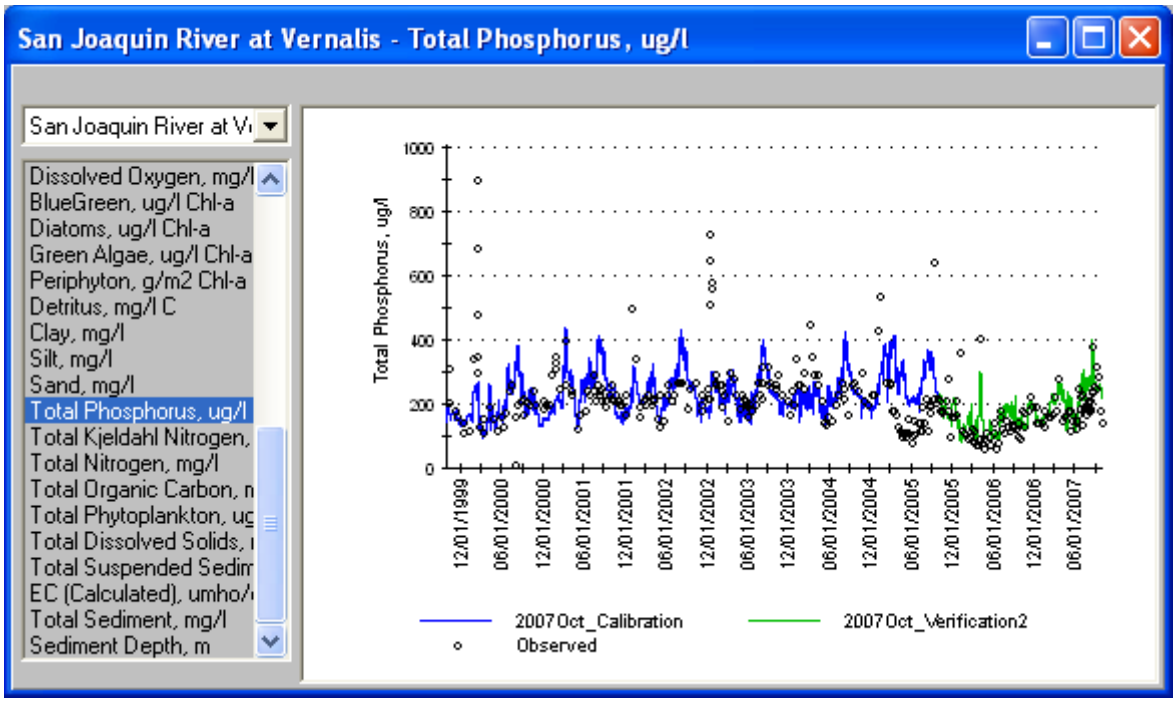

Figure A-11 Simulated vs Observed Total Phosphorus at Vernalis

Table A-16 shows the model errors for total phosphorus at Vernalis. Like phosphate, the total phosphorus simulation predicts too high a concentration in 2007, but unlike phosphate, the absolute error is less than during the calibration period. The problem with the phosphate simulation appears to be largely a matter of simulating the too much dissolved phosphorus in lieu of adsorbed and organic phases. Higher suspended sediment concentrations produce more adsorbed phosphorus, while higher phytoplankton produces more organic phosphorus. The model's under prediction of suspended sediment and phytoplankton is one cause of the prediction of too much dissolved phosphate.

Table A-16
Model Calibration and Verification Errors of Total Phosphorus at Vernalis

Simulation	Relative Error	Absolute Error
Calibration (2000-2005)	+1%	33%
Verification (2006)	+7%	27%
Verification (2007)	+14%	23%

Phytoplankton

The calibration (blue) and verification (green) simulations are shown with observed data (black circles) in Figure A-12. Since 2006 was a high flow year, residence time in the river was low and phytoplankton was not able to grow to its more typical concentration. 2007 was a lower flow year and exhibited high measured phytoplankton concentration. Simulated phytoplankton was significantly lower than observed in 2007.

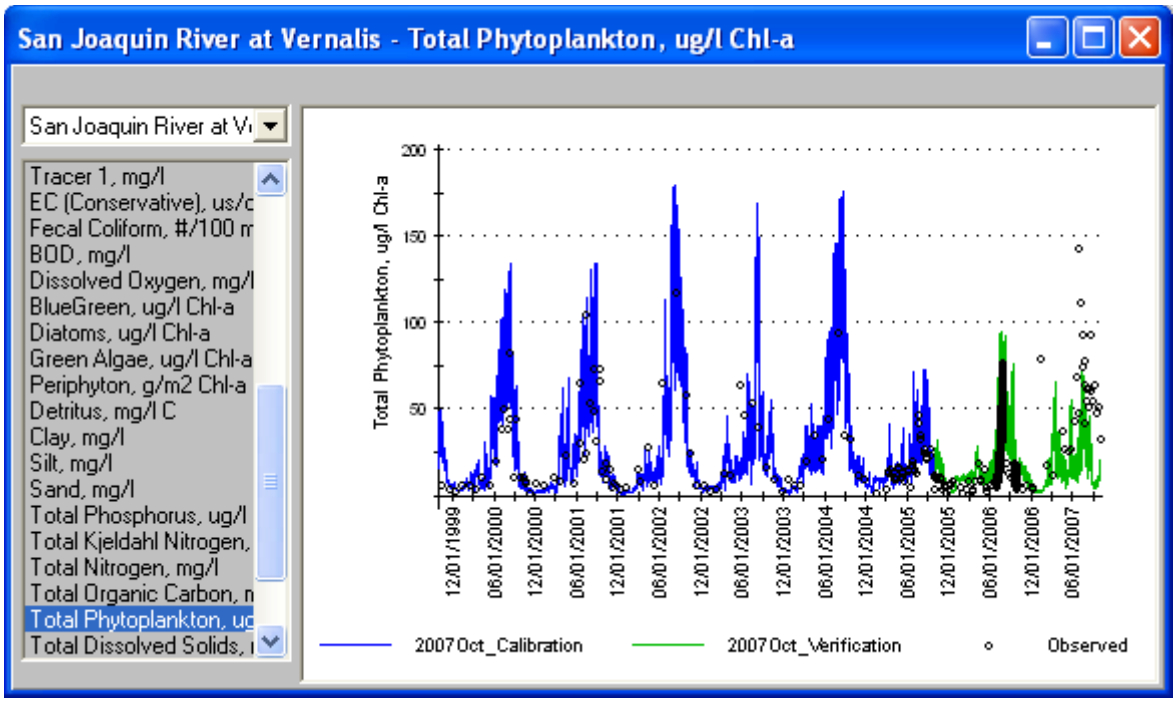

Figure A-12 Simulated vs Observed Phytoplankton at Vernalis

Table A-17 shows the model errors for total phytoplankton at Vernalis. The model over predicted the phytoplankton concentration in 2006, but underpredicted the phytoplankton in 2007. The latter was of greater concern because the low flow years have been more likely to experience low dissolved oxygen in the DWSC in response to organic loading of phytoplankton from upstream.

Table A-17
Model Calibration and Verification Errors of Phytoplankton at Vernalis

Simulation	Relative Error	Absolute Error
Calibration (2000-2005)	+8%	57%
Verification (2006)	+139%	140%
Verification (2007)	-38%	68%

Simulating travel time was very important for simulating phytoplankton since it followed a pattern of unlimited growth. It is particularly important in the upper reaches of the San Joaquin River since low flows can lead to long travel times and increasing phytoplankton biomass. As Figure A-2 indicates, however, the flow was simulated correctly in summer 2007 at Newman, just downstream of the Merced River confluence.

Another possible source of error is model inputs. The loading of phytoplankton seed into the upper reaches of the San Joaquin River comes from the San Joaquin River at Lander Avenue, Salt Slough, Mud Slough, and Merced River. All of those have adequate flow and phytoplankton measurements to produce reasonably accurate time series of phytoplankton load. The load from the San Joaquin River and Mud Slough were unusually low in 2007, but the

measured phytoplankton at Vernalis was similar to other dry years. Since the initial loading of phytoplankton in the upper reaches of the San Joaquin River serves as the seed for growth going downstream, there may be additional phytoplankton loading which is not simulated by the model.

The Salt Slough, Mud Slough, and Los Banos Creek monitoring stations are respectively about 5 miles, 8 miles, and 7 miles from the San Joaquin River. Any phytoplankton growth in those reaches is not currently accounted for in the model. Mud Slough flows into Los Banos Creek about 4 miles upstream of the San Joaquin River. For the sake of discussion, the portion of Los Banos Creek upstream of Mud Slough is considered Upper Los Banos Creek and the portion between Mud Slough and the San Joaquin River is Lower Los Banos Creek.

We can examine the monitoring data and travel times shown for June-September 2007 in Table A-18 to determine if modifications to the model are warranted. The estimate of potential growth assumes the growth rate defined in the model coefficients of 3.2 / day under optimum light, nutrient, and temperature conditions. The respiration rate is 0.15 / day and the mortality is 0.05 / day. Daily calculations from June through September were used to calculate growth under measured water quality.

Table A-18
Phytoplankton Growth Potential in Salt Slough, Mud Slough, and Los Banos Creek
June 1 – September 30 2007

Tributary	Estimated Travel Time, hours	Measured NH_4-N + NO_3-N, mg/l	Measured PO_4-P, µg/l	Average Estimated Potential Growth
Salt Slough	9	0.3 – 3.4	67 - 234	27%
Mud Slough	10	0.5 – 9.3	<5 - 59	11%
Upper Los Banos Creek	11	0.05 – 2.6	113 - 592	32%
Lower Los Banos Creek	7	1.0 – 10.0*	34 – 214*	21%

* Flow weighted average of Mud Slough and Upper Los Banos Creek

In Mud Slough, the dissolved phosphate concentration was often below the detection limit of the water quality monitoring as was thus a limiting nutrient for phytoplankton growth. Below the confluence of Mud Slough and Upper Los Banos Creek, however, there are ample nutrients for growth. The large estimated gain in phytoplankton load from simulating the slough and creek reaches downstream of the monitoring stations justifies making the change in the model.

Dissolved Oxygen

The calibration simulation is shown in blue and the verification simulation in green in Figure A-13. Observed data is shown in black circles. A cursory look at 2006 and 2007 shows that simulated dissolved oxygen was greater than observed in 2006 but less than observed in 2007.

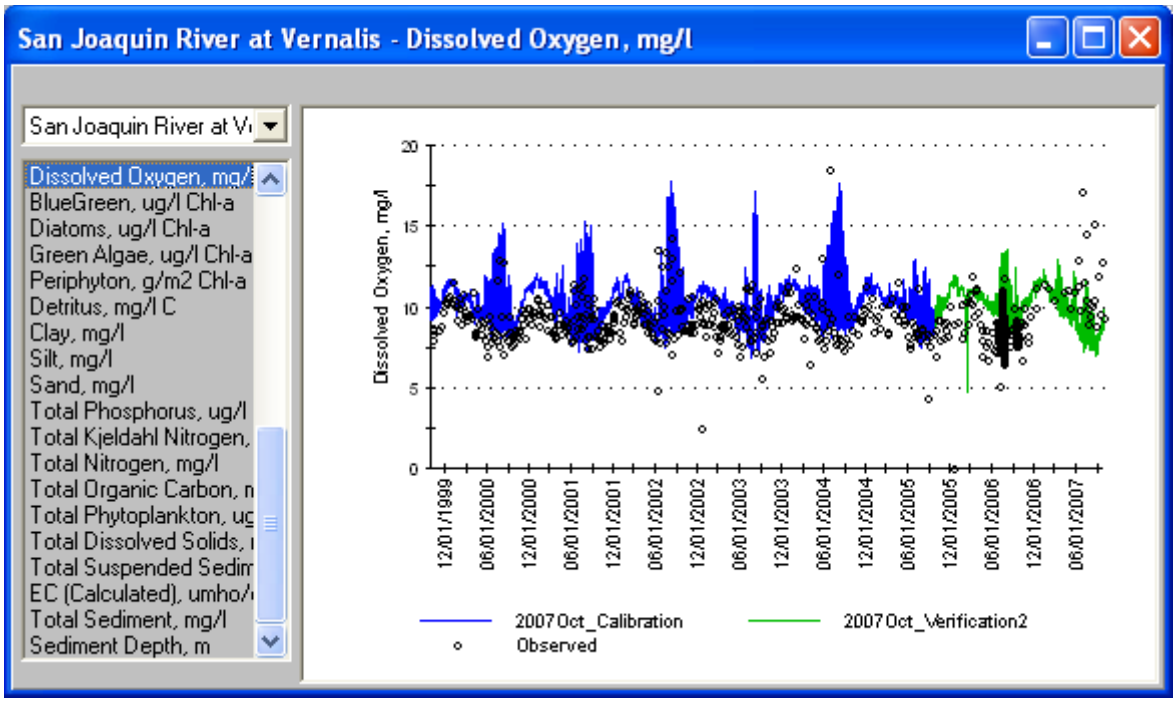

Figure A-13 Simulated vs Observed Dissolved Oxygen at Vernalis

Table A-19 shows the model errors for dissolved oxygen at Vernalis. The errors in both 2006 and 2007 are likely to be related to the model error of phytoplankton (Figure A-12). Since phytoplankton adds dissolved oxygen to the water at Vernalis through photosynthesis, the overprediction of phytoplankton in 2006 and under prediction in 2007 are correlated to the dissolved oxygen errors. Reducing the error in simulated phytoplankton concentration is likely to improve dissolved oxygen simulation.

Table A-19
Model Calibration and Verification Errors of Dissolved Oxygen at Vernalis

Simulation	Relative Error	Absolute Error
Calibration (2000-2005)	+10%	15%
Verification (2006)	+19%	21%
Verification (2007)	-13%	19%

Model Verification Conclusion

The objective of model verification is testing the model on a data set to which it has not been calibrated. If the model performs in a similar manner as its calibration, that adds confidence that the model will perform well when simulating different management options than actually occurred. The model verification is limited by the completeness of the data sets used to drive the model and evaluate its calibration.

The performance of the verification simulation matched that of the calibration for flow, temperature, suspended sediment, and total phosphorus. For water year 2006, the verification simulation of EC, phytoplankton, and dissolved oxygen exhibited greater error than during the calibration simulation. In 2007, the errors of ammonia, nitrate, total nitrogen, and phosphate were also in excess of the calibration error.

The data set for 2007 must be completed with the Merced River near Stevinson gaging data and diversion data for Patterson, El Solyo, and Banta-Carbona Irrigation Districts. Using the correct data rather than estimates may reduce model errors without otherwise changing the model. Since the phytoplankton measured at Salt Slough, Mud Slough, and Los Banos Creek probably undergoes significant growth before entering the San Joaquin River, the model domain will be expanded to include the reaches of those tributaries downstream of the monitoring stations. With those changes, the model is expected to provide more accurate results for nutrients, phytoplankton, and dissolved oxygen for simulations of 2006-2007.

The changes recommended to correct errors in the validation will also improve the performance of the model for performing simulations of proposed watershed management actions. These actions could include recycling of water from the Delta-Mendota Canal through the Newman Wasteway, reuse of irrigation water in the grasslands area to reduce pollutant loads in Mud and Salt Sloughs, and the addition of flow past the San Joaquin at Lander Avenue in accordance with the settlement agreement to restore continuous flow from Friant Dam to the Delta. The model simulations of these actions will provide guidance to stakeholders to determine those methods most likely to succeed at acceptable cost.

APPENDIX B: RESPONSE TO PEER REVIEW

Introduction

The San Joaquin River Group Authority asked Flow Science Incorporated to perform a review of the application of the WARMF watershed modeling framework to the San Joaquin River. The review (List and Paulsen 2008) performed by Susan Paulsen and Aaron Mead was based on the watershed model and documentation made available to San Joaquin River stakeholders. As investigators collecting data for the San Joaquin River and applying a watershed model based on that data, we welcomed feedback from individuals independent of the project. Scientific review strengthened the quality and utility of the work we were performing and introduced new information about which the investigators may not have been aware. Although a typical scientific peer review involves a panel of investigators from various backgrounds, we accepted the work done by Flow Science as an attempt to address the modeling from a broad-based perspective. It is in that spirit of scientific exchange that we composed this response to the draft of the review released in 2007.

This response directly addresses the issues raised by the review. Our primary concerns in data collection and modeling were the accurate simulation of those water quality parameters of greatest concern in the San Joaquin River: flow, electrical conductivity (as a measure of salinity), and phytoplankton. In addressing the comments in the review, our responses are in the context of the model's performance in simulating these parameters.

Responses to Specific Review Comments

The Flow Science review was divided into Summary and Review Comments sections. The summary section of the review discussed the purpose and scope of the San Joaquin River modeling. There was a detailed description of the modeling domains of WARMF, which simulated the San Joaquin River upstream of the Old River, and Link-Node, which simulated the tidal portion of the San Joaquin River through the Deep Water Ship Channel. We had no disagreement with the description of the two models, but we noted that the modeling effort at the time of the review was contractually focused on the WARMF model domain upstream of the Old River. Although WARMF was linked with the pre-existing Link-Node model, the latter model had not been substantially updated as part of this project at that time.

The review described the San Joaquin River modeling as "an extremely ambitious project" because of the complexity of simulating biochemical processes. Indeed, the interactions between light, nutrients, flow, and phytoplankton were complex but WARMF was chosen to model the San Joaquin River in part because it simulated those processes contributing to phytoplankton growth as they are understood by science. There were many coefficients involved in the

simulation, but the equations which describe phytoplankton growth were designed to work under many different conditions of flow and water quality. Under the specific conditions of the San Joaquin River, many of these coefficients did not strongly affect the simulated phytoplankton concentration, reducing the practical impact of uncertainty in certain model coefficients.

Review Comment 1

The review noted that difference between simulated and measured flow at the Patterson gage was greater than at other gages and further study of the discrepancy was warranted. In response to this discrepancy, the gage site at Patterson was studied. It was determined that the gage was not accurate at low flows. For this reason, this gage is not suitable for evaluating model calibration at this time.

The review discussed the dye studies performed in 1994 which the model attempted to duplicate to assess whether the simulated travel time was reasonable under two different flow regimes. The dye study was performed before the time period for which a complete dataset is available to drive model simulations, but since no other dye study had been conducted WARMF was run under similar flow regimes to those which occurred during the dye studies.

It is important to note that the river flows simulated by WARMF for comparison to the dye studies were not identical to flow during the dye studies. Table 4-3 of the WARMF Calibration Report (Systech 2006) compares the flows of the San Joaquin River at Vernalis, Stanislaus River at Ripon, Tuolumne River at Modesto, Merced River near Stevinson, and San Joaquin River at Lander Avenue. As indicated in Table B-20, although the net flow rate at Vernalis was similar between the dye study tests and the comparison simulations, there were large differences in flow rate of the major tributaries between the dye study time periods and the comparison time periods. The difference in flow coming from the upstream San Joaquin River at Lander Avenue was unknown because it was not measured in 1994. Because the simulated travel time from Salt Slough to Vernalis was sensitive to the flow rate along the river, the simulated travel time for the comparison periods should not be expected to precisely match the measured travel times of the dye study.

Table B-20
Difference of flows used for comparison with 1994 dye study and simulated travel time differences

	High Flow Comparison	Low Flow Comparison
Comparison	Flow, 8/1/2005 vs. 2/9/1994	Flow, 8/1/2004 vs. 6/20/1994
Flow, SJR at Lander Ave	Not measured in 1994	Not measured in 1994
Flow, Merced River near Stevinson	-32%	-42%
Flow, Tuolumne River at Modesto	+24%	+107%
Flow, Stanislaus River at Ripon	-26%	-30%
Flow, SJR at Vernalis	-0.4%	-7%
Total Travel Time	-18%	-3%

Since the difference in tributary flows had an unknown effect on the test results, a reasonable measure for this test is whether the difference in travel time is within the difference in tributary flows. As Table B-20 shows, the discrepancy between the simulated travel time and that in the dye study is small compared to the discrepancies between flows used for the simulation and those which occurred during the dye study. The low flow travel time difference of -18% was well within the -32% to +24% differences in tributary flows; the high flow travel time difference of -3% was also within the tributary flow differences of -42% to +107%. Because of this, we do not believe this comparison with the dye study provided a basis for the review's comment that "the model predicts significantly lower travel times (i.e., higher river velocities) than are indicated by field data".

The DSM2 model of the San Joaquin River was also tested against the dye study experiment. Initially, the DSM2 simulated travel times were 32% and 43% higher for the high flow and low flow conditions respectively. The cross-section geometry in DSM2 was then modified so that its travel times were 11% and 19% greater than field data, but further improvement was not practical. (DWR 2005)

We agreed with the recommendation of the review that new dye studies should be conducted, as this will provide a much stronger basis upon which to evaluate the simulated travel time.

The review indicated that there was an error in the calculation of percentiles in Table 4-1 of the WARMF Calibration Report. The percentile values for 2003 and 2004 were reversed. A corrected table with incorrect values struck out is shown below in Table B-21 and in Table 1.5 of the main body of this report.

Table B-21 (Corrected version of WARMF Calibration Report Table 4-1)
Average Annual Flows at Vernalis for Water Years 2000 to 2005

Water Year	Average Flow at Vernalis, cfs	Percentile (based on 1984-2005)
2000	3,920	62
2001	2,390	48
2002	1,930	38
2003	1,920	~~29~~33
2004	1,890	~~33~~29
2005	5,230	71

The review noted that only the Modesto meteorology station had been used for the watershed. After the calibration report was written, two additional meteorology stations were added, Manteca and Los Banos. Both have hourly data like the Modesto station. Over the simulation time period, the Manteca station has 23% more precipitation than Modesto; Los Banos has 14% less. The precipitation multipliers were used to adjust the precipitation falling on each catchment so that there was an even gradation of precipitation between meteorology stations.

Review Comment 2

The review comment questioned whether the kinematic wave approximation for routing flow was appropriate for the San Joaquin River given the results of the travel time comparison. As mentioned above, the travel time comparison described in the WARMF Calibration Report did not indicate a deficiency in the ability of the model to predict travel time given the large uncertainties in the test. The choice of a routing method used by a model matters most when the flow is rapidly changing. Since the critical time period for water quality in the San Joaquin River is during the dry season when flow does not change rapidly, there is less reason for concern that the kinematic wave approximation does not simulate travel time accurately. More complex routing mechanisms have drawbacks in increased simulation time and the potential for numerical instability.

Review Comment 3

The review noted the systematic underprediction of temperature as reported in the WARMF Calibration Report, and asked whether the error in temperature could effect water quality calibration since reaction rates are a function of temperature. WARMF used temperature correction in most chemical reactions as shown below, where C is concentration, K is the reaction rate at 20 ^{o}C, T is the temperature in ^{o}C, and θ is the temperature correction factor:

$$\frac{dC}{dt} = \theta^{(T-20)} KC$$

If the systematic temperature simulation error of the model is E, propagation of that error into reaction rate will produce an error in the reaction rate of θ^{E}. For the highest θ used in the San Joaquin River application of 1.083, the systematic error of 0.8 ^{o}C will cause an error in simulated reaction rate of -7%. Since reaction rates are calibration parameters, the model's representation of reaction rate K could be up to 7% higher than would be measured. The phytoplankton growth rate is modified using a triangular distribution. As applied to the San Joaquin River, the systematic temperature error could propagate into a phytoplankton growth rate error between -3% and +7%.

In response to the review, the temperature algorithms used in WARMF were upgraded to incorporate the effects of short wave radiation, long wave radiation, and evaporation upon the temperature. The changes reduced the error of the simulations.

Review Comment 4

The review stated, "the model is unable to consistently reproduce measured suspended sediment concentrations." The WARMF Calibration Report acknowledged that the model predicted peak concentrations of sediment not observed in measured data. If the objective of the modeling were to simulate annual sediment transport, this would be a critical issue. However, given the objectives of the modeling to simulate flow, EC, and phytoplankton, sediment simulation was most important for calculating light penetration into the river and adsorbed nutrient transport.

Since nutrients were in excess, the transport of adsorbed nutrients was not expected to be important with respect to phytoplankton concentration. To test the importance of sediment on light penetration and phytoplankton growth, the model was run with double the sediment load to determine the sensitivity of phytoplankton to sediment concentration. The results, shown starting on page 6-7 of the WARMF Calibration Report, indicated that phytoplankton was very insensitive to sediment concentration.

Review Comment 5

The sensitivity analysis of sediment loading performed in the WARMF Calibration Report addressed this comment that errors in simulation of sediment will propagate errors in other chemical constituents. Details of model coefficient values are listed in Appendix A of this report.

Review Comment 6

This comment noted the errors in model simulation at the Mossdale, at the downstream end of the WARMF simulation. The errors at Mossdale were generally greater than at Vernalis. A significant problem related to calibration at Mossdale was the assumption that there is unidirectional flow at that location. However, during low flow there are known to be tidal effects at the Mossdale monitoring station. The best solution would be to extend the domain of the Link-Node estuary model upstream to encompass the entire area of tidal influence. The domain of the WARMF model could then be restricted to the truly riverine sections of the San Joaquin River. Funding and contractual constraints did not allowed for extention of the Link-Node model, so the WARMF model domain boundary was set at the Old River. It would be desirable to modify the models' domains in the future if funding were available.

Review Comment 7

This comments noted the non-conservative EC simulated by WARMF is higher than observed EC at the Stevinson boundary condition in the very wet winter of 2004-2005 and suggested improving TSS predictions to correct the error. Non-conservative EC is calculated as the sum of dissolved cations and anions, and thus is not dependent upon the TSS concentration. It is believed that non-conservative EC averages higher than the conservative EC in simulation results because the model overestimated the pH and inorganic carbon concentration in the river. Although the model's calculations of non-conservative EC were included in simulation output and reports, the conservative EC is being used for decisions based upon model simulations. Conservative EC is simpler to apply (as it requires only EC data for model inputs) and does not incorporate uncertainties associated with individual ions into simulation results.

Review Comment 8

This comment noted the errors in ammonia identification identified in the WARMF Calibration Report. The report hypothesized that systematic disagreement between simulation results and observed data could be explained by phytoplankton respiration after sample collection, and the

review found this explanation to be plausible. Given the high nitrate concentration, however, it should be noted there was excess nitrogen for phytoplankton growth regardless of the cause of the discrepancy between simulated and observed ammonia concentrations.

Review Comment 9

This comment noted that the total nitrogen concentrations were well-correlated with measured values for stations other than Mossdale, while nitrate concentrations were close to observed values at all locations. As mentioned above, the assumption of unidirectional flow at Mossdale does not necessarily hold during low flow and could introduce simulation errors at Mossdale. Regardless, the model predictions of nitrogen indicated nutrient concentration well in excess of that needed for optimum phytoplankton growth.

Review Comment 10

The review comment stated "The WARMF model appears to consistently underpredict both phosphate and total phosphorus, especially peak concentrations." Although phosphate concentrations were generally underestimated by the model, Table 4-19 of the WARMF Calibration Report showed total phosphorus concentrations overestimated at Patterson and Maze Road, underestimated at Mossdale, and within 5% on average at Crows Landing and Vernalis. Like nitrogen, however, phosphorus was well in excess of concentrations which would limit phytoplankton growth.

Review Comment 11

The review states "Phytoplankton concentrations are predicted with a surprising degree of accuracy." Model simulations showed the phytoplankton growth to be largely unlimited, which made the simulations relatively insensitive to some processes which might be more important in other areas. We agreed with the review that 24 hour continuous sampling of phytoplankton would be valuable in learning more about diurnal cycles. Continuous monitoring of phytoplankton was preformed at several locations on the San Joaquin River in 2007.

Review Comments 12 and 13

Simulated and observed dissolved oxygen is discussed in these review comments. Model predictions were more accurate at some stations than at others, and predictions of the Link-Node model at Buckley Cove in the DWSC did not appear to be very sensitive to dissolved concentration at Mossdale. An examination of the transformations of dissolved oxygen within the Link-Node model had not been performed as of the time of the review.

Review Comment 14

We agreed with the review comment that phytoplankton growth did not appear to be sensitive to nutrient concentrations.

Review Comment 15

The review noted the limitation that comes with using the flow measured at Stockton as a model input for the Link-Node model. This was done because of the flow split which occurs at the Old River. In particular, this made it difficult to simulate the effect on the DWSC resulting from significant flow changes in the San Joaquin River. This is an important point to consider, and we agreed with the recommendation that the effect of significant changes in flow in the San Joaquin River should be taken into account when using the Link-Node model to simulate the DWSC. Although modifications of the flow regime of the Link-Node model were not made under this contract, this would be worth considering for future work.

Review Comment 16

The review comment stated, "this modeling effort represents an extremely ambitious undertaking, and one that is hampered by the lack of available field data for calibration and verification." Although additional data collection was always desirable, and a dye study in particular is recommended, the dataset for the San Joaquin River was quite extensive and lended considerable support to the modeling effort. The data included regular measurements of many parameters under different hydrologic regimes which provided good constraints for the WARMF model. Although the model could always be improved through additional data collection and calibration, we believed that the WARMF model is mature and ready to be used for its intended purposes: simulation of flow, EC, and phytoplankton.

Task 6-supplemental

DO TMDL Project
Draft Final Report 2008

2-D MODEL OF ALGAE FATE AND TRANSPORT BASED ON DYE TRACER STUDIES

Nigel W.T. Quinn, PhD, P.E.
Berkeley National Laboratory
1 Cyclotron Road, Bld 70A-3317H
Berkeley, CA 94720

Thomas Heinzer and Diane Williams
MPGIS, US Bureau of Reclamation/
Michael-Thomas Group
2800 Cottage Way
Sacramento, CA 95825

Søren Tjerry
DHI Water & Environment
319 SW Washington Street, Suite 614
Portland, OR 97204

Gary M. Litton, PhD, P.E.
School of Engineering
University of the Pacific
3601 Pacific Avenue
Stockton, CA 95211

Mark S. Brunell, PhD
School of Biology
University of the Pacific
3601 Pacific Avenue
Stockton, CA 95211

Abstract

During late summer of 2005 through 2007 dye tracer studies were conducted in conjunction with a Lagrangian algal fate study to improve understanding of algal dynamics between Vernalis and the Deep Water Ship Channel. Previous studies had shown a reduction in algal bimass in this reach of the river which was not explained by the flow bifurcation at Old River or by riparian diversions from the river at Banta Carbona Irrigation District or the private pumping stations along the river serving delta agriculture. The dye study was conducted in both Lagrangian and Eulerian modes – the Lagrangian study followed the peak dye concentration as it moved downstream in a moving boat that was fitted with instruments capable of simultaneous GPS positioning and real-time dye measurement – the Eulerian study was conducted from a boat moored at a fixed location that measured the dye pulse as it swept past. A hand-held instrument capable of simultaneously recording dye concentration and GPS coordinates was used to analyze the dye pulse as it was carried past the boat downstream. Dye trace profiles were plotted and qualitative descriptions of the longitudinal dispersion of the dye trace were obtained. In order to improve the simulation of algae dynamics in the reach between Vernalis and the Deep Water Ship Channel (especially the transition zone in the vicinity of Mossdale where the river becomes influenced by tidal dynamics and algae experience flow reversal accompanied by periods of quiescence as the flood tide transitions into an ebb tide) a more detailed dynamic model of the river reach was sought. A simple plug flow model was developed in MATLAB by Gary Litton, which was able to simulate the celerity of the dye pulse reasonably well. However to develop and understanding of the influence of river morphology on conservative dye transport and retardation - a two dimensional hydrodynamic flow model has been developed to account for such phenomena as eddying, which is caused by river sinuosity and that is a primary causal factor in longitudinal dispersion of both dye and algae in the River. After reviewing several candidate models – the new curvilinear version of the Danish Hydrologic Institute's Mike 21c code was chosen to perform the model simulations. This computer code has been used by many years by restoration scientists and engineers, has good user interfaces and contains a powerful visualization tool box that allows effective communication of results. This final report describes the development of the model, use of GIS to visualize the river bathymetry and the simulation experiments performed to date.

Introduction

Algal dynamics in a riverine system are complex, especially in a river such as the San Joaquin where the river transitions from a levee-constrained flow regime, in its middle reaches, to a tidally-dominated river as it enters the Delta (Lee and Lee; 2000, Chen and Tsai, 2002). The transition point location is dynamic and is affected primarily by flow volumes in the San Joaquin River and the amplitude of the ocean tides expressed at the Golden Gate Bridge. Flow volumes is the San Joaquin River are also highly dynamic – river diversions made by local water districts and unincorporated riparian diverters can change instream flow quite dramatically, especially in dry and critically dry years where River flow at Vernalis can be substantially below 1000 cfs and the largest four riparian diverters (including Banta Carbona Irrigation District located downstream of Vernalis) have the capability of removing flows in excess of 700 cfs from the River. (Kratzer et al., 1987). Irrigation return flows, rainfall runoff and wastewater treatment

plant discharges that flow into the River are also dynamic but do not typically account for flow variations that are as dramatic as the stopping and starting of pumped diversions. Simulation of water quality in the San Joaquin River system is even more complicated given the large number of discharge points along the river and the highly variable water quality discharged at each of these locations (Kratzer et al, 1987; Kratzer et al., 2004; Pate, 2001; Wilde, 2005). Each of these point source discharges as drainage collectors for large diverse watersheds. The salinity, nutrient and sediment content of these discharges is influenced by local soil conservation and water management practices (Kratzer et al., 2004). Since the modeling of algal dynamics is at the core of this study and many of the other upstream studies – it is clear than any realistic algae growth and decay model will first need to provide a realistic simulation of flow and water quality (Brown and Huber, 2004; Herr and Chen, 2006). The reach of the San Joaquin River between Vernalis and the Stockton Deep Water Ship Channel differs from the reaches upstream in that, with the exception of Banta Carbona Irrigation District, water returned to the river is derived from water diverted from the same source. Banta Carbona Irrigation District receives a portion of the annual water supply from the Delta Mendota Canal. The reach also passes through heavily urbanized areas – return flows from urban areas have a much different chemical signature than those return flows from irrigated lands. The reach between Vernalis and the Stockton Deep Water Ship Channel has significant sinuosity – tracking algal biomass between these points requires an understanding of how river morphology affects longitudinal dispersion. The Rhodamine dye trace studies conducted by the study team during 2005, 2006 and 2007 provide data on hydrodynamic longitudinal dispersion during the 3-5 day duration of each experiment. These data are used to evaluate the validity and future potential of a simulation model of flow and mass transport.

Hydrodynamic transport

Hydrodynamic turbulent mixing in rivers and streams has been studied for more than a century – the fundamental theory derives from Fourier's law of heat flow (1822) and Fick's (1855) concepts of molecular diffusion in fluids. These conceptual models relate the mass flux of a solute with the concentration gradient. Classical texts such as Carslaw and Jaeger (1959) provide solutions to many classical heat flow problems that involve molecular diffusion that are direct analogs of turbulent mixing in rivers. Under certain conditions "Fickian" turbulent mixing theory can be used to describe the mixing phenomena in rivers. Taylor (1953, 1954) developed the theory relating the spread of dissolved contaminants in laminar and turbulent flows to velocity gradients in the flow domain. He referred to flows where velocity gradients were present as "shear flows" and the mechanism of induced mixing and the "shear effect". The theory of shear flow dispersion is the most helpful in understanding the mechanics of longitudinal dispersion in rivers. Fischer et al. (1979) introduced the concept of "scales of turbulence" as a means of explaining how the velocity of a moving fluid varies in both space and time as a result of strong non-linearities in fluid motion – especially at large Reynold's numbers (the Reynolds number is a ratio of the inertial to the viscous forces in a fluid which is either laminar or turbulent). The effect of these non-linearities is to "spread the kinetic energy of the fluid motion over a range of eddy sizes through the interaction of the large and smaller scales of motion" (Fisher et al, 1979).

Fischer et al (1979) found it useful to describe turbulent mixing mathematically using the

diffusion equation together with a turbulent mixing coefficient in place of the molecular diffusion coefficient typical of Fickian mixing. Under ideal conditions of a straight channel of constant depth and large width (sufficient to minimize the shear induced by sidewalls) a cloud of tracer would grow until it filled the depth of the channel and then would continue to grow in volume in the directions of both length and breadth. The phenomenon of turbulent mixing can be described mathematically as a product of the Lagrangian length scale (a measurement of the distance a particle must travel before it forgets its initial velocity) and the intensity of the turbulence according to the following expression (Fischer et al., 1979):

$$\varepsilon_x = l_L [< U^2 >]^{½} \qquad [1]$$

Where : e_x = turbulent mixing coefficient
l_L = depth of flow
U = velocity of a particle

Experiments conducted by Laufer (1950) and other researchers have suggested that turbulence intensity on any flow contained by channel boundary (walls) is directly proportional to the shear stress imposed on the channel walls. Shear velocity is related to shear stress and fluid density by the relationship :

$$u^* = [\tau_o/\rho]^{1/2} \qquad [2]$$

Where : u^* = shear velocity
τ_o = shear stress
ρ = density of the fluid

For uniform open channels shear stress is calculated by a force balance according to the equation:

$$u^* = [gdS]^{½} \qquad [3]$$

Where : u^* = shear velocity
g = acceleration due to gravity
d = channel depth
S = channel bed slope

Channel mixing

Empirical studies of open channel flow by a number of investigators including Elder (1959), Jobson and Sayre (1970) and Csanady (1973) suggest developing separate mixing coefficients for vertical, transverse and longitudinal mixing. Breaking down these components of mixing can help develop generic functions that can be applied to rivers of various configurations.

Vertical mixing coefficients can be derived from the theoretical velocity profiles for the channel.. Theoretical velocity profiles show increased velocity with height above the bed – the boundary

layer next to the bed being the zone of greatest shear stress. Elder (1959) obtained the following equation for the vertical mixing coefficient ε_v based on an arithmetic law velocity profile :

$$\varepsilon_v = \kappa d u^*(z/d)[1 - (z/d)]$$

Where :
ε_v = vertical mixing coefficient
u^* = shear velocity
d = channel depth
z = vertical depth increment
κ = coefficient

Since there is no direct analog of the vertical mixing profile for transverse mixing – transverse mixing coefficients must be derived empirically. There is a large literature of transverse mixing experiments being conducted in regular irrigation canals and channels. Fischer et al. (1979) reviewed experiments by Lau and Krishnappan (1977) and Okoye (1970) which suggested a wide range of empirical values that could be approximated by the general expression :

$$\varepsilon_t \sim= 0.15\, d u^*$$

Where :
ε_t = transverse mixing coefficient
u^* = shear velocity
d = channel depth

Longitudinal mixing is considered by Fischer et al. (1979) to occur at about the same rate as transverse mixing in cases, where boundaries do not artificially restrict spreading. However some researchers, such as Sayre and Chang (1968), found that longitudinal mixing and spreading of polystyrene particles was as high as three times that of transverse spreading. Fischer et al. (1979), Aris (1956) and Elder (1959) discount the impact of turbulent eddies in causing longitudinal mixing and considers the shear flow dispersion coefficient caused by the velocity gradient to be much larger in value than the mixing coefficient due to turbulence. Elder (1959) suggested that the dispersion coefficient in a logarithmic velocity profile could be described as follows :

$$K = 5.93\, d u^*$$

Where :
K = dispersion coefficient
u^* = shear velocity
d = channel depth

The value of K in this relationship is approximately 40 times the expected magnitude of the turbulent mixing coefficient. Aris (1956) maintained that turbulent and shear mixing effects were additive and they dominating any effects due to longitudinal turbulent mixing alone. Fischer et al (1979) acknowledged that it is difficult to separate the mixing effects due to longitudinal turbulence and those due to shear forces alone in river dye experiments.

Channel curvature

Natural channels are rarely regular in cross section and in rivers such as the San Joaquin – channels are characterized by sharp bends, large sidewall irregularities such as groins and irregular depth profiles. Channel irregularities typically do not have much effect on vertical mixing – this has been verified empirically in flume experiments. However transverse and longitudinal mixing, are strongly affected by bends and sidewall irregularities. In general the greater the scale of the sidewall irregularity the faster the rate of transverse mixing. River studies by Holley and Abraham (1973), Jackman and Yotsukura (1977) and Mackay (1970), that were reviewed by Fisher et al. (1979), show values of $\varepsilon_t / d u^*$ in the range of 0.4 to 0.8 – when flow rounds a bend. In this case, the centrifugal forces induced by the flow tend to direct the flow towards the outside bank at the river surface – this is compensated by a reverse flow near the bottom of the river channel which induces transverse mixing to occur.

Although Elder's empirical analysis was found to work for transverse dispersion in real streams it was found to underpredict the rate of longitudinal dispersion (Fischer et al.,1979). Godfrey and Frederick (1970) and Yotsukura et al. (1970), whose work was summarized by Fischer et al. (1979), found values of $K / d u^*$ that ranged from 140 to over 7500 (in the instance of Yotsukura et al.'s study) – these are consistently higher than the values obtained by Elder (1959). Fischer et al.'s (1990) explanation for the wide range of values is that Elder didn't fully appreciate the fact that velocity varies across a typical stream – the profile used in Elder's analysis extended only over the depth of flow (d). Fischer et al. (1979) suggested that since the longitudinal dispersion coefficient is typically proportional to the square of the distance over which the shear flow profile extends. Given the typical cross-sectional topology of the San Joaquin River it follows that longitudinal dispersion is dominated (two orders of magnitude) by transverse mixing than by vertical mixing. The width to depth ratios of the San Joaquin River is generally greater than 10.

In the San Joaquin River, deep holes in the river channel up to 40 ft in depth, which typically occur immediately downstream of regions of constricted flow, can cause significant retardation of the dye and contribute to longitudinal dispersion. These deep holes in the River bed are sufficiently large to induce localized eddies as the River passes over the top of them. Although the vertical mixing may not be as important in causing dye retardation – having the dye trapped within a large eddy could induce greater shear flow than might otherwise occur – resulting in much more significant dye retardation than due to vertical mixing alone. Two dimensional modeling of the San Joaquin River is justified based on the fact that it has the ability to simulate the occurrence of shearing forces that appear to affect dye mixing and hence the degree of longitudinal dispersion. Although, modeling the River in three dimensions would provide even more information, this approach is computationally intense and beyond the scope of the current study.

Modeling Objectives

A number of candidate one-dimensional and two dimensional numerical model codes were considered for simulating dye dispersion within the San Joaquin River between the stations at Vernalis and Channel Point. The goal of the modeling effort is to improve the understanding of algae biomass fate and transport between the Vernalis monitoring station (the most downstream station not subject to tidal influence) and the Stockton Deep Water Ship Channel. Previous

monitoring studies provided evidence of a reduction in algal biomass within this reach of the San Joaquin River that could not be explained by River hydrology. The series of dye tracer experiments conducted by Gary Litton (team leader), Nigel Quinn and Mark Brunell over the three years of the project between 2005 and 2008 were designed to monitor the fate of a unit volume of water containing algae biomass (represented by the peak dye concentration) as it was conveyed along the River and into the Deep Water Ship Channel. A two dimensional hydrodynamic simulation model has been developed using Mike 21c, a state-of-the-art, curvilinear version of the Danish Hydrologic Institute's Mike 21 code, to simulate transport of the Rhodamine dye tracer. The rationale for this modeling approach is that accurate simulation of the transport of a conservative substance such as Rhodamine would provide greater assurance that the model was capable of simulating algae fate and transport. Without this proof of concept it is possible that algae losses in the system could be ascribed to the coefficients chosen for algae growth and decay. The Mike 21-c curvilinear model mesh allows the alignment of the computational model finite difference cells (elements) with the tortuosity of the river. This is a major advantage in the numerical simulation of dye dispersion and is more computationally stable than more traditional finite difference approaches that apply a regular grid mesh to the region containing the river.

Developing a computationally efficient and accurate curvilinear grid is difficult - the quality of the grid generation affects the performance of the model. Model accuracy is reduced when grid cells are not orthogonal or when the difference in cell sizes of adjacent cells is too great – accuracy is also compromised when grid cells are not aligned sufficiently closely to river bed contours to accurately describe river bathymetry. Bifurcations, branches, confluences and major diversion points have to be simulated as separate grids which are finally merged into the master model grid using a stepwise fitting algorithm that is included in the Mike 21c software. The tolerance between grid points at the merging boundary can be specified in the software. There is also a grid update option which applies smoothing algorithms to the model mesh – improving model orthogonality up to the point where it starts over-smoothing and distorting the mesh. This process is as much art as science.

The first phase of the project concentrated on developing an accurate and computationally efficient model mesh for the San Joaquin River between monitoring stations at Vernalis and at Rough and Ready Island (east of Burns Cut). Initial grid development required that the bounds of the model be defined prior to invoking the Mike 21c curvilinear grid generator. Digital imagery of the San Joaquin River between Vernalis and the Deep Water Ship Canal at Rough and Ready island was imported into ESRI's ArcMap software. The San Joaquin River cross-sectional profile was defined using the River levees – the slope break point along each levee, where the top of the levee and the levee banks join (on the river-side of each levee) determined the left and right banks. Defining the river boundaries required creating a photo-mosaic of almost 30 scenes – GIS line boundaries had to be edge patched to ensure that the final model domain was a closed polygon.

The second step was to determine a suitable mesh interval for the River cross-section. Having grid cells that are too widely spaced defining the River cross-section may fail to accurately simulate the River cross-sectional area along its length. Grid cells that are too small can significantly increase computation time and cause numerical dispersion errors if the width to

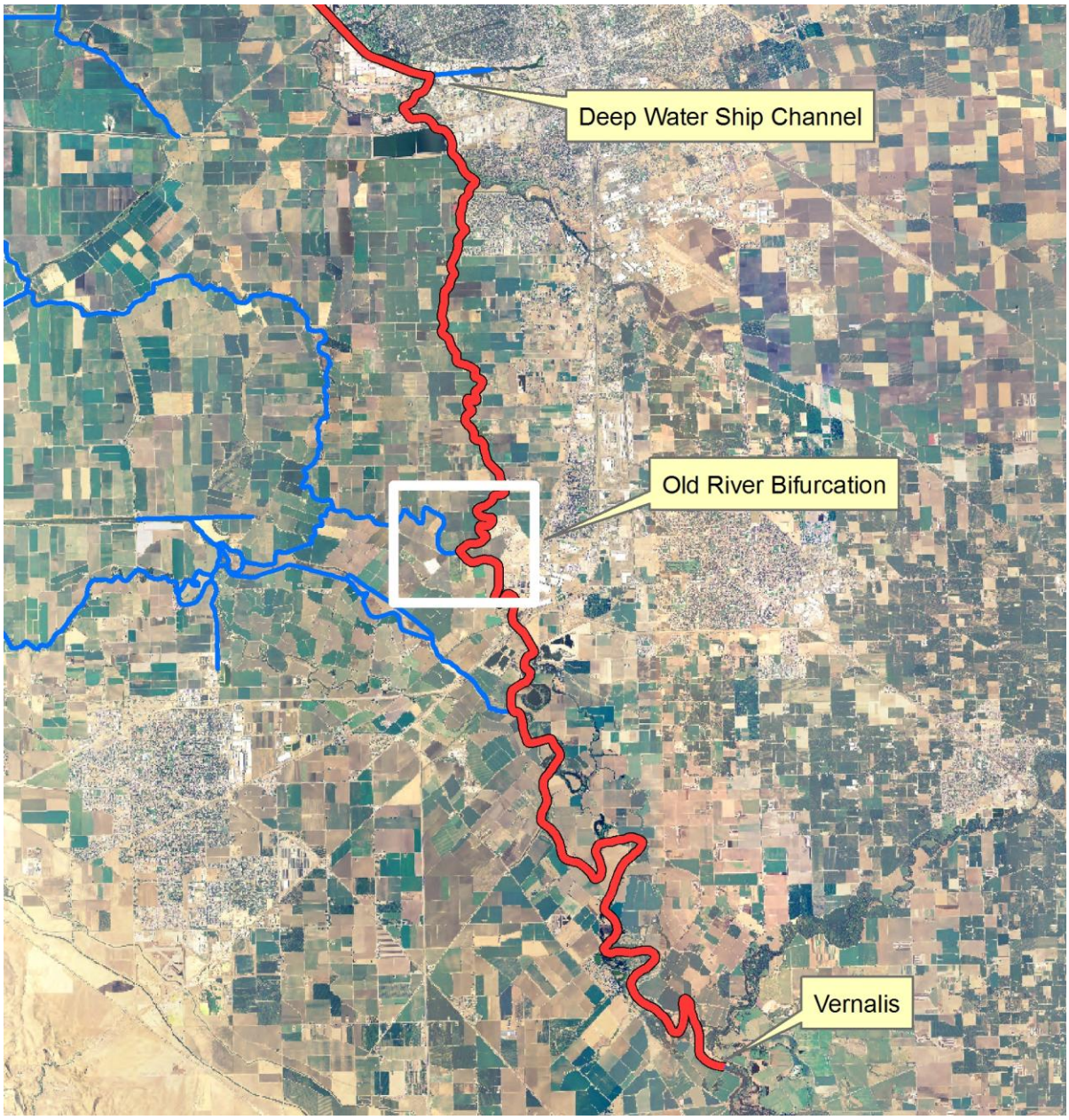

Figure 1. Mike 21c model reach from the Vernalis monitoring station to the monitoring station at Rough and Ready Island showing the confluence between the San Joaquin River and the Deep Water Ship Channel at the top of the image and the bifurcation at Old River.

length ratio is too small. Another potential problem that needed resolution was the presence of sand bars in the certain reaches of the flow domain. Truncation of a flow line due to an obstruction such as a sand bar can lead to numeric instabilities. However confining the River streamlines just to the inundated area would be very limiting – especially if flows decreased further, exposing more sand bars.

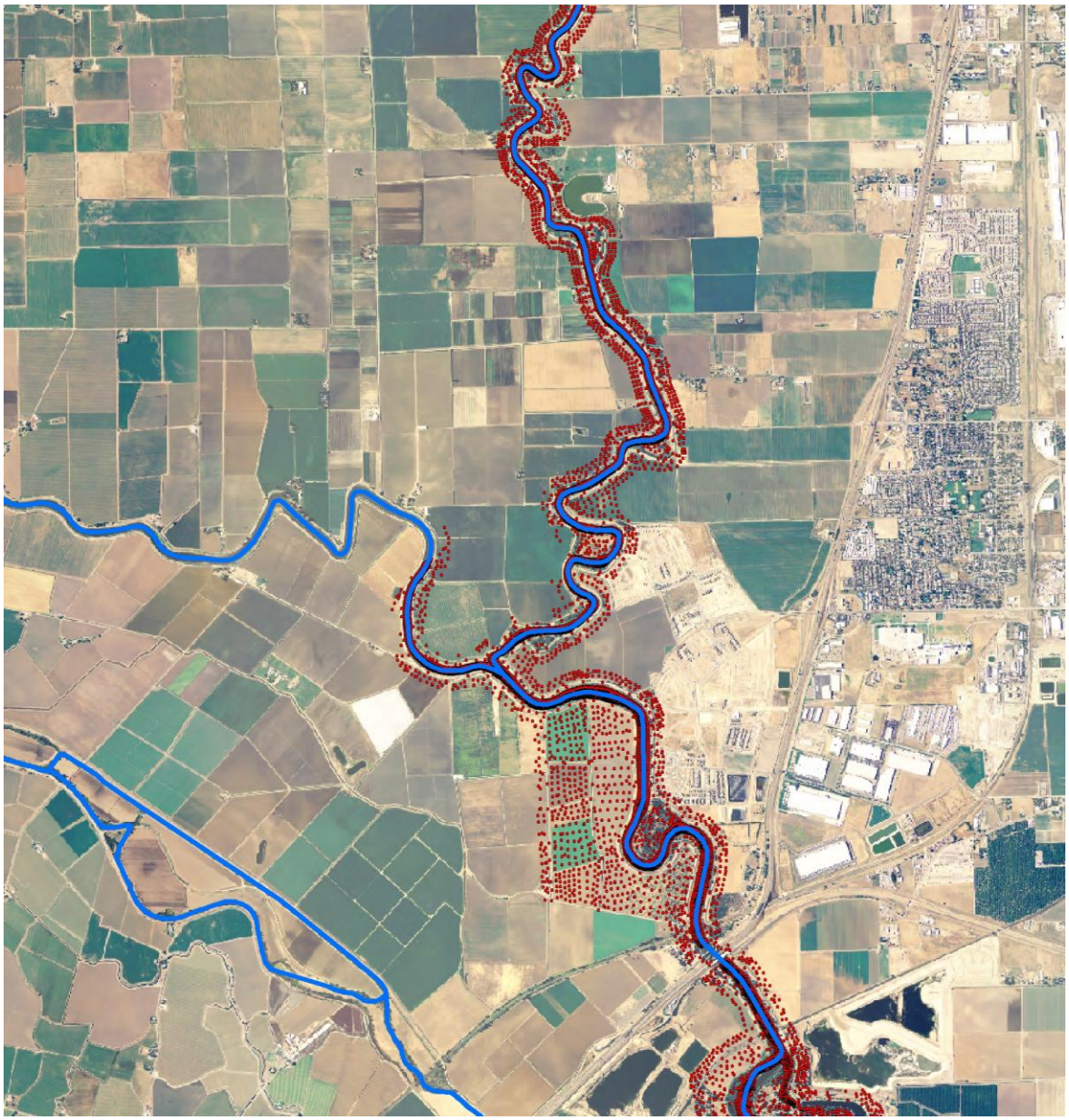

Figure 2. Model reach showing the US Corps of Engineers channel cross-section and DEM dataset that was made available through a US Bureau of Reclamation – Department of Water Resources cooperative agreement. Data is of sufficient refinement to allow accurate 3-D cross section profiles to be developed for the model study reach between the Vernalis and Rough and Ready Island monitoring stations.

This approach would also be ill-advised since the river bed is dynamic and continually in motion – the bed configuration using the existing cross-section and bathymetry data may be drastically changed as a result of a large flood. The approach taken was to allow the streamlines to pass around islands and objects in the River that were never inundated and to treat sand bars that were commonly inundated during high flows as part of the River.

San Joaquin River model bathymetry data

After the conceptual model and mesh configuration was completed the next step involved developing the dataset containing River bathymetry and cross-sectional profiles. The most comprehensive dataset produced for the model study reach is that produced by the US Army Corps of Engineers for the Sacramento and San Joaquin River Basins Comprehensive Study ((1997 – 2003).

River bathymetry and morphology is dynamic and it is unlikely that the survey data collected for this study depicts current conditions exactly given the lapse in time since these surveys were made. However, given the fact that the River is contained between levees along the entire model study reach, the Comprehensive Study data is considered to represent a reasonable "average" condition of River morphology.

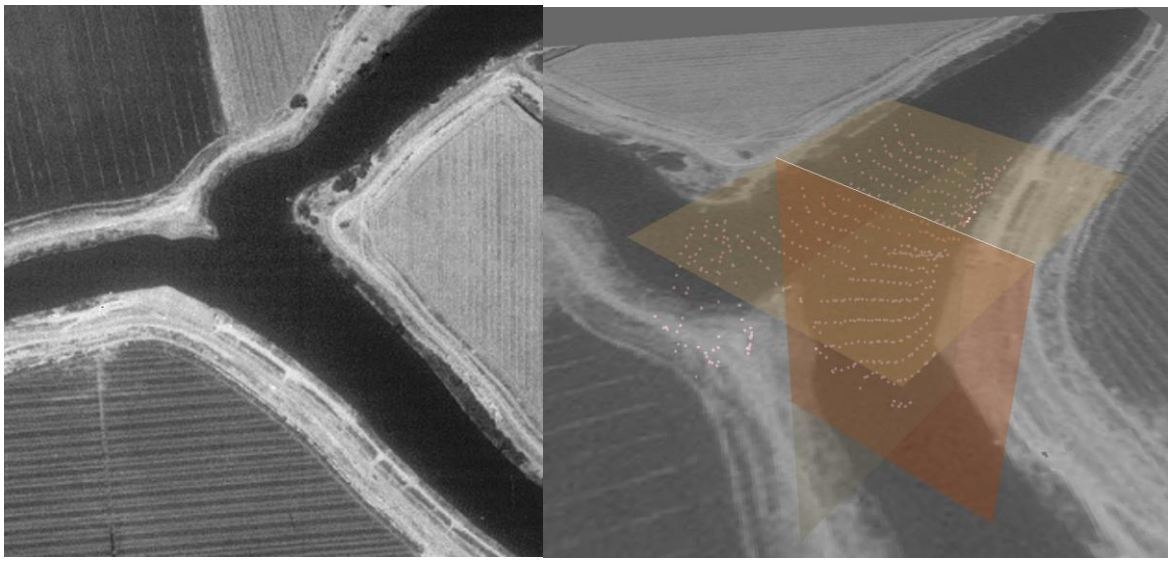

Figure 3. Plan view of the San Joaquin River bifurcation at Old River. USCOE cross section dataset is used to develop a 3-D rendering of the River morphology at this flow split.

Obtaining access to the US Corps of Engineers dataset was difficult and took more than 6 months to accomplish because of national security concerns that needed to be resolved. Final resolution was achieved through the intervention of the US Bureau of Reclamation which was able to obtain the data through a cooperative agreement of data sharing with the Department of Water Resources. Even after the data was rendered readable – considerable effort was required to process this large dataset so that it could be read into a geo-database. The geo-database used was Arc-Info GIS. Figure 2 shows the data points that were provided by the USCOE survey. The survey data extends beyond the River levees into the flood plain. For the purposes of the current study the cross-sectional profiles were clipped to the model domain defined by the levee slope break points.

The San Joaquin River bifurcation at the head of Old River is shown in Figure 3 together with a 3-dimensional image of the survey points used to obtain the River cross section and bathymetry.

The morphology of the junction dictates channel hydraulics which in turn affects the flow volume split between Old River and the main San Joaquin River channel. In the Mike 21c model the boundary condition at the Old River flow monitoring station is simulated as a dynamic head boundary that rises and falls with the tidal flux through the Delta.

Development of 3-D bed surface profiles

Although the purpose of this study is to improve the conceptual understanding of dye transport in the San Joaquin River reach between the monitoring stations at Vernalis and the Deep Water Ship Channel the model was developed and implemented within Mike 21c to serve future studies of algae fate and transport and the transport of other non-conservative constituents of concern. A model mesh configuration that would serve future simulations of algal biomass in the San Joaquin River would need to include the diversion at Banta Carbona Irrigation District, the flow split at Old River, the confluence at French Camp Slough and smaller confluences from minor

Figure 4. Detailed view of the confluence of the shallow (< 20ft) San Joaquin River discharging into the deeper Stockton Deep Water Ship Channel (30 – 40ft).

east-side sloughs (which have been shown to contribute significantly to River algae biomass during each ebb tide). The development of this configuration that allows the hydrodynamic impacts of these features to be represented requires that separate model meshes first be created within a GIS – these are then merged into the main model mesh using custom procedures within the Mike 21c software.

The initial dye studies using rhodamine dye as a conservative tracer, which are reported upon in this chapter, use the three primary boundary conditions i.e Vernalis, Old River and the Deep Water Ship Channel. This was done to speed up the initial model calibration process and deliver more timely output.

Figure 5 shows the bathymetry of the San Joaquin River as it empties into the much deeper Stockton Deep Water Ship Channel. During a typical tidal cycle San Joaquin River can flow into the Deep Water Ship Channel only to be pushed back into the River channel during the following flood tide. The potential transformations in water quality while the water is resident in the Ship Channel include decreases in turbidity, algal biomass concentration, temperature and dissolved oxygen – these should be simulated in order to fully understand the dynamics of water quality in

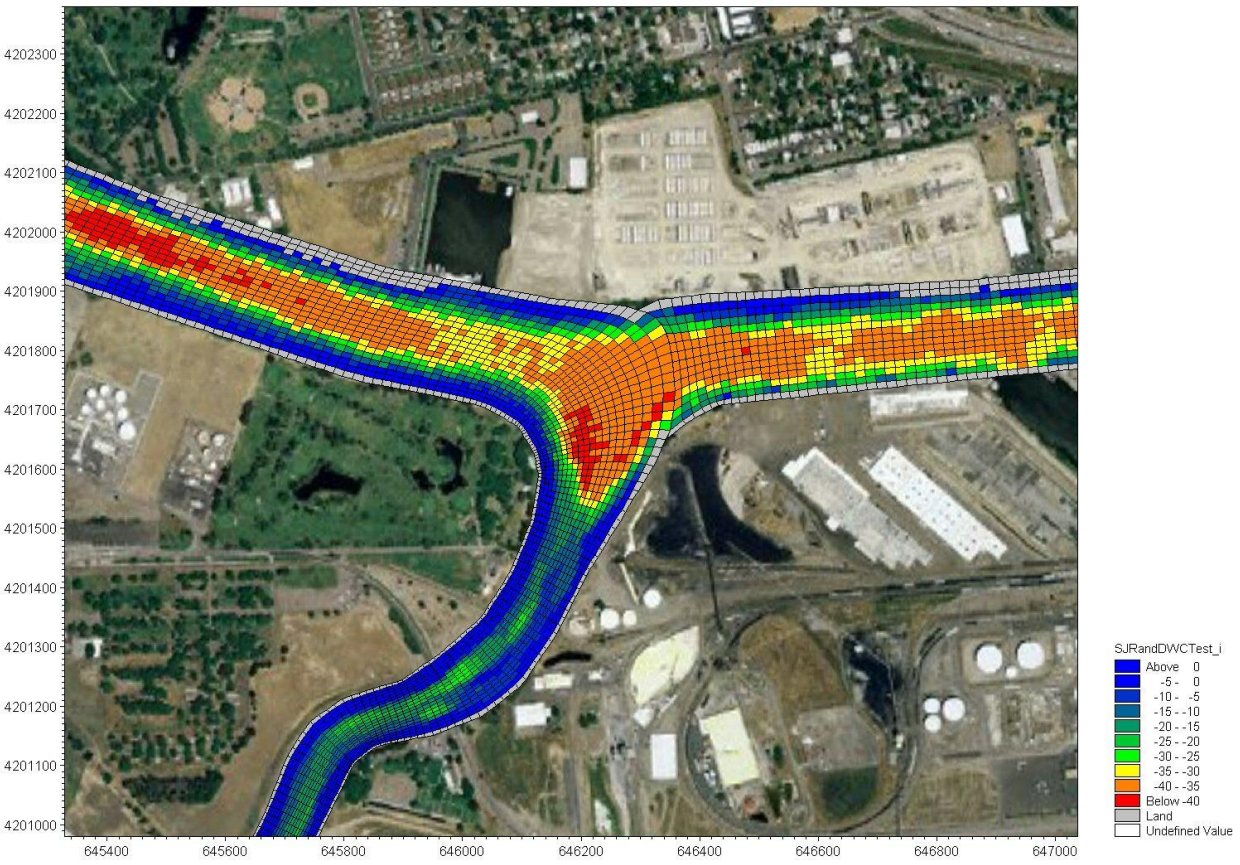

Figure 5. Model channel discretization at the San Joaquin River confluence with the Stockton Deep Water Ship Channel. Image shows the final result of merging a second model mesh (of the turning Basin) with the mesh of the main channel. Depth of channel shown in (negative) feet.

Figure 6. Model channel discretization at the San Joaquin River bifurcation with Old River.. Image shows the final result of merging a second model mesh (of the head of Old River) with the mesh of the main channel. Depth of channel shown in (negative) feet.

this transition zone. Under normal, positive flow downstream conditions, the tidal excursion in the San Joaquin River can be up to several miles in extent, depending on the flow conditions and the strength of the tidal pulse – this is usually sufficient to prevent the River discharge into the Ship Channel from re-entering the River channel more than once.

Figure 6 shows the bifurcation of the San Joaquin River at the head of Old River. A separate model mesh of the short reach of the Old River between the mouth and the monitoring station at Head is conjoined with the mesh of the San Joaquin River main channel using procedures contained within the Mike 21c software. Inspection of the transitional mesh shows that orthogonality has been maintained which should help to avoid numerical instability and lead to realistic simulation of the flow split.

Steady-state hydrodynamic model

Technical modeling staff at the Danish Hydrologic Institute suggested developing a steady-state model using a simple mesh configuration with only the major boundary conditions included to simplify the initial calibration process and to provide initial conditions for the simulation experiments. Complex hydrodynamic models typically require an initial "warm-up period" during which the model resolves numerical instabilities. The closer the initial river elevations specified in the model are to the measured data the more quickly the model will resolve the momentum and conservation equations that simulate the river hydrodynamics.

To develop the steady-state model the boundary conditions specified were the flux boundary at Vernalis (upper boundary of the model), an intermediate tidal head boundary at the Old River bifurcation and a lower tidal head boundary condition within the Deep Water Ship Channel at Rough and Ready Island. Figure 2 is an output plot from Mike 21c showing the head distribution along the entire San Joaquin River model reach.

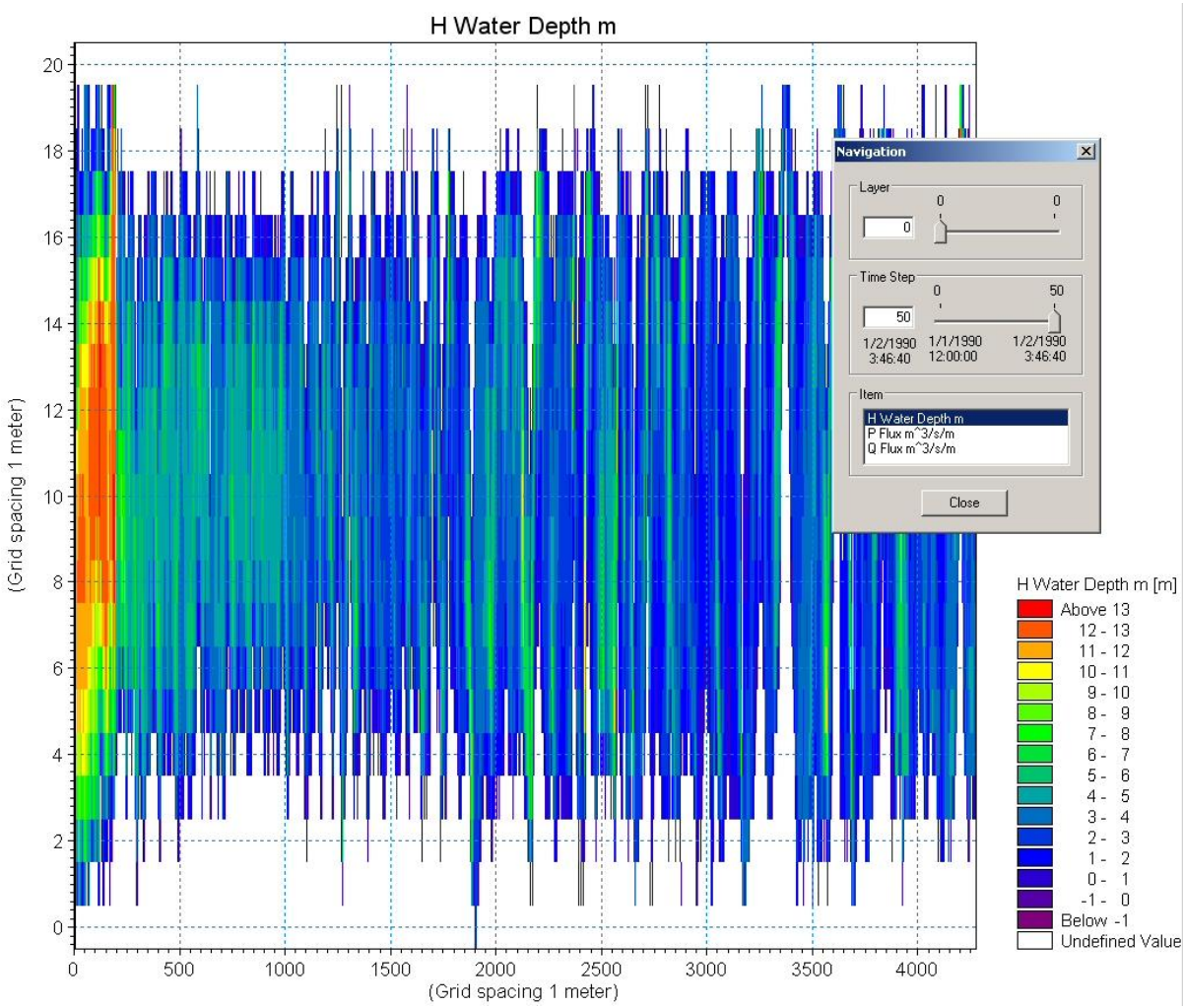

Figure 7. Steady-state water levels within the model finite difference mesh as seen from an orthogonal representation in Mike 21c. After the dynamic runs are complete, the head values are projected from orthogonal space into "real world" coordinates for visualization in a GIS and for use as initial conditions in subsequent runs.

Preparation of dye simulation data files

Dye release experiments were conducted every month between July and October during 2004, 2005, 2006 and 2007. In each of these experiments 50 lbs of concentrated Rhodamine WT dye was dispersed in the River adjacent to the Vernalis monitoring station using the Litton research vessel to apply the dye across the River cross-section and making use of the propeller wake from

both the research vessel and the smaller 14 ft Jon boat to mix the dye within the water column. Figure 8 shows the dye being pumped from the research vessel using an on-board peristaltic pump. Manual pouring was used during later dye experiments to achieve a faster rate of initial mixing. The research vessel is equipped with a continuously recording Rhodamine dye sonde, an accurate GPS recorder and a MatLab software interface that permitted the real-time dye concentration to be plotted, together the outputs from other sensors, with the vessel's exact location (Litton et al., 2007). This software program allowed the boat operator to find the dye peak concentration within the dye plume and stay within this dye prism as it was swept downstream.

Figure 8. Rhodamine WT dye dispersal from Litton research vessel with Jon boat riding in the wake of the larger boat to assist with vertical mixing of the dye. Uniform mixing within the water column was achieved within 2 – 3 miles downstream. The research vessel then drifted downstream attempting to stay with the dye concentration peak.

A second 50 lb container of dye was added to the existing dye peak, just below the Old River bifurcation, within the tidal reach of the River. This was necessary owing to the reduced dye

concentration as the effects of longitudinal dispersion, adsorption to organic matter and degradation in sunlight combined to diluted the dye signal. The mean celerity of the River declines within the tidal reach and the average water depth increases. Even with the added dye the peak dye concentration can be difficult to ascertain because of tidal dispersion.

Dye concentration measurements were made in both Langrangian (boat travels with the dye peak) and Eulerian (collected by a stationary boat and the dye passes downstream) experiments. Figure 9 is a typical set of Eulerian concentration profiles showing the manner by which the dye tracer disperses longitudinally as it moves downstream from Vernalis, encountering a variety of influences including channel irregularity, channel tortuosity, obstructions, groins, sand bars and other factors that increase dye retardation within the channel reach. Although the shapes of the dye plumes can be described by polynomial expressions the rate of longitudinal dispersion is significantly influenced by mixing and retardation factors which can vary with rate of flow and channel morphology, as previously discussed. Gary Litton (Litton et al., 2007) was able to simulate dye travel time reasonably well using a simple Matlab plug-flow model (Figure 10). However this model does not simulate the mechanisms of longitudinal dispersion, nor is it likely to be valid for all flow conditions in the River, especially within the reaches subject to tidal excursions. Simulation of the mechanisms of dye (and by inference algal biomass) can only be achieved with a more detailed numerical model of the River reach between the Vernalis and Rough and Ready monitoring stations such as the MIKE 21c model previously described.

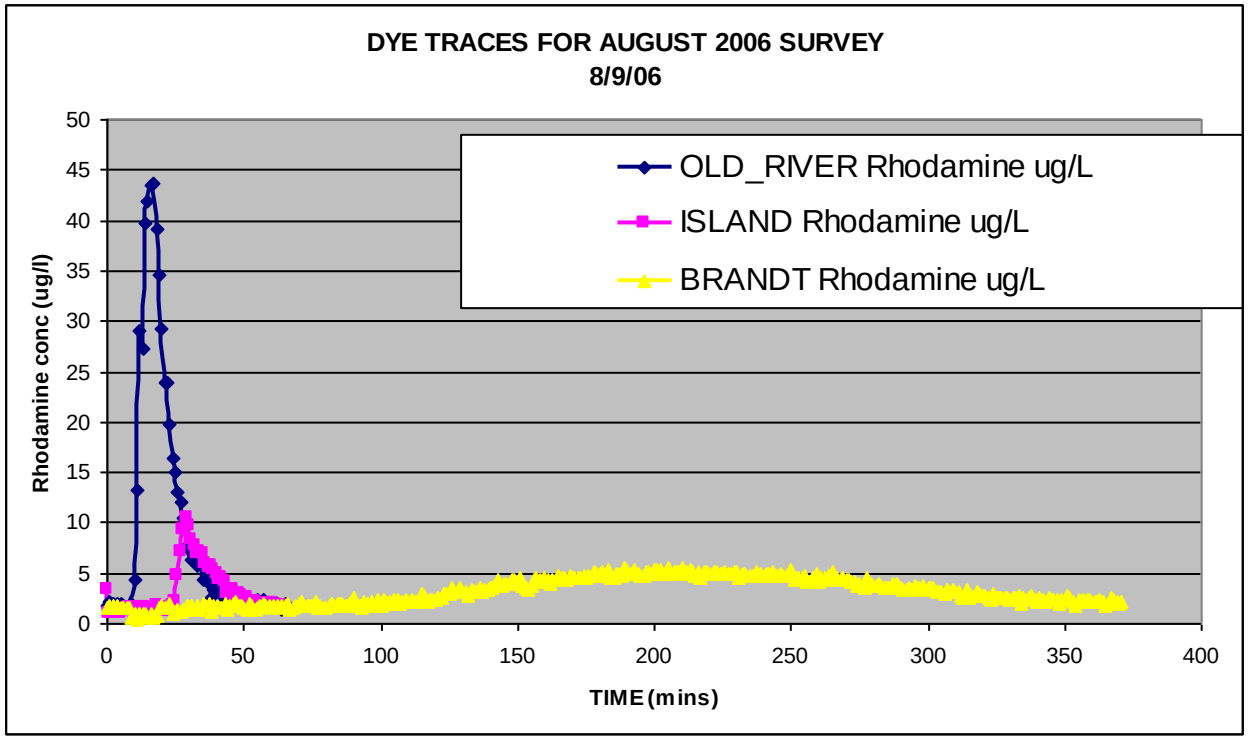

Figure 9. Dye longitudinal dispersion in the reach of the San Joaquin River between the Vernalis monitoring station and Dos Reis campground, located approximately 16 miles downstream.

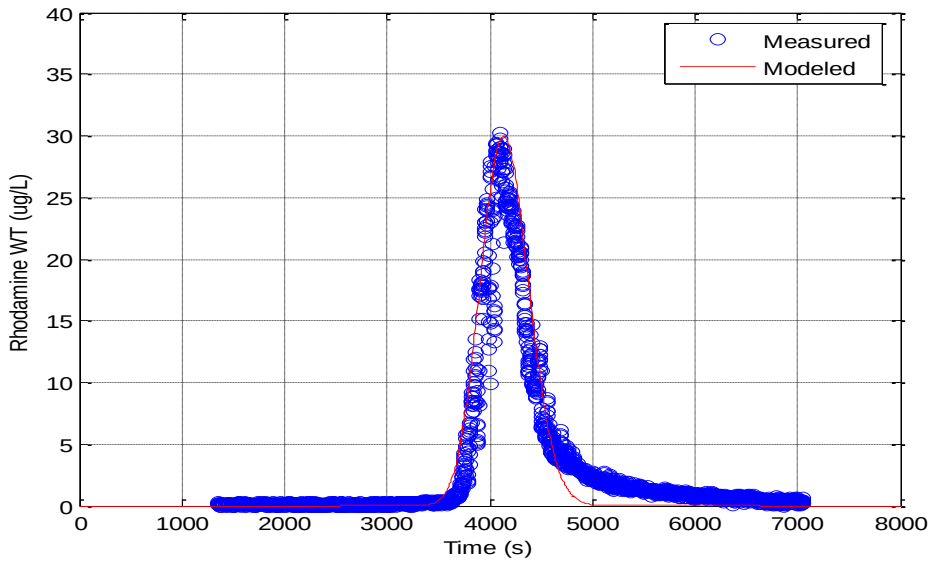

Figure 10. Comparison of measured and modeled Rhodamine WT concentrations in the San Joaquin River (river mile 53.07) using Litton MatLab model. Dye release occurred at river mile 53.7 (just downstream from the Head of Old River) at 2:30 a.m. on July 14, 2005.

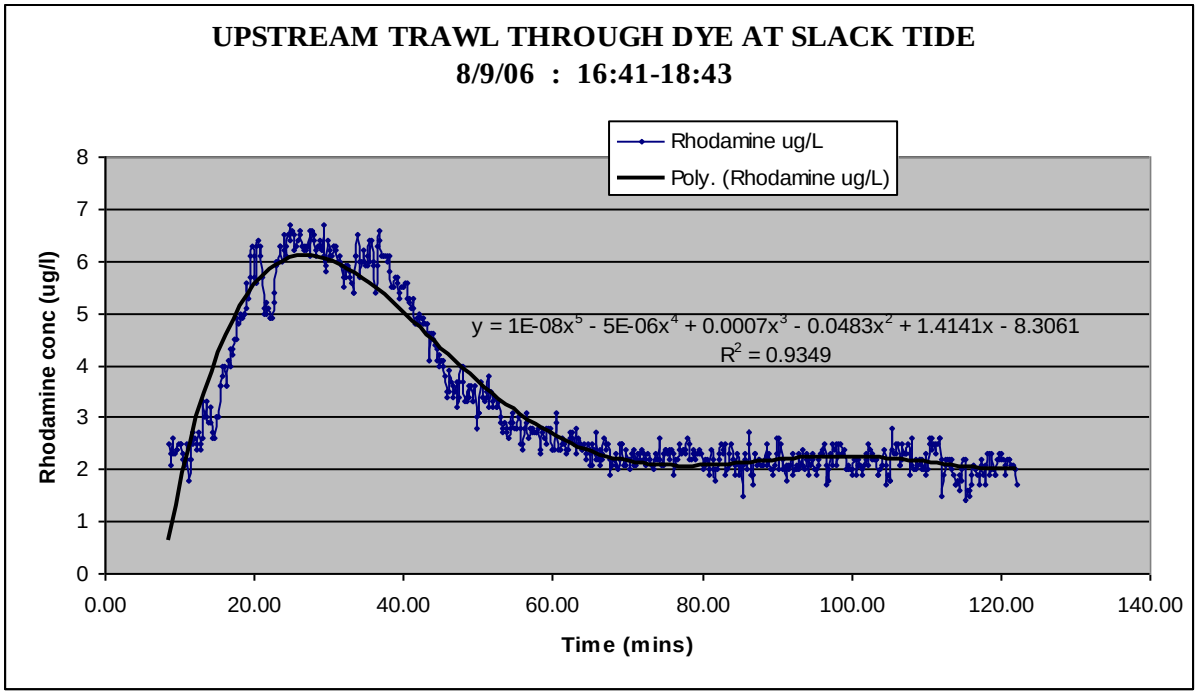

Figure 11. Upstream trawl through the dye starting at the (Brickyard) SBC Stack site (river mile 45.0) starting at 4:41 p.m. on August 8, 2006.

Figure 11 is a Rhodamine dye trace obtained by trawling upstream during slack tide (tidal reversal during which time advective flow is zero). In this instance the transition is from an ebb tide to a flood tide. The sharp dye front is pushed back through the lower concentration dye cloud which essentially destroys the shape of the dye pulse, especially during low flow hydrologic conditions where tidal excursions are greater owing to the smaller volume of water opposing the flood tide. It is expected that eddying and secondary flows would be more prevalent under low flow hydrologic conditions resulting in increased longitudinal dispersion of dye.

Preliminary results of Mike 21c simulations

Two numerical simulations of the dye experiments were selected to represent both high and low River hydrology and to fully test the stability of the MIKE 21c code. The first experiment conducted in March 2005, although outside the typical period of low dissolved oxygen conditions in the San Joaquin River which occur in late summer and early fall, provided a number of useful dye traces against which to compare the numerical model. Flows recorded at Vernalis during March 2005 were above 5,000 cfs and produced a dye transport flow regime which was strongly advective. This created more of a plug-flow regime in the non-tidal River reach below Vernalis and resulted in a minimal number of tidal excursions in the tidal reach, before the dye passed into the Ship Channel.

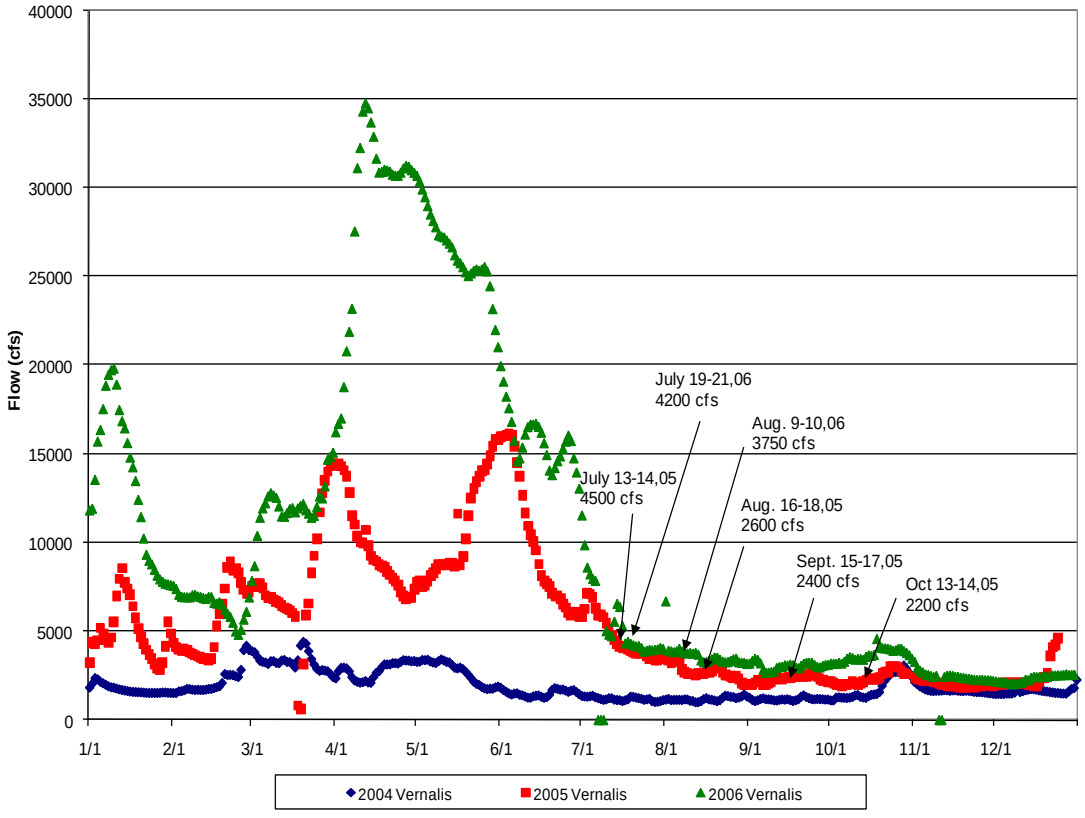

Figure 12. Flows at Vernalis 2004 – 2006 showing dates of dye experiments.

The second dye experiment chosen was started on September 20, 2007 and lasted approximately 6 days. During the latter part of 2007 the San Joaquin River experienced hydrology similar to that in 2004, with extremely low flows at Vernalis and conditions that produced very little advection through the tidal reaches of the River between Mossdale and the Deep Water Ship Channel. Under these conditions eddies and secondary flows become more dominant in their tendency to disperse dye and the number of tidal excursions is large before the dye finally passes into the Stockton Deep Water Ship Channel.

Model simulation experiments

Numerical simulations with MIKE 21c require the development of an input data deck which provides initial and boundary conditions and initial values for parameters such as bed cohesion, eddy viscosity and bed roughness that affect dispersion. The simulations are performed in three steps. The first step requires that the model be supplied with realistic heads at each grid cell since stage measurements are available at a small number of gauging stations along the River. This is achieved most efficiently by running the model iteratively until it reaches a steady-state condition, as previously described. The stage values at the steady-state condition are used as initial conditions for a transient run of the model. For the March 2005 dye experiment – the MIKE 21c model took 59 hours on a 3.0 GHz Dell computer with a dual Xeon processor to achieve a steady-state condition. A parallelized beta version of the MIKE 21c code was provided by DHI Inc. – once this was properly functional it reduced the computation time to one quarter of the time. The parallelized code performs approximately 1.2 million computational points/sec – whereas the non-parallelized code runs at 300,000 computational points/sec.

A transient run is then made using the "hot start" initial condition files using a time step that is as large as possible that still allows the model to run to completion. This is a trial and error procedure – the larger the model time step the quicker the model runs to completion. For the highly advective, March 2005 flow condition, a 15 second time step was found to be desirable. However the August 2007 model run – which spawns more eddies and secondary flows owing to the smaller flow volumes – the time step had to be reduced to 1 second.

After a successful flow simulation was achieved the simulation was re-run to simulate transport of Rhodamine dye. MIKE 21c does not contain a water quality module that can be used to simulate dye transport – rather we were advised by DHI to use the sediment transport capability of MIKE 21c and to simulate dye transport as sediment with properties of zero settling velocity (neutral density) and with zero bed cohesion. The simulation was started approximately 5 days in advance of the dye (sediment) injection to allow the model to stabilize and was continued for another 15 days after the initial dye injection to allow all of the dye to be pushed out of the River. The strongly advective March 2005 simulation ran efficiently without any major problems – however the weakly advective case was inherently unstable and did not run to completion with the parameter values initially selected.

On the advice of Søren Tjerry the alluvial resistance model, which is contained within the MIKE 21c River Morphology module, was run to address the tendency for the flow to concentrate on River point bars. This phenomenon occurs naturally because the flow path is shorter over the bars than in the outer bend scours. To make the flow more sensitive to the depth, the algorithm causes the flow to deflect away from shallow areas into deeper areas. Using a Manning

coefficient of M=32 for all water depths the flow tends to concentrate on point bars, looks un-natural and is prone to instabilities. Using the applied alluvial resistance model - Manning's M is set to a value of 32 for deep water, while for shallow regions (depth of 1m or less) M is set equal to 10. A higher bed resistance is always stabilizing for low flow cases. Smoothing the bathymetry, and lowering the time-step to 1 second, raising the eddy viscosity to 2 m^2/s and using an alluvial resistance where $M = 10 * h^{0.5}$ were steps taken to get the model to run to completion.

Model Scenario run – Vernalis high flow > 5000 cfs : March 23, 2005

The first dye release experiment was conducted on March 23, 2005 with Vernalis as the dye release point. Figure 13 shows the longitudinal dispersion of the dye plume as the dye is transported downstream. The first dye concentration profile is obtained by driving the boat downstream through the dye peak – the second is obtained from a stationary boat as the dye moves past the instrument. These plots are primarily in the non-tidal reaches of the San Joaquin River under moderately high flow conditions which minimizes the effect of tidal excursions.

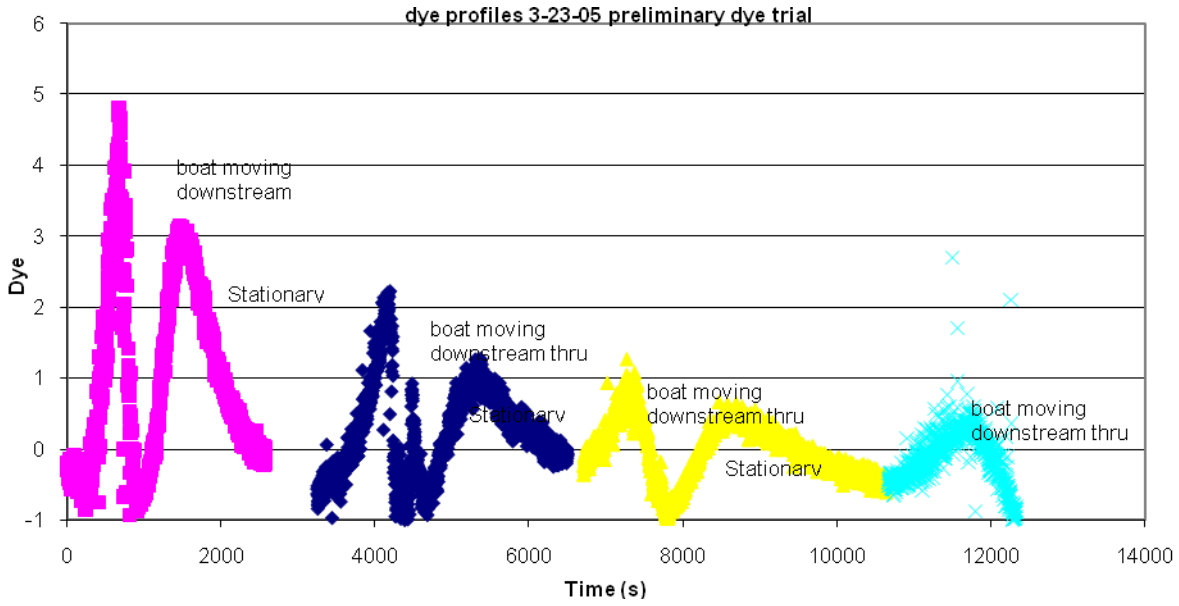

Figure 13. Dye profiles collected for the preliminary dye trail on March 23, 2005. Release point was Vernalis and dye profiles were obtained by alternately driving the boat through the dye cloud and waiting for the dye to pass the stationary boat.

MIKE 21c simulations results are shown in Figure 14. This shows snapshots from an animation of the dye release experiment. The San Joaquin River has been broken into smaller reaches and placed on the viewing screen from right to left to allow the entire simulation to be viewed on a single screen. The color ramped dye concentrations in the animation show the strongly advective

dye pulse. The tidal excursion during this experiment was small owing to the large volume of water passing along the San Joaquin River which resists the force of the flood tide.

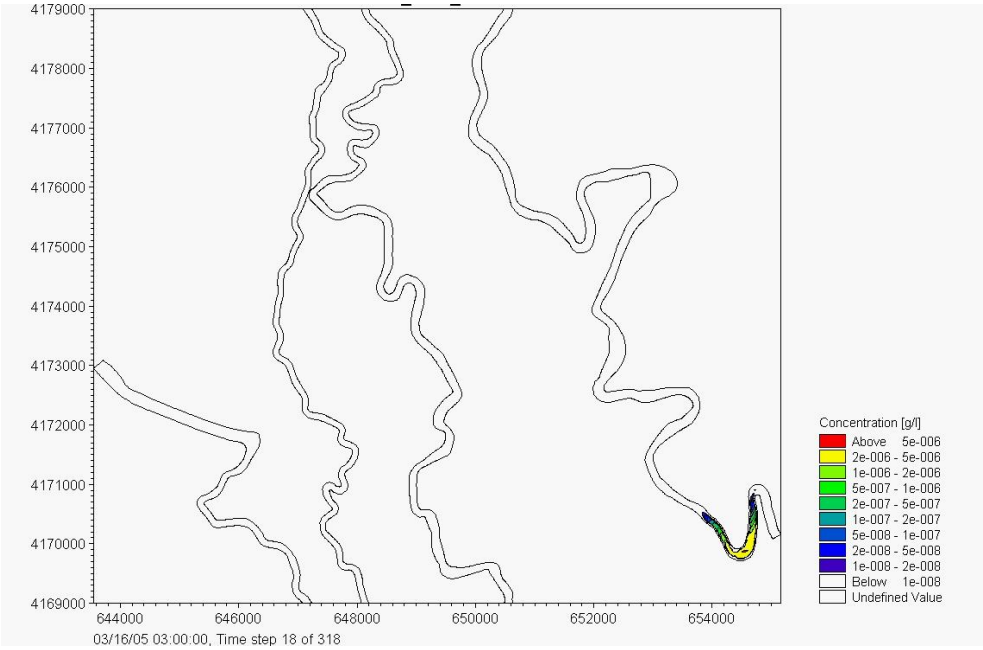

Figure 14-1. Downstream from dye release – 03/16/08 : 03:00:00. Time step 18.

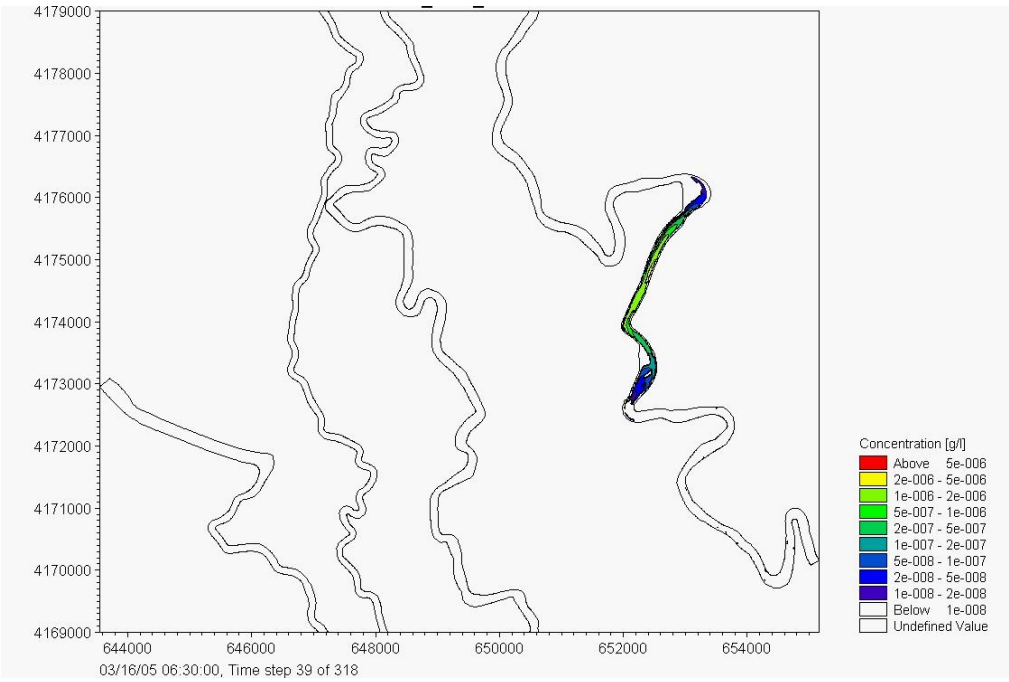

Figure 14-2. Downstream from dye release – 03/16/08 : 06:30:00. Time step 39.

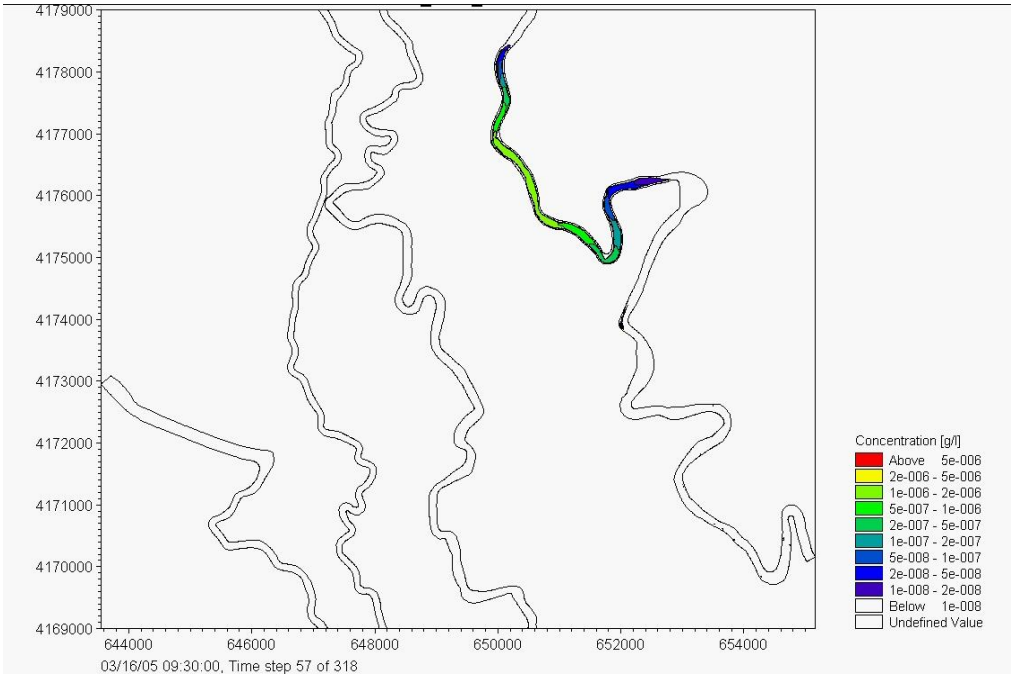

Figure 14-3 Downstream from dye release – 03/16/08 : 09:30:00. Time step 57.

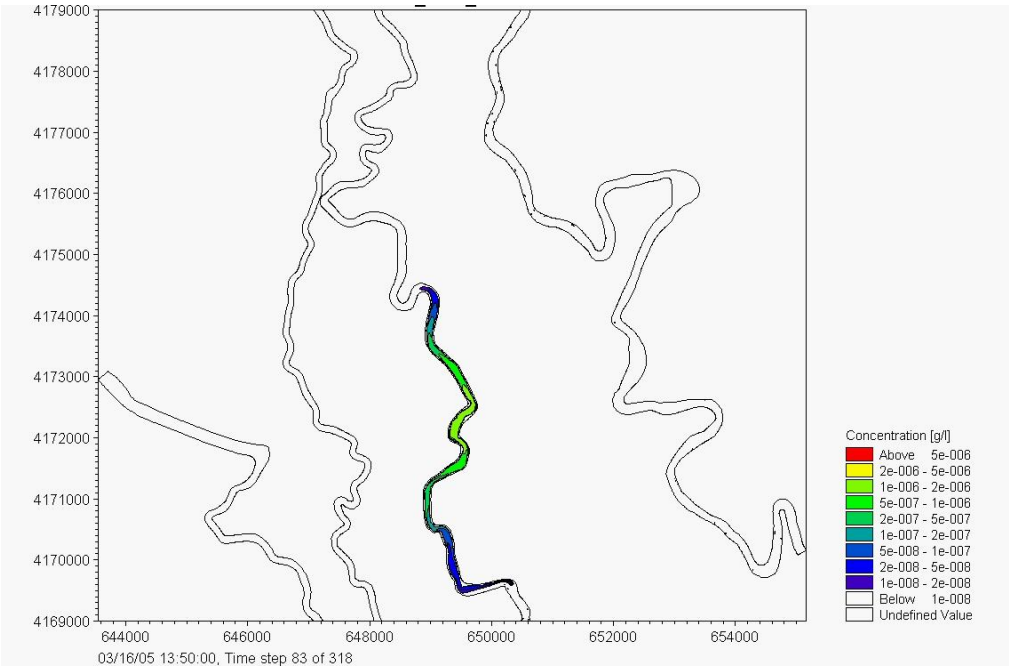

Figure 14-4 Downstream from dye release – 03/16/08 : 13:50:00. Time step 83.

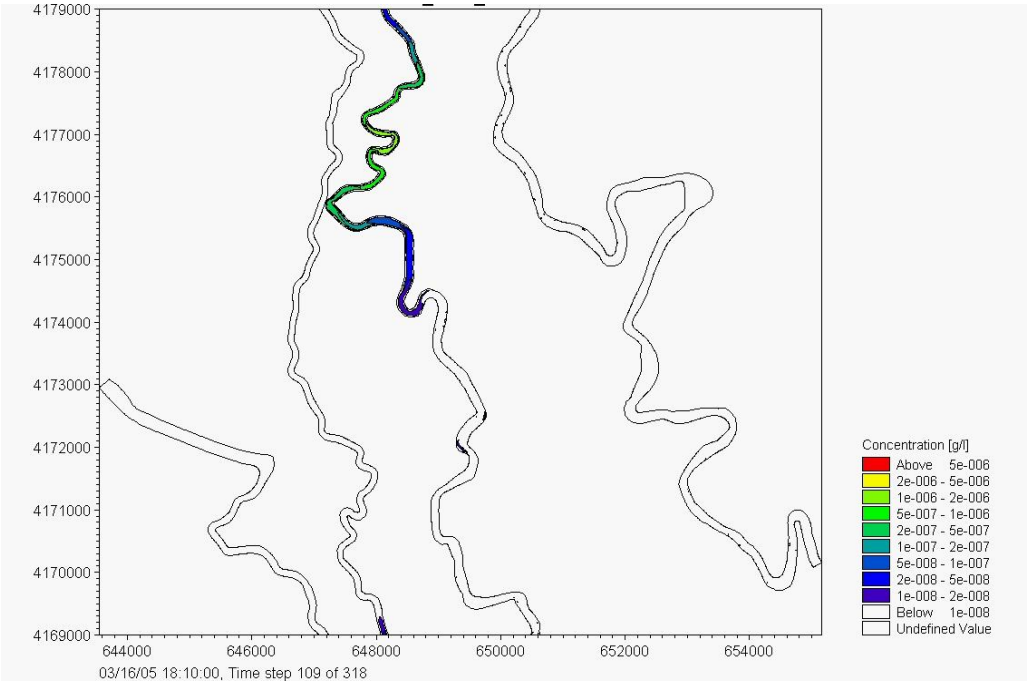

Figure 14-5. Downstream from dye release – 03/16/08 : 18:10:00. Time step 109.

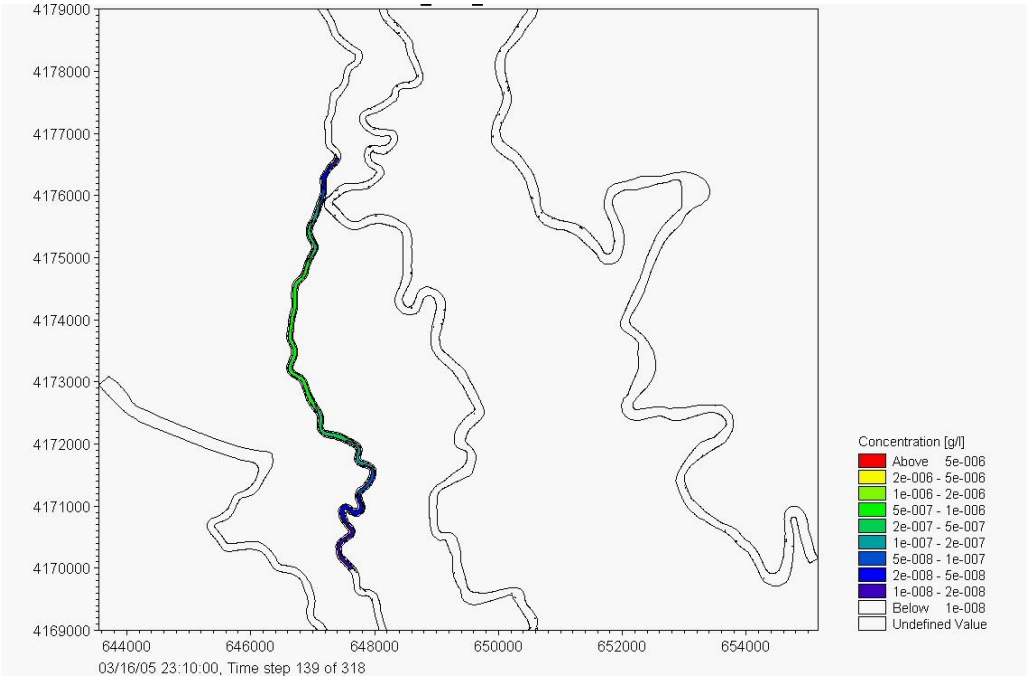

Figure 14-6. Downstream from dye release – 03/16/08 : 23:10:00. Time step 139. Dye shown in tidally-influenced reach of the San Joaquin River.

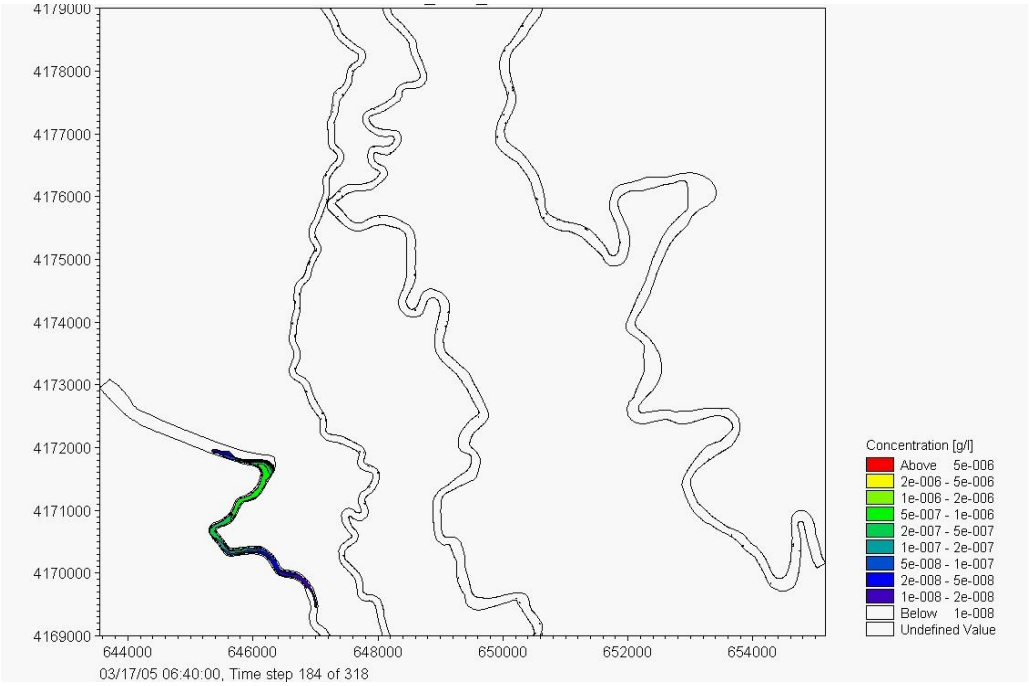

Figure 14-7. Downstream from dye release – 03/17/08 : 06:40:00. Time step 184. Dye shown just entering the Deep Water Ship Channel after 1 tidal excursion.

Model Scenario run – Vernalis low flow < 1000 cfs : September 20, 2007

The second dye release experiment was conducted on September 20, 2007 with downstream of the Head of Old River as the dye release point. Figure 15 shows the longitudinal dispersion of the dye plume as the dye is transported downstream. The dye concentration profile is recorded at

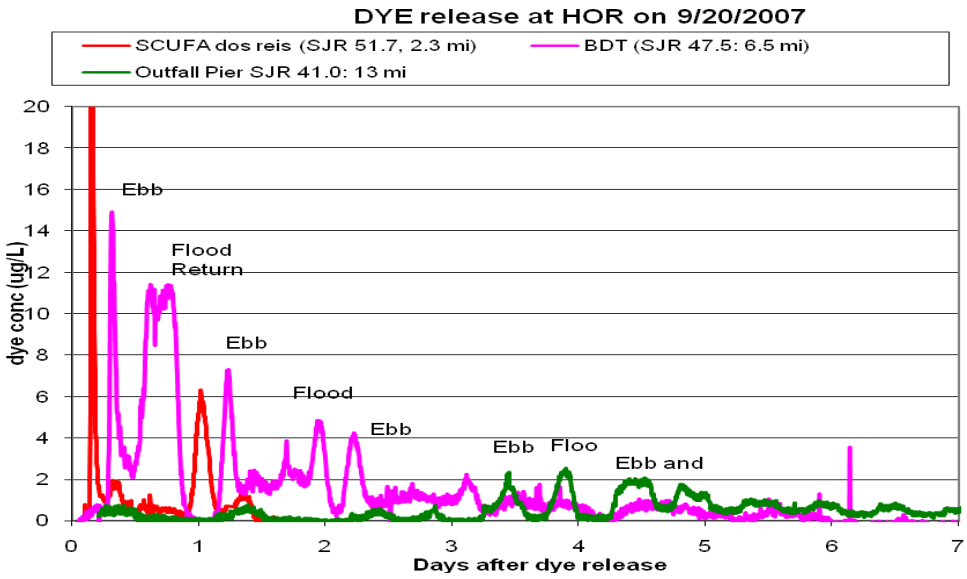

Figure 15. Dye concentration profiles in the tidal reach of the San Joaquin River showing the frequency of tidal excursions against a weak advective outflow.

three observation platforms – (1) the Dos Reis campground site – 3 miles downstream from the HOR dye release location; (2) Brant Bridge (BDT) – a little over 6 miles downstream from HOR; and (3) the Outfall Pier – located about 1 mile from the entrance to the Deep Water Ship Channel and about 13 miles downstream from HOR.

Figure 15 shows the series of flood and ebb tidal excursions that continue over the six days after the dye release on 9/20/2007. The first dye peak is very sharp at Dos Reis as would be expected – the second dye peak is somewhat dispersed but still strong as the sensor picks up the second ebb tide almost 23 hours later. It is interesting to observe that the first flood tide (after the initial strong ebb tide) provides a very weak dye signal. This may be caused by the weakness of the tidal excursion which failed to push the center of the dye cloud past the sensor at the Dos Reis dock. The Brandt Bridge station sees the dye peak concentration approximately 8 hours after the dye release. This is a strong signal – probably due to the strength of the ebb tide. Each subsequent flood tide tends to broaden and attenuate the dye peak. The signal disappears after day 5. At the Outfall Pier the first strong Rhodamine dye signal is observed on the ebb tide about 3.5 days after the dye release on September 20. The dye peaks, although attenuated, remain surprisingly distinct even after three tidal reversals. The signal disappears from the system after day 5.

Figures 16-1 through 16-7 show the model simulated dye concentration profiles along the San Joaquin River starting from Old River (model node 1850) down through the Deep Water Ship Channel and the Rough and Ready monitoring Stations (model node 0). At this time the model node numbers have not been mapped to River mile. The dye concentration in g/m^3 is also scaled for each plot – which makes it difficult to make a direct comparison to the data shown in Figure 15. This will be improved after further work. However it is clear that the distinct dye concentration profiles that were observed in the field data also are observed in the model simulations. The model appears to be producing the right amount of longitudinal dispreson from a purely qualitative assessment.

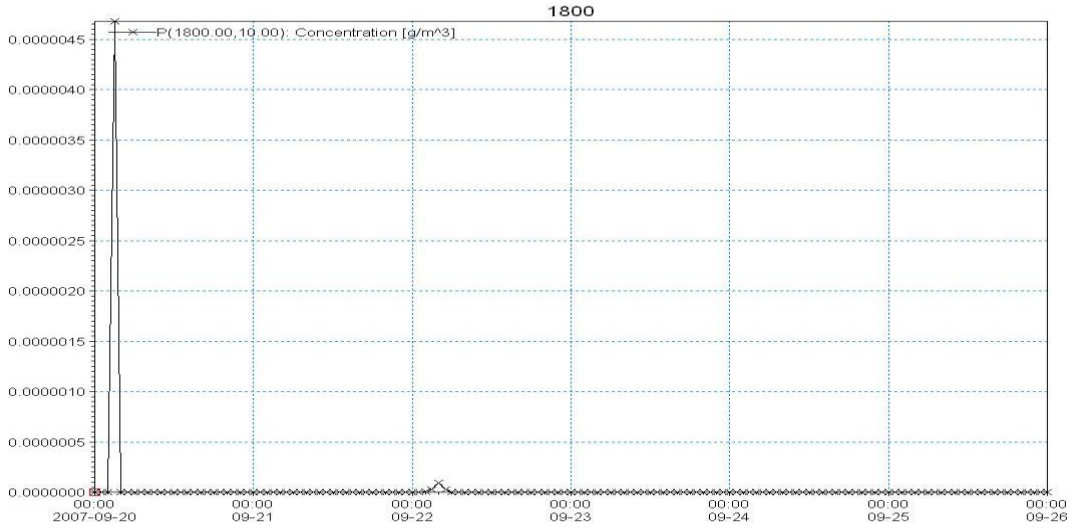

Figure 16-1. Dye concentration profile at model node 1800 immediately downstream of Old River.

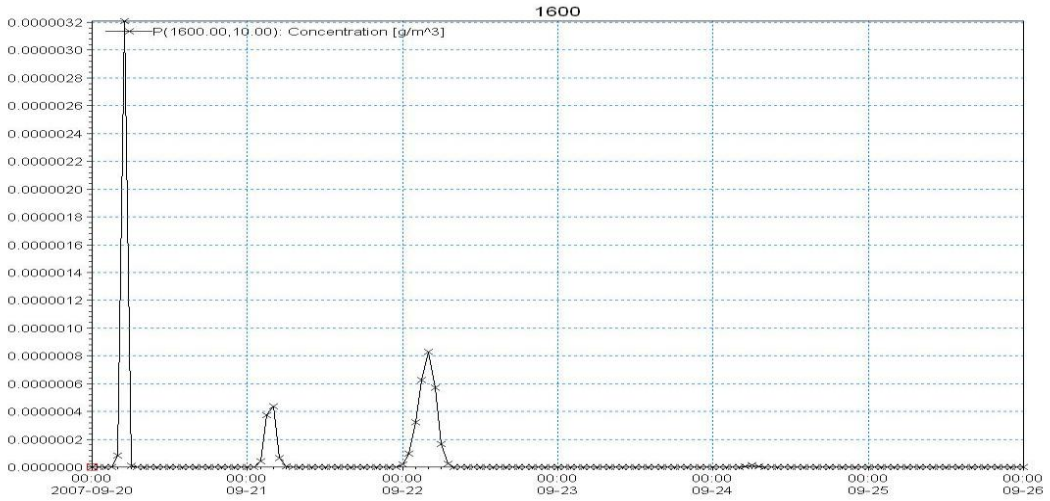

Figure 16-2. Dye concentration profile at model node 1800 downstream of Old River.

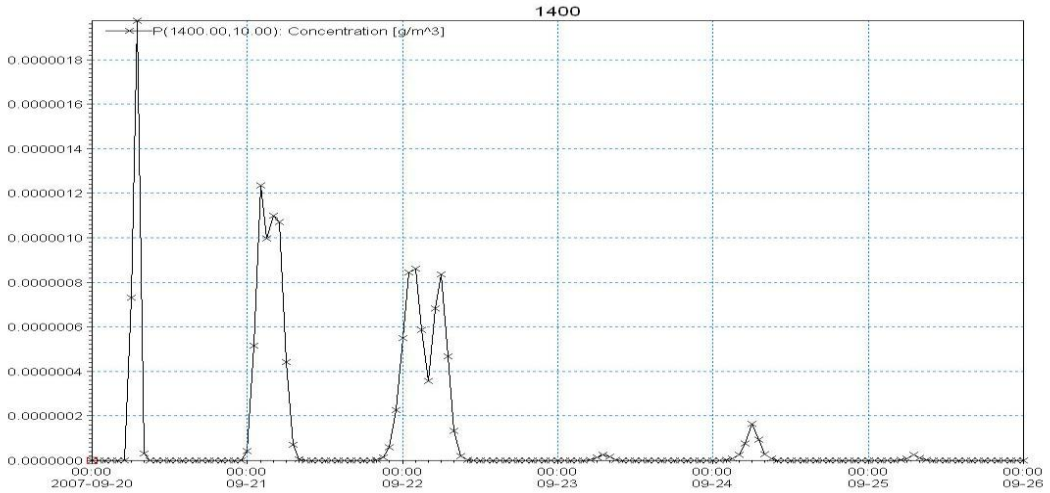

Figure 16-3. Dye concentration profile at model node 1400.

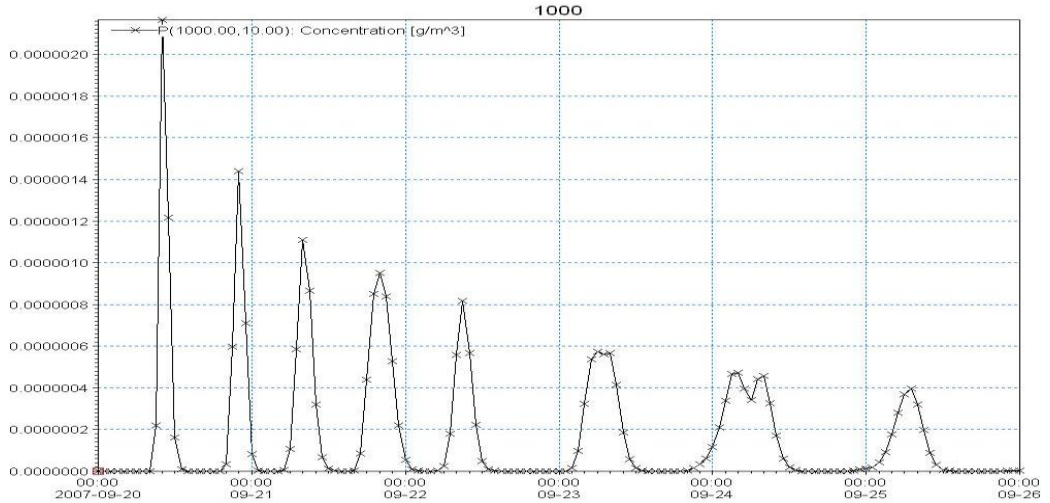

Figure 16-4. Dye concentration profile at model node 1000.

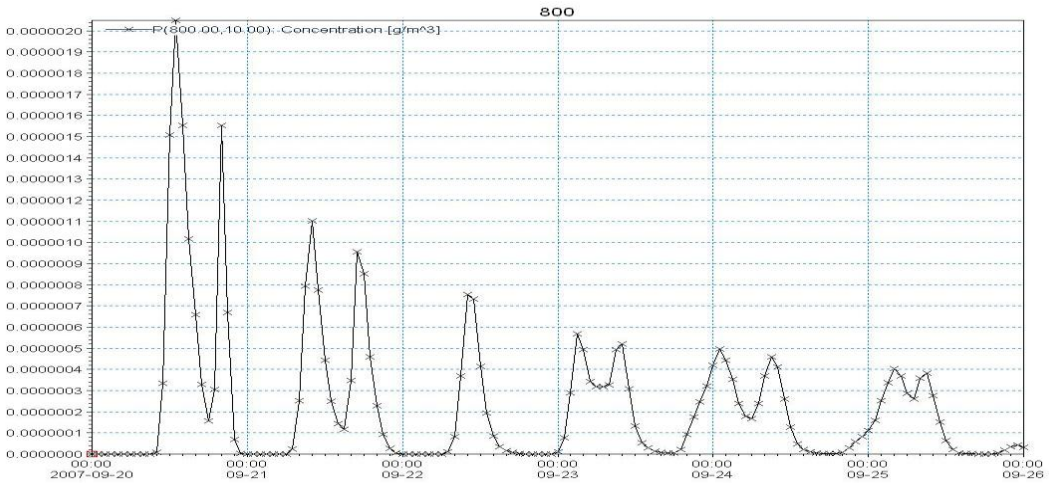

Figure 16-5. Dye concentration profile at model node 800.

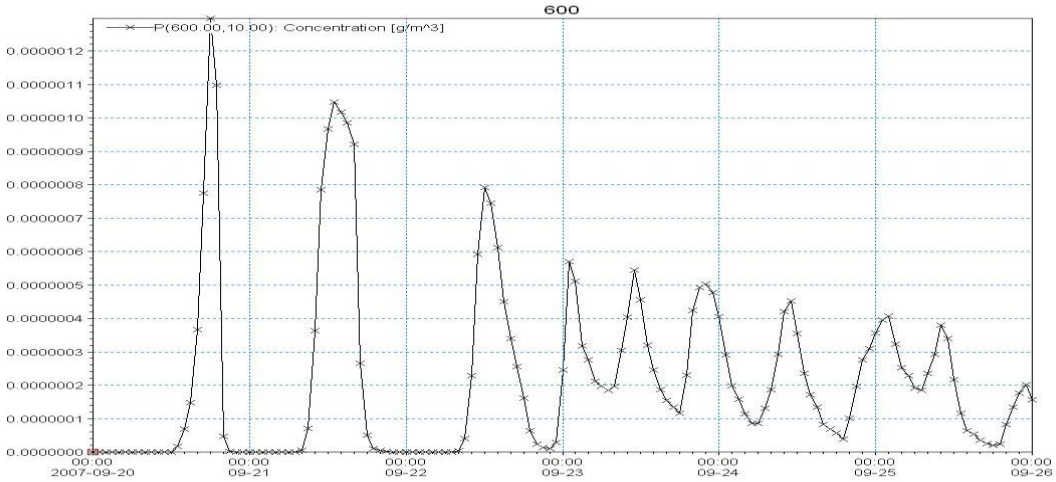

Figure 16-6. Dye concentration profile at model node 800.

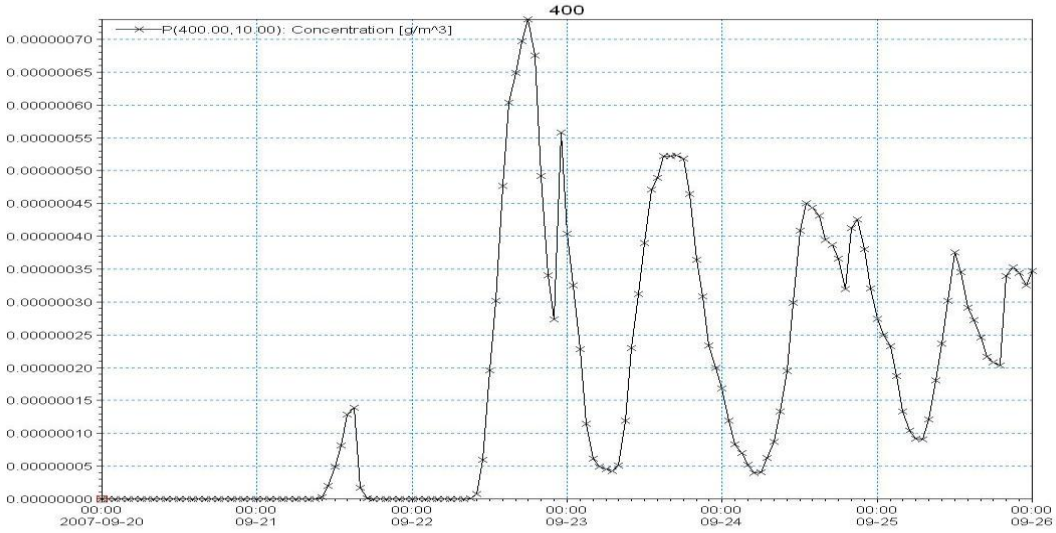

Figure 16-7. Dye concentration profile at model node 400 upstream of the DWSC.

In Figure 16-7 the model simulation shows a reasonably identifiable dye signal 3 days after the release of the dye just downstream from the Head of Old River. The field data picked up the dye signal after about 3.5 days. The model simulation shows a gradual decay through day 6 of the experiment. The decay of the signal was more rapid in the case of the field data. This is likely a result of the assumption being is being made to simulate the dye as non-cohesive, neutrally buoyant sediment. In reality Rhodamine dye concentrations decay because of adsorption to organic matter and sediment and due to a natural decay in the fluorescent property of the dye. This issue can be dealt with through calibration or by introducing a decay term for the Rhodamine dye.

Conclusions

A state-of-the-art numerical simulation model of the lower San Joaquin River between Vernalis and the Rough and Ready Island monitoring station within the Stockton Deep Water Ship Channel has been developed to provide a working tool that captures some of the field observations made by the Litton team during 2005 – 2007. The numerical modeling approach uses the Danish Hydrologic Institute's MIKE 21c model code which has a new curvilinear mesh feature which allows the model to more accurately simulate the complex dynamics of flow along a highly sinuous River reach with high variable bathymetry. Preliminary model simulations have demonstrated the model's significant potential as a research and decision support tool to further improve the understanding of dye and algal fate and transport in the San Joaquin River. A well-calibrated two-dimensional simulation model of the River can significantly reduce the costs associated with real-time monitoring.

Acknowledgements

This study is an extension of the Task 8 project, led by Dr Gary Litton, entitled "Linking the San Joaquin River to the Stockton Deep Water Ship Channel". Gary's leadership on this task was truly impressive and without the use of his small fleet of boats and customized monitoring equipment the vast and unique data set that has been collected over the past 3 years would not have been realized. This was one of the most satisfying study team experiences I have encountered in my 20 years working in the San Joaquin Basin. We are grateful to Joseph McGahan and Nettie Drake for their work in administering this grant work and to Will Stringfellow who distilled our collective ideas into a workable proposal that allowed the work to be funded. Also to the California Bay-Delta Authority and the various Project Managers who guided this multi-agency project to a successful conclusion.

References

Brown, R. and A. Huber. 2005: "Initial Simulation of 2000-2003 Flows and Water Quality in San Joaquin River Using DSM2-SJR Model", Jones and Stokes, Sacramento, CA

Carslaw H.S. and J.C. Jaeger, 1959. Conduction of Heat in Solids. 2nd edition. Oxford

University Press, London.

Chen C. W. and W. Tsai. 2002. Improvements and Calibrations of Lower San Joaquin River DO Model. Final Report for CALFED Grant 99-B16, and DWR 4600000989, Systech Engineering, Inc., San Ramon, CA 94583.

Csanady G.T. 1973. Turbulent Diffusion in the Environment. Geophysics and Astrophysics Monographs. Volume 3.

Fick A. 1855. On Liquid Diffusion. Philso. Mag. 4(10), 30-39. (referenced in Fischer et al. 1979).

Fischer H.B., E.J. List, R.C.Y. Koh, J. Imberger and N. H. Brooks, 1979. Mixing in Inland and Coastal Waters. Academic Press Inc.

Foe C., M. Gowdy and M. McCarthy. 2002. Strawman Load Allocation of Responsibility Report. Draft, Central Valley Regional Water Quality Control Board, Sacramento, CA. Jones & Stokes. 1998. Potential Solutions for Achieving the San Joaquin Dissolved Oxygen Objectives, Prepared for City of Stockton, Jones & Stokes, Sacramento, CA

Fourier J.B.J. 1922. Theorie Analytique de la Chaleur. Didot, Paris (referenced in Fischer et al. 1979).

Godfrey R.G.and Frederick, B.J. 1970. Dispersion in Natural Streams. US. Geological Survey Professional Paper, 433-B. (referenced in Fischer et al. 1979).

Herr J. and C.W. Chen 2006. Forecasting Procedure Report. Task 6 Report for Upstream San Joaquin River Monitoring and Investigations Project (A CALFED Directed Action Project), Systech Engineering, Inc., San Ramon, CA.

Holley E.R. and G. Abraham. 1973. Laboratory Studies on Transverse Mixing in Rivers. J. Hydraul. Res. 11, 219-253. (referenced in Fischer et al. 1979).

Jackman A.P. and Yotsukura N. 1977. Thermal Loading of Natural Streams. U.S. Geological Survey Professional paper 991. (referenced in Fischer et al. 1979).

Kratzer C.R., P.J. Pickett, E.A. Rashimawi, C.L. Cross, and K.D. Bergerson. 1987. An Input-Output Model of the San Joaquin River from the Lander Avenue Bridge to the Airport Way Bridge : Technical Committee Report No. N.Q. 85-1. California Water Resources Control Board, Sacramento, CA.

Kratzer C.R., P.D. Dileanis, C. Zamora, S. R. Silva, C. Kendall, B.A. Bergamaschi and R. A Dahlgren. 2004. Sources and Transport of Nutrients, Organic Carbon, and Chlorophyll-a in the San Joaquin River Upstream of Vernalis, California, during Summer and Fall, 2000 and 2001 : Water Resources Investigations Report 03-4127, US Geological Survey, Sacramento, CA.

Lee G.F. and A.J. Lee. 2000. Synopsis of Issues in Developing the San Joaquin River Deep Water Ship Channel DO TMDL : available from http://www.gfredlee.com/ SJRsynopsis.pdf. Lehman, P.W., J. Sevier, J. Giulianotti, and M. Johnson. 2004. Sources of Oxygen Demand in the Lower San Joaquin River, California, Estuaries, Vol. 27, No. 3, pp 405-418.

Litton G.M., M. Brunell, N.W.T. Quinn and J.C. Monroe. 2007. Task 8. Linking the San Joaquin River to the Stockton Deep Water Ship Channel. Interim task Report # 3. University of the Pacific, Stockton, CA.

Mackay. J.R. 1970. Lateral Mixing of the Laird and Mackenzie Rivers Downstream from their Confluence. Can. J. Earth Sci. 7, 111-124. (referenced in Fischer et al. 1979).

Pate T. 2001. DSM2 San Joaquin Boundary Extension : in Chapter 5 of Methodology for Flow and Salinity Estimates in the Sacramento-San Joaquin Delta and Suisun Marsh, 22nd Annual Progress Report to the State Water Resources Control Board in Accordance with Water Right Decision 1485, Order 9, Department of Water Resources, Sacramento, CA.

Wilde J. 2005. Using Dye-Injection Study to Revise DSM2-SJR Geometry : in Chapter 2 of Methodology for Flow and Salinity Estimates in the Sacramento-San Joaquin Delta and Suisun Marsh, 26th Annual Progress Report to the State Water Resources Control Board in Accordance with Water Right Decision 1485, Order 9, Department of Water Resources, Sacramento, CA.

Yotsukura, N. H.B. Fischer and W.W. Sayre 1970. Measurement of Mixing Characteristics of the Missouri River between Sioux City, Iowa and Plattsmouth, Nebraska. US Geological Survey Water Supply Paper 1899-G. (referenced in Fischer et al. 1979).